Desulfurization and Denitrogenation of Bitumen-Derived Gas Oils using Functionalized Polymers

A Thesis Submitted to the College of Graduate and Postdoctoral Studies
In Partial Fulfillment of the Requirements for the
Degree of Doctor of Philosophy
In the Department of Chemical and Biological Engineering
University of Saskatchewan
Saskatoon, SK
Canada

By

Prachee Misra

PERMISSION TO USE

In presenting this thesis in partial fulfillment of the requirements for a Postgraduate degree from the University of Saskatchewan, I agree that the Libraries of this University may make it freely available for inspection. I further agree that permission for copying of this thesis in any manner, in whole or in part, for scholarly purposes may be granted by Dr. Ajay Dalai and Dr. John Adjaye, who supervised my thesis work, or in their absence, by the Head of the Department or the Dean of the College of Engineering. It is understood that any copying or publication or use of this thesis or parts thereof for financial gain shall not be allowed without my written permission. It is also understood that due recognition shall be given to me and to the University of Saskatchewan in any scholarly use which may be made of any material in my thesis.

Requests for permission to copy or to make other uses of materials in this thesis/dissertation in whole or part should be addressed to:

Head of the Department
Chemical and Biological Engineering
University of Saskatchewan
57 Campus Drive
Saskatoon, Saskatchewan S7N 5A9
Canada

ABSTRACT

Recent developments in the petroleum refinery processes are focused on the production of ultra-low sulfur fuels due to the stringent environmental regulations. Heavy crude oil, also known as the synthetic crude derived from the oil sands is emerging as one of the sources to meet the present and future energy demands. However, heavy oil contains high concentration of heterocyclic sulfur and nitrogen compounds. A major challenge in achieving deep hydrodesulfurization with the conventional hydrotreating technology is the inhibition and deactivation of the catalyst caused by heterocyclic nitrogen compounds. Amongst the sulfur compounds present in the petroleum feed, benzothiophene and its derivatives are unsusceptible to conventional hydrotreating catalyst leading to impediment in achieving deep hydrodesulfurization. There is a critical need for the improvement in hydrotreating technologies to reduce sulfur and nitrogen levels in the fuels derived from unconventional resources. Therefore, a pre-treatment process using functionalized polymers has been developed for the removal of nitrogen and sulfur compounds from gas oil via charge transfer complex mechanism. Functionalized polymer comprises of polymer support, linker and π-acceptor; these parts were modified to enhance nitrogen and sulfur removal.

The research work was divided into five phases. The first phase was focused on studying the effects of different electron withdrawing π-acceptors on the nitrogen and sulfur removal. Three π-acceptors with 2, 3 and 4 electron withdrawing nitro groups attached on the fluorenone moiety were synthesized; viz., 2,7-dinitro-9-fluorenone (DNF); 2,4,7-trinitro-9-fluorenone (TriNF) and 2,4,5,7-tetranitro-9-fluorenone (TENF), respectively. Porous polymer support [copolymer of glycidyl methacrylate and ethylene glycol dimethacrylate, poly (GMA-co-EGDMA)] was functionalized with the π-acceptors via hydroxylamine linker. The optimized polymers successfully removed 14.4 wt.% of total nitrogen and 1.4 wt.% of total sulfur from light gas oil at room temperature. It was found that the removal of these impurities is due to the formation of charge transfer complexes between π-acceptor functionalized polymers and heterocyclic nitrogen and sulfur species present in gas oil. In the second phase, the effects of changing the linker length on nitrogen and sulfur removal was studied. The linkers were varied from a two-carbon (diaminoethane, DAE (2)), a three-carbon (diaminopropane, DAP(3)) to a four-carbon (diaminobutane, DAB(4)) containing compounds while the functionalized polymer consisted of

identical polymer support, poly (GMA-co-EGDMA) and π-acceptor (TENF). 19 wt.% removal of nitrogen compounds from light gas oil was observed using diaminopropane (DAP(3)) substituted polymers in a batch reactor at ambient temperature with polymer to oil loading ratio of 1:4 wt./wt.

In the third phase, polymers with high internal phase emulsion (polyHIPEs) were synthesized to study the effects of polymer support on the removal of nitrogen and sulfur compounds from bitumen-derived gas oil. Four different types of polymer supports were prepared by varying the amount of monomers (unsaturated polyester resin, glycidyl methacrylate and divinylbenzene) and the type of porogen (toluene or tetrahydrofuran). All four polymer supports were functionalized with identical π-acceptor (TENF) and tested in a batch reactor at ambient temperature. 14.6 wt.% of total nitrogen was removed while no significant sulfur removal was observed. Reusability studies were performed by regenerating the used polymers with toluene. Regenerated polymer was capable of removing 8.2 wt.% of total nitrogen in second contact with light gas oil.

A fundamental insight into the role of π-acceptors forming charge transfer complexes with heterocyclic nitrogen and sulfur compounds was obtained in the fourth phase of this work. Adsorption isotherms were studied using model nitrogen and sulfur compounds (quinoline, 9-ethylcarbazole and dibenzothiophene) in a batch reactor at three sets of temperature (298 K, 313 K and 328 K). Calculation of the thermodynamic parameters disclosed the exothermic and spontaneous nature of the adsorption of quinoline, 9-ethylcarbazole and dibenzothiophene over functionalized polymer. The polymeric adsorbent was found selective towards the removal of nitrogen compounds and the adsorption capacity followed the order: quinoline > dibenzothiophene > 9-ethylcarbazole. In the last phase, hydrotreatment of polymer treated heavy gas oil was studied in a trickle bed reactor at industrial conditions. The combination of adsorption and catalysis has resulted in 94.3% hydrodesulfurization (HDS) and 63.3% hydrodenitrogenation (HDN) as compared to 93.1% HDS and 60.5% HDN activities during hydrotreatment of heavy gas oil using conventional NiMo/γ-Al_2O_3 catalyst.

ACKNOWLEDGEMENT

I am taking this opportunity to convey my appreciation to everyone who supported me in the completion of my Ph.D. research work. Firstly, I would like to express my deepest gratitude to my supervisors, Drs. Ajay Dalai and John Adjaye for providing me with an opportunity to work under their aspiring guidance. I am very much thankful to them for the immense knowledge and for motivating me to grow as a researcher. This thesis would not have been possible without their constant supervision and support.

I would like to thank my advisory committee members, Drs. Venkatesh Meda, Catherine Niu, Jafar Soltan, and Stephen Foley, for their valuable inputs throughout my program, and for improving the quality of research. I am grateful to Drs. Jackson Chitanda, Ali Abedi, and Sandeep Badoga for their contributions in the laboratory. I am thankful to Dr. Satyendra Chaurasia for encouraging and helping me throughout my studies. I also acknowledge the assistance with the analytical instruments from Ms. Heli Eunike and Mr. Richard Blondin.

I sincerely acknowledge the financial support from Natural Science and Engineering Research Council of Canada (NSERC), the University of Saskatchewan, MITACS, and Syncrude Canada Limited.

Lastly, I would like to wholeheartedly thank my parents (Mrs. Nirvesh Misra and Mr. Ashok Kumar Misra) who always believed in me and gave me the strength and courage to set higher targets in life, my sister (Dr. Medha Misra) for her unparalleled support throughout my life, my dear husband (Dr. Munish Sharma) whose love and motivation is a blessing beyond words, and my parents-in-law (Mrs. Meera Sharma and Mr. Megh Raj Sharma) for encouraging me throughout my Ph.D. program.

DEDICATION

This thesis is dedicated to my parents

Mrs. Nirvesh Misra and Mr. Ashok Kumar Misra

TABLE OF CONTENTS

LIST OF TABLES

LIST OF FIGURES

NOMENCLATURE

2,4-DMDBT	2,4-dimethyldibenzothiophene
4,6-DMDBT	4,6-dimethyldibenzothiophene
4-MDBT	4-methyldibenzothiophene
AIBN	azobisisobutyronitrile
Al_2O_3	aluminum oxide
API	American Petroleum Institute gravity of petroleum liquids, dimensionless
ATM	atmospheric
BET	Brunauer-Emmett-Teller method
BN	basic nitrogen compounds
BT	benzothiophene
BTU	British thermal unit
C1-C4DBT	alkyl substituent containing one to four carbon atoms on DBT
C_{Ar}%	percentage aromatic content
$CDCl_3$	deutrated chloroform
C_e	equilibrium concentration of the solute in the model feed (ppm)
C_i and C_f	initial and final concentrations (ppm)
Ci	concentration of species, i (ppm)
CTC	charge transfer complex
D	distribution coefficient
DAB(4)	diaminobutane
DAE (2)	diaminoethane
DAP(3)	diaminopropane
DBT	dibenzothiophene
DDS	direct desulfurization
DFT	density-functional theory

DLS	dynamic light scattering
DMDBT	dimethyldibenzothiophene
DMF	N,N-dimethylformamide
DMSO	dimethyl sulfoxide
DNF	2,7-dinitro-9-fluorenone
DVB	divinylbenzene
E%	extraction efficiency
EGDMA	ethylene glycol dimethacrylate
EIA	U.S. Energy Information Administration
FBP	final boiling point
FCC	fluid catalytic cracking unit
FTIR	Fourier transform infrared spectroscopy
GMA	glycidyl methacrylate
H_2-TPR	H_2-temperature programmed reduction
HC	hydrocarbon
HDA	hydrodearomatization
HDM	hydrodemetallization
HDN	hydrodenitrogenation
HDS	hydrodesulfurization
HGO	heavy gas oil
HOMO	highest occupied molecular orbital
HYD	hydrogenation
IBP	initial boiling point
K	thermodynamic equilibrium constant
K_F	Freundlich adsorption constant (mmol/g) $(L/mg)^{1/n}$
K_L	Langmuir isotherm constant (L/mg)
LGO	light gas oil

LHSV	liquid hourly space velocity (s^{-1})
LUMO	lowest unoccupied molecular orbital
Me	methyl
M_f	model feed weight (g)
MF	model feed
MMF	mixed model feed
MoS_2	molybdenum sulfide
M_s	mass of solid adsorbent (g)
N	nitrogen
NBN	non-basic nitrogen compounds
NMR	nuclear magnetic resonance
NN	hydrazine
OECD	Organization for Economic Cooperation and Development
ON	hydroxylamine
PA	polystyrene
PF	polystyrene (Fluka)
PGMA	copolymer of GMA and EGDMA, poly (GMA-co-EGDMA)
PN	pyromellitic dianhydride
polyHIPE	polymer with high internal phase emulsion
PS	silica coated polystyrene
q	adsorption capacity (mmol/g)
q_e	equilibrium adsorption capacity (mmol/g)
q_m	maximum monolayer coverage capacity (mmol/g)
R	universal gas constant (J mol^{-1} K^{-1})
R^2	coefficient of regression for the reaction models, dimensionless
R_L	separation factor
S	sulfur

SCO	synthetic crude oil
SEM	scanning electron microscopy
$S_{N/S}$	selectivity factor
SRGO	straight run gas oil
T	temperature (°C)
TCN	4,5-dicyano-2,7-dinitrofluorenone
TEA	triethanolamine
TENF	2,4,5,7-tetranitro-9-fluorenone
TGA	thermogravimetric analysis
THF	tetrahydrofuran
TriNF	2,4,7-trinitro-9-fluorenone
UPR	unsaturated polyester resin
VDU	vacuum distillation unit
VTB	vacuum topped bitumen
WS_2	tungsten sulfide
XRD	X-ray diffraction
$\Delta G°$	Gibbs free energy (kJ mol^{-1})
$\Delta H°$	change in enthalpy (kJ mol^{-1})
$\Delta S°$	change in entropy (J mol^{-1} K^{-1})

Chapter 1: Introduction and Thesis Outline

1.1 Introduction

With the increasing world's population and the rapid development of emerging economies, the world's demand for energy is projected to accelerate substantially [1]. Science and technology must play a vital role in accommodating the growth in energy demand while meeting the aggressive environmental regulations. Continuous research is needed to identify processes to mitigate emissions in the most economically efficient ways. Due to strong inclination towards liquid fuels for transportation, 95% of the world transportation fuel is produced from crude oil. Harnessing conventional oil resources is easier and economical while exploration and utilization of unconventional oil is devious. However, liquid fuels from unconventional resources are expected to dominate the conventional oil market, as conventional oil subsides [2]. Unconventional oil tends to be heavier, complex and requires intensive processing before it can be used as transportation fuel. Heavy oil derived from unconventional oil resources has higher concentration of refractory sulfur and nitrogen impurities which needs to be removed in order for the fuel to meet the environmental regulations [3]. In refineries, crude oil is subjected to numerous processes such as, cracking, reforming, isomerization, hydrotreating, and hydrocracking to deliver clean and affordable transportation fuels. Catalysts play an important role in increasing the efficiency of these processes [4]. Hydroprocessing is one of the important catalytic processes in petroleum refineries which is used to remove metals, oxygen, sulfur, and nitrogen hetero atoms and to saturate carbon-carbon bonds. It is used extensively for improving the quality of heavy oil feedstock before processing the feed in downstream refinery processes such as, catalytic reforming, fluid catalytic cracking, and hydrocracking. Prominence of hydrotreating has increased in recent years due to the implementation of ultra-low sulfur diesel specifications. Present day refineries are aiming towards the production of low sulfur petroleum feedstocks in order to meet the environmental regulations worldwide. Hydrotreating includes catalytic hydrodesulfurization (HDS), hydrodenitrogenation (HDN), hydrodemetallization (HDM), and hydrodearomatization (HDA) of the feed, which is carried out at high temperature and pressure in the hydrotreating

reactors with excess hydrogen consumption. Sulfur compounds such as, thiophene, benzothiophene, and its methyl substituted derivatives are resistant to the hydrotreating catalyst which decreases the hydrotreating efficiency of the process [5]. Moreover, nitrogen containing compounds present in the oil competitively adsorb onto the catalyst active sites causing inhibition and deactivation of the catalyst [6] which directly impacts the commercial profit of the refineries. Majority of the nitrogen is present as aromatic heterocyclic compounds with fused benzene rings. Typically, six-membered ring compounds such as, quinoline and acridine are basic nitrogen compounds whereas, five-membered ring compounds such as, indole and carbazole are non-basic nitrogen compounds [7]. Hydrogen consumption and process severity can be reduced by improving the catalyst life, activity and selectivity, which will also result in enhanced hydrotreating process efficiency. Through the improvement in petroleum refining technology, production of cleaner fuels is possible with reduced energy requirement and minimal impact on our environment.

Another approach to achieve deep HDS is the non-catalytic treatment of feed. The principle behind using non-catalytic processes is the selective adsorption of nitrogen and sulfur impurities at ambient temperature without using H_2. Non-complex designs, easy operational requirements and comparatively low cost are some of the advantages responsible for their worldwide popularity among researchers. Porous adsorbents such as activated carbon derived from wood, coke, coconut husk and coal have been studied for the removal of sulfur and nitrogen compounds from liquid hydrocarbon feed [8–10]. Various zeolites [11–13], ionic liquids [14,15] and metal-organic frameworks [16,17] have also been utilized in the field of denitrogenation and desulfurization of fuels. Moreover, hydroprocessing catalyst inhibiting nitrogen species such as indole, carbazole and alkyl substituted carbazoles can be removed by using functionalized polymers capable of adsorbing these compounds prior to hydrotreatment [18,19]. These compounds are often referred to as non-basic nitrogen compounds because the lone pair of electrons on the nitrogen atom is delocalized within the aromatic system, in contrast to the basic nitrogen compounds where the lone pair of electrons is localized on the nitrogen atom. Due to the formation of π-electron cloud, these compounds are electron rich and can act as electron donors. However, fluorenone derived compounds like 2,4,7-trinitro-9-fluorenone (TriNF) and 2,4,5,7-tetranitro-9-fluorenone (TENF)

are electron poor due to the presence of electron withdrawing nitro groups and can act as electron acceptors.

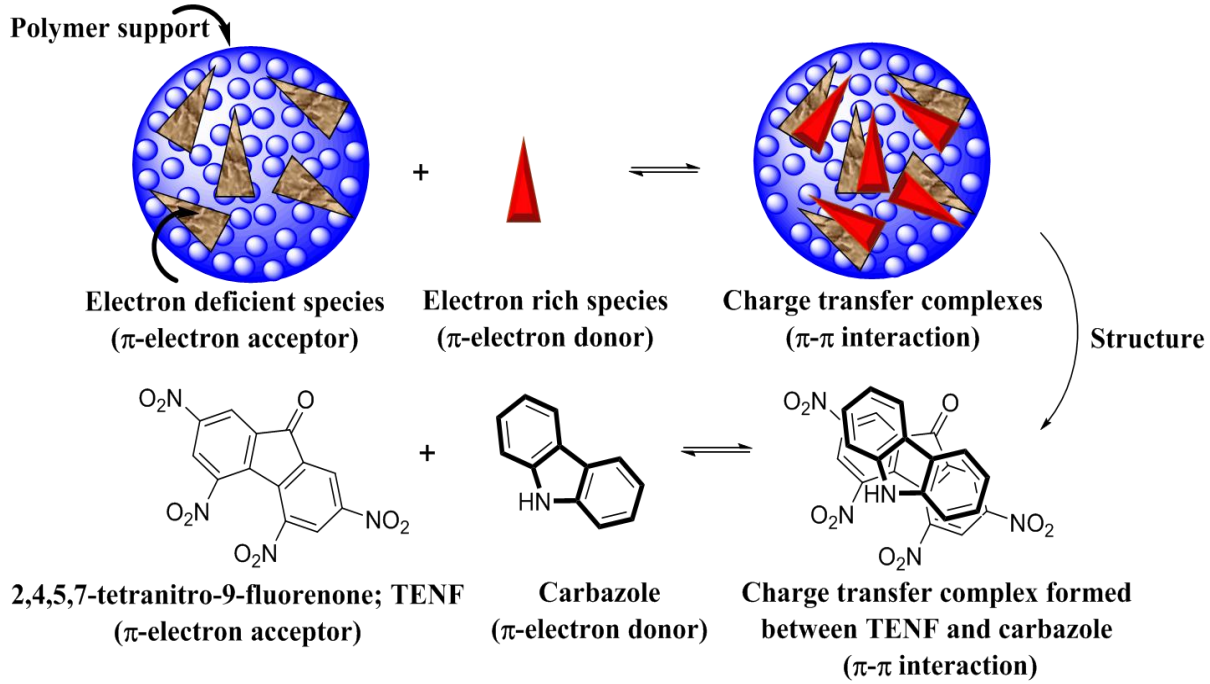

Figure 1.1: Visual representation of the formation of charge transfer complex between electron donor and electron acceptor.

As shown in Figure 1.1, these electron donor and acceptor compounds are capable of forming charge transfer complexes (CTC), resulting in the removal of inhibiting nitrogen compounds from gas oil [20–22]. The π-acceptors can be easily immobilized on porous polymer supports to enhance the adsorption process, and also to prevent leaching of the π-acceptors in gas oil. Therefore, the aim of this research was to improve the efficiency of hydrotreating process by removing the catalyst inhibiting impurities before hydrotreating by developing a highly efficient functionalized polymer. Functionalized polymers consist of three components: polymer support, linker, and π-acceptor, as shown in Figure 1.2. In this work, various functionalized polymers were synthesized and tested for adsorbing nitrogen and sulfur impurities from bitumen-derived gas oils. Effects of changing the polymer support, linker, and π-acceptor on the functionalized polymer efficiency to remove nitrogen and sulfur impurities were studied. Regeneration and reusability tests were performed to make the process economical for refineries. Furthermore, the effects of integrating adsorption and hydrotreating on improving the efficiency of the process were also studied.

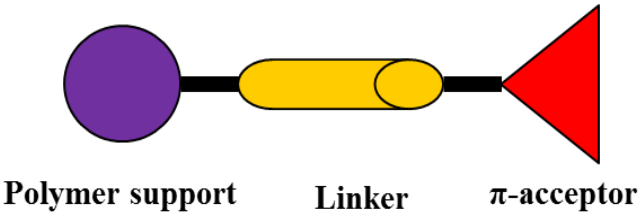

Figure 1.2: Components of functionalized polymers.

1.2 Knowledge gaps

A review of the research articles to date, focussing on the pre-treatment of bitumen-derived gas oils has led to the following knowledge gaps:

1. Research on nitrogen and sulfur removal from gas oils using functionalized polymers requires attention. There are limited studies on the selective removal of nitrogen compounds from bitumen-derived gas oil using π-acceptor functionalized polymers.
2. Role of fluorenone derived π-acceptors in the formation of charge transfer complexes with electron rich nitrogen and sulfur compounds has not been studied in detail.
3. Change in the polymer performance by altering the linker length of π-acceptor functionalized polymers is not reported in literature, and the interaction effects are not known yet.
4. There is no literature available on using polymers with high internal phase emulsion (polyHIPEs) for the removal of nitrogen compounds from gas oil.
5. Effect of the removal of nitrogen compounds prior to hydrotreatment of bitumen-derived gas oils is limited.

1.3 Hypotheses

1. Pre-treatment with π-acceptor functionalized polymers will eliminate refractory sulfur and nitrogen compounds from bitumen-derived gas oils which will improve the overall efficiency of the hydrotreating process.
2. Increasing the number of electron withdrawing nitro groups attached to the π-acceptor will increase the removal of nitrogen and sulfur compounds.

3. Increasing the length of linker in functionalized polymer will reduce the steric hindrance around π-acceptor molecules, which can enhance the nitrogen removal efficiency.
4. Increase in adsorption capacity can be achieved by immobilizing π-acceptors on the polymers with high internal phase emulsion.
5. It is hypothesized that hydrodesulfurization (HDS) and hydrodenitrogenation (HDN) activities of the gas oil may be improved by reducing the nitrogen content before hydrotreating reactions in a trickle bed reactor.

1.4 Research objectives

Based on the literature review discussion in Chapter 2 of this thesis, the research objectives and sub-objectives were set for this work. The main objective of this research is to improve the efficiency of hydrotreating processes by removing nitrogen and sulfur species from bitumen-derived gas oil using π-acceptor functionalized polymers. Following are the sub-objectives involved to accomplish the overall objective:

1. To study the role of π-acceptors in the removal of nitrogen and sulfur compounds from bitumen-derived gas oils.
2. To investigate the effects of linker length on the denitrogenation and desulfurization of gas oils.
3. To improve the textural properties of functionalized polymers by synthesizing polymers with high internal phase emulsion. Also, studying the regeneration and reusability of the complexing agents.
4. To study the adsorption isotherms, thermodynamic parameters and charge transfer complex interactions between electron donors and acceptors.
5. Performing the hydrotreatment studies on the polymer treated gas oil feedstock using conventional NiMo/γ-Al_2O_3 catalyst.

1.5 Organization of the thesis

This thesis contains 8 chapters covering detailed synthesis, characterization, testing and conclusions from all the phases of the research. Chapter 2 is dedicated to the literature review in the field of crude oil refining. Recent advances in non-catalytic methods for the removal of

nitrogen and sulfur impurities, mechanism of charge transfer complex formation, inhibitory effects of heterocyclic nitrogen compounds, and hydrotreating of bitumen-derived gas oils are reviewed.

Chapter 3 discusses the effects of various electron withdrawing π-acceptors on the nitrogen and sulfur removal efficiency of functionalized polymer. It describes the charge transfer complex formation ability of nitrogen and sulfur compounds with various fluorenone based π-acceptors. Chapter 4 presents the effects of changing the length of linker in functionalized polymers. Synthesis of polymers with various linkers, their textural and chemical characterization, batch adsorption test results along with optimization of process parameters such as, temperature, time, and particle loading are reported. Chapter 5 covers the effects of changing the polymer support on the adsorption efficiency of the polymeric adsorbents. This included the synthesis and characterization of polymers with high internal phase emulsion (polyHIPE), batch adsorption experimental details, and regeneration and reusability tests.

Chapter 6 deals with the adsorption isotherms, spectroscopic characterization of the charge transfer complexes and calculation of the thermodynamic parameters of adsorption using model feed. Chapter 7 explains the advantages of using functionalized polymers for the pre-treatment of heavy gas oil. Hydrotreating activity of NiMo-supported catalyst and the role of functionalized polymers in enhancing the hydrotreating activities are reported.

Chapter 8 summarizes the critical findings from all five phases of the work and provides recommendations for possible future work in this area.

Chapter 2: Literature review

This chapter provides a comprehensive literature review related to the research accomplished in this work. Increasing demand for liquid transportation fuel has intensified the exploitation of heavy oil and bitumen as refinery feedstock. Researchers all over the world are involved in improving the processes related to crude oil refining, due to the stringent environmental regulations. This chapter discusses the challenges associated with reducing the nitrogen and sulfur content of petroleum feedstock along with an overview of the energy demand, crude oil production, hydrotreating technology, catalyst inhibition, and novel methods to reduce the concentration of sulfur and nitrogen compounds present in crude oil.

2.1 Global energy consumption

Global energy consumption is increasing significantly due to the rapid economic growth and expanding populations in developing countries. As the living standards in growing economies improve, energy demand increases due to the structural changes, increase in transportation equipment, and expanding capacity to produce goods for domestic and international markets. U.S. Energy Information Administration (EIA) reported a 48% increase in total world consumption of energy from 2012 to 2040 in their International Energy Outlook 2016 report. This report assess the energy consumption for European Union, Organization for Economic Cooperation and Development (OECD) and non-OECD nations (outside the Organization for Economic Cooperation and Development). As shown in Figure 2.1, total energy consumption is projected to increase to 629 quadrillion British thermal units (Btu) in 2020 from 549 Btu in 2012, which is expected to reach 815 quadrillion Btu by 2040. In 2012, transportation sector which includes rail, road, air, and water transportation means accounted for 25% of total world energy consumption. It is expected to increase at a rate of 1.4%/year from 2012 to 2040. Industrial sector utilizes natural gas and petroleum products for the manufacturing, agriculture, and mining operations. A total of 54% of total energy was consumed by the industrial sector in 2012, which is expected to increase from 2012 to 2040 at a rate of 1.2%/year. Globally, the building sector consumes one-fifth of the total world energy and is expected to expand at a rate of 1.5%/year.

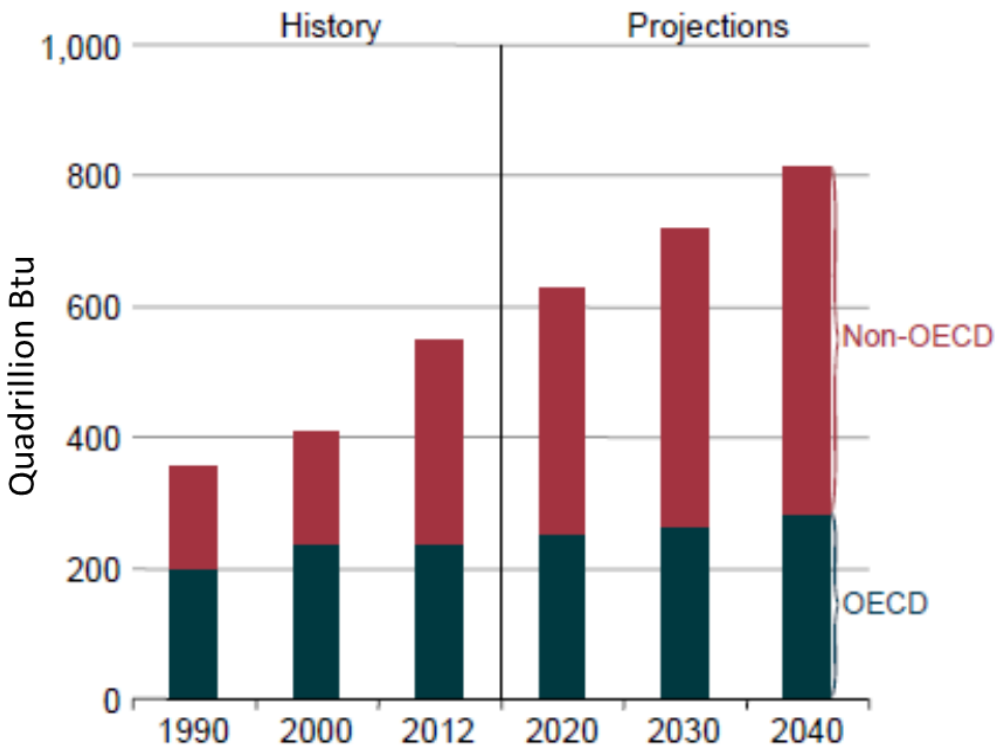

Figure 2.1: Total world energy consumption (Organization for Economic Cooperation and Development (OECD) and non-OECD nations) from 1990 to 2040 (Adapted from U.S. Energy Information Administration, EIA 2016 report).

Liquid fuels, natural gas, and coal are the fossil fuel resources exploited to meet the increasing energy demand. However, adverse environmental effects of fossil fuel emissions and sustained prices have expanded the use of renewable energy resources and nuclear power. Renewable energy is growing at a rate of 2.6%/year due to the government policies for cleaner environment, whereas, the nuclear energy increase rate is 2.3%/year. In 2040, energy from fossil fuels (liquid fuels, natural gas, and coal) will account for 78% of total energy consumption (as shown in Figure 2.2). Liquid fuel consumption is expected to increase in transportation and industrial sectors, while a decline can be expected in residential and electric power sectors due to increasing use of alternative energy resources [23].

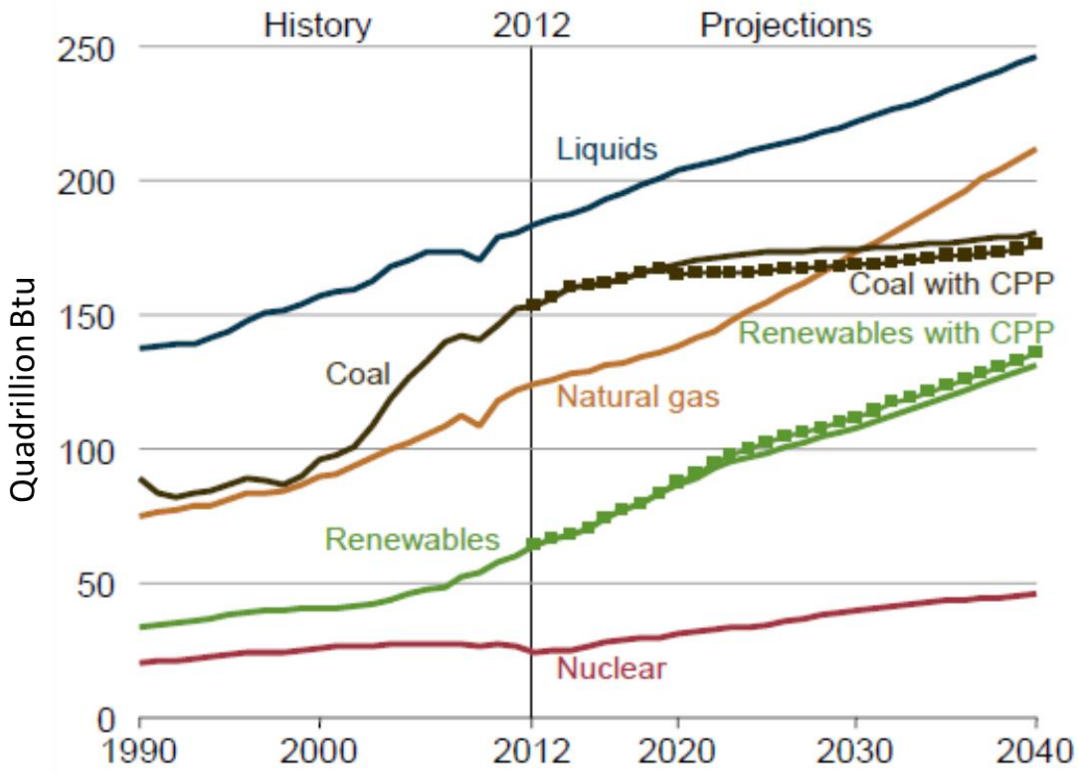

Figure 2.2: World energy consumption by energy source from 1990 to 2040 (Adapted from U.S. Energy Information Administration, EIA 2016 report). Dotted lines for coal and renewables show projected effects of the U.S. Clean Power Plan (CPP).

2.2 Crude oil production and characterization

Crude oil is one of the major energy sources used in transportation and industrial sector. Heavy oil or synthetic oil derived from oil sands is one of the alternative source of liquid fuels. Natural Resources Canada has reported that Canada has the world's third largest (10.3%) proven oil resources which can be recovered with the existing technological conditions. Canada accounts for 171 billion barrels of proven oil reserves, out of which 166.3 billion barrels is present in the form of oil sands [24]. Oil sands are naturally occurring deposits of bitumen consisting of approximately 10-12% bitumen, 4-6% water, and 80-85% sand and clay. As defined by R. Murray Gray [25], bitumen is a natural mixture of solid and semi-solid hydrocarbons. Bitumen is a heavy and unconventional form of crude oil, containing a large amount of middle distillates as compared to the conventional crude oil. Heavy oil is a mixture of hydrocarbons, organic compounds such as

sulfur, nitrogen and oxygen, and metals such as vanadium, nickel, copper and iron. It is usually characterized by high viscosity, low API gravity, low hydrogen to carbon ratio and high content of metals, sulfur, and nitrogen. As shown in Table 2.1, conventional crude oil, bitumen, and heavy oil can be characterized based on their physical properties.

Table 2.1: Properties of conventional crude oil, bitumen and heavy oil [25,26].

Material	Density (g/cm^3)	Viscosity, mPa.s	API gavity
Conventional crude oil	-	10	25-37
Bitumen	> 1	$> 10^5$	< 10
Heavy oil	0.934 - 1	10^2 - 10^5	20 - 10

Typical Athabasca oil sands derived bitumen and its products contain 14% light gas oil, 30% vacuum distillates and 56% vacuum topped bitumen (VTB) [27]. Light gas oil and heavy gas oil are distillate products of bitumen refining. Heavy gas oil is a cut from vacuum distillation unit. It can also be obtained from atmospheric distillation unit as a heavy stream. Boiling range of HGO varies with the type of crude. Table 2.2 summarizes the properties of LGO and HGO from typical Athabasca bitumen.

Table 2.2: Feed characteristics of narrow cuts from VTB obtained from Athabasca bitumen refining [27].

Characterization parameters	Light gas oil (LGO)	Heavy gas oil (HGO)
Cut range (°C)	343 −	343 - 524
Yield (wt.%)	14	50
Microcarbon residue (wt.%)	0	0.3
Sulfur content (wt%)	1.77	3.25
Nitrogen content (wtppm)	0.02	0.19

Concentration of nitrogen and sulfur compounds in crude oil varies depending upon the initial and final temperatures of distillation, and the nature of crude oil. Bitumen-derived heavy gas oil (HGO) contains high sulfur (approx. 4 wt.%) and nitrogen (approx. 0.3 wt.%) content as compared to the conventional crude oil (sulfur: approx. 2.5 wt.% and nitrogen: approx. 0.13 wt.%) which makes the hydrotreating processes challenging [28]. Apprehension of the types, quantities and chemical behavior of nitrogen compounds present in feedstock is important for the development of a novel method for their removal. Nitrogen in the gas oil feedstock is present predominantly as heterocyclic aromatic compounds. Non-basic (five membered ring) and basic (six-membered ring) are the two types of aromatic nitrogen compounds present predominantly in the Athabasca bitumen. In the basic moieties, the lone pair of electrons is not part of the aromatic system and extends in the plane of the ring whereas, in non-basic nitrogen compounds, the lone pair of electrons on the nitrogen atom is delocalized around the aromatic ring [20]. Table 2.3 summarizes the types of nitrogen compounds present in crude oil.

Thiols, sulfides and disulfides, thiophenes, benzothiophenes, dibenzothiophenes are the major sulfur compounds present in gas oil. Heavy oils contain ≥ 3-ring polycyclic sulfur compounds, including benzonaphthothiophene, dibenzothiophene and its alkyl-substituted derivatives such as, 4-methyldibenzothiophene and 4,6-dimethyldibenzothiophene [29]. Figure 2.3 shows the typical heterocyclic sulfur compounds found in heavy oil feedstock. These thiophenic compounds are least reactive and difficult to remove during hydrotreatment process. Sulfides (R_1-CH_2-S-CH_2-R_2), disulfides (R_1-CH_2-S-S-CH_2-R_2) and thiols (R-SH) are other forms of reactive sulfur compounds found in oil.

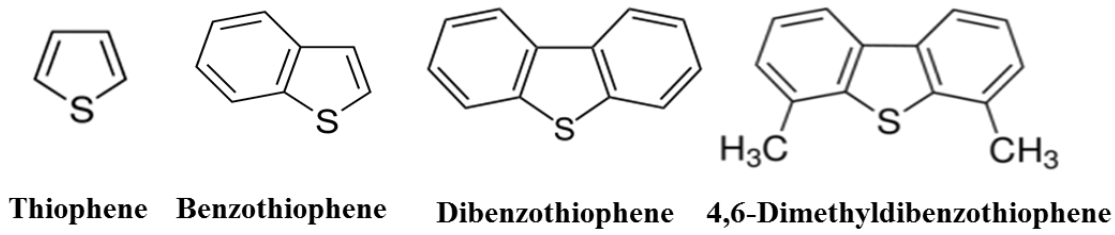

Figure 2.3: Examples of sulfur containing compounds found in gas oil feedstock.

Table 2.3: Representative nitrogen compounds present in gas oil [30].

Name	Formula	Representation
Non-heterocyclic compounds		
Aniline	$C_6H_5NH_2$	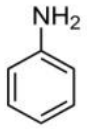
Non-basic heterocyclic compounds		
Pyrrole	C_4H_5N	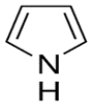
Indole	C_8H_7N	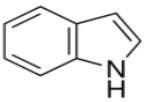
Carbazole	$C_{12}H_9N$	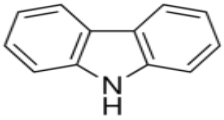
Basic heterocyclic compounds		
Pyridine	C_5H_5N	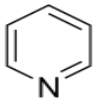
Quinoline	C_9H_7N	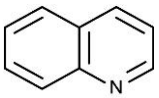
Acridine	$C_{13}H_9N$	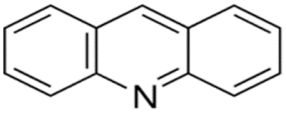

2.3 The hydrotreating process

As shown in Figure 2.4, hydrotreating is an integral part of oil refining process. Removal of sulfur, nitrogen, metals, and aromatic saturation are referred to as hydrodesulfurization (HDS), hydrodenitrogenation (HDN), hydrodemetallization (HDM), and hydrodearomatization (HDA), respectively. Hydrotreatment process is a group of technologies involving catalytic reactions in the presence of hydrogen at elevated temperatures (350-400 °C) and elevated pressures (8 – 10 MPa) to fulfill the following objectives [31]:

- Removal of hetero-atoms such as S and N from crude oil.

- Improvement of FCC feedstock quality due to lower sulfur content.
- Hydrogenation of aromatics.
- Improves stability of the final feedstock for storage
- Removal of heavy metals, such as Vanadium and Nickel

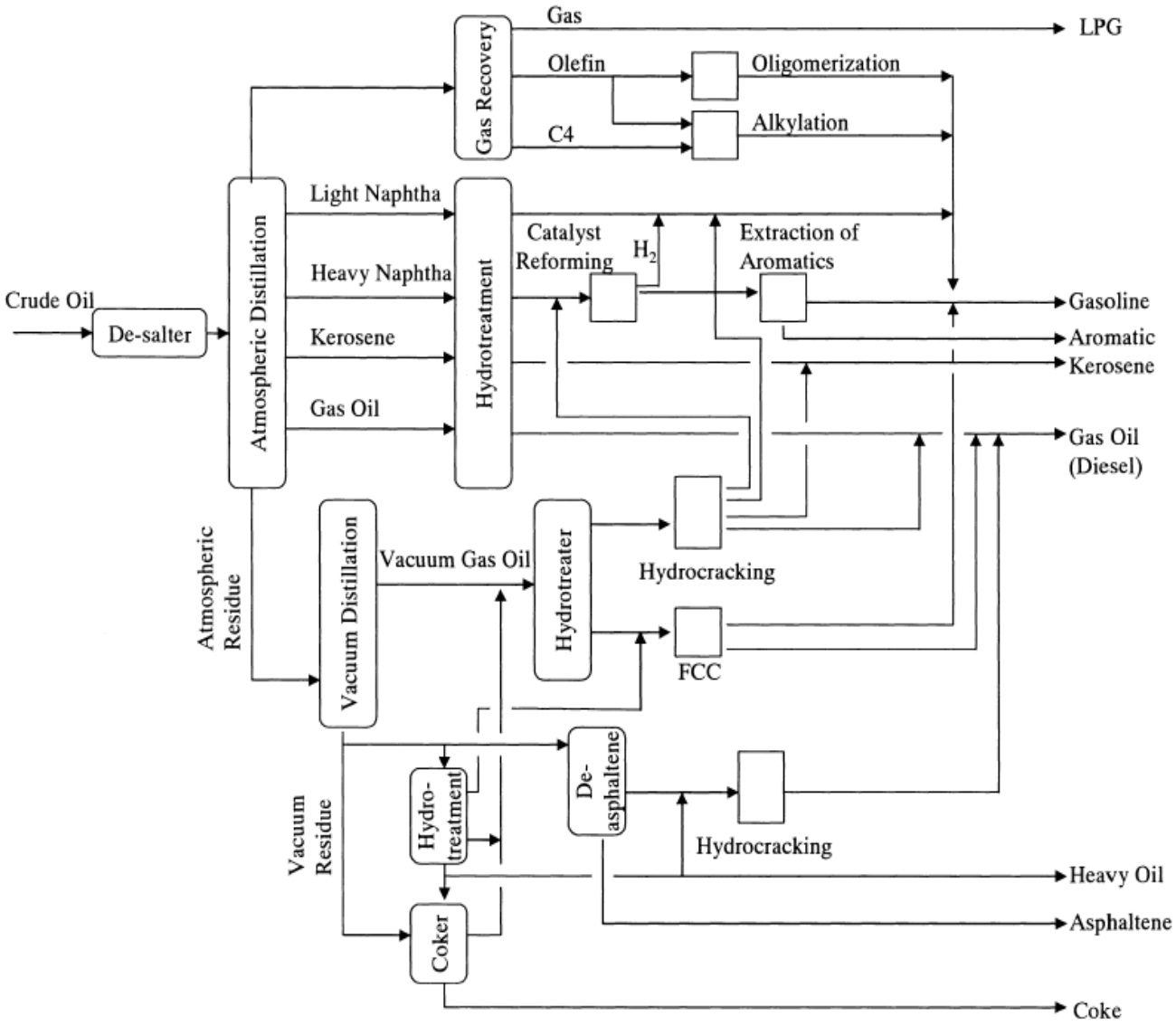

Figure 2.4: Significance of hydrotreatment in a stream of petroleum refining process (Adapted from Mochida & Choi 2004 [32]).

Alumina supported Mo- and W-based sulfides with promoters of Ni and Co sulfides are highly favored hydrotreating catalysts in industries. Cobalt-promoted Mo/γ-Al_2O_3 is preferred for hydrodesulfurization, while use of nickel is favored for hydrodenitrogenation reactions. Additives, such as phosphorus and boron are also widely applied to increase the hydrotreating activity. Owing to large surface area (200-300 m^2/g), pore size control, affinity to sulfide for high dispersion, high mechanical strength and lower cost, alumina is believed to be the best balanced support (Mochida et al., 2004). According to James G. Speight, hydrotreating catalysts are active in their sulfide forms, such as molybdenum sulfide (MoS_2) and tungsten sulfide (WS_2) [33]. Structure of NiMoW sulfided hydrotreating catalyst is shown in Figure 2.5.

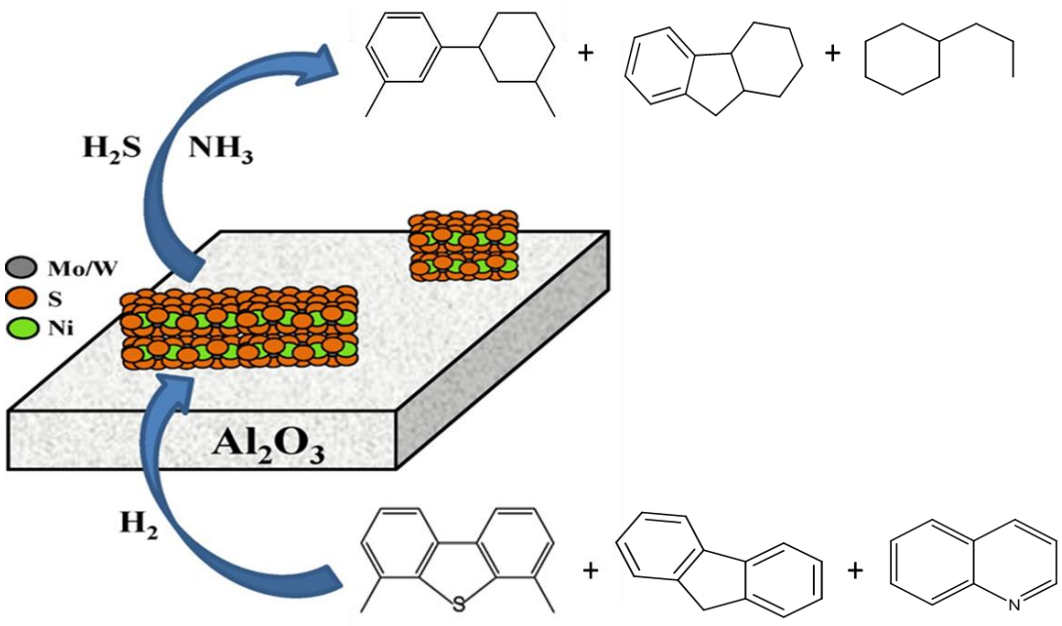

Figure 2.5: Structure of NiMoW sulfided hydrotreating catalyst on a support (Adapted from González-Cortés et al. 2014 [34]).

The choice of the process depends primarily on the boiling range of the feedstock which is dictated by its molecular weight distribution. During the hydrotreatment process, sulfur, nitrogen, and oxygen heteroatoms are removed in the form of hydrogen sulfide, ammonia, and water. Metals are simultaneously removed by HDM reactions. Sulfur compounds such as thiols and disulfides are readily reactive and are removed under mild hydrotreating reaction conditions. HDS of aromatic

organosulfur compounds proceeds by two routes: (i) direct desulfurization (DDS) and (ii) hydrogenation. Figure 2.6 shows the HDS mechanism for hydrogenation of 4,6-DMDBT via DDS and hydrogenation routes.

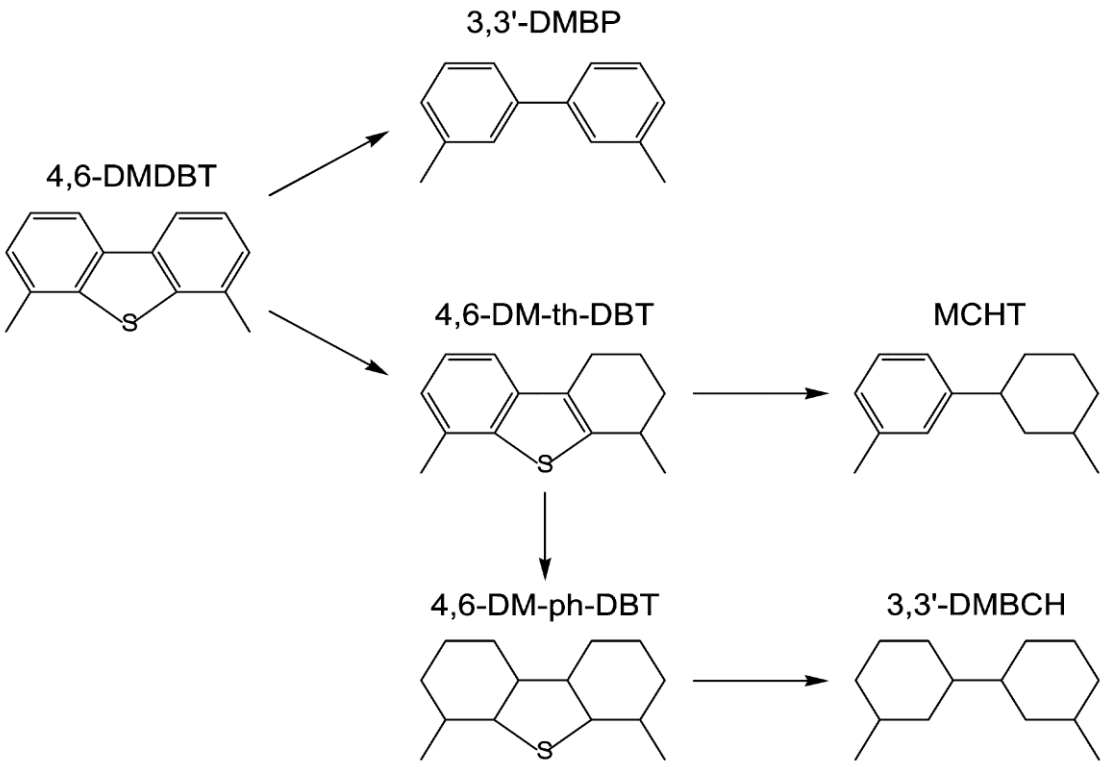

4,6-DMDBT: 4,6-dimethyldibenzothiophene; 3,3´-DMBP: 3,3-dimethylbiphenyl; 4,6-DM-th-DBT: 4,6-DM-tetrahydro-DBT; MCHT: methylcyclohexyltoluene; 4,6-DM-ph-DBT: 4,6-DM-perhydro-DBT; 3,3´-DMBCH: 3,3-dimethylbicyclohexyl

Figure 2.6: Hydrodesulfurization reaction mechanism (Adapted from Egorova & Prins 2004 [35]).

Approaches to ultra-deep HDS include the removal of refractory thiophenic compounds and their derivatives, particularly 4,6-DMDBT [32]. However, the heterocyclic ring has to be hydrogenated before the breaking of carbon-nitrogen bond, therefore, HDN reaction network is much more complicated than the HDS. Removal of nitrogen compounds proceeds through the hydrogenation of aromatic ring, followed by hydrogenolysis of the carbon-nitrogen bond. Quinoline is found in

abundance in the middle distillates. Hence HDN reaction pathway for quinoline is a good representation of industrial HDN processes. Figure 2.7 represents the HDN of quinoline [36].

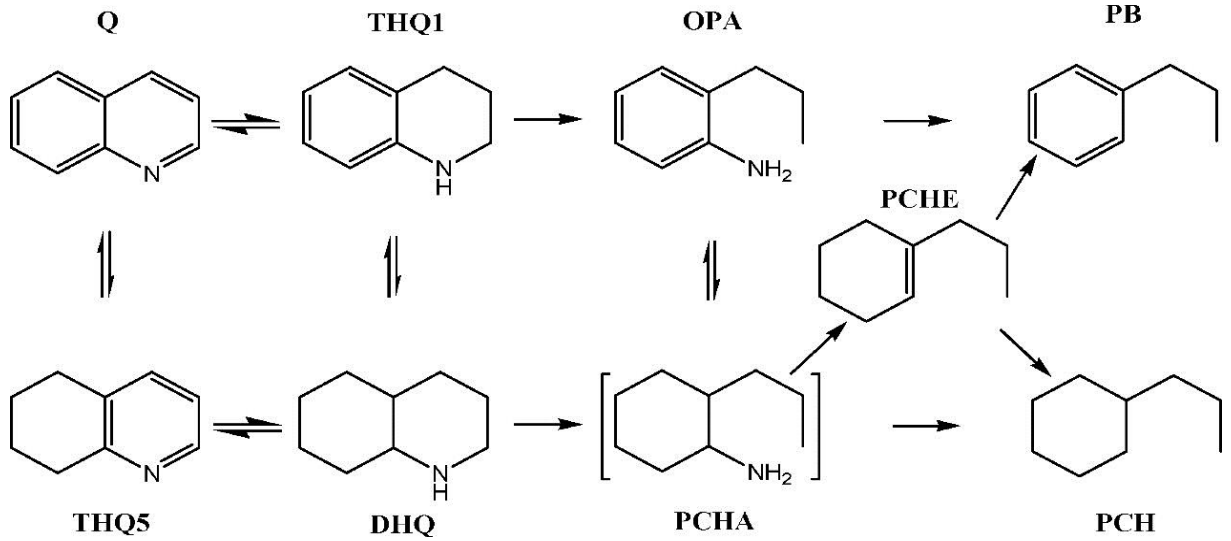

Q-quinoline; THQ1-1,2,3,4-tetrahydroquinoline; OPA-ortho-propylaniline; PB-propylbenzene; THQ5-5,6,7,8-tetrahydroquinoline; DHQ-decahydroquinoline; PCHA-2-propylcyclohexylamine; PCHE-propylcyclohexene; PCH-propylcyclohexane

Figure 2.7: Reaction pathway for HDN of quinoline (Adapted from Lu et al. 2007 [36]).

2.4 Inhibitory effects of heterocyclic nitrogen compounds

Nitrogen compounds naturally occurring in gas oil have been characterized among the strongest HDS inhibitors and a large amount of work has been devoted to their inhibition studies and removal. Upon achieving high levels of desulfurization, when the concentration of refractory sulfur compounds is very low then the polyaromatics and nitrogen compounds naturally occurring in feed inhibit the HDS conversion through competitive adsorption [37].

Han et al. proclaimed the inhibiting effects of quinoline, indole and carbazole on the HDS of 4,6-DMDBT via direct desulfurization step (DDS) and hydrogenation (HYD) routes. Indole inhibited DDS route, while quinoline intensely inhibited HYD route. Carbazole equivalently inhibited DDS and HYD [38]. For carbazole, Nagai et al. [39] and LaVopa et al. [40] reported a strong inhibiting effect on the HDS reactions of thiophene and dibenzothiophene, comparable to those of the basic

compounds pyridine, piperidine and acridine. The high value of the adsorption characterizing carbazole was attributed to products of a rapid hydrogenation converting it to basic compounds. To prove the usefulness of nitrogen removal and to evaluate the effect of its concentration in gas oil, Choi et al. [41] studied HDS reactions using conventional straight run gas oil (SRGO) and its denitrogenated gas oils. Hydrotreating at 340°C reduced the total sulfur content from 14354 ppm to 19 ppm and 120 ppm for 80% and 64% denitrogenated gas oil, respectively. While, sulfur as high as 311 ppm was detected after hydrotreating of untreated SRGO under same conditions. Beltramone et al. [42] concluded that basic strength of nitrogen species is not directly related to the inhibition of HYD and HDS reactions of DBT and 2,4-DMDBT; and it increases in the order: quinoline < tetrahydroquinoline < indole < indoline < ammonia.

Laredo et al. [43] described that the inhibiting effects of non-basic nitrogen compounds, indole and carbazole on HDS of dibenzothiophene were comparable to that of the basic nitrogen compound, quinoline. The inhibition increases in the order: carbazole < quinoline < indole. They also reported that the inhibiting effects of individual nitrogen compounds were very strong, even at concentrations as low as 5 ppm. In a similar study, the inhibiting effect of non-basic nitrogen compound indole was comparable to that of indoline and o-ethylaniline for the HDS of dibenzothiophene [44].

Tao et al. [45] studied the inhibiting effects of quinoline and indole on hydrodesulfurization of thiophenic compounds present in straight-run gas oil. It was found that the inhibiting effect of quinoline on HDS of gas oil is higher as compared to indole. As shown in Figure 2.8, upon increasing N/S concentration in the feed, a significant inhibition was observed in HDS activity. The HDS of refractory sulfur compounds (dibenzothiophene and its derivatives) was strongly inhibited by the increase in nitrogen concentration, while the HDS of thiophene and benzothiophene was slightly inhibited. They concluded that the HDS of sulfur compounds due to the presence of inhibiting nitrogen species decreases in the following order: 4,6-DMDBT > 4-MDBT > C1DBT > DBT > C2-C3DBT (C1-C4DBT are alkyl substituent containing one to four carbon atoms).

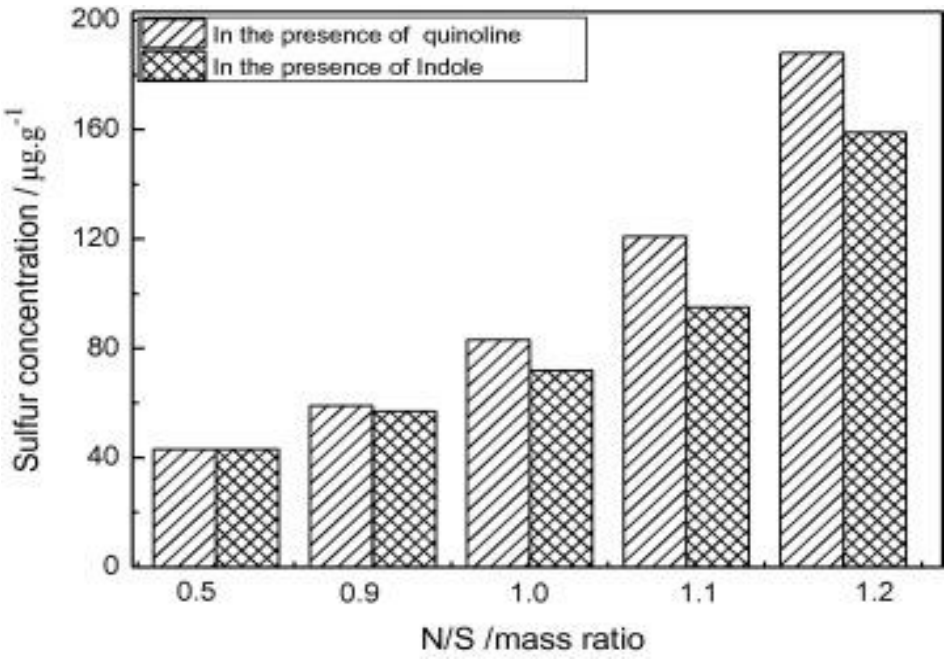

Figure 2.8: HDS of straight run gas oil using NiW/Al_2O_3 catalyst with different N/S concentration. (Adapted from Tao et al. 2017 [45]).

2.5 Recent advances in non-catalytic methods for the removal of inhibitors

In order to improve the efficiency of the hydrotreating process, two main routes can be followed: one is the removal of refractory sulfur compounds, such as 4,6-DMDBT and another is the removal of HDS inhibitors such as pyridine, acridine, carbazole and its derivatives before hydrotreating. The present state of art in denitrogenation of middle distillates using adsorbent materials has been reviewed by Laredo et al. [46]. Various non-catalytic processes including zeolites, activated alumina, mesoporous molecular sieves, ionic liquids, ion exchange resins, metal organic frameworks and activated carbon from numerous sources such as wood, coke, and coal have been studied for the removal of nitrogen species. Also, transition metal salts such as $CuCl_2.2H_2O$ have been utilized due to their ability to extract basic and heterocyclic nitrogen compounds from the synthetic crude oil by complex formation. Ahmed et al. [17] impregnated phosphotungstic acid on metal-organic framework for the adsorption of nitrogen containing compounds from a model fuel. Table 2.4 summarizes different non-catalytic approaches for the removal of nitrogen and sulfur compounds from crude oil. Some of these methods are effective only in the removal of basic nitrogen and sulfur compounds. None of them proved to be really efficient and economical for

removing non-basic nitrogen compounds from distillates. However, π-acceptor functionalized polymers have shown promising results in the removal of heterocyclic nitrogen and sulfur compounds from various petroleum feedstocks.

Table 2.4: Various non-catalytic methods for the denitrogenation and desulfurization of petroleum feed.

S.No.	Method	Remarks	Reference
1.	Ion exchange resins	Effective for basic nitrogen species removal	[47]
2.	Activated carbon	Polycyclic aromatics and sulfur removal	[48]
4.	Metal organic frameworks	Expensive and preparation is difficult	[17]
5.	Transition metal salts ($CuCl_2.2H_2O$)	Removal of basic nitrogen and other heterocyclic compounds	[49]
6.	Copper zeolites	Adsorb sulfur compounds	[50]
7.	Titania nanotubes	Adsorption of sulfur and nitrogen compounds	[51]

2.6 Adsorption isotherms and thermodynamics

Adsorption is a widely used process due to less operational cost, specific target, and high efficiency in removing the contaminant from a wide variety of chemical processes. Additionally, adsorption is a feasible process when dealing with highly toxic contaminants present in low or high concentrations. Establishing the most appropriate adsorption equilibrium correlation is crucial for quantitative comparison of the adsorbent behavior for different adsorption systems, for the successful design of the adsorption system, and for determining adsorption parameters. Adsorption isotherms are the equilibrium relationships which provide insights into the distribution of adsorbate between two phases for a particular adsorbate and adsorbent system [52]. Adsorption isotherms facilitate the measurement of equilibrium binding capacities and adsorption affinities for adsorbents. The Langmuir and Freundlich adsorption models have been widely used to analyze

the equilibrium adsorption of heterocyclic nitrogen and sulfur compounds present in the diesel fuels [9,17,48,53–56].

Langmuir Isotherm: Langmuir empirical model assumes monolayer adsorption, where the adsorption occurs at fixed number of identical and equivalent sites, with no lateral interaction between the adsorbed molecules, even on adjacent sites [57]. It refers to the homogeneous adsorption, where each molecule possess constant enthalpy and all sites possess equal affinity for the adsorbate. The mathematical expression of the Langmuir isotherm model is as follows:

$$q_e = \frac{q_m K_L C_e}{1+K_L C_e} \qquad (2.1)$$

Where, q_e (mmol/g) is the equilibrium adsorption capacity, q_m (mmol/g) is the maximum monolayer coverage capacity on the surface of the polymer, K_L (L/mg) denotes the Langmuir isotherm constant, which is an energy constant, indicating intensity of adsorption and C_e is the equilibrium concentration of the solute in the model feed (ppm).

Freundlich Isotherm [58]: This simple power law model describes non-ideal and reversible adsorption which is not restricted to the formation of monolayer. This model is usually applied to heterogeneous organic systems with non-uniform distribution of adsorption heat and affinities which justifies the applicability of the model in the present context. The mathematical expression of the Freundlich isotherm model is as follows:

$$q_e = K_F C_e^{1/n} \qquad (2.2)$$

Where, K_F and 1/n are Freundlich adsorption constants. K_F, (mmol/g) $(L/mg)^{1/n}$ is an indicator of the adsorption capacity, while 1/n is a measure of adsorption intensity or surface heterogeneity.

Bu et al. [48] studied competitive adsorption of heterocyclic sulfur compounds and polycyclic aromatic compounds for the desulfurization of diesel fuels. Langmuir and Freundlich models were used to study the adsorption capacities and adsorption equilibrium constants. Langmuir isotherm fit of the adsorption of various adsorbates on activated carbon sample is shown in Figure 2.9. Adsorption selectivity of activated carbon followed the following order: naphthalene < fluorene < dibenzothiophene < 4,6-dimethyl dibenzothiophene < anthracene < phenanthrene.

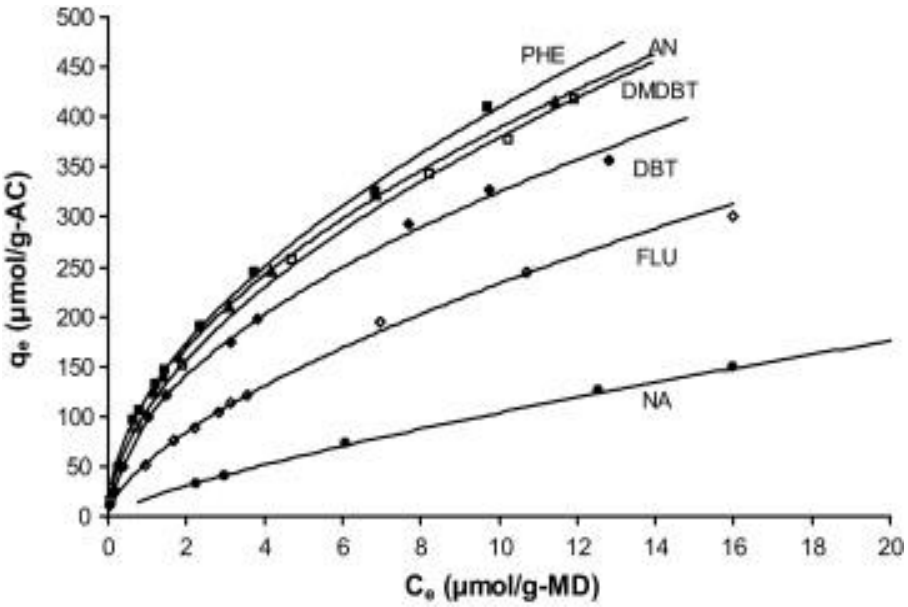

Figure 2.9: Adsorption isotherms of various heterocyclic sulfur compounds and polycyclic aromatic compounds on activated carbon sample at 303 K. Solid lines represent the data fitting using Langmuir isotherm (Adapted from Bu et al. 2011 [48]).

In adsorption process, the liquid phase (adsorbate) is contacted with the solid phase (adsorbent) and the distribution of adsorbate between liquid and solid phase depends on the affinity of the adsorbent towards adsorbate. Calculation of phase equilibrium between solute and solid adsorbent is the most significant contribution of thermodynamics to adsorption processes [59]. Amount of nitrogen and sulfur species adsorbed on adsorbents as a function of their remaining concentration in the model feed is represented by adsorption isotherms; which is the foundation of thermodynamic calculations. Thermodynamic parameters, such as change in Gibbs free energy $\Delta G°$, change in enthalpy $\Delta H°$, and change in entropy $\Delta S°$ (see Equation 2.3) are determined to investigate the effects of temperature on inherent energy changes, and to determine the thermodynamic feasibility of the process.

$$\Delta G° = \Delta H° - T\Delta S° \qquad (2.3)$$

Wen et al. [9] studied the adsorption of heterocyclic nitrogen compounds (quinoline, indole, and carbazole) and sulfur compounds (dibenzothiophene and 4,6-dimethyldibenzothiophene) present in model feeds, light cycle oils, and shale oil over activated carbon. Based on the thermodynamics study, it was concluded that the adsorption of heterocyclic nitrogen and sulfur compounds over

activated carbon is favorable and spontaneous in nature. Van't Hoff plots were used to determine the change in enthalpy (ΔH°) and change in entropy (ΔS°) by calculating the slope and intercept of the plots. Complexation enthalpies of 1,3,5-trinitrobenzene (electron acceptor) with aromatic hydrocarbons, such as benzene, meitylene, durene, and hexamethylbenzene (electron donors) have been measured between -1.84 to -18.28 kJ/mol by Thompson et al. 1966 [60].

2.7 Functionalized polymers for the pre-treatment of petroleum feedstock

2.7.1 Selective charge transfer complex formation

Association of an electron donor with an electron acceptor results in the formation of intermolecular donor-acceptor complexes. Heterocyclic nitrogen and sulfur compounds are electron rich and can act as π-donors. Π-acceptors are electron deficient and are capable of forming charge transfer complexes with π-donors. Lowest unoccupied molecular orbital (LUMO) of the π-acceptor interacts with highest occupied molecular orbital (HOMO) of the π-donor, resulting in the formation of charge transfer complexes. Milenkovic et al. [61] considered the electron-rich structure of alkyl-dibenzothiophenes and developed a highly selective method for their removal from gas oil by the formation of charge transfer complexes (CTCs). They reported the formation of an insoluble CTC between dibenzothiophene derivatives and a π-acceptor (TENF). Alkyldibenzothiophenes, which constitute a major portion of sulfur-containing molecules were removed from the gas oil. 16% and 14% decrease in sulfur impurities was observed from gas oil containing 860 ppm and 11300 ppm of total sulfur, respectively.

A variety of aromatic compounds, with or without heteroatoms present in the gas oil can compete with DBTs and may also form CTCs. Calculation of the highest occupied molecular orbital (HOMO), as shown in Table 2.5, can illustrate their complexing abilities. The higher the HOMO level of the considered π-donor, the lower will be their oxidation potential and therefore the stronger their association with π-acceptors.

Also, the rate of complexation and strength of interaction is best with lowest LUMO energy levels of the π-acceptors (the lower the LUMO level, the stronger will be the interaction with the donor

molecules). Tested π-acceptors with high capability for charge transfer complex formation are shown in Table 2.6.

Table 2.5: Summary of HOMO energy levels of π-donors [61–63].

π-donors	**Name**	**HOMO (eV)**
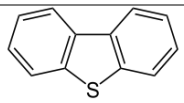	Dibenzothiophene (DBT)	-8.60
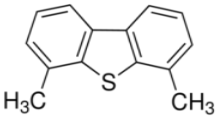	4,6-Dimethyldibenzothiophene (4,6-DMDBT)	-8.51
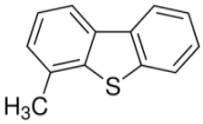	4-Methyldibenzothiophene (4-MDBT)	-8.55
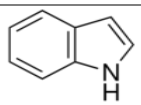	Indole	-8.38
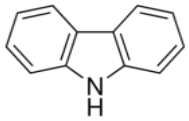	Carbazole	-8.08

Moreover, the energy calculations based on the density-functional theory (DFT) support the selectivity of the 2,4,5,7-tetranitro-9-fluorenone (TENF) to form CTC with alkyldibenzothiophenes [64]. Macaud et al. [30] considered previous studies on the removal of alkyldibenzothiophenes from gas oils by the formation of charge transfer complexes. Due to the structural similarities between carbazole and dibenzothiophene, they expected nitrogen compounds to form CTC with π-acceptors. However, profound analysis of TENF structure by Sevignon et al. [65] revealed that the oxygen atoms of the two nitro groups attached at 4- and 5-positions are too close to each other in planar conformation. Due to this steric repulsion, these two nitro groups rotate to form an angle of 30° with the middle plane of the molecule resulting in the deviation from its planer structure and hinder the approach of the electron donors to form the CTC. Thus, a new π-acceptor molecule, 4,5-dicyano-2,7-dinitrofluorenone was synthesized and immobilized on a hydrophobic support (polystyrene resin) to form charge transfer complex with

4,6-DMDBT. Steric strain was strongly reduced and the fluorenone moiety is almost planer by the introduction of linear cyano group in the 4- and 5- positions. Furthermore, this novel π-acceptor is expected to be stable because the symmetry of the molecule is not modified. This functionalized polymer was used for the deep desulfurization of the diesel feed containing 390 ppm sulfur which was reduced to 40 in four steps. Moreover, this resin could be regenerated with toluene and reused up to 10 times without loss of activity.

Table 2.6: Summary of π-acceptors tested for CTC formation [66].

π-acceptors	**Name**	**LUMO (eV)**
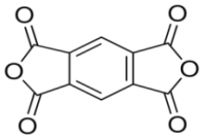	Pyromellitic dianhydride (PN)	-2.67
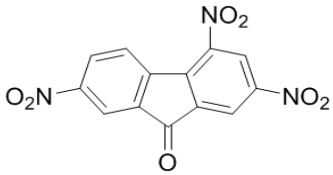	2,4,5-trinitro-9-fluorenone (TriNF)	-2.94
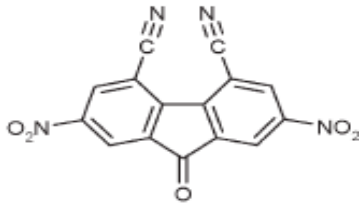	4,5-dicyano-2,7-dinitrofluorenone (TCN)	-3.03
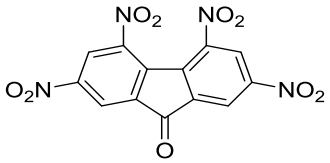	2,4,5,7-tetranitro-9-fluorenone (TENF)	-3.34

2.7.2 Polymer supports for the immobilization of π-acceptors

Selective adsorption of dibenzothiophenes from diesel feeds by formation of charge transfer complexes with immobilized π-acceptor molecules has been explored by Lemaire et al. [5]. Because of the similar structures of heterocyclic nitrogen and sulfur compounds found in

petroleum feed, Macaud et al. [30] expected nitrogen compounds to form CTC with π-acceptors. However, crude oil contains a large variety of aromatic compounds, capable of forming CTC which could in turn compete with indole and carbazole. Since N-containing compounds are more polar than S-containing compounds, synthesis of a polar polymer with electron deficient sites can selectively complex N-compounds as compared to other aromatics present in the feed.

Sevignon et al. [65] studied the desulfurization of Straight Run oil (SR) using 4,5-dicyano-2,7-dinitrofluorenone immobilized on poly(styrene) via hydrazone linker (see Figure 2.10) and successfully eliminated 23% of the total sulfur present in the diesel feed. Selective removal of non-basic nitrogen compounds from diesel feed via charge transfer complex mechanism was investigated by Macaud et al. [20]. A total of 60 wt% of nitrogen compounds were removed from Straight Run oil using π-acceptor immobilized on a hydrophilic support whereas only 30 wt.% of nitrogen removal was obtained from the immobilized polymer with lipophilic support.

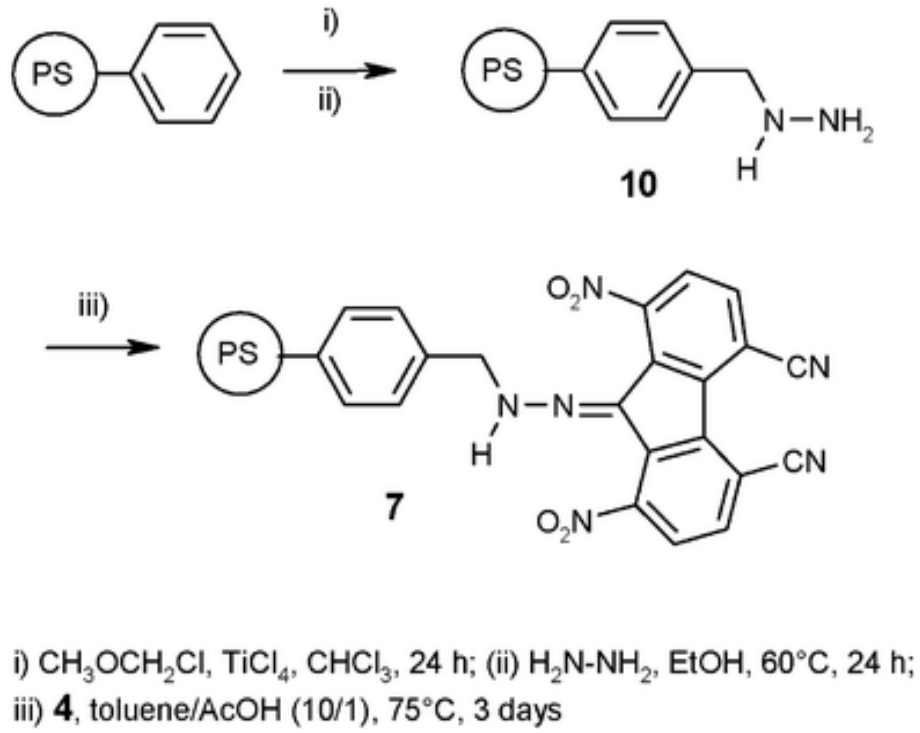

Figure 2.10: 4,5-dicyano-2,7-dinitrofluorenone immobilized on poly(styrene) for the selective removal of sulfur compounds from transportation fuels (Adapted from Sevignon et al. 2005 [65]).

Using π-acceptor molecules covalently attached on hydrophilic support (as shown in Figure 2.11), Macaud et al. [30] selectively removed non-basic nitrogen species from diesel feed by the formation of charge transfer complexes. It is stated that dibenzothiophene and carbazole have similar HOMO values. Also, sulfur compounds are 20 times more concentrated than nitrogen compounds in gas oil feedstock; thus, the carbazole / dibenzothiophene selectivity can be very low. However, the polar nature of nitrogen compounds can be utilized to make the polymer selective for nitrogen removal. Nitrogen selectivity can be improved by immobilizing π-acceptor on hydrophilic polymer support. Lemaire et al. [66] selected the polymer support from the group consisting poly (glycidyl methacrylate), commercial macroporous polystyrenes and polystyrene synthesized concentrated emulsion, called polyHIPE for the selective removal of sulfur and nitrogen compounds from gas oil and light cycle oil. A linking compound, called "linker" was used to immobilize the π- acceptor on these supports.

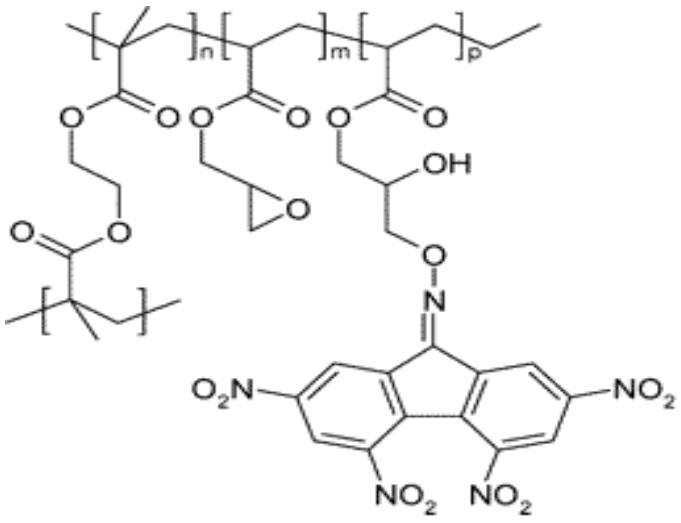

Figure 2.11: TENF immobilized on a hydrophilic polymer support for the selective removal of non-basic nitrogen compounds from diesel feed (Adapted by Macaud et. al. 2004 [30])

In a recent study, PGMA was chosen as the polar support for immobilization of π-acceptor TENF, which led to a very selective complexation of non-basic nitrogen compounds. It was observed that the polymers with highest TENF coupling have the highest nitrogen removal and the one with

lowest TENF coupling have the lowest nitrogen removal [67]. Table 2.7 summarizes the grafting amount of the π-acceptor, TENF on various polymer supports used by Lemaire et al. [66].

Table 2.7: Immobilization rate of TENF on various supports.

Functionalized polymers	Immobilization rate (mmol/g)
PA-NN-TENF	0.60
PS-NN-TENF	0.14
PH-NN-TENF	0.76
PGMA-NN-TENF	0.22
PF-ON-TENF	0.74
PGMA-ON-TENF	0.56
PA-N-TENF	0.76

Lemaire et al. [68] selected polymeric materials from PGMA and polyphenols. It was proposed that, for the selective adsorption of N-compounds, the polymer must have 30 to 90 wt.% from monomer, which comprises of acrylates, methacrylates, phenols, acrylamides, substituted ethylene oxides, isocyanates and acrylonitriles. Adsorption tests were carried out in a batch process at room temperature and atmospheric pressure with a hydrocarbon/polymer ratio of 3:1.

2.7.3 Regeneration and reusability of the reagents

In order to move the adsorbed polyaromatic compound from the bed of the functionalized polymer, it can be eluted by an electron donor solvent. The electron donor solvent is capable of establishing a donor-acceptor interaction with the π-acceptor functionalized polymer. Among many available solvents, benzene, toluene, xylene, and aromatic petroleum cuts (C_9-C_{12}) are preferred due to the HOMO energy level greater than -9.80 eV [66].

Multiple rounds of adsorption of nitrogen and sulfur compounds over regenerated bed of a functionalized polymer showed that the polymers are sufficiently stable. The graft amount of π-

acceptor (TENF) on polystyrene before and after the operation cycles as measured by FTIR is shown in Table 2.8.

Table 2.8: FTIR data for the graft amount of TENF on polymer support after 6 cycles of regeneration [66].

TENF loading in complexing agent	Before testing	After 6 cycles
	0.72 (± 0.5)	0.69 (± 0.5)

For the purpose of regeneration, Macaud et al. [30] easily achieved the regeneration of the nitrogen loaded complexing agent by washing with toluene. Rizwan et al. [67] performed the contact study in order to establish the reusability of the polymer. The sample with highest nitrogen removal was further utilized by washing it multiple times with toluene and then contacting it second and third time with heavy gas oil. Nitrogen removal rate was found to be consistent, which confirmed the reusability of the synthesized polymer.

Chapter 3: Immobilization of fluorenone derived π-acceptors on polymer support for the removal of refractory sulfur and nitrogen species from bitumen derived gas oil: Effect of π-acceptor

---

A similar version of this chapter has been published as a research article and a part of this work was presented at the following conferences:

- Misra, P., Chitanda, J. M., Dalai, A. K. & Adjaye, J. "Immobilization of fluorenone derived π-acceptors on poly (GMA- co-EGDMA) for the removal of refractory nitrogen species from bitumen derived gas oil". *Fuel* (2015) 145, 100–108.
- Misra, P., Dalai, A. K. & Adjaye, J. "Selective removal of nitrogen species from bitumen derived gas oil using π-acceptor immobilized polymers: efficient approach towards improving hydrotreatment technology". *AIChE 2014 Annual Meeting*, Atlanta, Georgia, USA, 16-21 November 2014.
- Misra, P., Dalai, A. K. & Adjaye, J. "Removal of refractory nitrogen species from bitumen procured gas oil using a series of fluorenone derived π-acceptors". *Oil Sands 2014*, University of Alberta, Edmonton, AB, Canada, 28-30 April 2014.
- Misra, P., Rizwan, D., Dalai, A. K. & Adjaye, J. "Denitrogenation of bitumen derived gas oils using immobilized polymers". *63rd Canadian Chemical Engineering Conference*, Fredericton, NB, Canada, 20-23 October 2013.

Contribution of the Ph.D. candidate

Polymer synthesis, characterization, testing and data analysis was done by Prachee Misra. Synthesis and batch adsorption set-up was designed and installed by Prachee Misra with assistance from Dr. Jackson Chitanda. All the manuscript writing and revision work was done by Prachee Misra based on the suggestions from Drs. Ajay Dalai, John Adjaye, and Jackson Chitanada.

Contribution of this chapter to the overall Ph.D. work

This part of work was focused on the synthesis of functionalized polymers with different π-acceptors for the removal of sulfur and nitrogen impurities from bitumen-derived gas oil.

3.1 Abstract

A pretreatment process employing porous polymer support coupled with electron withdrawing π-acceptors has been developed for the selective removal of refractory nitrogen compounds from gas oil via charge transfer complex (CTC) mechanism. Copolymer of glycidyl methacrylate and ethylene glycol dimethacrylate, poly (GMA-co-EGDMA) was used as the porous polymer support for the immobilization of fluorenone based π-acceptors. In order to study the effect of various π-acceptors, 2,7-dinitro-9-fluorenone (DNF); 2,4,7-trinitro-9-fluorenone (TriNF) and 2,4,5,7-tetranitro-9-fluorenone (TENF) were immobilized on poly (GMA-co-EGDMA) via hydroxylamine (ON) linker. BET, CHNOS elemental analysis, SEM and TG/DTA were employed for determining the chemical and physical properties of the synthesized compounds. Characterization by FT-IR revealed the immobilization of π-acceptor on the polymers. Total Nitrogen/Sulfur analyzer affirmed the decrease in total nitrogen and sulfur content of bitumen derived light gas oil (LGO) after pre-treatment with immobilized polymers. This decrease in total nitrogen content of gas oil is a direct consequence of the formation of charge transfer complexes between π-acceptors immobilized polymer and heterocyclic nitrogen species present in gas oil. Furthermore, spectroscopic features of the charge transfer interactions between π-acceptors and basic and non-basic nitrogen species were confirmed by UV-vis spectrophotometer. ^{13}C NMR was used to calculate the decrease in aromatic content after treatment. The optimized polymers were successful in removing up to 14.4 wt.% of the total nitrogen content in a single contact using 25 wt% of the immobilized polymers with respect to LGO while only 1.4 wt.% of the total sulfur moieties were removed at 25°C.

3.2 Introduction

For the production of ultra-low sulfur fuel and to meet the stringent environmental regulations, the improvement of hydrotreating process by the removal of catalyst inhibitors, like nitrogen-containing compounds (N-compounds) is worth considering. N-compounds deactivate the catalysts used in the downstream secondary processing (such as fluid catalytic cracking and hydrocracking) of petroleum feedstock at a much faster rate than expected because of poisoning and inhibition by these nitrogen bearing species [69]. Moreover, nitrogen heterocycles affect the quality of the final product by the formation of insoluble sediments and gums [70]. Removal of

nitrogen compounds from heavy oil will restrain their irreversible adsorption onto the acidic sites of hydrotreating catalyst, thus improving sulfur elimination. These N-compounds are present predominantly in heterocyclic aromatic rings which can be classified into basic (e.g. pyridine, quinoline, etc.) and non-basic (e.g. indole, carbazole, etc.) nitrogen species. Synthetic crude oil derived from Athabasca bitumen contains alkyl-substituted carbazoles as major type of non-basic nitrogen compounds. Also, aliphatic amine and nitriles are the non-heterocyclic organo-nitrogen compounds present but in noticeably small amount and have the capability to denitrogenate quickly as compared to heterocyclic compounds [71]. Therefore, in order to achieve high levels of desulfurization and to reduce both deactivation and permanent poisoning of active sites of catalysts, it is necessary to eliminate nitrogen compounds, particularly carbazoles and indoles, which are less reactive in hydrotreating process.

Removal of refractory sulfur and nitrogen compounds by non-catalytic processes is emerging as a new trend in hydrotreating of heavy oils because it reduces the hydrogen consumption and can be achieved at less severe operating conditions. Functionalized polymers have shown promising results in the removal of nitrogen and sulfur-containing compounds [5][66][30][61]. A polymer based on poly (glycidyl methacrylate) that is functionalized with, 2,4,5,7-teranitro-9-fluorenone, has demonstrated high selectivity towards non-basic nitrogen species present in HGO extracted from the Athabasca oil sands without showing any significant effect on the basic nitrogen or sulfur species [67]. Although the removal of 6.7% nitrogen compounds was observed during pre-treatment of HGO with polymer, higher hydrodesulfurization (HDS) and hydrodenitrogenation (HDN) activities were reported during the hydrotreatment of HGO using a trickle bed reactor. The treated HGO has HDS of 96.7% and HDN of 70.1%; while untreated HGO has HDS of 90.5% and HDN of 60.5% [72]. In this regard, research interests in charge transfer complexes (CTCs) for the selective removal of heterocyclic nitrogen compounds from bitumen derived gas oils have increased and this work focuses on the effect of different π-acceptor moieties immobilized on the poly (GMA-co-EGDMA) henceforth referred to as PGMA (which is a reactive polymer due to the presence of epoxy functional group in its structural unit) via hydroxylamine linker for the removal of nitrogen species from bitumen-derived gas oil; in order to produce highly denitrogenated feed for hydrotreating applications.

3.3 Experimental details and methodology

3.3.1 Materials

The functional monomer, glycidyl methacrylate; the crosslinker, ethylene glycol dimethacrylate; poly[N-vinyl-2- pyrrolidone] (Mw~55,000 g/mol), 1-dodecanol (≥98.0%), cyclohexanol (99.0%), N,N-dimethylformamide (anhydrous 99.8%), acetone oxime (≥98.0%), potassium carbonate (≥99.0%), 9-fluorenone (98%), fuming nitric acid (90%) and p-toluene sulfonic acid monohydrate (≥98.5%) were purchased from Sigma Aldrich. Concentrated sulfuric acid (95-98%) was purchased from Fischer Scientific. The radical initiator Azobisisobutyronitrile was purchased from Molekula Ltd., and distilled water was used for making the aqueous phase. Dimethyl sulfoxide spectrophotometric grade (>99.9%) was purchased from VWR, deutrated chloroform (D, 99.8%) was purchased from Cambridge Isotope Laboratories, Inc. and potassium bromide (99+ %) for spectroscopy, IR grade was purchased from Acros Organics. Bitumen-derived light gas oil used throughout this study was provided by Syncrude Canada Ltd. All the chemicals were used as received.

3.3.2 Synthesis of π-acceptor immobilized polymers

Synthesis of 2,7-dinitro-9-fluorenone (DNF)

2,7-dinitroflourenone was synthesized by the method of nitration of fluorene described by Morgan and Thomason [73] with slight modifications as shown in Figure 3.1. 150.0 mL of fuming HNO_3 (90%) was added to 30.0 g of 9-fluorenone in a 250.0 mL three-necked flask, fitted with a dropping funnel and two condensers. The solution was placed in an oil bath at 100 ^{o}C and was refluxed for 3 h. Reddish brown solution formed was cooled at ambient temperature and DNF was obtained as yellow crystals which was subsequently filtered, washed with water and dried at 90 °C for 24 h. It was recrystallized with glacial acetic acid to obtain the purified sample. *Elemental Analysis*, Anal. Calcd. For $C_{13}H_6N_2O_5$: C(57.78), H(2.22), N(10.37), O(29.63); Found: C(58.20), H(1.98), N(10.62), O(29.21).

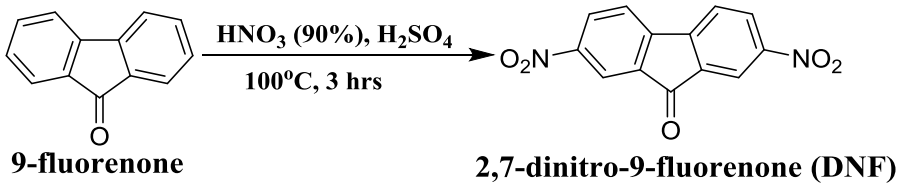

Figure 3.1: Reaction scheme for the synthesis of 2,7-dinitro-9-flourenone.

Synthesis of 2,4,7-trinitro-9-fluorenone (TriNF)

As shown in Figure 3.2, a method reported by Orchin and Woolfolk, [74] was used for the synthesis of 2,4,7-trinitroflourenone with modifications. One litre three-necked flask, fitted with a dropping funnel and two condensers, was charged with 55.0 mL of conc. H_2SO_4 and 120.0 mL of conc. HNO_3 (70%). The solution was placed on a preheated oil bath at 100 °C. To this refluxing mixture, a solution of 5.15 g of 9-fluorenone in 60.0 mL of conc. H_2SO_4 was added from the dropping funnel over a period of 1 h. Thereafter, a nine hour addition of a solution comprising of HNO_3 (88.0 mL) and H_2SO_4 (80.0 mL) was followed. After cooling the reaction for 10 h, it was slowly added to 4.0 L beaker filled with ice. This addition resulted in the precipitation of a yellow solid, which was filtered through a frit and washed with distilled water until all the acid was washed. The yellow crystals were dried at 100 °C for 24 h to obtain TriNF. *Elemental Analysis*, Anal. Calcd. For $C_{13}H_5N_3O_7$: C(49.59), H(1.68), N(13.38), O(35.59); Found: C(49.80), H(1.43), N(13.81), O(34.96).

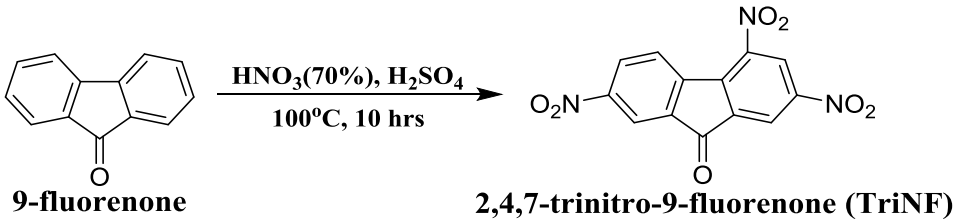

Figure 3.1: Reaction scheme for the synthesis of 2,4,7-trinitro-9-flourenone.

Synthesis of 2,4,5,7-tetranitro-9-fluorenone (TENF)

The synthesis of 2,4,5,7-tetranitroflourenone is shown in Figure 3.3 and follows the method used by Newman and Lutz [75]. A 2.0 L three-necked flask, fitted with a dropping funnel and two condensers, was charged with 115.0 mL of conc. H_2SO_4 and 195.0 mL of fuming HNO_3 (90%).

The solution was placed on a preheated oil bath at 110 °C. To this refluxing mixture, a solution of 10.9 g of 9-fluorenone in 126.0 mL of conc. H_2SO_4 was added from the dropping funnel over a period of 1 h. Thereafter, a 9 h addition of a solution comprising of HNO_3 (142.5 mL) and H_2SO_4 (168.0 mL) followed. After cooling the reaction for 10 h, it was slowly added to 4.0 L beaker filled with ice. This addition resulted in the precipitation of a yellowish solid, which was filtered through a frit and washed with distilled water until all the acid was washed off. The obtained yellow powder was dried at 100 ^oC overnight to obtain TENF. *Elemental Analysis*, Anal. Calcd. For $C_{13}H_4N_4O_9$: C(43.35), H(1.12), N(15.55), O(39.98); Found: C(43.40), H(1.20), N(16.03), O(39.96).

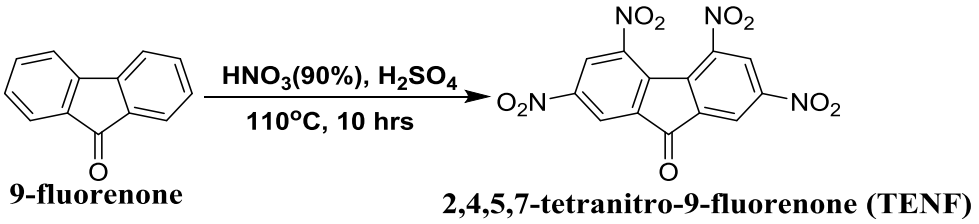

Figure 3.2: Reaction scheme for the synthesis of 2,4,5,7-tetranitro-9-flourenone.

Synthesis of copolymer of GMA and EGDMA (PGMA)

PGMA beads were synthesized by radical suspension polymerization of glycidyl methacrylate (GMA) and ethylene glycol dimethacrylate (EGDMA) using azobisisobutyronitrile as radical initiator according to the method described by Rizwan et al., [67]. Epoxy content of the synthesized polymer was determined using a hydrochlorination method, which is based on the addition of hydrogen chloride to the epoxy group, producing a chlorohydrin. It was found to be about 4.5 wt.% per gram of polymer.

Procedure for attaching hydroxylamine linker on PGMA (PGMA-ON)

In a 1.0 L three-necked flask fitted with a condenser, a mixture of acetone oxime (12.6 g) and N,N-dimethyl formamide, DMF (110.0 mL) was charged. The mixture was heated at 100 °C and potassium carbonate, K_2CO_3 (26.2 g) was added. 20.5 g of PGMA beads were added and the mixture was stirred at 400 RPM for 24 h. Upon completion of the reaction, the beads were filtered through a frit and washed with distilled water and ethanol. The obtained beads were dried at 90 °C

for 24 h to get yellow powder of oxime substituted PGMA, hereafter referred to as 'PGMA-ON'. Synthesis follows reaction scheme shown in Figure 3.4 [67].

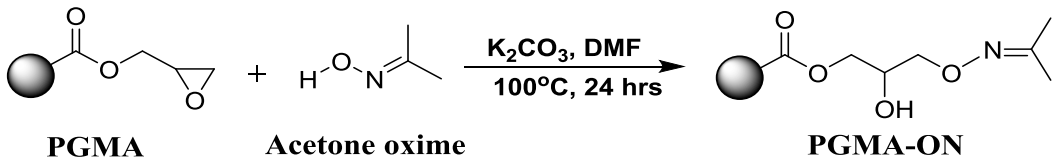

Figure 3.4: Reaction scheme for the substitution of epoxy ring with acetone oxime.

General procedure for immobilizing π-acceptors on PGMA

The last stage of the synthesis involved immobilization of π-acceptors, DNF, TriNF and TENF on PGMA via hydroxylamine linker; hereafter referred to as 'PGMA-ON-DNF, PGMA-ON-TriNF and PGMA-ON-TENF' respectively. 15.9 g of π-acceptors (DNF, TriNF, or TENF) were mixed with 270 mL of acetic acid at 100 °C in a three-neck flask with condenser. 14.7 g of p-toluene sulfonic acid monohydrate was dissolved in the mixture. Afterwards, 58.7 g of PGMA-ON beads were added. The mixture was allowed to reflux for 3 days. The product obtained was filtered through frit and washed with toluene and then dried at 90 °C for 24 h. The reaction for synthesis of PGMA-ON-TENF is shown in Figure 3.5. Similarly, all π-acceptor immobilized polymers were obtained.

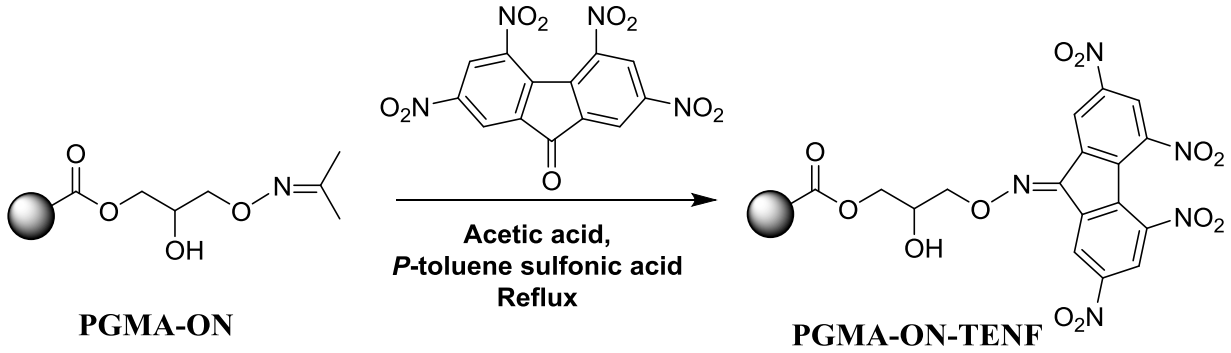

Figure 3.5: Reaction scheme for the immobilization of TENF on PGMA.

3.3.3 Characterization techniques

The Brunauer–Emmett–Teller (BET) surface area, pore diameter and pore volume of the polymer samples were determined by analyzing the adsorption and desorption of N_2 at 77 K with a Micromeritics 2000 ASAP analyzer. Samples were degassed in vacuum at 150 °C and textural properties were calculated from desorption isotherms using the multipoint BET method. The pore diameter, pore volume, and pore size distribution were computed using the Barrett-Joyner-Halenda (BJH) method. Scanning electron microscopy images for the PGMA and π-acceptor functionalized PGMA samples were taken by dissolving a small amount of each sample in millipore water and sonicated for 20 min. A few drops of the mixture were transferred to the aluminium slab and allowed to dry. The slab was then sputter-coated with gold to improve secondary electron signals and to reduce charging. The analysis was performed with JEOL 6010LV SEM.

Thermo gravimetry/differential thermal analyzer (TG/DTA) was used to determine thermal stability of the synthesized beads using a TA instrument, Q-5000 model. 10-15 mg of sample was heated to 500 °C and mass loss of polymer was recorded at 20 s intervals at a heating rate of 10 °C/min under nitrogen atmosphere(40 and 60 mL/min). Carbon, hydrogen, nitrogen and oxygen content for all stages of polymer synthesis was determined using Vario EL III CHNOS elemental analyzer, in triplicate, after heating the samples at 100°C for 24 h. 6-8 mg of polymer samples were combusted for the analysis. Amount of oxygen was calculated by difference. Fourier transform infrared (FT-IR) spectra were obtained using a PerkinElmer Spectrum GX instrument to determine the characteristic functional groups present during different stages of the polymer synthesis. The spectra were recorded in the range of 400−4000 cm^{-1}. The spectrum for each analysis was averaged over 16 scans. The spectra of the samples were obtained by using KBr pellet technique. For making the pellets, 1 g of sample was mixed thoroughly in 4 g of KBr. UV-vis spectra were recorded on Shimadzu UV mini 1240 spectrophotometer. Known quantities of samples were dissolved in dimethyl sulfoxide to prepare 0.025 M solutions of π-acceptors and 0.075 M solutions of N-compounds. Quartz cuvette were used for the analysis inside spectrophotometer.

The total sulfur and nitrogen content of the gas oil was measured by Antek-Model 9000 Nitrogen/Sulfur analyzer using pyro-fluorescence technique following ASTM D5453 method and

pyro-chemiluminescence technique following ASTM D4629 method respectively. Liquid ^{13}Carbon Nuclear Magnetic Resonance (^{13}C NMR) spectra were recorded for gas oil samples. A 500 MHz Bruker Advance NMR Spectrometer was used to determine the aromatic content of the light gas oil before and after the removal of nitrogen species. Inverse gated decoupling with 2000 scans and pulse delay of 4 s were set as the operating parameters. All samples were dissolved in deutrated chloroform ($CDCl_3$) in 1:1 ratio. The treated and untreated oil samples were analyzed with Varian model CP-3800 Simulated Distillation using ASTM D2887 method. Simulated distillation version 5.5 software was used for data collection and processing. Additional details on the characterization techniques are mentioned in the previous work from our group [28][69][67][76].

3.4 Results and discussion

3.4.1 Characterization of π-acceptor immobilized polymers

To confirm the synthesis of PGMA, substitution of epoxy ring with acetone oxime and immobilization of π-acceptors on PGMA, FT-IR spectra were recorded and shown in Figure 3.6. The characteristic peaks in the range of 1250-1265 cm^{-1} and 810-950 cm^{-1} represent symmetrical and asymmetrical stretching of the epoxy ring and peak at 1735 cm^{-1} is due to carbonyl carbon (C=O); which confirms the presence of epoxy ring on the synthesized PGMA. Upon the ring opening in the second stage, characteristic peaks in the range of 1650 cm^{-1} confirm the successful substitution of acetone oxime functionality [67]. Also, a broad hydroxyl (–OH) band near 3500 cm^{-1} represents the ring opening reaction in epoxy group [77]. Moreover, the π-acceptors, DNF, TriNF and TENF contain two, three and four nitro groups on fluorenone meoity. Immobilization of these electron acceptors on PGMA was confirmed by the appearance of the additional peaks due to symmetrical and asymmetrical stretching vibrations of nitro group (O=N–O) at 1367 cm^{-1} and 1540 cm^{-1} [78]. All IR peaks were in consensus agreement with the expected results, which clearly signify that the desired polymers were synthesized.

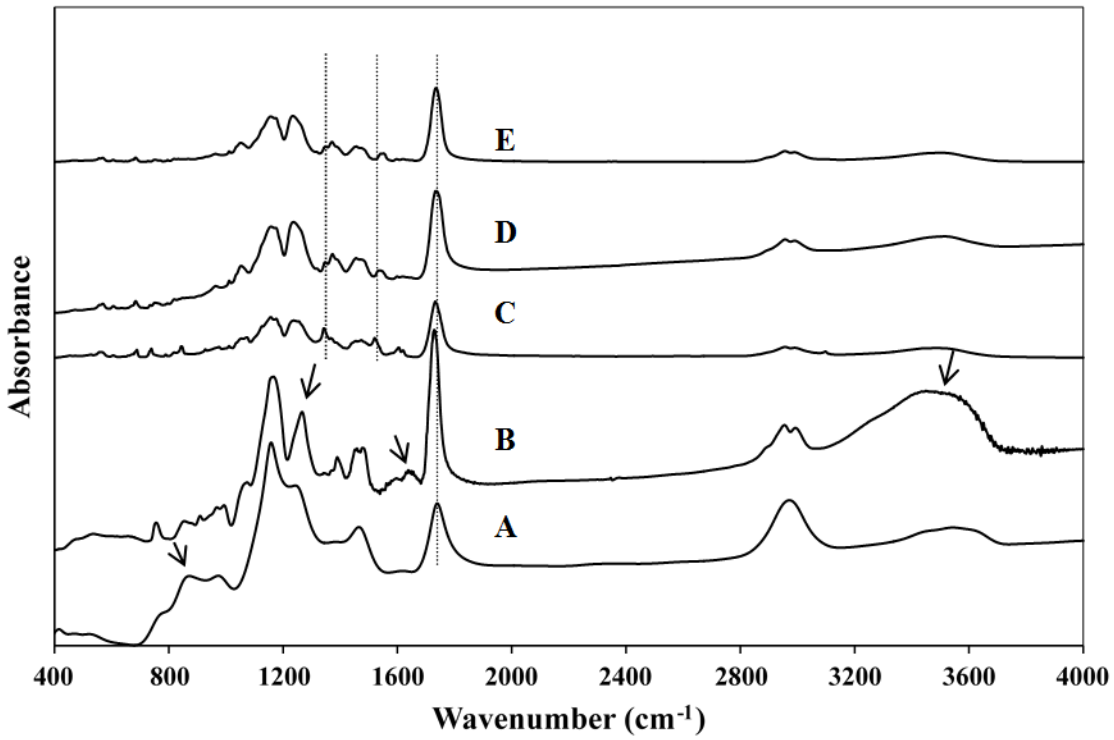

Figure 3.6: FT-IR spectra of (A) PGMA, (B) PGMA-ON, (C) PGMA-ON-DNF, (D) PGMA-ON-TriNF, and (E) PGMA-ON-TENF.

Scanning Electron Microscope was used to determine the surface morphology of the synthesized polymers. The cross-section of the beads was observed to analyze the quality and shape of PGMA with and without immobilization of π-acceptors. All micrographs were taken under the same magnification (X 15,000) as shown in Figure 3.7. The PGMA beads formed were uniform and spherical in shape with size ranging from 0.2 to 0.3 μm. The size of the synthesized beads was optimum for the nitrogen adsorption studies because high diffusional constraints are observed in beads with larger particle diameter which hinders the transportation of reactants and products; thus making them unsuitable for this study [79]. The addition of π-acceptors in the reaction system leads to the formation of pores with smaller particle diameter. Moreover, spherical PGMA beads were distorted after the immobilization of DNF, TriNF, and TENF on PGMA via hydroxylamine linker. This observation was affirmed by the results obtained from the analysis of textural properties.

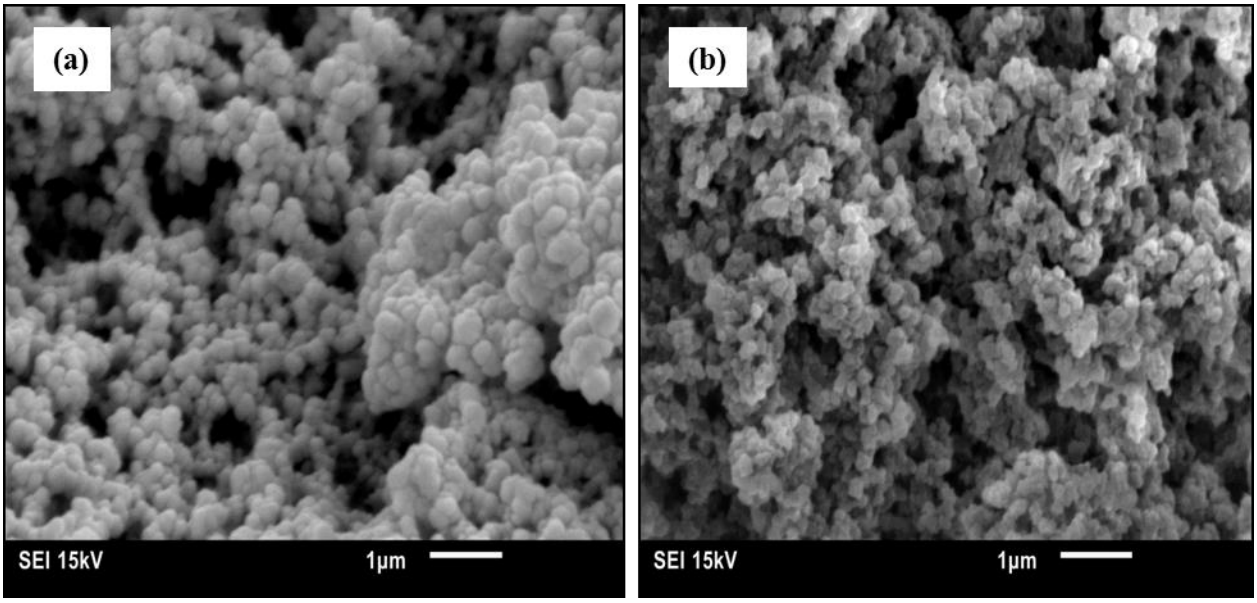

Figure 3.7: SEM images of (a) PGMA and, (b) π-acceptor immobilized polymers.

Effects of immobilization of π-acceptors on surface area, pore size, and pore volume of PGMA beads were determined by BET surface area and BJH pore size distribution methods. As shown in Figure 3.8, N_2 adsorption-desorption isotherms for PGMA and DNF, TriNF, TENF immobilized PGMA are of type IV with weakly pronounced hysteresis loop which is in agreement with the pore size values obtained by BJH method. Isotherms obtained for different polymers are identical which clearly indicates that the structure of hydrophilic polymer support, PGMA remained intact even after the immobilization of π-acceptors. On comparing the textural properties (as shown in Table 3.1) of PGMA beads with and without hydroxylamine linker, 15% decrease in the surface area was observed with only a slight decrease in the pore size and pore volume due to the substitution of epoxy ring with acetone oxime functionality. Marginal increase in surface area based on the amount of nitro groups present in fluorenone based π-acceptors was observed when DNF, TriNF and TENF were immobilized on PGMA beads via hydroxylamine linker. The surface area increased from 55 m^2/g to 63 m^2/g, 62 m^2/g and, 57 m^2/g for PGMA-ON-DNF, PGMA-ON-TriNF, and PGMA-ON-TENF, respectively. Electron acceptor DNF has least (two) nitro groups on fluorenone meoity and has the highest surface area and pore volume while TENF with four nitro groups has the lowest surface area and pore volume amongst all immobilized polymers. As calculated by BJH method, the pore size for all polymer samples varies from 18-24 nm. High

surface area and larger pore sizes are key factors in determining the efficiency of the synthesized polymers to adsorb nitrogen compounds present in gas oil.

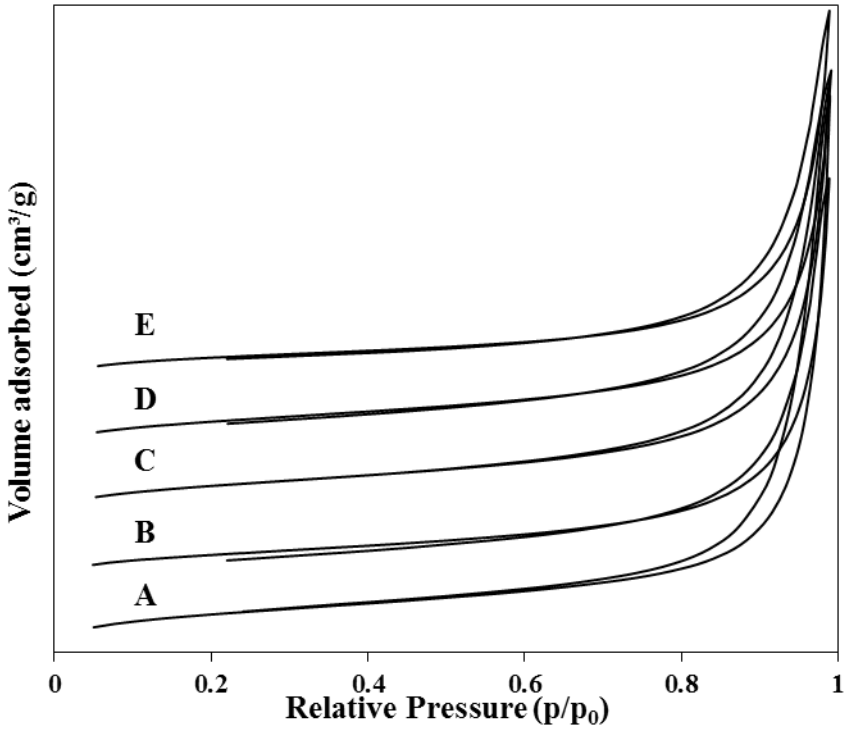

Figure 3.8: Adsorption-desorption isotherms of (A) PGMA, (B) PGMA-ON, (C) PGMA-ON-DNF, (D) PGMA-ON-TriNF, and (E) PGMA-ON-TENF polymers.

Table 3.1: Textural properties of PGMA and π-acceptor immobilized PGMA beads.

Sample	**Surface area (m^2/g)**	**Average pore size (nm)**	**Pore volume (cm^3/g)**
PGMA	65 ± 2	24	0.40
PGMA-ON	55 ± 1	20	0.29
PGMA-ON-DNF	63 ± 1	20	0.32
PGMA-ON-TriNF	62 ± 2	18	0.28
PGMA-ON-TENF	57 ± 1	23	0.27

Elemental analysis was performed to know the elemental composition of the polymers and to ascertain the immobilization of π-acceptors. All samples were analyzed for their C, H, N, O, and S content. In order to prepare DNF, TriNF and TENF immobilized polymers, the same batch of PGMA was used. Noteworthy increase in elemental nitrogen and decrease in elemental carbon of PGMA-ON signifies the substitution of epoxy ring with acetone oxime functionality. As shown in Table 3.2, subsequent immobilization of π-acceptors steered an increase in elemental nitrogen to 3% for PGMA-ON-DNF, 1.4% for PGMA-ON-TriNF, and 1.6% for PGMA-ON-TENF due to the presence of nitro groups on fluorenone moiety. However, this increase was highest for DNF which can be explained as follows: higher amount of DNF moieties were immobilized on PGMA as compared to their other counterparts. The reduction in carbon content from 59% to about 56% was consistent for all successive stages of synthesis. It implies that the structure of PGMA modified with hydroxylamine (–ON) linker remained intact even after the immobilization of electron acceptors. All these observations reveal the successful synthesis of different π-acceptor immobilized polymers.

Table 3.2: Elemental analysis of polymers at various stages.

Sample	Nitrogen (%)	Carbon (%)	Oxygen* (%)	Hydrogen (%)
PGMA	0.1	59.7	32.2	8.1
PGMA-ON	1.1	56.9	33.4	8.5
PGMA-ON-DNF	3.0	56.8	33.3	6.8
PGMA-ON-TriNF	1.4	56.9	34.6	7.8
PGMA-ON-TENF	1.6	55.7	34.9	7.8

*Oxygen content was calculated by difference

Figure 3.9 shows the TGA thermograms of PGMA and all the π-acceptor immobilized polymers which are thermally stable up to 230 °C and then mass loss begins for all the samples as the temperature increases. An abrupt weight loss for PGMA beads was observed at 310 °C [77].

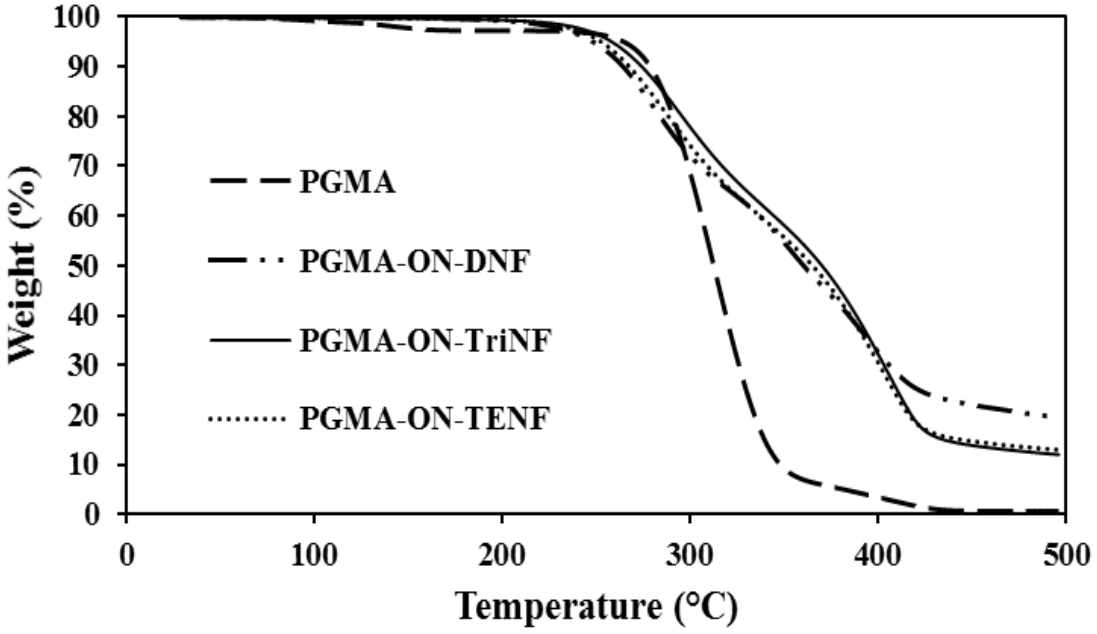

Figure 3.9: TGA thermograms of PGMA and π-acceptor immobilized polymers.

The thermal degradation of pure PGMA proceeds by a one-step process, which is reflected as one distinct peak in the DTG curve (Figure 3.10). Thermal degradation temperatures of PGMA showed that the degradation was due to polymer surface decomposition and random chain scission [80]. On the other hand, DNF immobilized PGMA degrade in three steps and reaches to a maximum at 270 °C. Moreover, TriNF and TENF immobilized PGMA degrade in two steps, which is evidenced by the appearance of distinct peaks in DTG thermograms in Figure 3.10. Stepwise degradation of DNF, TriNF and TENF immobilized polymers indicate that every π-acceptor immobilized on PGMA had different thermal stabilities giving rise to the separate derivative peaks. Sequence of chemical modifications is clearly evidenced in the thermograms. Immobilization of the π-acceptors makes the polymer more susceptible to thermal degradation. However, up to the processing temperatures of 200 °C, the π-acceptor immobilized beads can still be safely used. Since these beads are used for the removal of refractory nitrogen species present in bitumen derived gas oil, which sometimes require relatively higher temperatures, the synthesized immobilized polymers are of great practical importance.

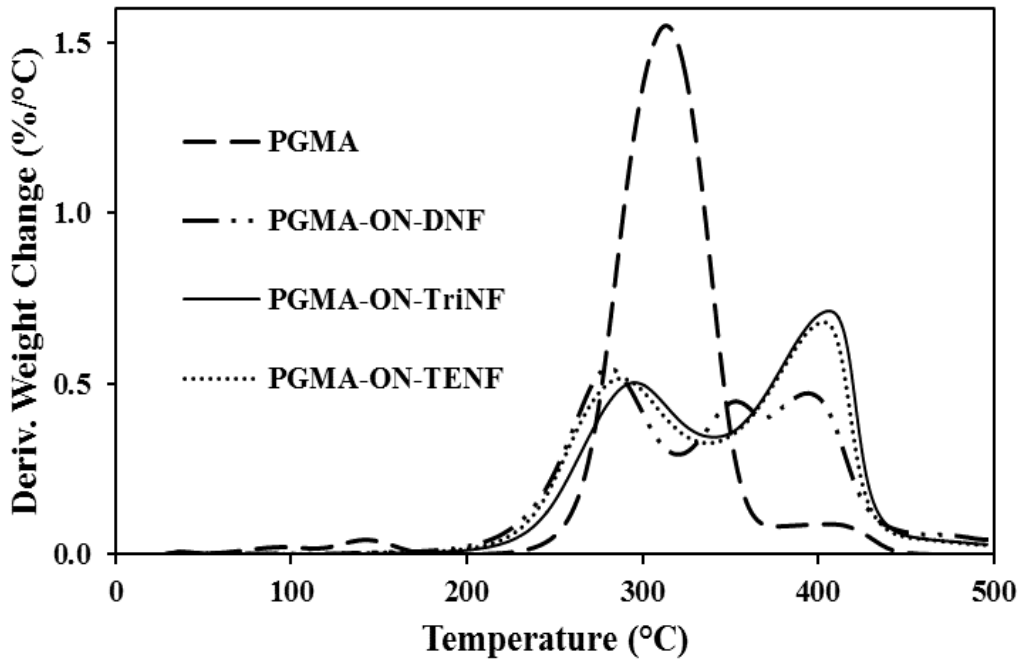

Figure 3.10: DTG thermograms of PGMA and π-acceptor immobilized polymers.

3.4.2 Studies on adsorption of sulfur and nitrogen compounds

3.4.2.1 Evaluation of charge transfer complexes

Acridine, pyridine, quinoline and alkyl-substituted carbazoles are the major types of nitrogen heterocyclic compounds present in Athabasca derived gas oil [28][71]. Hence, 9-ethyl carbazole (9EC) and acridine are the two representative heterocyclic nitrogen compounds present in bitumen derived gas oil which were studied for evaluating the charge transfer phenomena. Efforts were made to understand the selectivity of the synthesized polymers towards the donor molecules. The charge transfer complexes formed between heterocyclic nitrogen compounds and fluorenone-derived π-acceptors were easily identifiable by the color change upon mixing. Separate solutions of known concentrations (0.025 M) of the three π-acceptors (DNF, TriNF and TENF) and electron donors, 9-ethyl carbazole and acridine, were prepared in dimethyl sulfoxide (DMSO). No significant color change was observed when solutions of π-electron donors and acceptors were mixed in 1:1 ratio by taking 2 mL of each solution. To enhance the charge transfer phenomena, the concentration of electron donors was increased to 0.075 M. Again the donor and acceptor solutions were mixed in 1:1 ratio to a total volume of 4 mL. Spontaneous color changes were

observed. Figure 3.11 shows the change in energy and color when charge-transfer complexes (CTC) are formed. 9EC was a transparent solution in DMSO while the π-acceptors DNF, TriNF and TENF formed colors ranging from light yellow to orange in DMSO. The color of the complexes formed became darker from deep orange to blackish as the electron-deficiency of the fluorenone derivatives increases. However, acridine was light yellowish in DMSO and formed nearly the same colored complexes as 9EC when dissolved in the π-acceptors.

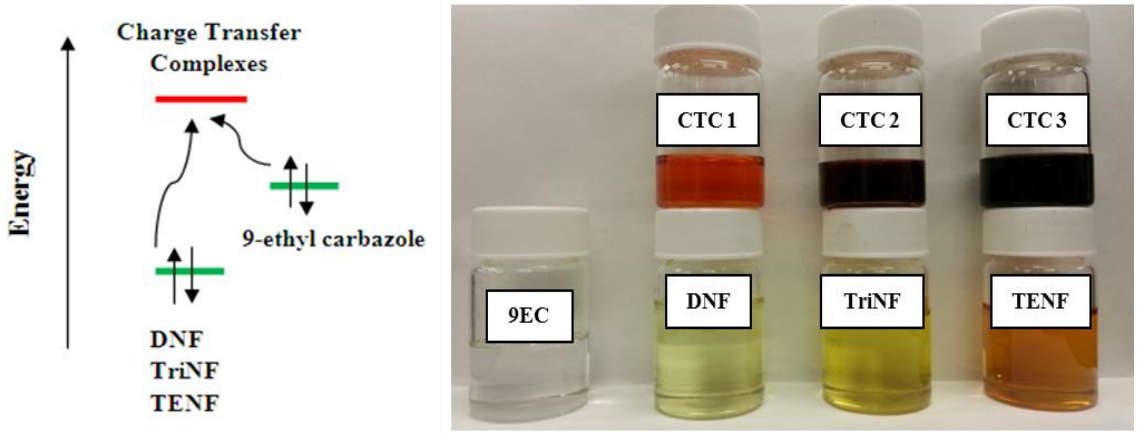

Figure 3.11: (a) Energy schematic of electron donor-acceptor interaction in charge transfer complex formation phenomena, and (b) the color change observed by mixing electron donor with π-acceptors in DMSO solvent in 1:1 ratio at 25°C (CTC-1, 2, 3 are charge transfer complexes between 9EC and DNF, TriNF, and TENF respectively).

In an effort to verify the formation of charge transfer complexes, a series of UV-vis spectra were obtained. A new absorption band is detected when intermolecular charge transfer complexes are formed due to electron transfer between the donor and acceptor molecules. All donor and acceptor moieties do not show a significant absorption band in the visible region, but the charge transfer complexes show a broad spectrum in the visible region ranging from 450 nm to 750 nm [81]. As shown in Figure 3.12, the absorption spectrum of 9EC in DMSO has the maximum absorption (λ_{max}) around 360 nm which is in agreement with the absorption range for carbazole derivatives [82]. Electron acceptors, DNF, TriNF and TENF do not show any absorption bands after 450 nm, which is consistent with the absorption bands for TriNF as shown by Hu et al. [83]. As shown in Figure 3.12 (a), the charge transfer complex between 9EC and DNF showed an absorption band

around 550 nm. Similarly, a broad absorption band from 490 nm to 650 nm was apparent when a charge transfer complex was formed between 9EC and TriNF as shown in Figure 3.12 (b). TENF is one among the strongest known π-acceptors [66] and the absorption band was very prominent as observed in Figure 3.12 (c), which lies in the visible region centered about 620 nm when charge transfer complex was formed between 9EC and TENF.

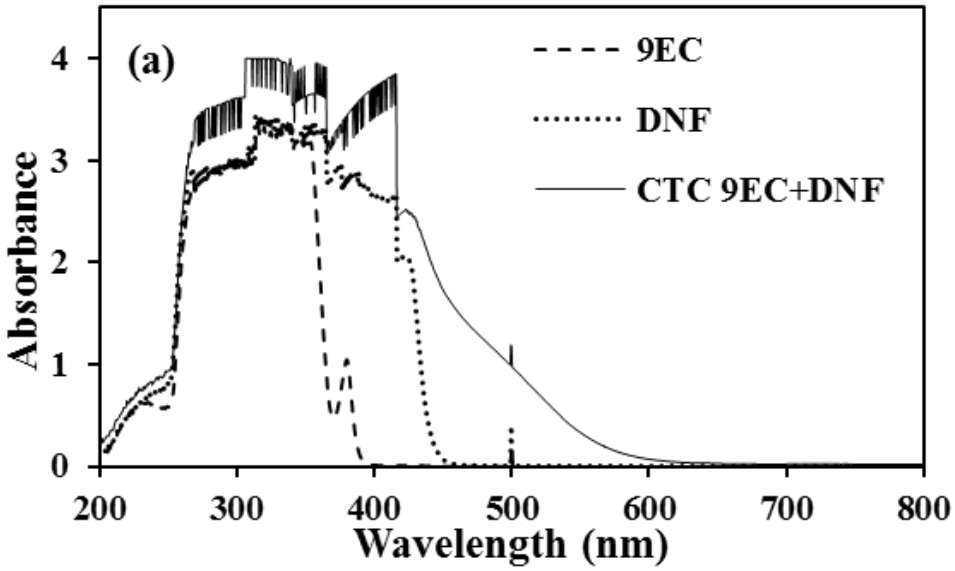

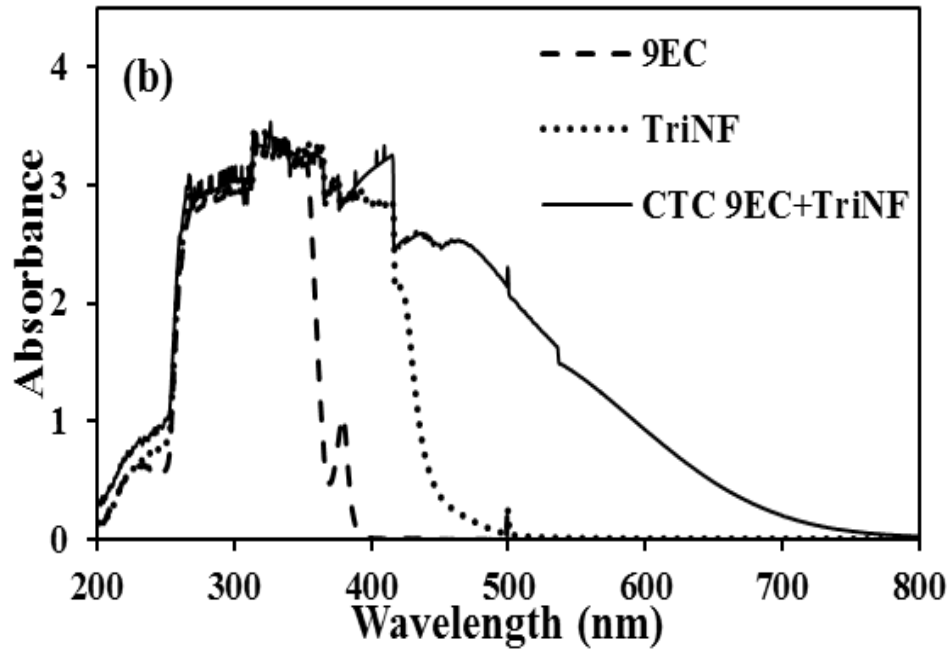

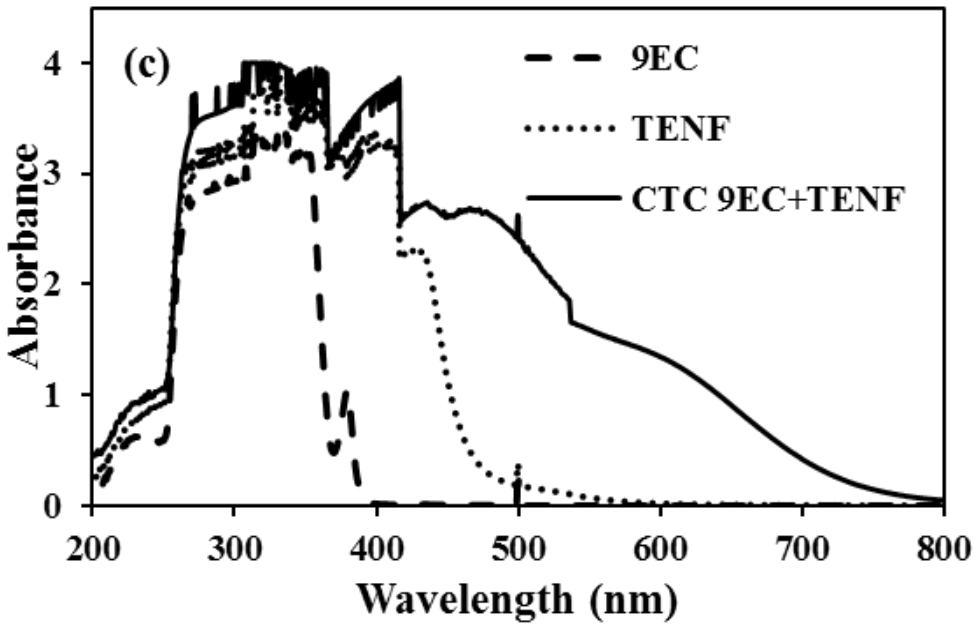

Figure 3.12: UV-vis absorption spectra of CTC between donor 9-ethyl carbazole and the acceptors: (a) 9EC-DNF, (b) 9EC-TriNF, and (c) 9EC-TENF in DMSO for 1:1 molar mixture.

The charge transfer complexes were observed at lower absorption wavelength for acridine and the electron acceptors. Maximum absorption bands for acridine are around 250 nm and 420 nm. The complex formed by mixing acridine and DNF in 1:1 molar ratio has broad absorption band in the visible region around 480 nm as observed in Figure 3.13 (a). Figure 3.13 (b) and (c) show similar absorption bands for acridine-TriNF and acridine-TENF complexes at around 490 nm and 550 nm respectively. As observed in the above analysis, intermolecular charge interaction exhibits different absorption bands in the visible region, implying the complex formation between heterocyclic N-compounds and the π-acceptors.

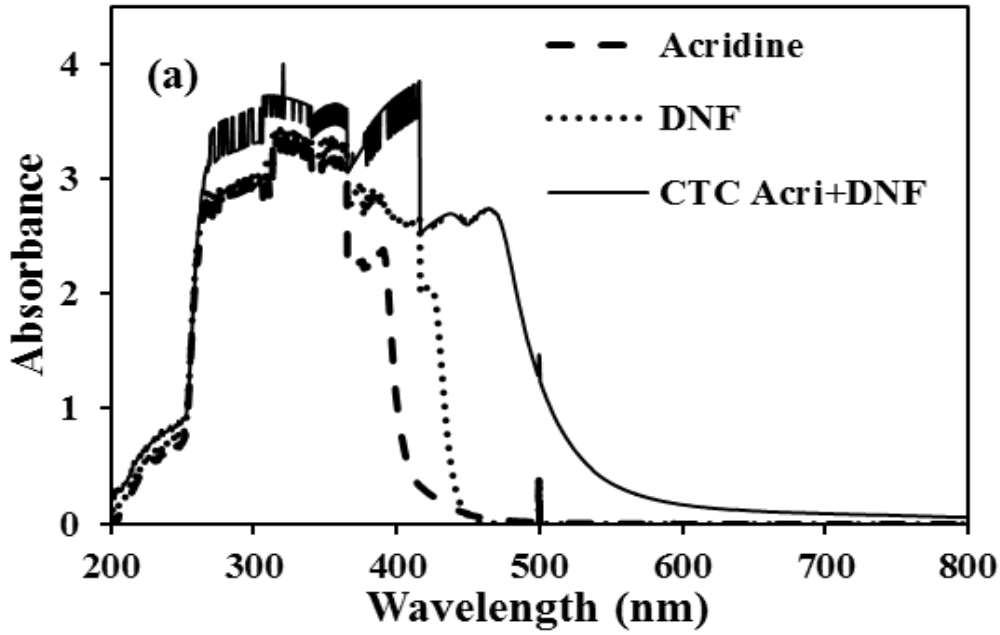
(a)
Acridine
DNF
CTC Acri+DNF
Absorbance
Wavelength (nm)
0
1
2
3
4
200
300
400
500
600
700
800

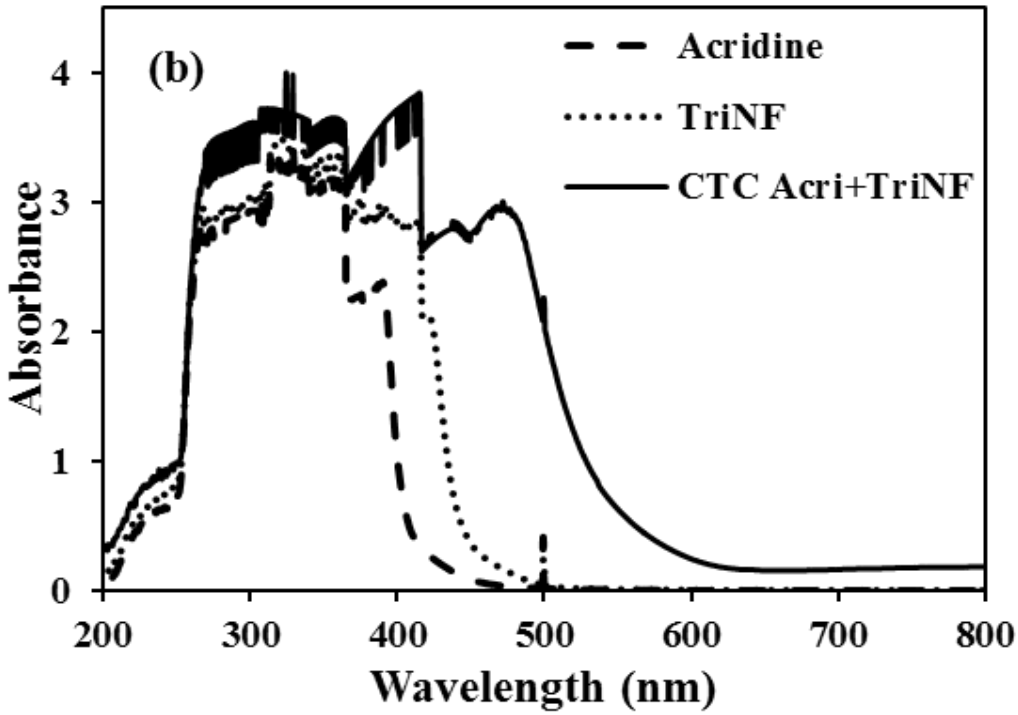
(b)
Acridine
TriNF
CTC Acri+TriNF
Absorbance
Wavelength (nm)
0
1
2
3
4
200
300
400
500
600
700
800

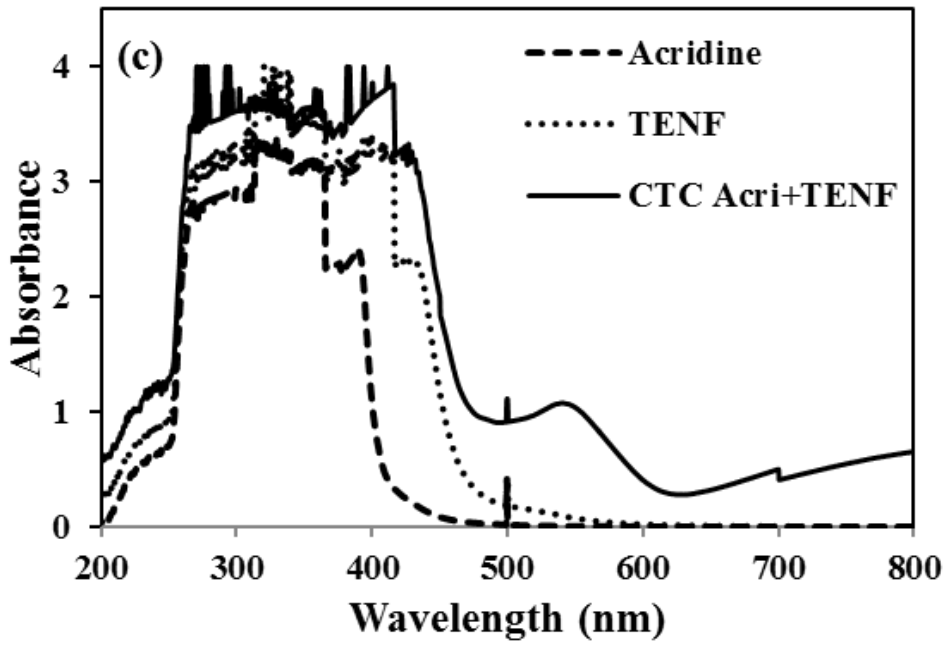

Figure 3.13: UV-vis absorption spectra of CTC between donor Acridine and the acceptors: (a) Acridine-DNF, (b) Acridine-TriNF, and (c) Acridine-TENF in DMSO for 1:1 molar mixture.

3.4.2.2 Denitrogenation of bitumen derived light gas oil

Selectivity of synthesized polymers towards heterocyclic sulfur and nitrogen compounds present in gas oil was evaluated; the performance tests for DNF, TriNF and TENF immobilized PGMA were conducted in a batch reactor using bitumen derived light gas oil. The sulfur and nitrogen removal efficiencies of the polymers were tested at the following conditions: Temperature = ambient [22°C], Pressure = atmospheric, Mechanical stirring = 400 RPM, Polymer : LGO ratio = 1:4 and Time = 24 hour. Percent nitrogen and sulfur removal is an indicator to determine whether changing the π-acceptors has an influence on the selectivity towards nitrogen compounds and their subsequent removal from LGO.

Total nitrogen and sulfur removal was calculated as follows:

$$\text{N/S removal (\%)} = \frac{\text{N/S in untreated LGO (ppm)} - \text{N/S in treated LGO (ppm)}}{\text{N/S in untreated LGO (ppm)}} \qquad (3.1)$$

As shown in Figure 3.14, all functionalized polymers were capable of removing the nitrogen species present in light gas oil accompanied with the removal of small amount of sulfur species. DNF immobilized polymer has the lowest nitogen removal efficiency with only 9.4 wt.% decrease in total nitrogen. Inferior performance of PGMA-ON-DNF is due to the presence of lesser number of electron withdrawing nitro groups on the fluorenone moeity in DNF. However, PGMA-ON-TriNF and PGMA-ON-TENF removed 14.4 wt.% and 11.2 wt.% of the total nitrogen content, respectively.

It was observed that PGMA-ON-TriNF has the highest percentage nitrogen removal despite of the presence of only 3 nitro groups as compared to PGMA-ON-TENF which has 4 nitro groups attached to fluorenone moeity. This can be explained by the profound analysis of TENF structure by Sevignon et al. [65], which revealed that the oxygen atoms of the two nitro groups attached at 4- and 5- positions are too close to each other in planer conformation. Due to this steric repulsion, these two nitro groups rotate to form an angle of 30^0 with the middle plane of the molecule resulting in the deviation from its planer structure and hinder the approach of the electron donors to form the CTC. On the other hand, the steric strain was strongly reduced in TriNF functionalized polymer which distinctly explains its prime performance amongst all π-acceptor immobilized polymers synthesized for this study. Simultaneously, a small amount (0.5-1.5 wt.%) of total sulfur compounds were removed by PGMA-ON-DNF, PGMA-ON-TriNF, and PGMA-ON-TENF which exhibits the selectivity of these polymers towards nitrogen species present in bitumen derived gas oil. In order to ensure the reliability on nitrogen and sulfur removal rates of polymers, the tests were conducted three times for each sample and the average was taken as the percentage removal of nitrogen and sulfur species. Moreover, blank tests were performed to confirm that removal is entirely due to the efficiency of synthesized π-acceptor immobilized PGMA beads.

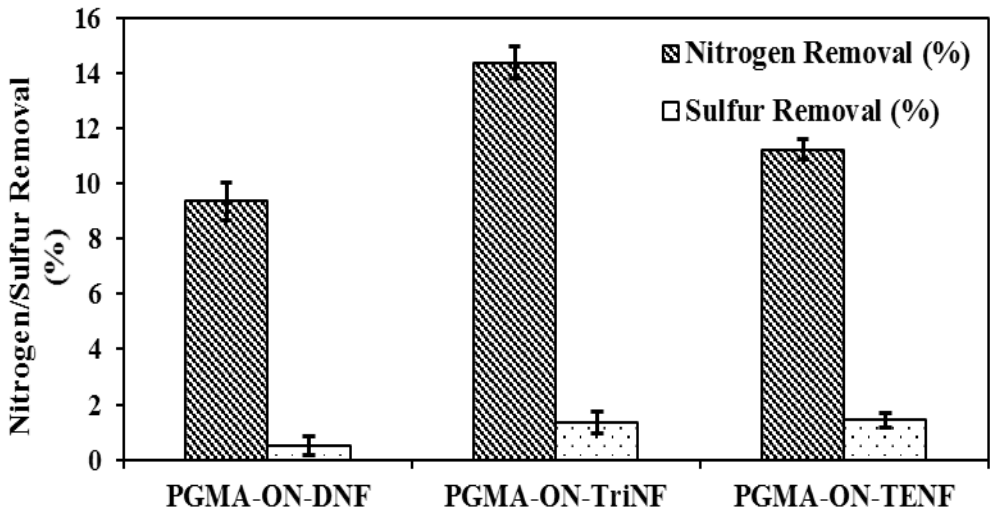

Figure 3.14: Percent nitrogen and sulfur removed during the first contact with light gas oil.

To further analyze the effect of pre-treatment of light gas oil by π-acceptor immobilized polymers, ^{13}C NMR was used to determine the change in the aromatic content of gas oil after the removal of nitrogen and sulfur species. Hydrodearomatization (HDA) is one of the important hydrotreatment processes which involve the hydrogenation of the aromatics, thus improving the gas oil feedstock quality. NMR was used to measure the carbon content in the aromatic environment present in the gas oil samples. The intensities over saturated hydrocarbon range (0-50 ppm) and aromatic hydrocarbon range (110-150 ppm) in ^{13}C NMR plot were integrated and the ratio of carbon in aromatic hydrocarbons to saturated hydrocarbons revealed the aromatic content of the gas oil [76]. A total of 30.2% aromatic content was found in the analysis of untreated LGO which remarkably decreased in all the treated LGO samples. The highest dearomatization activity was observed for PGMA-ON-TriNF which reduced the total aromatic content from 30.2% to 25.7%. Besides, total aromatic content of 27.9% and 27.2% was calculated for PGMA-ON-DNF and PGMA-ON-TENF, respectively. This decrease in the aromatic content is evidently due to the removal of heterocyclic nitrogen and sulfur species present in the gas oil. Conclusively, all PGMA samples immobilized with π-acceptors are capable of adsorbing the aromatics; the dearomatization activity follows the order PGMA-ON-TriNF > PGMA-ON-TENF > PGMA-ON-DNF.

3.4.2.3 Characterization of treated light gas oil

There are significant changes in the quality and physical properties of Athabasca derived LGO after treatment with TriNF immobilized polymer, such as reduction in sulfur and nitrogen content as measured by N/S analyzer. The average nitrogen content in heavy gas oil derived from oil sands is approximately 4000 ppm [28]. However, the light gas oil feed used for this study contains 1676 ppm of nitrogen content which was reduced to 1416 ppm after treatment with PGMA-ON-TriNF. Also, 1.8 wt.% reduction in total sulfur content was observed with an increase in the initial and final boiling point of the treated light gas oil (as shown in Table 3.3). The boiling point distribution as recorded by Simulated Distillation exhibits an increase in the initial and final boiling point of the polymer treated sample of gas oil. In addition, decrease in the aromatic content of LGO from 30.2% to 25.7% was observed upon treatment with PGMA-ON-TriNF.

Table 3.3: Characterization of bitumen derived light gas oil (LGO) and PGMA-ON-TriNF treated LGO.

Parameter	**LGO**	**PGMA-ON-TriNF treated LGO**
Sulfur content (ppm)	29257	28718
Nitrogen content (ppm)	1676	1416
Density (g/ml)	0.90	0.88
Aromatic content (%)	30.2	25.7
Simulated distillation:		
IBP (ºC)	159	167
FBP (ºC)	502	506

3.5 Conclusions

π-acceptors immobilized on porous polymer support are capable of removing heterocyclic nitrogen and sulfur compounds from bitumen derived gas oil which has high concentration of these impurities. In order to improve the denitrogenation of LGO, three different flourenone based π-

acceptors were successfully synthesized and tested for nitrogen removal. These π-acceptors form charge transfer complexes with heterocyclic nitrogen and sulfur species which was evident by the appearence of new bands in the visible region of absorption spectra as detected by UV-vis spectrophotometer. PGMA beads formed by the direct polymerization of monomers were used as support to prevent the leaching of π-acceptors in gas oil and feasibility of filteration after pre-treatment. The π-acceptors were immobilized on the PGMA beads in a three step procedure. FT-IR spectra of the final stage which deals with coupling of DNF, TriNF and TENF onto the oxime functionality showed the immobilization of organic compounds on PGMA. Among the three types of polymers with different electron acceptors, PGMA-ON-DNF has lowest efficiency towards nitrogen removal despite of the highest surface area (63 m^2/g) due to the presence of lesser number of electron withdrawing nitro groups in the structure. Specific surface area of 62 m^2/g and 57 m^2/g was recorded by BET method for PGMA-ON-TriNF and PGMA-ON-TENF, respectively. High surface area and absence of steric repulsion due to nitro groups in PGMA-ON-TriNF as compared to PGMA-ON-TENF can be attributed to the highest nitrogen removal efficiency. Hence, pre-treatment of LGO with TriNF immobilized PGMA has proved that it is capable of removing 14.4 wt.% of total nitrogen species in single contact with gas oil at room temperature.

Chapter 4: Synthesis and characterization of functionalized poly(glycidyl methacrylate) based particles for the selective removal of nitrogen compounds from bitumen derived gas oil: Effect of linker length

---

A similar version of this chapter has been published as a research article in Energy & Fuels:

- Chitanda, J. M., Misra, P., Abedi, A., Dalai, A. K. & Adjaye, J. D. "Synthesis and characterization of functionalized poly(glycidyl methacrylate)-based particles for the selective removal of nitrogen compounds from light gas oil: Effect of linker length". *Energy & Fuels* (2015) 29, 1881–1891.

Contribution of the Ph.D. candidate

Polymer synthesis, characterization and testing was done by Prachee Misra. Data analysis was done by Prachee Misra with assistance from Dr. Ali Abedi. Dr. Jackson Chitanda wrote the manuscript. Revision and rebuttal work was done by Prachee Misra based on the suggestions from Drs. Ajay Dalai, John Adjaye, and Jackson Chitanada.

Contribution of this chapter to the overall Ph.D. work

This part of work was focused on investigating the effects of increasing the linker length on the selective removal of nitrogen impurities from bitumen-derived gas oil.

4.1 Abstract

In this work, four poly (glycidyl methacrylate-co-ethylene glycol dimethacrylate) poly [GMA-co-EGDMA] functionalized particles were synthesized and characterized, and tested in gas-oil adsorption. Particles consisted of identical polymer support poly(GMA-co-EGDMA), henceforth referred to as PGMA, and π-acceptor moiety (2,4,5,7-tetranitroflorenone, TENF), while the linkers (linear diamines) were varied from a two-carbon (diaminoethane, DAE (**2**)), a three-carbon (diaminopropane, DAP(**3**)) to a four-carbon (diaminobutane, DAB(**4**)) containing compounds. The particles notation takes the form: PGMA-DAE(**2**)-TENF, PGMA-DAP(**3**)-TENF, PGMA-DAB(**4**)-TENF and PGMA-DAB(**4**)5-TENF, where 5 denotes the synthesis in 5% (vol./vol.)

linker and 95% (vol./vol.) toluene solution, while for other three, 100% (vol./vol.) linker was used. Particles were characterized by, among others, Fourier transform infrared spectroscopy (FT-IR), thermogravimetric analysis (TGA), elemental carbon, hydrogen, nitrogen and sulfur analysis (CHNS) and scanning electron microscopy (SEM). The change in linker length did not result in a significant effect on loading as similar amounts of TENF were immobilized on the polymeric particles regardless of the linker length. From the adsorption studies of light gas oil (LGO), results showed that diaminopropane (PGMA-DAP(**3**)-TENF) substituted particles gave the highest % adsorption of nitrogen compounds, followed by the diaminobutane (PGMA-DAB(**4**)-TENF)-based particles, while no significant differences between the particles with diaminoethane (PGMA-DAE(**2**)-TENF) and PGMA-DAB(**4**)5-TENF were observed. The results further showed that all the four types of particles selectively adsorbed nitrogen compounds, while the sulfur concentration in LGO remained unchanged under the following adsorption process conditions: ambient temperature (24 °C), time (24 h), particles to oil loading ratio (1:4 wt./wt.) and stirring speed (400 rpm). Generally, steric hindrance around the TENF molecules, on the surface of the particles, had a major role to play in the adsorption process than the length of the linker.

4.2 Introduction

Due to stringent environmental regulations that require the reduction of sulfur content in gasoline to 10 ppm, tremendous interest in the research world has been generated into improving the current methods that are being used for the reduction of sulfur [20,84–90]. The main technique employed industrially for the treatment of gasoil is referred to as hydrotreating process. This process mainly involves the removal of sulfur (hydrodesulfurization, HDS), nitrogen (hydrodenitrogenation, HDN), aromatic compounds (hydrodearomatization, HDA) and metals (hydrodemetallization, HDM) [91]. Failure to remove these contaminants from the oil feed will have detrimental effects on the catalyst, equipment and the quality of the final product. Hydrotreating process is a catalytic process that is conducted at hydrogen pressure between 8-9 MPa, 360-420 °C as the temperature range and using mainly, NiMo and CoMo/Al_2O_3 based-catalysts. Under these conditions, sulfur and nitrogen containing compounds produce H_2S and NH_3, respectively as by-products. These side products, in conjunction with unreacted aromatic and other nitrogen compounds inhibit/deactivate the catalyst, hence reducing the efficiency of HDS process [92,93]. Possible alternatives to improving this process is either (a) the development of new and improved catalysts, (b) the use of

a non-catalytic process [9,94–98] or (c) a combination of a non-catalytic (pre-treatment) and a catalytic step in a single process set-up [87,99,100]. Two types of aromatic nitrogen compounds exist in a petroleum feedstock: basic and non-basic compounds. In basic nitrogen (BN) compounds such as pyridine and acridine, the lone pair of electrons on the nitrogen atom does not participate in the delocalized π-electron cloud. While the lone pair of electrons in the non-basic compounds (NBN), such as indole and carbazole are a part of the delocalized π-electrons. This characteristic makes the NBN compounds less reactive than the basic compounds and were thought to be spectator compounds [28,101].

However, studies have shown that under the hydrotreating conditions, non-basic compounds are converted to basic compounds and increase the competition for the catalyst active site with sulfur containing compounds [37,69,102]. Therefore, there is a need to remove both basic and non-basic nitrogen compounds in order to avoid drastic decrease in catalytic activity and catalyst lifetime. A number of methods have been proposed to remove nitrogen compounds, however, most of them have been found to be selective towards basic nitrogen compounds.

Among the promising techniques is the formation of a charge transfer complex (CTC) between π-acceptor moiety functionalized on a polymeric support and π-donor compounds found in the gasoil such as BN, NBN, aromatics and sulfur containing compounds [20,64,67,103,104]. The functionalized particles consist of three parts: polymer support, linker and the π-acceptor moiety. The support used in this work is highly cross-linked polymeric particles consisting of glycidyl methacrylate (GMA) and ethylene glycol dimethacrylate (EGDMA). The readily reactive epoxide functionality on the GMA monomer makes attachment of the linkers, in this case diamines, possible [105]. The CTC formation could be affected by steric hindrance that is, how far the π-acceptor moiety is stretched (extended) from the polymeric support. The effect of linker length on the selective adsorption of non-basic nitrogen compounds has never been discussed before. Furthermore, there is limited study on the adsorption of NBN species using hydrophilic functionalized polymeric materials. It is hypothesized that a longer linker would reduce steric hindrance, therefore would allow for more interaction between the adsorbent and adsorbate. Moreover, more linker per polymer backbone (bead) would increase the amount of the π-acceptor on the surface of the particles as illustrated in Figure 4.1. Additionally, limited regeneration and

optimization studies on the adsorption studies by polymers exist in the literature [61,103,106]. Herein, the effect of linker length on the selective removal of nitrogen, and subsequent adsorption optimization study were investigated and are reported.

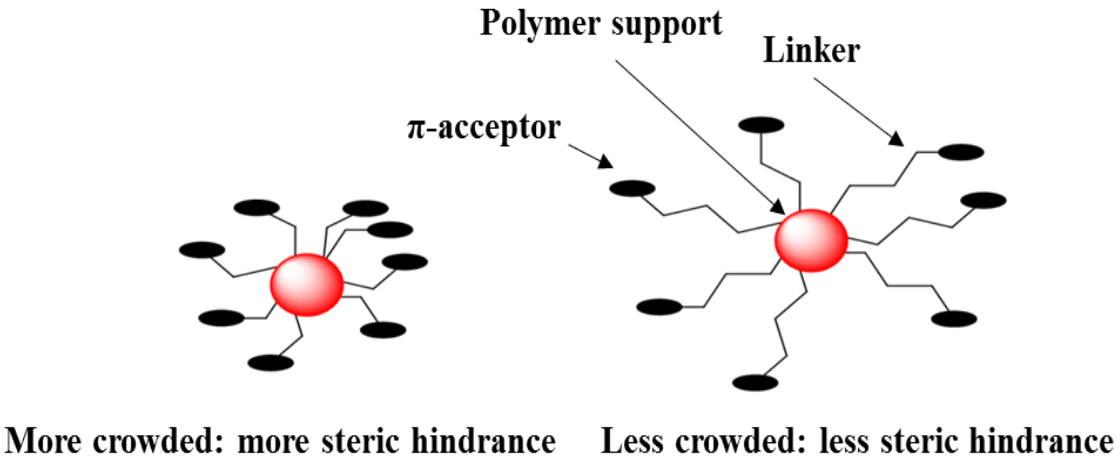

Figure 4.1: Visual comparison of particles with shorter linkers (left) to ones with longer linkers (right).

4.3 Experimental Details and Methodology

4.3.1 Materials

The following materials were purchased from Sigma-Aldrich and were used as received: glycidyl methacrylate (GMA), ethylene glycol dimethacrylate (EGDMA), poly[N-vinyl-2-pyrrolidone] (PVP) (Mw ~ 55,000 g/mol), 1-dodecanol (98.0%), cyclohexanol (99.0%), N,N-dimethylformamide (anhydrous 99.8%), Fluorenone, fuming nitric acid and sulfuric acid, 1,2-diaminoethane (≥99.0%), 1,3-diaminopropane (≥99.0%) and 1,4-diaminobutane (≥99.0%). Azobisisobutyronitrile was purchased from Molekula Ltd. A sample of bitumen-derived light gas oil, whose characteristics are shown in Table 4.1, was provided by Syncrude Canada Ltd., Edmonton. AB, Canada.

Table 4.1: Characteristic properties of light gas oil (LGO).

Parameters	**LGO**
Boiling range (°C)	200-450
Sulfur content (ppm)	28,612
Nitrogen content (ppm)	1,508
Non-basic Nitrogen content (ppm)	889
Basic Nitrogen content (ppm)	619
Aromatic Carbon content (ppm)	28,526
Density (g/ml)	0.9

4.3.2 Synthesis of π-acceptor and polymer support

Synthesis of π-acceptor (2,4,5,7-tetranitrofluorenone, TENF)

Synthesis of 2,4,5,7-tetranitrofluorenone (TENF), the π-acceptor moiety on the particles was accomplished following a procedure described by Newman et al [75]. TENF was characterized by three techniques namely; NMR [^{1}H NMR DMSO δ 8.97 (s, 2H, aromatic protons), 8.77(s, 2H, aromatic protons)], Mass spectroscopy [MS-EI, $C_{13}H_4N_4O_9$ $[M]^+$ = 360:] and Elemental Analysis [Cal (% wt./wt.): C, 43.4; H, 1.12; N, 15.6; O, 40.0, found: C, 42.6; H, 1.50; N, 15.4; O, 40.5]. All these results were consistent with the expectations of pure TENF.

Synthesis of poly (GMA-co-EGDMA)

Synthesis of particles consisting of poly (GMA-co-EGDMA)-linker-TENF required a three step synthesis procedure, with each stage involving a modified experimental setup, as shown in Figure 4.2. Table 4.2 shows a summary of components, chemicals and their respective quantities used. Step 1 involved the synthesis of the copolymer poly (GMA-co-EGDMA) (henceforth referred to as PGMA) as described by Svec et. al. [107], with slight modifications. Thus, a 2 L three-neck flask fitted with a mechanical stirrer, and a valve for purging nitrogen was utilized. The reactants (active phase) were mixed in three different sets, with 85.5 g of glycidyl methacrylate and 36.75 g of ethylene glycol dimethacrylate being mixed with 1.2 g of the radical initiator azobisisobutyronitrile. Separately, the inert phase was prepared by mixing 147.9 g of cyclohexanol

and 14.7 g of dodecanol; and finally, a solution consisting of 9.0 g of polyvinylpyrrolidone in 900 ml of distilled water was prepared. The three solutions were then stirred at 400 rpm in the 3-neck flask, in an inert nitrogen environment. The reaction was performed at 70 °C for the first 2 h, and then at 80 °C for another 6 h. Once the reaction was completed, the system was allowed to cool for 2 h, while it was still stirred; the synthesized copolymer was then washed multiple times with distilled water and then with ethanol to remove any soluble components. The PGMA beads were then dried at 90 °C for 24 h to obtain about 100 g of the desired polymeric material.

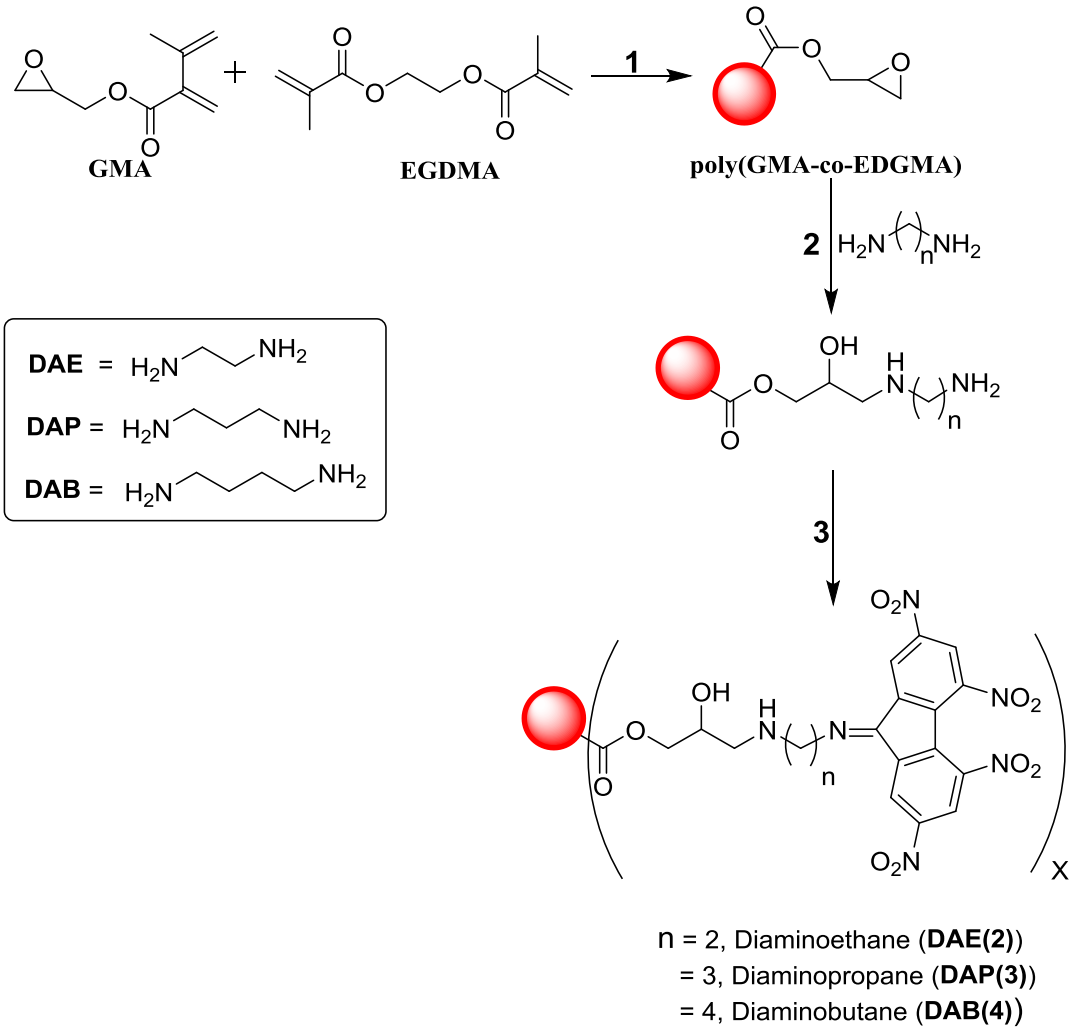

Figure 4.2: Synthesis of particles of PGMA-co-EGDMA functionalized with a π-acceptor, 1. AIBN, cyclohexanol (98.6 g), dodecanol (9.8 g), polyvinylpyrrolidone (6.0 g) and distilled water (600 mL) @ 70 °C (2 h) then @ 80 °C (6 h). 2. DAE, DAP or DAB (neat reaction), @ 80 °C, 24 h. 3. Glacial CH_3COOH, Toluene, TENF, 100 °C.

4.3.3 General procedure for attaching a diamine linkers to particles

The synthesis procedure involves substitution of the epoxy ring with a linker utilizing a modified experimental setup as that described in the literature [108–110]. Briefly, to a 500 mL two-necked flask incorporated with a mechanical stirrer and placed on a 100 °C pre-heated oil bath was added a 150 mL of the respective diamine, NH_2-(CH_2)n-NH_2, where n = 2, 3 and 4, (Figure 4.2, Step 2). To this flask, PGMA beads (61.5 g) were added slowly. The heterogeneous mixture was stirred at 400 rpm for 24 h. Upon completion of the reaction, the polymeric beads were washed several times with distilled water, then with ethanol. Further, washing using isopropyl ether in a soxhlet apparatus was done for 48 h and then, the obtained particles was left for drying at 90 °C for 24 h.

4.3.4 Synthesis of functionalized polymers

The final stage of the synthesis involved coupling of the π-acceptor compound to the PGMA-NH-(CH_2)n-NH_2 particles (Figure 4.2, Step 3). Thus, toluene (150 mL) and acetic acid (10 mL) were added to a 500 mL two-necked flask incorporated with a mechanical stirrer and placed on a 100 °C pre-heated oil bath. Then, TENF (2.45 g, 0.679 mmol) was added to the above flask. After complete dissolution of TENF, PGMA beads (6.20 g) were added slowly. This heterogeneous mixture is left to stir at 400 rpm and reflux for 3 days. The color for beads, upon addition, changed from white to brown. Once the reaction was completed, the modified beads were filtered and washed several times with toluene. Further, washing was done using toluene in a soxhlet apparatus for 48 h and then kept for drying at 90 °C for 24 h. The notation for the four particles that were synthesized, as shown in Scheme 4.1 are: PGMA-DAE(**2**)-TENF, PGMA-DAP(**3**)-TENF, PGMA-DAB(**4**)-TENF and PGMA-DAB(**4**)5-TENF. As shown in Figure 4.2, the three linkers used in the synthesis are diaminoethane (DAE(**2**)- 2 carbon linker), diaminopropane (DAP(**3**)-3 carbon linker) and diaminopropane (DAB(**4**)-4 carbon linker). Accordingly, through the epoxy ring-opening reaction, PGMA-DAE(**2**), PGMA-DAP(**3**), PGMA-DAB(**4**) were synthesized using 100% of the linker as solvent (Figure 4.2, Step 2). While, PGMA-DAB(**4**)5 was prepared in 95% toluene and 5% of diaminobutane (number 5 denotes 5% content of the linker in solution). Finally, (Figure 4.2, step 3) diamine attached particles were reacted with the π-acceptor, TENF, to obtain their corresponding TENF functionalized particles, as shown in Figure 4.3.

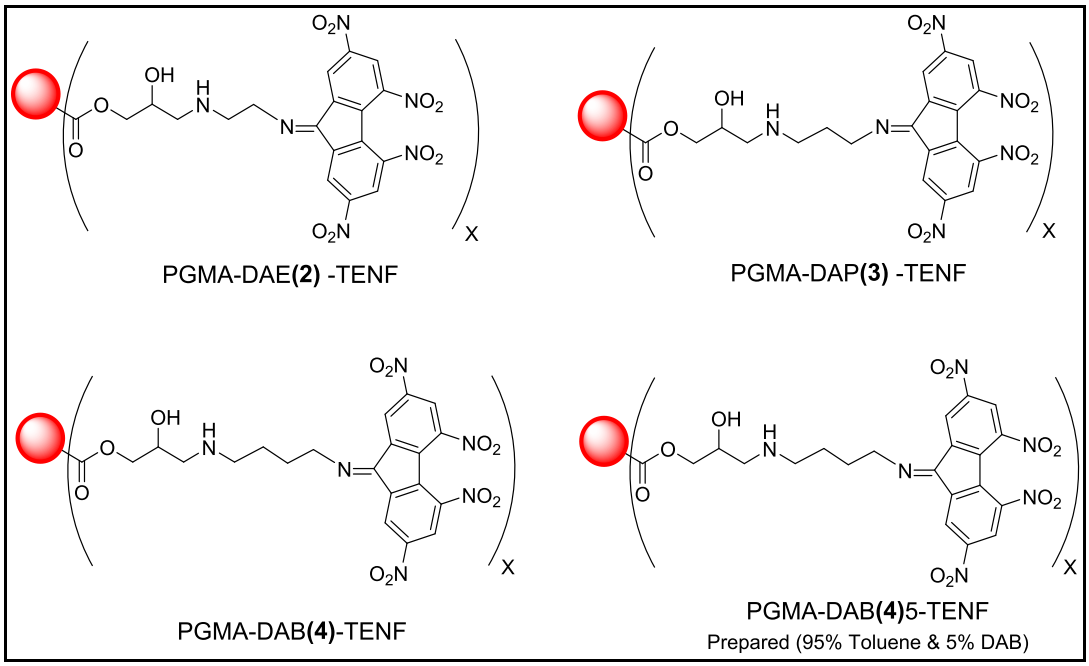

Figure 4.3: Summary of the TENF functionalized particles: PGMA-DAB(4)5-TENF was prepared in 95% toluene and 5% diaminobutane.

4.3.5 Instrumentation

Micromeritics ASAP 2000 analyzer (Micromeritics, Norcross, GA, USA) was utilized for the determination of The Brunauer–Emmett–Teller (BET) surface area, pore volume (Barret-Joyner-Halenda (BJH) method), and pore diameter of the particles samples. Prior to analysis, the samples were degassed under vacuum for 1.5 hours at 150 °C. The adsorption and desorption isotherms of N_2 were carried out at liquid nitrogen temperature (77 K). The hydrochloric acid-dioxane method was utilized to determine the α-epoxide content on the particles.[37] Scanning electron microscopy (SEM) JEOL 6010LV (JEOL USA Inc., Peabody, MA, USA) was used to analyze the morphology and quality of the synthesized particles. Thermal stability of the synthesized beads was determined using thermogravimetric analyzer, Q-5000, V20.13 (TA instruments, New Castle, DE, USA). Samples (ca. 10-15 mg) were heated in an inert atmosphere from 25 °C to 600 °C at a heating rate of 10 °C/min. The Vario EL III CHNS elemental analyzer (Elementar Americas Inc., Mt. Laurel. NJ, USA) was used to determine the percent content (wt./wt.) of carbon (C), hydrogen (H) and nitrogen (N) atoms. Fourier transform-infrared spectroscopy (FT-IR) was performed using a PerkinElmer Spectrum GX system (PerkinElmer, Waltham, MA, USA) in order to determine the

characteristic functional groups present during different synthesis steps. Samples were mixed and grounded with potassium bromide, KBr and placed in the hydraulic press to make sample discs. The discs were placed in the instrument at room temperature, where the average spectrum run was determined after 32 scans with a nominal 4 cm^{-1} resolution. Total nitrogen and sulfur content in gas oil samples was analyzed using the Antek model 9000NS combustion analyzer (ANTEK Instruments, Inc., Houston TX, USA). Boiling point distributions for all samples were determined by simulated distillation (SimDist., ASTM D2887) using a Varian/AC Analytical instrument (AC Analytical Instrument, Houston, TX, USA). Nuclear magnetic resonance data was obtained by dissolving samples in DMSO-d_6 /or $CDCl_3$ and analyzed using a Bruker 500 MHz NMR instrument (Bruker BioSpin Corporation, Billerica, MA, USA). Briefly, to obtain total percent aromatic carbon content, the feed/product was dissolved in $CDCl_3$ (1:1 ratio) and run under the following conditions (ASTM D5292-99(2014): 4s pulse delay, 28 KHz and inverse gated H_2 decoupling and 2500 scans. Percent aromatic carbon content (% C_{Ar}) is then calculated from the equation: % C_{Ar} = (A/A+B)*100, where A is the integral value of the aromatic portion of the spectrum (100 to 170 ppm) and B is the one for aliphatic carbons (-10 to 70 ppm). Particle size measurements were obtained using a Malvern Zetasizer Nano ZS instrument (Malvern Instruments Ltd, Westborough, MA, USA). The size distribution of particles in water was obtained by measuring the light scattered ($\theta = 173°$) by particles (dynamic light scattering, DLS) illuminated with a laser beam, using the CONTIN algorithm to analyze the decay rates that are a function of the translational diffusion coefficients of the particles. All the data analysis was performed in automatic mode. The measured data, presented in volume distribution, was obtained as an average value of 20 runs, with triplicate measurements within each run.

4.4 Results and discussion

4.4.1 Determination of epoxy content of PGMA particles

The α-epoxide content present in the PGMA particles was determined using the hydrochloric acid-dioxane method [111], which is based on the addition of hydrogen chloride to the sample in order to convert the epoxy group, on the particles, to chlorohydrin. The amount of acid consumed is then correlated to the epoxy content. Consequently, the epoxy content was calculated to be approximately equal to 1.1 mmol/g of particles [4.5 % (wt./wt.)], consistent with other published

literature.[28] Its worth mentioning that theoretically, the total epoxy content of the synthesized PGMA particles should roughly be equal to 4.9 mmol/g of particles and therefore, the cited titration method determines some epoxy groups, especially those exposed on the surface of the particles [112–115]. Based on this result, the synthesized PGMA particles have about 22.4 % of the epoxy on the surface, while 77.6 % is embedded in the polymer matrix.

4.4.2 Scanning Electron Microscopy (SEM) and Dynamic Light Scattering (DLS) analysis

In order to determine the morphology and size (size distribution) of the synthesized particles, scanning electron microscopy (SEM) and dynamic light scattering (DLS) were utilized. For SEM, samples were mounted onto aluminum slabs with the support of carbon paint, and were then gold coated, by vacuum sputtering, so as to improve secondary electron signals and to reduce charging. As shown in Figure 4.4 (a), the synthesized un-functionalized particles (PGMA) revealed spherical-shaped beads of size ranging from 0.2 to 0.32 µm. Average particle size and size-distribution were determined in aqueous suspensions using dynamic light scattering (DLS). The results in Figure 4.4 (b) show a narrow size distribution (Polydispersity Index [PDI] = 0.19) with the majority of the particles having size distributions centered at 1481 nm (volume distribution). The differences in the particle sizes measured by the two methods are due to the fact that SEM measurements suggest an average primary particle size in solid state whereas, in DLS, the hydrodynamic diameter of aggregated particles in aqueous solution were most likely obtained, consequently giving larger sizes compared to those obtained from SEM.

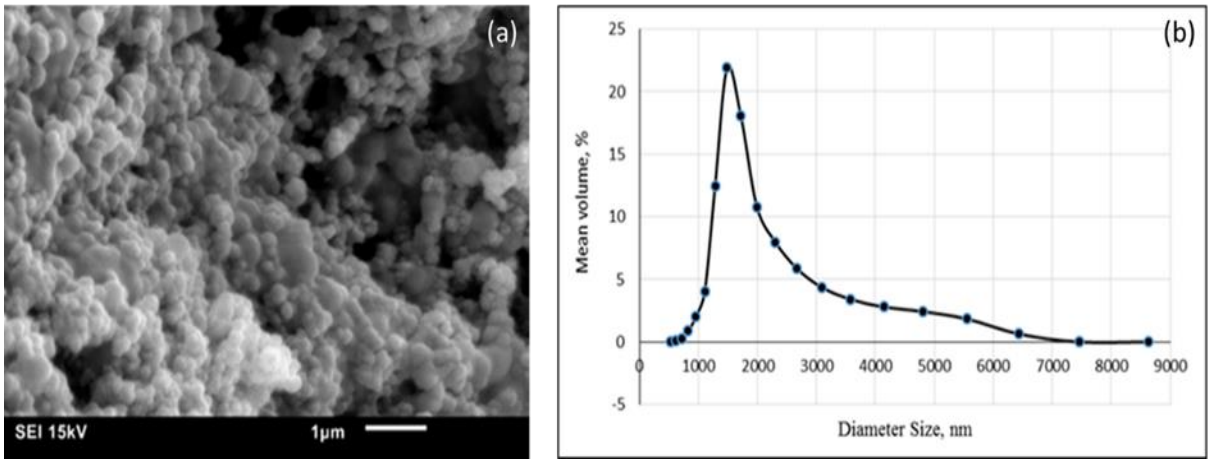

Figure 4.4: (a) SEM image taken at 15 kV and (b) size distribution measured by DLS of un-functionalized PGMA.

4.4.3 FT-IR functional group determination and Thermal Gravimetric Analysis (TGA)

Characteristic functional groups present during different synthesis steps were analyzed by the FT-IR instrument. Figure 4.5 shows FT-IR representative spectra of the successive synthesis in the PGMA-DAP(**3**) series and reveals significance differences among the sequential product samples. The spectrum from the analysis of PGMA shows characteristic peaks of the epoxy group (C-O-C) vibration frequencies at 1069, 908 and 853 cm^{-1} and stretching frequency at 1153 cm^{-1}, whereas the peaks at 1730 and 1154 cm^{-1} are attributed to the characteristic stretching frequency signal of a carbonyl (C=O) and ether (C-O) groups on an ester functionality. In PGMA-DAP(**3**), upon ring-opening, almost all epoxy signals disappear, while the broad signal at 3455 cm^{-1} is intensified. This signal denotes the presence of the hydrogen-bond stretching vibrations of hydroxyl (O-H) and amino (N-H) functionalities, consistent with literature [110,116]. The signal at 2942 cm^{-1} is attributed to the presence of sp^3 and sp^2 C-H stretching frequencies [116]. Finally, further reaction of PGMA-DAP(**3**) with TENF introduces extra signals at 1542 and 1344 cm^{-1}, corresponding to symmetrical and unsymmetrical stretching frequencies, respectively, of the nitro groups (O=N-O) on the π-acceptor (TENF) (shown in Figure 4.5) [117]. This data clearly indicates that the desired functionalized particles have been synthesized successfully.

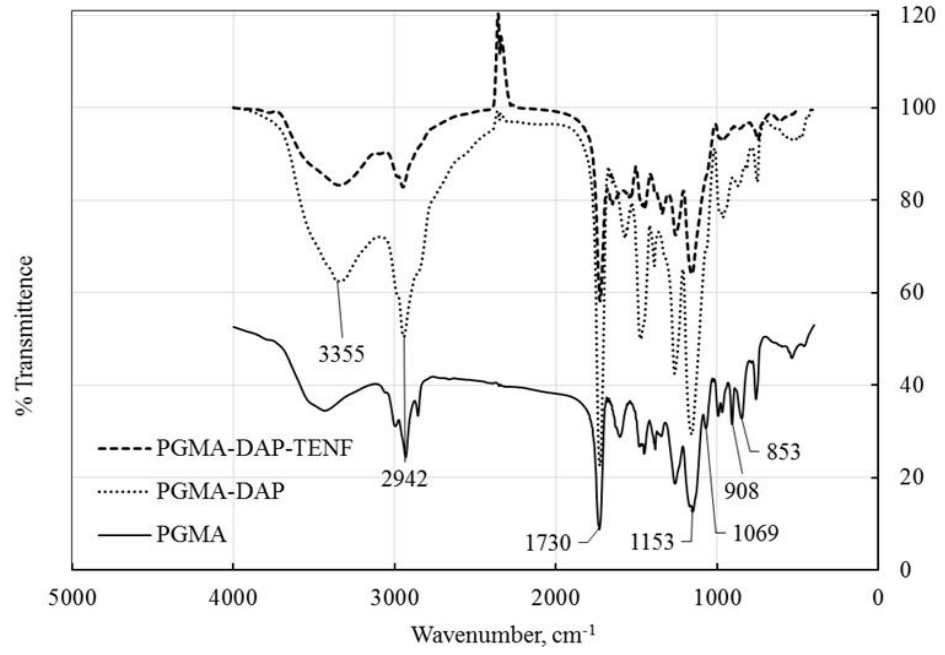

Figure 4.5: FT-IR spectra of a PGMA, PGMA-DAP(3) and PGMA-DAP(3)-TENF.

FT-IR analysis (Figure 4.6), shows the over-layered spectra of the fully functionalized particles: PGMA-DAE(**2**)-TENF, PGMA-DAP(**3**)-TENF, PGMA-DAB(**4**)-TENF and PGMA-DAB(**4**)5-TENF. It was observed that the signals from all the four particles were consistent with the expected results: somewhat disappearance of peaks attributed the epoxy ring and the appearance of peaks that are linked to the nitro groups associated with the π-acceptor moiety. It was further noted that the peaks got more intense as we progressed from a shorter to a longer linker. Since all the corresponding peaks appear at the expected wavenumbers, this observation could be due to an increase in sample concentration, which results in an apparent increase in functional group intensities.

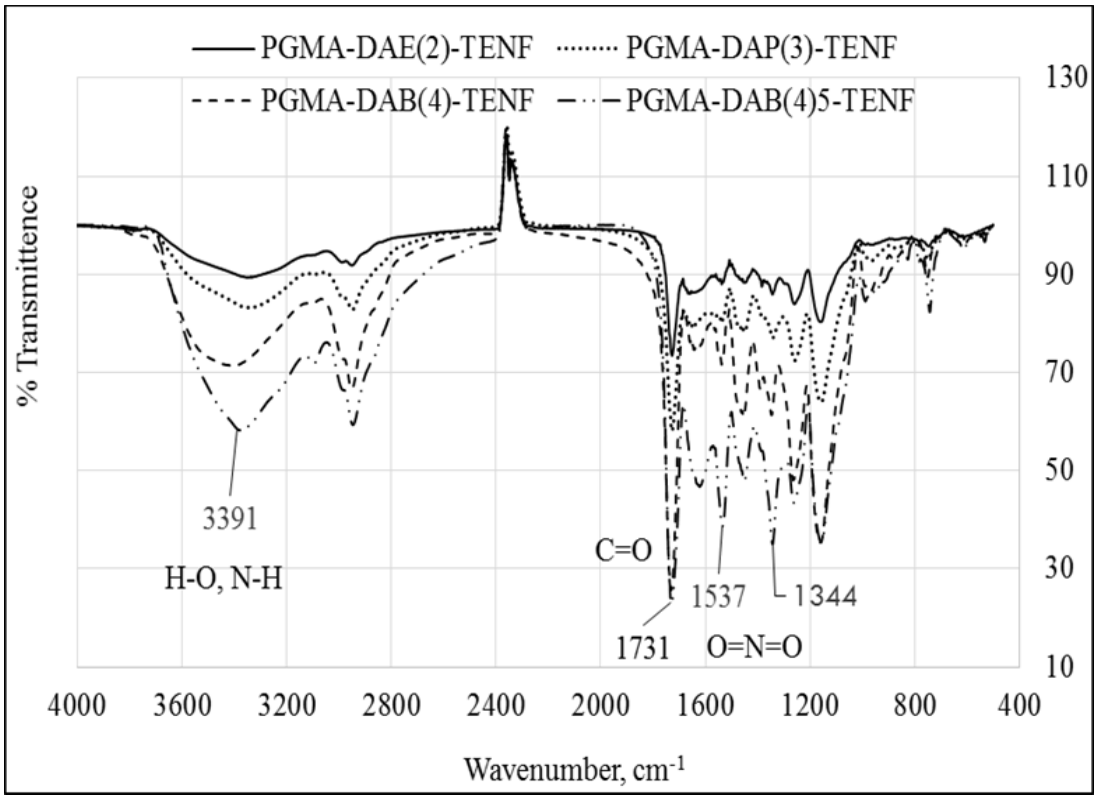

Figure 4.6: Over-layered spectra of TENF functionalized particles, PGMA-DAE(2)-TENF, PGMA-DAP(3)-TENF, PGMA-DAB(4)-TENF and PGMA-DAB(4)5-TENF.

To determine the stability and hence, decomposition temperatures of the synthesized particles, 10-15 mg samples were placed in the TGA instrument. All measurements were conducted in a nitrogen purge (40 mL/min) and after equilibration at 25 °C, they were heated to 600 °C at a

ramping rate of 10 °C/min. Figure 4.7 shows the dynamic weight loss (TGA) curve and its corresponding derivative curve (DTG), for the epoxy-functionalized PGMA particles. The results showed two major decomposition temperatures that were above 200 °C. For clarity Figure 4.8, shows representative curves using one set of particles consisting of PGMA, PGMA-DAP(**3**) and PGMA-DAP(**3**)-TENF, in addition to that of TENF. The two-step degradation process was also observed in all the particles synthesized, as evidently shown in the derivative weight loss (DTG) curves for PGMA-linker and PGMA-linker-TENF series (Figures 4.9 (a) and (b), respectively). One observable difference in the particle series in Figure 4.8, is that there is an increase in particle's residual at temperatures higher than 450 °C. At 500 °C, for instance, 5.6 % and 20.7 % of material remains for PGMA-DAP(**3**) and PGMA-DAP(**3**)-TENF, respectively, whereas almost all the material degraded when PGMA was heated above 450 °C.

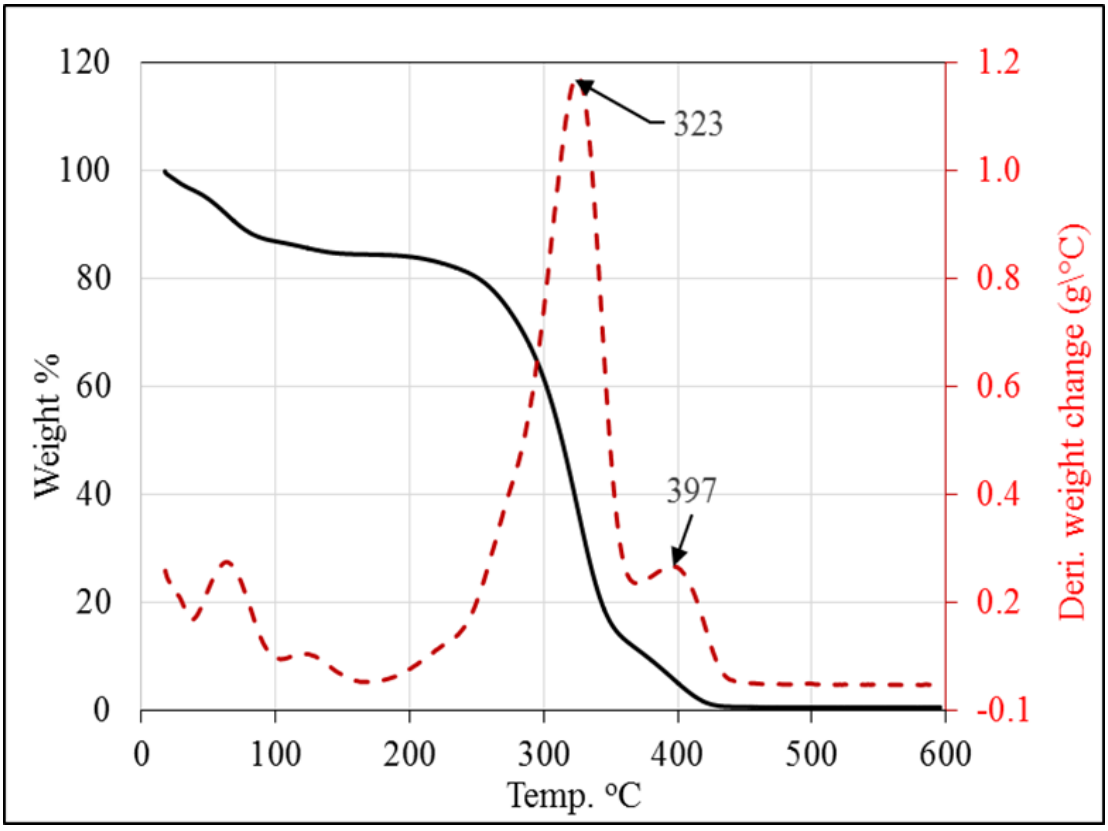

Figure 4.7: Dynamic weight loss (TG) curves and its derivatives (DTG) for PGMA.

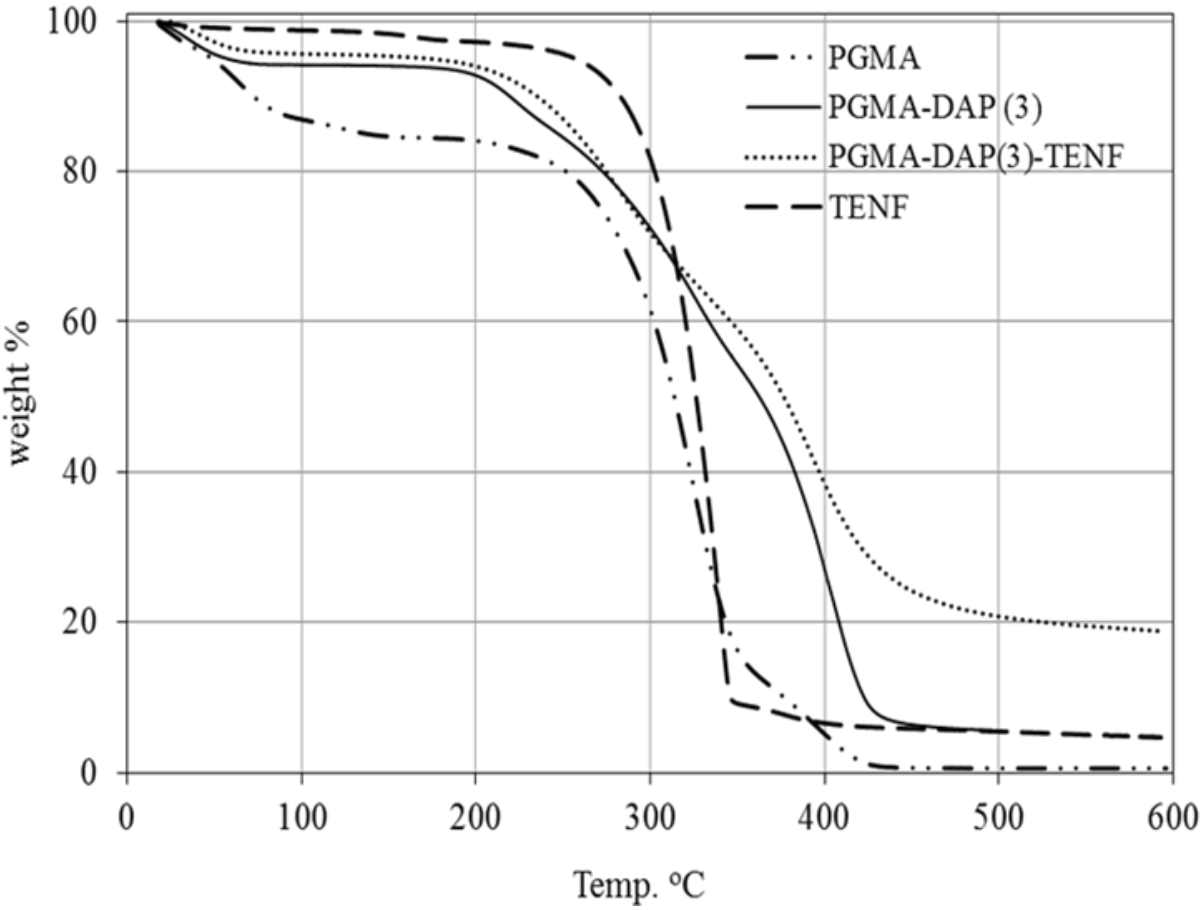

Figure 4.8: TGA plot of PGMA, PGMA-DAP(3), PGMA-DAP(3)-TENF and TENF.

Figures 4.9 (a) and (b), further, show another difference in the degradation profiles of PGMA compared to the PGMA-linker and PGMA-linker-TENF particles. There is a large peak in the starting PGMA profile appearing at ~ 323 °C and a smaller peak at ~ 397 °C ($T_{max}1$ and $T_{max}2$, correspondingly as shown in Table 4.3 and Figure 4.9 (a)). The opposite is observed for PGMA-linker particles i.e. their respective smaller peaks appear at 260-330 °C range ($T_{max}1$) while larger peaks come about 406-414 °C ($T_{max}2$).

Over the same temperature range, PGMA-linker-TENF particles show two peaks of similar heights. The average temperature range for these peaks is 278-286 °C (for the first decomposition step) and 371-394 °C (for the second decomposition step). The temperature at the start of

decomposition (T_{onset}) for PGMA and PGMA-linker particles is observed to be around 200 °C, whereas the one for PGMA-linker-TENF particles seems to appear at a slightly lower temperature (~ 175 °C). These results indicate that the overall functionality has changed and this therefore results in complete change in degradation profiles. However, the overall thermal stability of each series of particles remain the same over the temperature range studied (180-450 °C).

As shown in Table 4.3, the percent weight loss for PGMA, appearing at the first decomposition step, was estimated to be 69%. This corresponds to a total grafting amount of about 4.8 mmol/g of particles. Interestingly, this is consistent with the total epoxide content of the PGMA particles (~ 4.9 mmol/g particles). The percent weight loss for PGMA-Linker particles ranged from 35.7 to 38.4 (1.9 to 2.2 mmol/g) and 30.3 to 36.3 (0.62 to 0.71 mmol/g) for the PGMA-Linker-TENF particles. These results, based on the first degradation step, show that the amount grafted on these particles are almost the same regardless of the linker used.

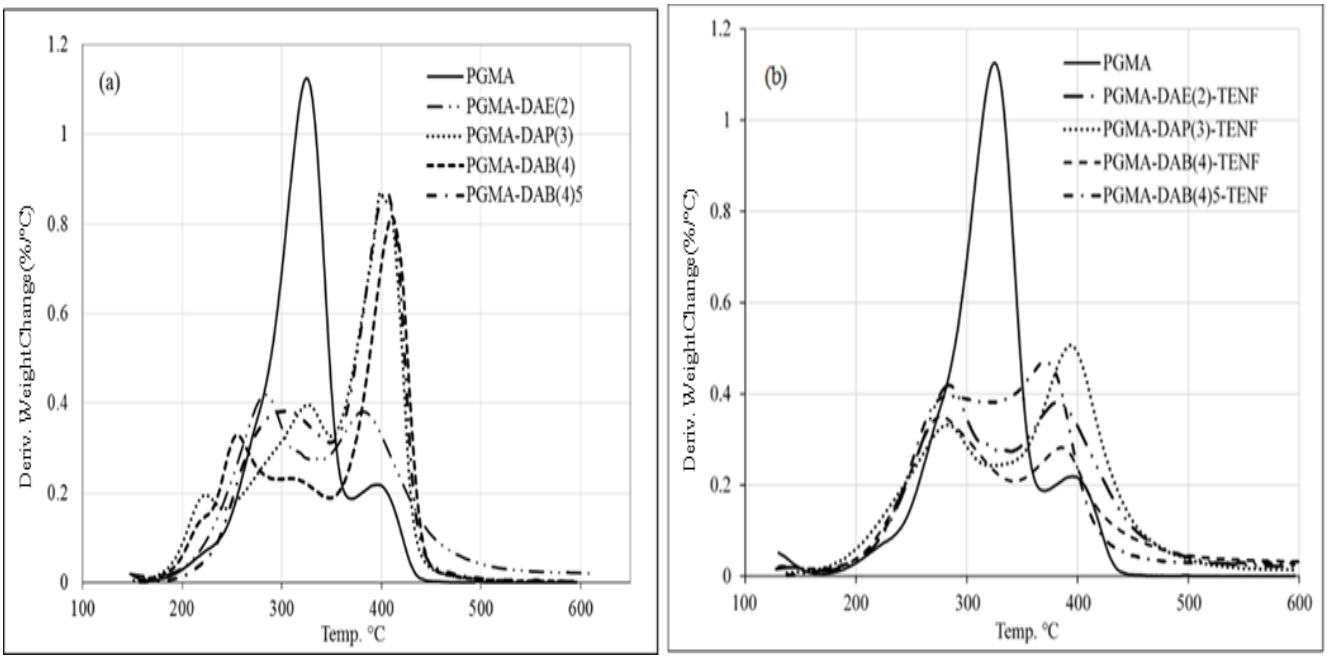

Figure 4.9: Dynamic weight loss derivatives (DTG) curve: (a) PGMA-linker series and (b) PGMA-linker-TENF series.

Table 4.3: TGA and DTG chracteristic properties of the synthesized particles.

Particles	T_{onset}	T_{max} (°C)		Residue (wt.%) @ 500 °C	weight loss (wt.%) @ 1st step	Total graft amount @ 1st step (mmol/g)
		$T_{max}1$	$T_{max}2$			
PGMA	202	323	397	0.1	69.0	4.8
PGMA-DAE(2)	195	330	407	0.7	35.7	2.2
PGMA-DAP(3)	199	327	406	5.6	37.2	2.1
PGMA-DAB(4)	200	300	407	6.1	35.7	1.9
PGMA-DAB(4)5	200	260	414	3.8	38.4	2.0
PGMA-DAE(2)-TENF	175	286	382	26.9	36.3	0.71
PGMA-DAP(3)-TENF	174	282	394	20.7	30.2	0.58
PGMA-DAB(4)-TENF	178	278	386	39.5	33.0	0.62
PGMA-DAB(4)5-TENF	176	282	371	25.7	33.7	0.63

4.4.4 CHNS elemental analysis and BET surface area determination

To determine the elemental composition of the synthesized particles, 7-10 mg samples were combusted using Vario EL III CHNS elemental analyzer. The results of the analysis are shown in Tables 4.4. Table 4.4 (a) shows, in addition the elemental compositions, the elemental ratios of initial PGMA and after the linker attachment, also shown are linker loadings. The same parameters for the fully functionalized particles are shown in Table 4.4 (b). The same batch of PGMA was used as a starting material in all cases, therefore it has the same percent composition, by mass, of carbon (56.8%), hydrogen (7.2%) and nitrogen (0.0%). Upon the ring-opening reaction with the various linkers, there is an increase in the elemental nitrogen content; from 0% to 7.6 % for PGMA-DAE(**2**) [linker loading = 2.7 mmol/g], 7.2 % for PGMA-DAP(**3**) [linker loading = 2.6 mmol/g], 8.6 % for PGMA-DAB(**4**) [linker loading = 3.1 mmol/g] and 4.9% for PGMA-DAB(**4**)5 [linker loading = 1.8 mmol/g]. The total nitrogen and hydrogen content increased, resulting in lower C/N and C/H atomic ratios. The observed increase in elemental nitrogen is attributed to the fact that the attached linkers contain nitrogen atoms that were absent in the initial starting material. Particles consisting of PGMA-DAB(**4**) gave the highest linker loading. There was no significant difference

between PGMA-DAE(**2**) and PGMA-DAP(**3**), while PGMA-DAB(4)5 gave the lowest linker loading of 1.8 mmol/g particles, as expected (only 5% linker was used). Furthermore, addition of the π-acceptor (TENF) caused a further general increase in elemental nitrogen content. For instance, in PGMA-DAE(**2**), it was 7.6 % and increased to 8.7 % for PGMA-DAE(**2**)-TENF [0.21 mmol/g], therefore give a lower C/N ratio and a slightly higher TENF loading than all the particles, as shown in Table 4.4 (b). These observations are due to the presence of nitro groups present on the π-acceptor moiety (TENF). Again, all these observations indicate the successful particle functionalization.

Table 4.4: Elemental (CHNS) analysis of synthesized functionalized particles.

(a)	**Elemental Comp. %(wt./wt.)**			**Atomic ratio**		**Linker loading**
	C	**H**	**N**	**C/H**	**C/N**	**mmol/g**
PGMA	56.7	7.2	0.0	7.9	0.0	-
PGMA-DAE(2)	51.7	7.4	7.5	7.0	6.9	2.68
PGMA-DAP(3)	54.7	8.8	7.2	6.2	7.6	2.57
PGMA-DAB(4)	54.5	8.8	8.6	6.2	6.3	3.07
PGMA-DAB(4)5	55.7	8.5	4.9	6.6	11.4	1.75
(b)	**Elemental Comp. %(wt./wt.)**			**Atomic ratio**		**TENF loading**
	C	**H**	**N**	**C/H**	**C/N**	**mmol/g**
PGMA	56.7	7.2	0.0	7.9	0.0	-
PGMA-DAE(2)-TENF	53.8	6.5	8.7	8.3	6.2	0.21
PGMA-DAP(3)-TENF	52.6	7.2	7.8	7.3	7.3	0.11
PGMA-DAB(4)-TENF	55.6	6.6	9.4	8.4	5.9	0.14
PGMA-DAB(4)5-TENF	55.6	7.5	5.6	7.4	9.9	0.12

In order to determine the best synthesis condition for maximum π-acceptor attachment, two polymeric materials (PGMA-DAB(**4**)-TENF and PGMA-DAB(**4**)5-TENF) were synthesized. On

the latter, as mentioned earlier, the number *5* denotes the use of 5% of diaminobutane and 95% toluene as the solvent mixture. While for the former, and for any other particles synthesized, a neat reaction (100% linker) was used. Although there is more linker on PGMA-DAB(**4**) than on PGMA-DAB(**4**)5, the amount of TENF attached is the same in both cases. The CHNS results, therefore, clearly reveal that there is no advantage in using a 100 % linker concentration, since the amount of TENF attached is almost the same.

The specific surface area of the synthesized functionalized particles was determined using the Brunauer-Emmett-Teller (BET) method, while their pore volumes were obtained from the analysis of the adsorption branch using the Barret-Joyner-Halenda (BJH) method. All particles gave similar adsorption isotherms, so for clarity, only the isotherm for PGMA-DAP-TENF is shown in Figure 4.10. The BET isotherms clearly shows that the synthesized particles exhibit a class IV isotherm and are therefore considered to be mesoporous materials, this is consistent with other published articles [79].

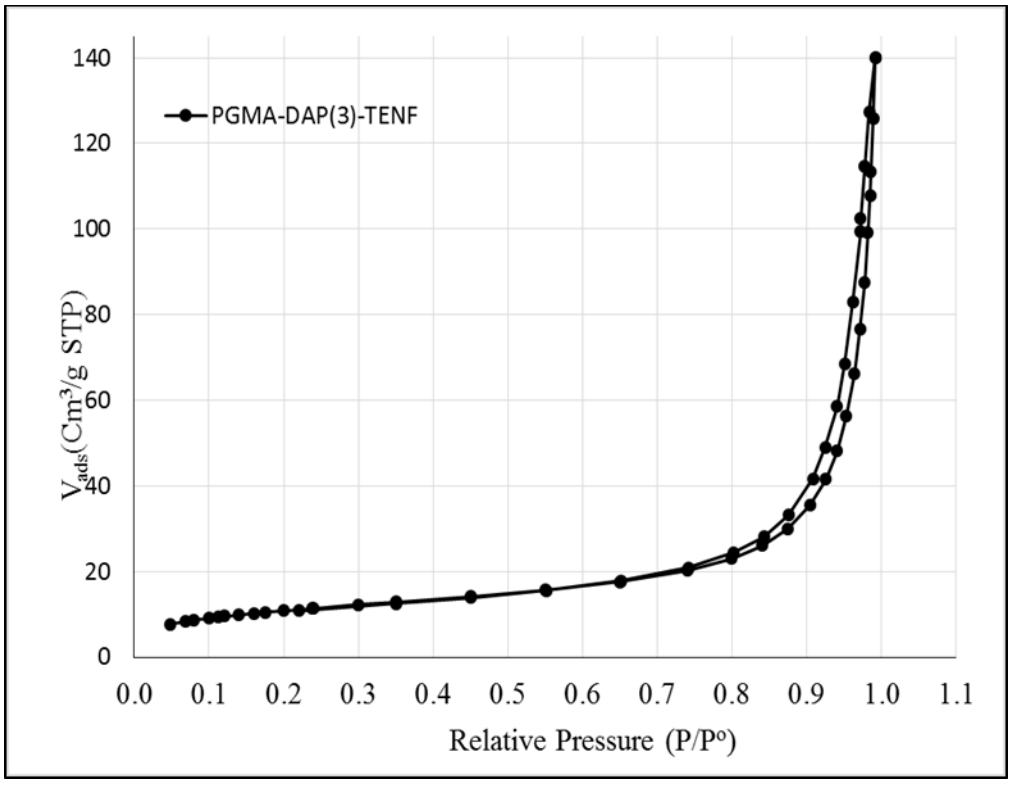

Figure 4.10: Sample pattern of adsorption-desorption isotherms: PGMA-DAP-TENF.

Within experimental error (± 4 m^2/g), the BET surface area for PGMA-DAE(**2**) (34 m^2/g) and PGMA-DAP(**3**) (41 m^2/g) did not change from the initial value of PGMA (38 m^2/g). However, there was an increase in surface area for the particles PGMA-DAB(**4**) and PGMA-DAB(**4**)5 which gave surface areas of 50 and 56.0 m^2/g, respectively, as shown in Table 4.5 (a). The pore diameter ranged from 16 to 19 nm, regardless of linker-particle functionalization. It was observed that, upon attaching the π-acceptor, the BET surface area and pore volume for DAB-TENF functionalized particles decreased, as shown in Table 4.5 (b). The particles, PGMA-DAB(**4**)-TENF, consisting of the longest linker and at 100% linker concentration during synthesis, gave the highest reduction in surface area from 50 to 25 m^2/g and pore volume from 0.22 to 0.07 m^3/g. On the other hand, the fully functionalized particles, PGMA-DAE(**2**)-TENF and PGMA-DAP(**3**)-TENF showed no change in either surface area, pore volume or pore diameter when compared to their immediate precursor particles. These results are consistent with highly cross-linked particle network that is stable under functionalization and testing conditions.

Table 4.5: BET surface area, pore volume and pore diameter of the synthesized particles.

(a)	**Surface area (m^2/g) ± 4**	**Pore volume (m^3/g)**	**Average pore diameter (nm)**
PGMA	38	0.14	16
PGMA-DAE(2)	34	0.14	17
PGMA-DAP(3)	41	0.17	17
PGMA-DAB(4)	50	0.22	16
PGMA-DAB(4)5	56	0.22	19
(b)	**Surface area (m^2/g) ± 4**	**Pore volume (m^3/g)**	**Average pore diameter (nm)**
PGMA-DAE(2)-TENF	36	0.13	16
PGMA-DAP(3)-TENF	39	0.17	19
PGMA-DAB(4)-TENF	25	0.07	14
PGMA-DAB(4)5-TENF	47	0.16	13

4.4.5 Batch adsorption studies

The light gas oil (LGO), used in this study, has characteristics shown in Table 4.1, and was tested as follows; To a batch-type reactor, kept at ambient temperature (24 °C), was added TENF-functionalized particles and gas oil in a ratio of 1:4 (wt./wt.) (1 g of particles to 4 g of oil). The mixture was stirred at 400 rpm for 24 h and then suction filtered to separate the treated oil from the particles. The used particles were then washed with acetone and air dried. The dried particles are regenerated using a soxhlet extractor at 110 °C using toluene for 48 h. The regenerated particles are then dried at 100 °C for 12 h. The total nitrogen and sulfur content of the oil before (initial) and after treatment (final) was determined by the N/S analyzer. The percent of either nitrogen or sulfur adsorbed was calculated using equation 4.1.

$$\%\ \text{N (or S) adsorbed} = \frac{\text{initial ppm N (or S)} - \text{final ppm N (or S)}}{\text{initial ppm N (or S)}}\ \text{x}\ 100 \qquad (4.1)$$

Results in the adsorption studies of light gas oil (LGO), showed that diaminopropane (DAP(**3**)) substituted polymer gave the highest adsorption (19%), followed by the diaminobutane (DAB(**4**))-based polymer, as shown in Figure 4.11. No significant difference between the particles with diaminoethane (DAE(**2**)) and DAB(**4**)5. Although, PGMA-DAE(**2**)-TENF had the highest TENF attachment, the amount of nitrogen adsorbed was lower than PGMA-DAP(**3**)-TENF and PGMA-DAP(**4**)-TENF. This is could be due to steric hindrance around the attached TENF molecules. On average, the synthesized particles were restored to their original state after regeneration, the concentration of adsorbed nitrogen after regeneration gave similar results as with fresh particles, except for DAP particles that experienced a 6% decrease (from 19.0 to 13.0 %). For this particular material, the decrease could be due to insufficient regeneration time, because at similar regeneration conditions, all the other particles were restored to their original state. The length of the linker did not have a significant effect on loading as similar maximum amounts of TENF were immobilized on the polymeric particles regardless of the linker length. However, it is interesting to note that all particles were very selective for adsorption of nitrogen containing compounds, for the percent concentration of sulfur in the feed remained unchanged as shown in Figure 4.11.

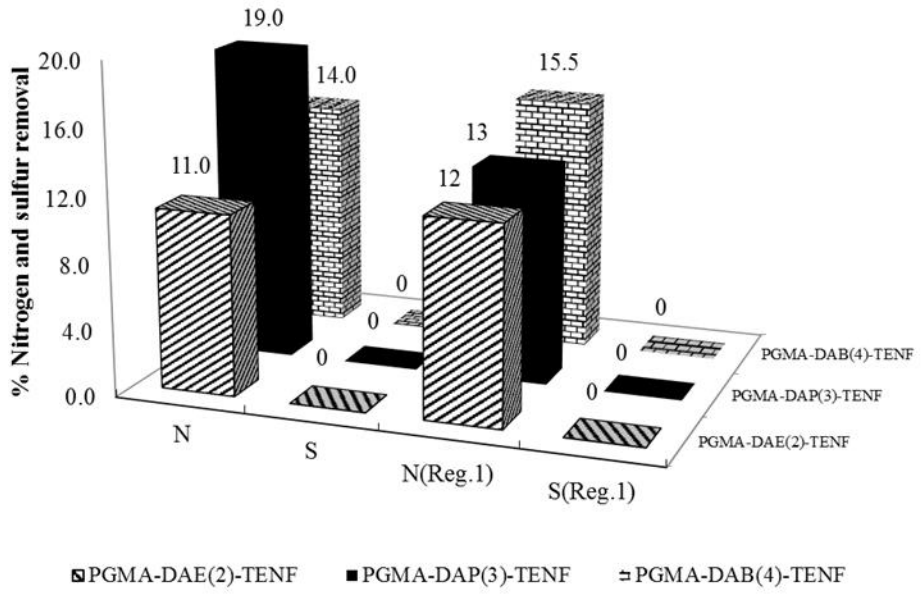

Figure 4.11: Adsorption results using fresh and regenerated particles at conditions: 24 °C, 24 h and 4:1 oil to particle ratio. N and S are nitrogen and sulfur, respectively.

4.4.6 Optimization of process parameters

Various parameters such as temperature, time, stirring rate and adsorbent to adsorbate loading ratio, affect the adsorption process. Design Expert® software (version 6.0.11, State-Ease Inc., Minneapolis, USA) was utilized to investigate the effect of each parameter on the adsorption process. Thus, the experimental design, data analysis, quadratic model buildings, and 3-D graphs (response surface and contour) were obtained from the 20 suggested experiments from the software. Table 4.6 shows the three parameters and their corresponding ranges that were utilized to generate the 20 experiments. Temperature ranged from 24 to 60 °C, time from 1 to 48 hours and oil to particles loading ratio varied from 4:1 to 10:1 (wt./wt., represented as 4, 5 to 9 in Figures 4.12 (a) and (c)). Particles of PGMA-DAP(**3**)-TENF were selected for this study due to higher nitrogen removal obtained from earlier studies. To fit the response function of nitrogen removal, regression analysis was performed. The quadratic model for the nitrogen removal in terms of coded factors, after excluding the insignificant terms is shown in equation 4.2.

$$\text{Total 'N' removal} = 12.25 + 0.28\mathbf{A} - 0.37\mathbf{B} - 1.12\mathbf{C} + 3.48 \times 10^{-3}\mathbf{AB} + 0.021\mathbf{AC} + 0.011\mathbf{BC} - 5.90 \times 10^{-3}\mathbf{A}^2 + 5.91 \times 10^{-3}\mathbf{B}^2 - 0.068\mathbf{C}^2 \quad (4.2)$$

Where, **A** = Temp. (^{o}C), **B** = Time (h) and **C** = ratio of Oil to particle loading (wt./wt.).

The interaction effect of the three parameters (temp., time and loading ratio) are plotted in three-dimensional (3-D) response surface and contour graphs as shown in Figures 4.12. Each plot has two parameters (either temp., time or loading ratio) on the x- and y-axes and the z-axis is the % nitrogen adsorbed by the particles. The agitation rate was kept at a constant value of 400 rpm. From the plots, it was observed that the lower the loading ratio, the higher the nitrogen removal (Figures 4.12 (a) and (c)). Lower oil loading ratio means there is a higher concentration of oil per gram of particles compared to a higher loading ratio (less concentrated). Therefore, more nitrogen is removed from the oil in a more concentrated mixture. Because of the viscosity of the oil, there were challenges connected to mixing/stirring, therefore the lowest loading ratio that was employed is 1:4 (wt./wt. particles to oil ratio). It was further observed that the longer the contact time between the particles and the oil, the higher the adsorption of nitrogen compound (Figures 4.12 (b) and (c). Finally, increase in temperature had an increase in the nitrogen adsorption to some extent then decreased as temperature increases toward 53 °C. The formation of the charge transfer complex (CTC) is an exothermic process; hence the slight/minimum effect of an increase in temp is acceptable [118,119]. To the contrary, lower temperature would actually increase the nitrogen removal. To check the validation of the model, the optimization analysis showed that at the following conditions: temp. = 31 °C, time = 38 h and 1:5.2 (by wt.) loading ratio, maximum nitrogen removal of 12.5% would be obtained. The experimental study resulted in 12.9 % nitrogen removal, which is within the experimental error. It is consistent with the predicted result.

Table 4.6: Optimization parameters and their corresponding range.

		Levels	
Variables	**Symbols**	**-1.41**	**+1.42**
Temperature (°C)	A	24	60
Time (h)	B	1	48
Oil to particle loading ratio (wt./wt.)	C	1:4 (4)	1:10 (10)

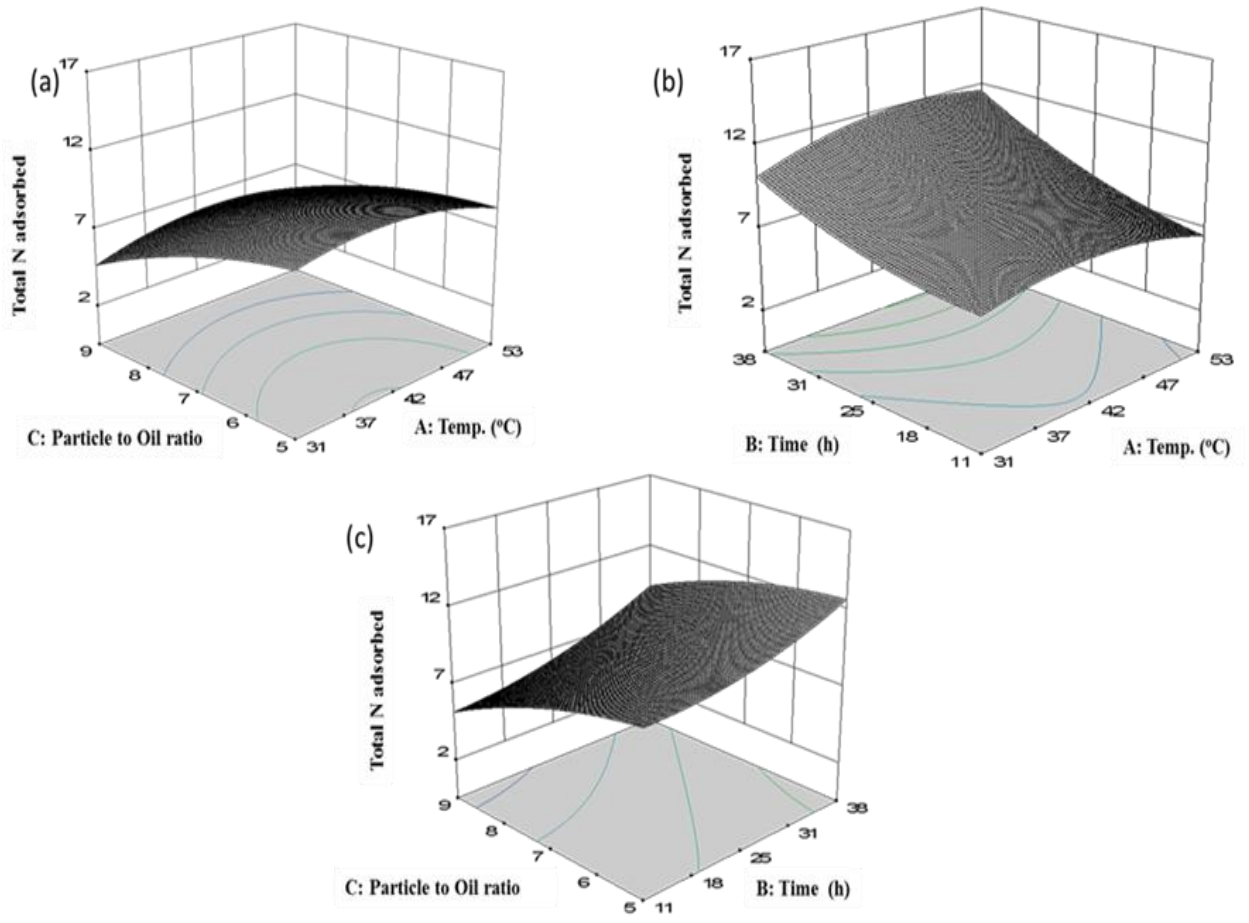

Figure 4.12: The three-dimensional response surfaces: (a) effect of loading ratio and temperature, (b) effect of time and temperature and (c) effect of ratio of oil to particle loading and time on the nitrogen adsorbed.

4.5 Conclusions

The focus of this research was to study the effect of the length of the linker on the particles towards the selective adsorption of nitrogen compounds from light gas-oil (LGO). To this effect, four PGMA-based functionalized polymeric materials, (PGMA-DAE(**2**)-TENF, PGMA-DAP(**3**)-TENF, PGMA-DAB(**4**)-TENF and PGMA-DAB(**4**)5-TENF, with variable linker lengths and different reaction conditions, were successfully synthesized. These particles were fully characterized by, among others, FT-IR, TGA, elemental CHNS, and SEM. The length of the linker did not have a significant effect on loading as similar amounts of TENF were immobilized on the polymeric particles regardless of the linker length. The results from the adsorption studies of light

gas oil (LGO), showed that diaminopropane (PGMA-DAP(**3**)-TENF) substituted particles gave the highest adsorption, followed by the diaminobutane (PGMA-DAB(**4**)-TENF)-based particles. No significant difference between the particles with diaminoethane (PGMA-DAE(**2**)-TENF) and PGMA-DAB(**4**)5-TENF. Although, PGMA-DAE(**2**)-TENF had slightly higher TENF attachment, the amount of nitrogen adsorbed was lower than that by PGMA-DAP(**3**)-TENF and PGMA-DAP(**4**)-TENF. This could be due to steric hindrance around the attached TENF molecules that limits the interaction with the feed. Interestingly, all the particles selectively adsorbed nitrogen compounds, for the sulfur content in the feed remained unchanged after the adsorption process. Further studies are underway to determine the effect of this pre-treatment procedure on the hydrotreating process of light gas oil.

Chapter 5: Selective removal of nitrogen compounds from gas oil using functionalized polymeric adsorbents: Effect of polymer support

---

A similar version of this chapter has been published as a research article and was presented at the following conferences:

- Misra, P., Chitanda, J. M., Dalai, A. K. & Adjaye, J. "Selective removal of nitrogen compounds from gas oil using functionalized polymeric adsorbents: Efficient approach towards improving denitrogenation of petroleum feedstock". *Chemical Engineering Journal* (2016) 295, 109–118.
- Misra, P., Dalai, A. K. & Adjaye, J. "Removal of nitrogen species from bitumen-derived gas oil prior to hydrotreating: Efficient approach towards improving refinery feedstock". *251st ACS National Meeting & Exposition*, San Diego, California, USA, 13-17 March 2016.
- Misra, P., Dalai, A. K. & Adjaye, J. "Advancement in the conventional hydrotreatment technology by removing sulfur and nitrogen species from heavy gas oil using π-acceptor functionalized polyHIPEs". *65th Canadian Chemical Engineering Conference*, Calgary, AB, Canada, 4-7 October 2015.

Contribution of the Ph.D. candidate

Polymer synthesis, characterization, testing and data analysis was done by Prachee Misra. All the manuscript writing and revision work was done by Prachee Misra based on the suggestions from Drs. Ajay Dalai, John Adjaye, and Jackson Chitanda.

Contribution of this chapter to the overall Ph.D. work

This part of work was focused on the synthesis and functionalization of polymers with improved textural properties and their application in selectively removing nitrogen compounds.

5.1 Abstract

A major challenge in achieving deep hydrodesulfurization with the conventional hydrotreating technology is the inhibition and deactivation of the catalyst caused by heterocyclic nitrogen compounds. In this research, novel polymeric adsorbents were introduced for the selective removal of nitrogen compounds from bitumen-derived light gas oil. Synthesis of polymers with high internal phase emulsion (polyHIPEs) was carried out using a monomeric mixture of unsaturated polyester resin, glycidyl methacrylate and divinylbenzene. To facilitate the selective removal of nitrogen compounds, reactive epoxy groups present in glycidyl methacrylate were used to functionalize the polyHIPEs with a fluorenone based π-acceptor, 2,4,5,7-tetranitro-9-fluorenone (TENF). Successful application of the synthesized polymers was found in the batch adsorption experiments at ambient temperature. Functionalized polyHIPEs were capable of selectively adsorbing nitrogen species from light gas oil. The optimum ratio of monomers was found to be one of the key factors in determining the polymer performance. Particles with high glycidyl methacrylate content with toluene as the porogenic solvent were capable of removing 14.6 wt.% of nitrogen compounds. Reusability studies were performed successfully by regenerating the used polymers with toluene, which aids the separation of complexing agent and the adsorbed nitrogen species.

5.2 Introduction

Refractory sulfur compounds, such as dibenzothiophene and alkyl substituted dibenzothiophenes and hydrotreating catalyst inhibiting nitrogen species, such as indole, carbazole and alkyl substituted carbazoles can be removed by using functionalized polymers capable of adsorbing these compounds prior to hydrotreatment [18,19]. Over the last few years, researchers have been synthesizing highly functionalized polymers which can be modified for a variety of applications. Glycidyl methacrylate (GMA) containing emulsion-templated porous polymers were functionalized by Kimmins et al. [120] for biocatalysis. Emulsion droplets can be used to template the micro-spherical structures in solution phase synthesis [121]. Ruckenstein et al. [122] synthesized polymer-supported biocatalysts for their application in vinylation reaction. Mert et al. [123] prepared polyester-glycidyl methacrylate based polyHIPEs for heavy metal removal. In their study, heavy metal ions such as Silver, Copper and Chromium were successfully adsorbed on the

polyHIPE monoliths. Jungbauer et al. [124] have extensively mentioned about the removal of large biomolecules using polymethacrylate monoliths. Hence, polyHIPEs have demonstrated their great potential as separation media. However, these polyHIPEs were never used in the petroleum related research.

This work focuses on the synthesis, functionalization and characterization of polymers with high internal phase emulsion for the removal of refractory sulfur and nitrogen compounds from bitumen-derived light gas oil (LGO). The polymer monoliths were prepared using unsaturated polyester resin (UPR), glycidyl methacrylate (GMA) and divinylbenzene (DVB) as monomers in the continuous phase, hereafter referred to as polyHIPEs. Reactive epoxy groups were used to functionalize the polyHIPEs with π-acceptor, TENF. All functionalized polyHIPEs have characteristic textural properties which ease the adsorption of different types of heterocyclic nitrogen and sulfur compounds from refinery feed.

5.3 Experimental details and methodology

5.3.1 Materials

The functional monomer; glycidyl methacrylate (≥97.0%), the diluent monomer; divinyl benzene (80%), triethanolamine (≥99.0%), Anhydrous N,N-dimethylformamide (99.8%), acetone oxime (≥98.0%), 9-fluorenone (98%), fuming nitric acid (90%), tetrahydrofuran (99.9%), and p-toluene sulfonic acid monohydrate (≥98.5%) were purchased from Sigma Aldrich. Unsaturated polyester resin was purchased from Viking Plastics Ltd., Edmonton, Canada. Concentrated sulfuric acid (95-98%) and toluene (99.9%) were purchased from Fisher Scientific. The radical initiator Azobisisobutyronitrile (AIBN) was purchased from Molekula Ltd., and distilled water was used for making the aqueous phase. Potassium carbonate (≥99.0%) was purchased from Alfa Aesar. Potassium bromide (99+%) for spectroscopy, IR grade was purchased from Acros Organics. Bitumen-derived light gas oil (LGO) used in this work was provided by Syncrude Canada Ltd. All the chemicals were used as received.

5.3.2 Preparation of π-acceptor functionalized polyHIPEs

5.3.2.1 Synthesis of polyHIPEs

Unsaturated polyester resin (UPR), glycidyl methacrylate (GMA) and divinylbenzene (DVB) were the monomers used in the preparation of polymers with high internal phase emulsion; additionally,

triethanolamine (TEA) was used as an emulsifier with toluene or tetrahydrofuran (THF) as the porogen. Water formed the aqueous phase to produce polyHIPEs with 85% internal phase. Radical initiator Azobisisobutyronitrile (AIBN) facilitated the cross-linking of the HIPEs which was accomplished through curing of UPR with GMA and DVB mixtures. Four different types of polyHIPEs were prepared by varying the amount of monomers and the type of porogen (monomer: porogen = 1:1 (wt%/wt%)) used in the polymerization process. Table 5.1 shows the different composition variations of the synthesized polyHIPEs, which were named according to their UPR/GMA/DVB content as follows: P1 (70/18/12 with Toluene), P2 (70/18/12 with THF), P3 (30/50/20 with Toluene) and P4 (30/50/20 with THF). The schematic for step-wise synthesis of polyHIPEs is shown in Figure 5.1 and follows the method used by Mert et al. [123]. UPR, GMA, DVB, toluene/THF and TEA were mixed in a 500 mL round bottom flask and stirred at room temperature with a magnetic stirrer at 350 rpm. Afterwards, AIBN was added and the mixture was allowed to stir for 30 min. 85 mL of water was added drop-wise with constant stirring to form the internal phase. Cream-like emulsion was formed when the mixture was stirred for another 60 min. To obtain the porous monoliths, the emulsion was transferred to the mold and the internal phase was removed after curing of the dispersed phase at 80 ºC for 24 h. Methanol was used for the purification of the resulting polymer by soxhlet extraction. Subsequently, the polyHIPEs were dried in vacuum for 24 h at 60 ºC.

Table 5.1: Composition of ingredients for the synthesis of polyHIPEs.

PolyHIPE sample name	**Monomer composition (wt%)**			**Porogen Toluene/THF (wt%)**	**Initiator AIBN (wt%)**	**Emulsifier TEA (wt%)**	**Aqueous phase volume (mL)**
	UPR	**GMA**	**DVB**				
P1	70	18	12	Toluene, 100	2	30	85
P2	70	18	12	THF, 100	2	30	85
P3	30	50	20	Toluene, 100	2	30	85
P4	30	50	20	THF, 100	2	30	85

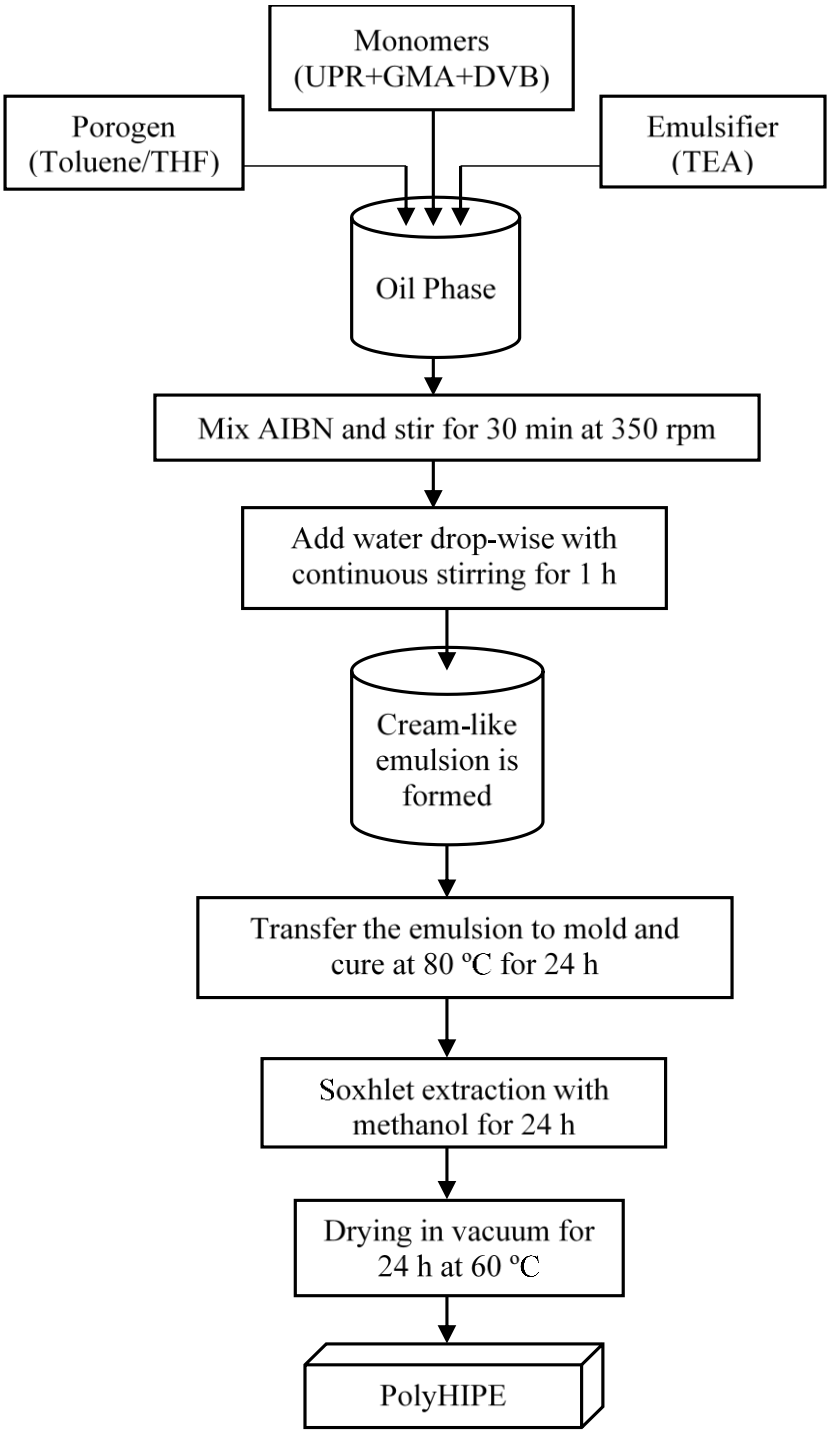

Figure 5.1: Schematic for step-wise synthesis of GMA-polyester based poly (high internal phase emulsion)s (polyHIPEs).

5.3.2.2 Procedure for immobilizing π-acceptor on polyHIPEs

Reactive epoxy groups present in GMA were used for the modification of synthesized polyHIPEs. Acetone oxime (represented as, –ON) was used as a linker between polyHIPEs and the π-acceptor, TENF. A mixture of acetone oxime (15 g) and N,N-dimethyl formamide (130 mL) was charged in a 250 mL two-necked flask fitted with a condenser. The mixture was heated at 100 °C and 32 g of potassium carbonate was added while stirring the mixture at 300 rpm. Finally, 24 g of the polyHIPE monoliths were added and the mixture was stirred for 24 h. Once the reaction was complete, polymer beads were filtered and washed with distilled water and ethanol. The modified polyHIPEs were dried at 80 °C for 24 h. In this method, the linker was attached to the monoliths using epoxy groups as the reactive platform and the oxime substituted polyHIPEs P1, P2, P3 and P4 were named as, P1-ON, P2-ON, P3-ON and P4-ON, respectively.

Finally, π-acceptor (TENF) was immobilized on all four modified polyHIPEs (P1-ON, P2-ON, P3-ON and P4-ON) via oxime linker; hereafter referred to as P1-ON-TENF, P2-ON-TENF, P3-ON-TENF and P4-ON-TENF, respectively. 5.3 g of TENF was mixed with 90 mL of acetic acid in a two-neck flask with condenser at 100 °C. Then, p-toluene sulfonic acid monohydrate (5 g) was added to the mixture. Afterwards, 19.5 g of modified polyHIPEs obtained in the second stage were added. The mixture was allowed to stir at 300 rpm and was refluxed for 3 days. TENF immobilized polyHIPEs obtained from this reaction were filtered through frit and washed with toluene and dried in vacuum for 24 h at 80 °C to get the yellow powder. The synthesis follows reactions as conducted by Misra et al. [22] for the immobilization of TENF on poly (GMA-co-EGDMA) beads. Reaction scheme for all the stages of π-acceptor functionalized polyHIPE is shown in Figure 5.2.

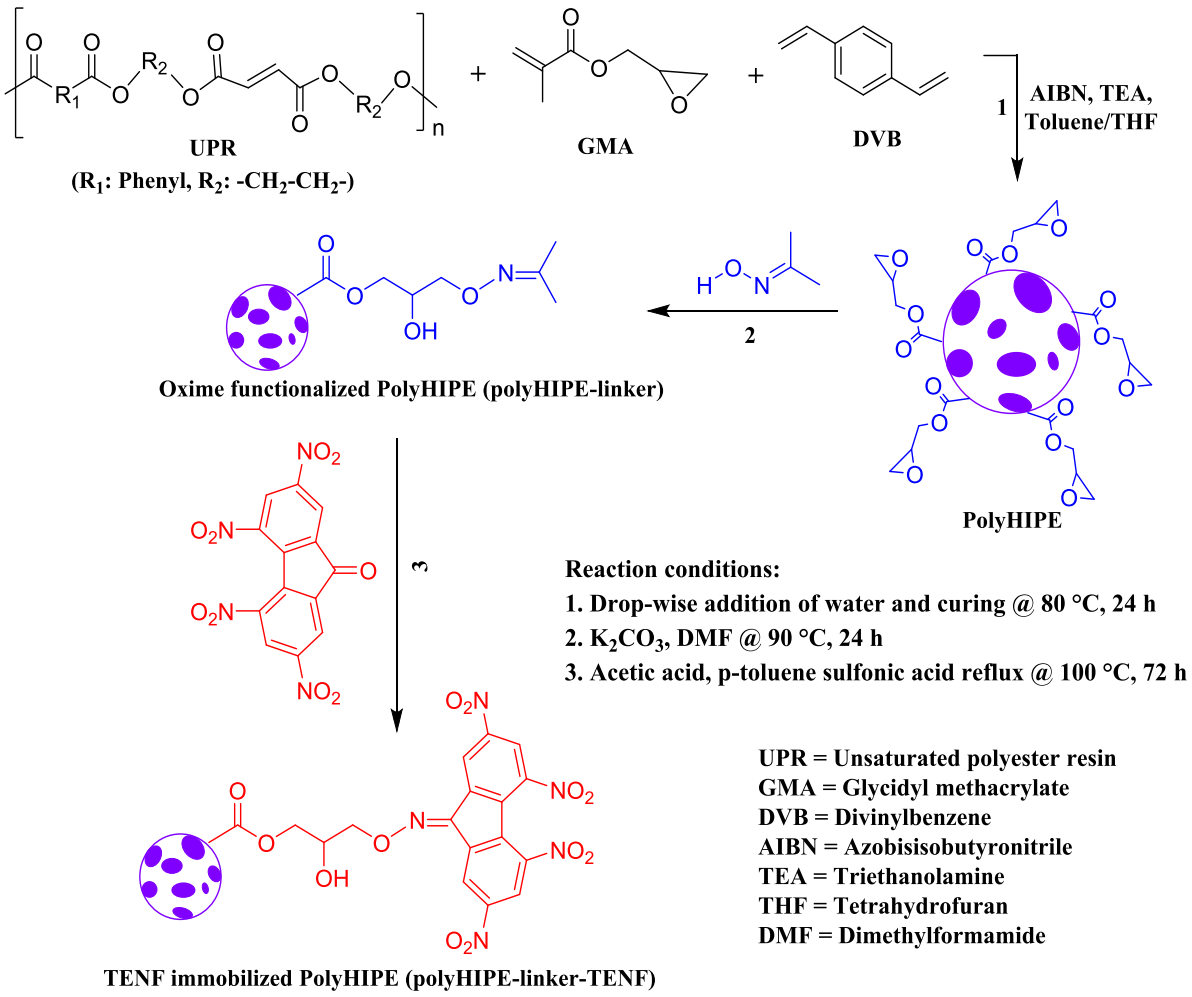

Figure 5.2: Reaction scheme for the synthesis of π-acceptor functionalized polyHIPE.

5.3.3 Characterization techniques

Textural properties of the polyHIPE samples were determined by Micromeritics 2000 ASAP analyzer (Micromeritics, Nacross, GA, USA) using Brunauer–Emmett–Teller (BET) method. Analysis was performed using N_2 at 77 K. Scanning electron microscopy images for polyHIPEs and π-acceptor functionalized polyHIPEs were obtained by Hitachi field emission scanning electron microscope (FE-SEM) SU6600 machine at 2.0 kV and different magnifications. Thermal gravimetric/differential thermal analyzer (TG/DTA) from TA instrument, Q-5000, V20.13 model (TA instruments, New Castle, DE, USA) was used to determine the thermal degradation profiles of the polymer beads. Carbon, hydrogen, nitrogen and oxygen content for all stages of polymer synthesis was determined using Vario EL III CHNS elemental analyzer (Elementar Americas Inc.,

Mt. Laurel, NJ, USA). In order to determine the characteristic functional groups present in the polyHIPE samples, Fourier transform infrared (FT-IR) spectra were obtained using a PerkinElmer Spectrum GX instrument (PerkinElmer, Waltham, MA, USA). Total sulfur and nitrogen content of the untreated and treated light gas oil was measured by Antek Model 9000 Nitrogen/Sulfur analyzer (ANTEK Instruments Inc., Houston, TX, USA) using pyro-fluorescence technique (ASTM D5453 method) and pyro-chemiluminescence technique (ASTM D4629 method), respectively.

5.4 Results and discussion

5.4.1 Polymerization of GMA based polyHIPEs

Cross-linking of double bonds of unsaturated polyester with the monomer mixture of GMA and DVB and subsequent removal of aqueous phase was performed to obtain the polyHIPEs. Radical initiator, AIBN helped in the cross-linking of UPR/GMA/DVB mixture. TEA was used as an emulsifier to stabilize the water in oil emulsion which forms salts by reacting with carboxylic groups of UPR and these salts provide the stability during the removal of dispersed phase at 80 ºC. In order to reduce the viscosity of the mixture, DVB was used as the diluent monomer which also promotes the cross-linking of the polymer. As shown in Table 5.2, the surface area of the polyHIPEs increases while the pore size decreases on increasing the amount of GMA and DVB and reducing the polyester resin in the continuous phase of the mixture. Resulting polyHIPE, P3 has the highest surface area of 6.4 m^2/g as compared to P1 and P2. Higher surface area may be attributed to the higher cross-linking of the monomer mixtures. THF and toluene are considered as suitable solvents for UPR [123], so they were added in the monomer phase to increase the surface area of polyHIPEs. However, a note-worthy decrease in the surface area was found for P4, where THF was used as a porogen instead of using toluene. Similar trends were seen on comparing P1 and P2 in which toluene and THF were added, respectively. As compared to THF, when toluene was used as a porogen, it resulted in polyHIPEs with higher surface area and lower pore sizes. Substantial change in the pore sizes of polyHIPEs is observed by changing the type of porogen. Similar trends in pore sizes of the macroporous polymers were observed by Steinke et al. [125] where mean pore diameters were observed in the range of 4.2-16.8 nm.

Table 5.2: Effect of monomer composition on the textural properties of polyHIPEs.

PolyHIPEs (UPR/GMA/DVB)	Surface area (m^2/g)	Average pore size (nm)
P1 (70/18/12 with Toluene)	2.0	8.8
P2 (70/18/12 with THF)	1.6	22.3
P3 (30/50/20 with Toluene)	6.4	8.7
P4 (30/50/20 with THF)	0.7	16.1

These polyHIPEs were synthesized for their application in the removal of heterocyclic nitrogen and sulfur impurities from light gas oil. Therefore, in the final stage of synthesis, the electron acceptor is immobilized on polyHIPEs via oxime linker by opening of the epoxy ring. Therefore, it is important for epoxy groups to maintain its chemical integrity. Characteristic functional groups present in the particles were determined by FT-IR spectra. Consistently, 16 scans in the range of 400-4000 cm^{-1} were performed for the background and the sample. KBr was used for the sample preparations. As shown in Figure 5.3, vibration frequencies at 845 cm^{-1}, 908 cm^{-1} and 1270 cm^{-1} are due to the asymmetric and symmetric stretching of epoxy groups (C–O–C) [22] in all the polyHIPEs which suggest that the chemical integrity of epoxy group is maintained during the synthesis. Distinctive methacrylate ester peak at 1725 cm^{-1} is attributed to the stretching vibrations of carbonyl group (C=O) [120]. C–H stretching frequencies (sp^2 and sp^3) are shown by the peak at 2942 cm^{-1}. Broad peak at 3500 cm^{-1} represents the hydroxyl group (–OH) present in the polyHIPEs [18].

Thermal gravimetric analysis (TGA) was performed to determine the stability and degradation profiles of all the synthesized GMA based polyHIPEs. For the analysis, 10-20 mg of polymers were placed in platinum pans in the TA instrument. After equilibration at 33 ºC, the analysis was done under nitrogen with balance and sample purge flowrates of 40 mL/min and 60 mL/min, respectively. The samples were decomposed at a ramping rate of 10 ºC/min up to 600 ºC.

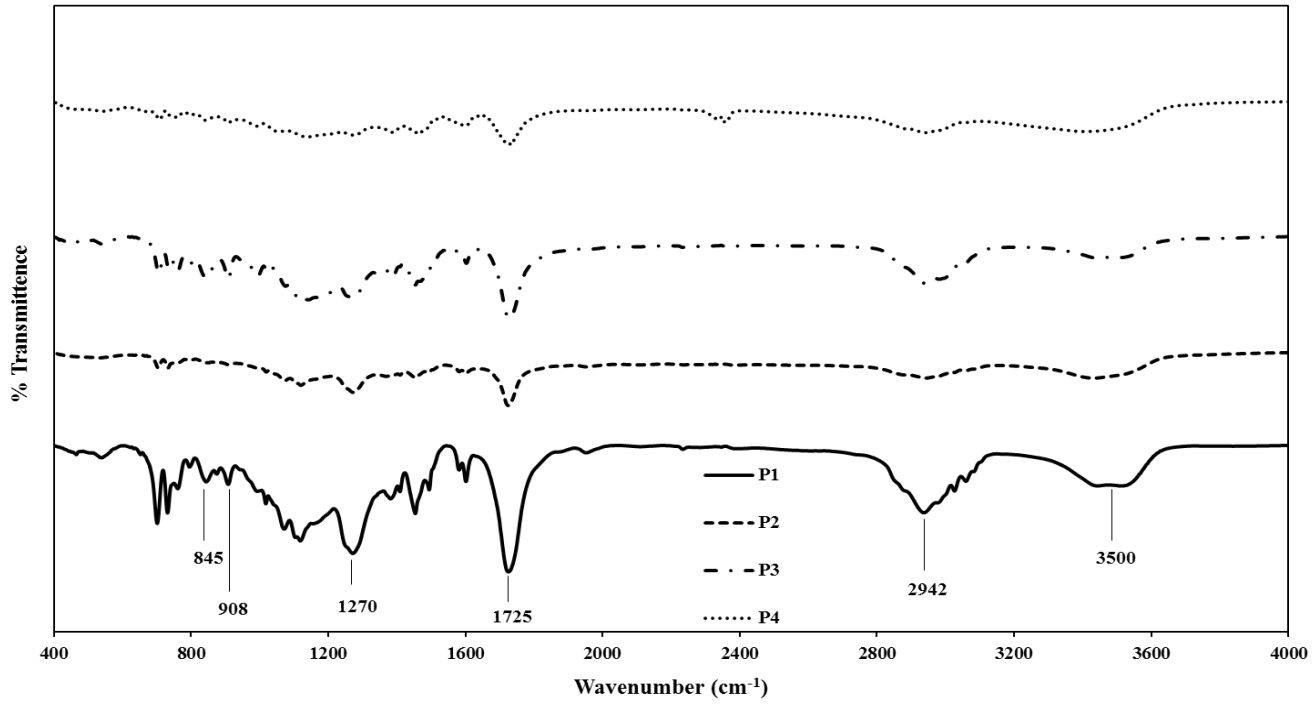

Figure 5.3: FT-IR spectra of GMA based polyHIPE particles.

Thermal weight loss and the corresponding derivative weight loss for P1, P2, P3 and P4 are shown in Figure 5.4. All the polymers were stable up to 250 ºC, which is within the working temperature range of polyHIPEs for the removal of nitrogen and sulfur impurities from light gas oil and the two major decomposition temperatures were recorded above 300 ºC. Thermal degradation of polyHIPEs proceeds in two steps as shown by the derivative weight loss curves in Figure 5.4 (b). In the first step, small peaks at 340-375 ºC are due to the random chain scission, followed by the surface decomposition at higher temperatures (390-420 ºC). P2 is the most stable amongst all four polyHIPEs, which had the onset of the decomposition temperature at 311 ºC. One clear difference in the polyHIPE series shown in Figure 5.4 (a) is that the residual at 600 ºC is more in the polyHIPEs where THF is used as the porogen. At 600 ºC, 8.1% and 7.3% of material remains for P2 and P4, respectively, whereas only 5.6% and 4.8% of material remains for P1 and P3, respectively.

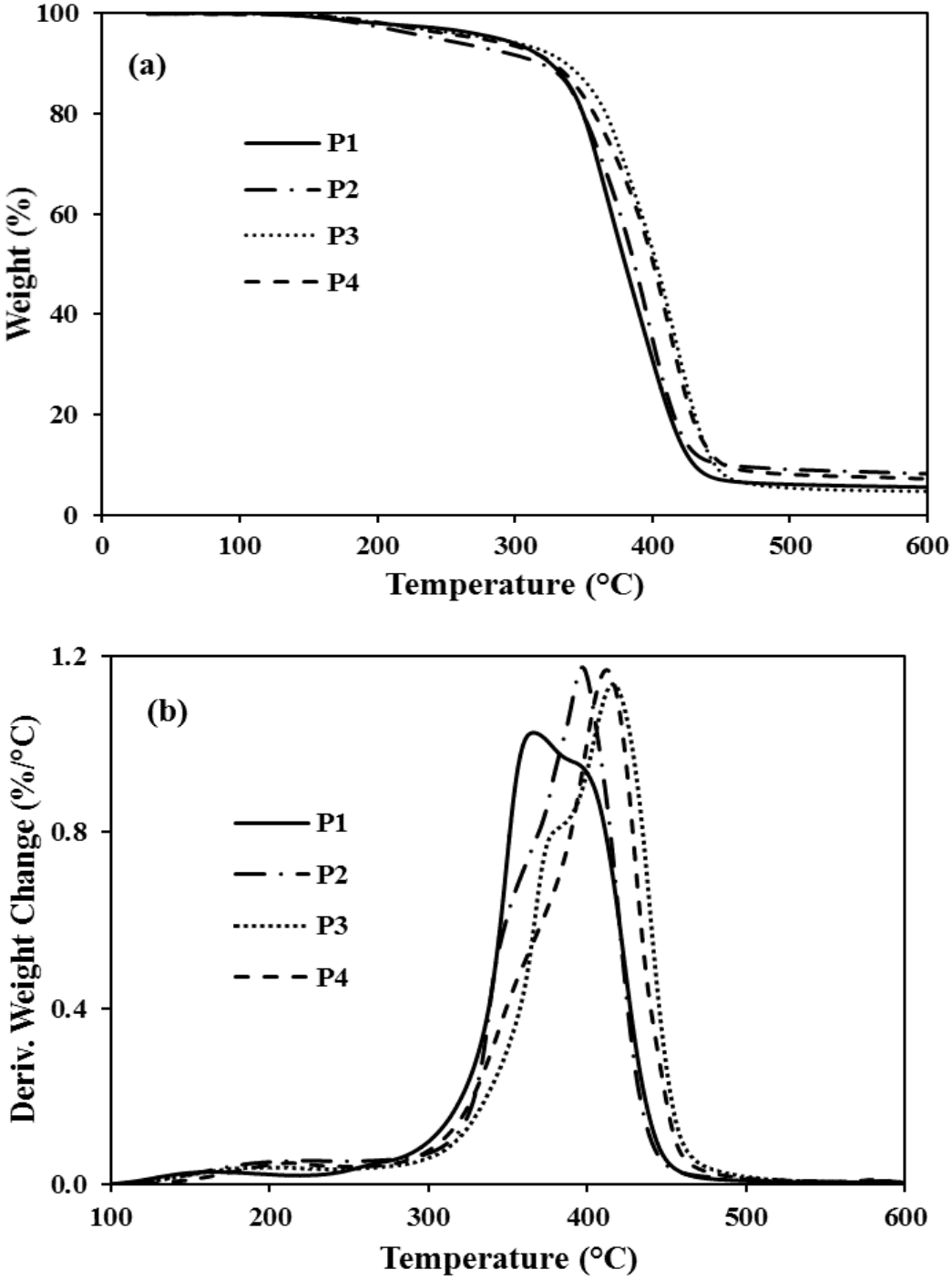

Figure 5.4: (a) TGA thermograms (heating rate 10 ºC/min) of polyHIPEs, and (b) DTG curves of polyHIPE particles.

5.4.2 Functionalization of GMA based polyHIPEs with acetone oxime and preparation of π-acceptor immobilized polyHIPEs

Figure 5.5 shows a representative FT-IR spectra that compares polyHIPE (P1) in all stages of π-acceptor immobilized polyHIPE (P1-ON-TENF) synthesis. Notable differences in the spectra of the succeeding polymer samples are observed. Acetone oxime linker was attached to the polyHIPEs synthesized in the earlier stages, by ring-opening reaction of the reactive epoxy group. This results in the disappearance of almost all the signals related to the epoxy group: 845 cm^{-1}, 908 cm^{-1} and 1270 cm^{-1}. A new peak at 1610 cm^{-1} could be assigned to the oxime functionality of the linker. Also, the broad hydroxyl peak was intensified at 3460 cm^{-1} [18]. Finally, immobilization of the π-acceptor, TENF on the P1-ON introduces the signals for the symmetric and asymmetric stretching of the nitro groups (O=N–O) at 1500 cm^{-1} and 1367 cm^{-1}, respectively [19]. Similar data was obtained for all four polyHIPE samples. These signals established that TENF was successfully immobilized on all polyHIPEs via oxime functionality resulting in the synthesis of the desired particles.

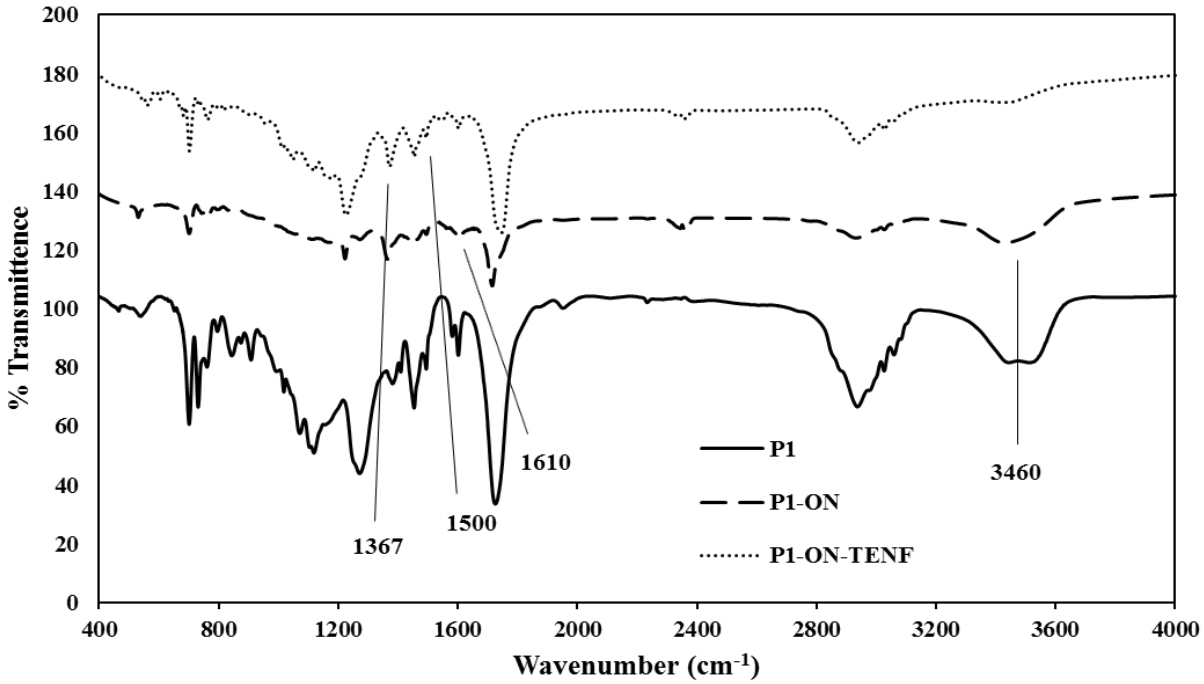

Figure 5.5: Comparison of FT-IR spectra of polyHIPE and TENF functionalized polyHIPEs: (a) P1, (b) P1-ON and (c) P1-ON-TENF.

Furthermore, CHNS analysis acknowledged the presence of oxime functionality on the polyHIPEs as the composition of elemental nitrogen increased after attaching the oxime linker. Samples were combusted in CHNS analyzer in order to determine the elemental composition of the polyHIPEs functionalized with acetone oxime. Epoxy ring present in polyHIPEs was substituted with oxime functionality to facilitate the immobilization of π-acceptor in the later stages. A comparison of the results showing an increase in the nitrogen content for all polyHIPE samples after substituting oxime functionality is shown in Table 5.3. A consistent increase of ~0.2% nitrogen was observed for P1-ON, P2-ON and P4-ON as compared to their initial counterparts. However, P3-ON exhibited a higher increase in the elemental nitrogen content upon ring opening reaction, where, nitrogen content increased from 0.39% to 1.17%. This may be attributed to the higher amount of GMA used in the synthesis. Increased elemental nitrogen content is a clear indication of the fact that nitrogen atoms are present in the linker. In addition to the elemental composition, the atomic ratios were also calculated. A significant decrease in carbon to nitrogen ratio was observed for all oxime functionalized polyHIPEs due to an increase in the total nitrogen content.

Table 5.3: CHNS elemental analysis of polyHIPEs and oxime functionalized polyHIPEs.

Sample Name		**Elemental composition**				**Atomic ratio**	
		%(wt./wt.)					
		Nitrogen	**Carbon**	**Hydrogen**	**Oxygen**	**C/H**	**C/N**
Polymer-1	P1	0.46	71.20	6.85	21.50	10.40	156.48
	P1-ON	0.74	71.94	7.01	20.31	10.26	97.35
Polymer-2	P2	0.54	69.16	6.88	23.43	10.06	129.27
	P2-ON	0.70	68.07	6.77	24.46	10.06	97.24
Polymer-3	P3	0.39	69.93	7.34	22.34	9.53	181.17
	P3-ON	1.17	66.34	7.43	25.06	8.93	56.75
Polymer-4	P4	0.88	65.12	7.66	26.34	8.50	73.83
	P4-ON	1.09	64.24	7.50	27.17	8.56	58.99

As mentioned before, the epoxy ring present in GMA was further modified by ring opening with acetone oxime. Oxime functionalized polyHIPEs provide an adaptable platform for the immobilization of π-acceptor, TENF. As shown in Table 5.4, a general increase in the surface area of all polyHIPE monoliths was observed after attaching the acetone oxime linker on the polyHIPE particles. Moreover, after the immobilization of the π-acceptor (TENF) consistent decrease in the surface area of polyHIPE samples is observed. However, the pore size of the final polyHIPE-linker-TENF particles increases predominantly as compared to polyHIPE-linker series for all the polymers except for the polymer-1, where the pore size decreased from 13.7 nm to 8.9 nm. Despite having low surface areas (0.2-30 m^2/g), the large channels present in polyHIPEs could facilitate the adsorption of large nitrogen compounds.

Table 5.4: Comparison of the BET surface area and pore size of polyHIPEs, acetone oxime functionalized polyHIPEs (polyHIPE-ON) and TENF immobilized polyHIPEs (polyHIPE-linker-TENF).

Sample Name		**Surface area (m^2/g)**	**Average pore size (nm)**
Polymer-1	P1	2.0	8.8
	P1-ON	9.6	13.7
	P1-ON-TENF	9.0	8.9
Polymer-2	P2	1.6	22.3
	P2-ON	3.4	9.6
	P2-ON-TENF	2.2	21.4
Polymer-3	P3	6.4	8.7
	P3-ON	38.6	6.6
	P3-ON-TENF	30.0	9.5
Polymer-4	P4	0.7	16.1
	P4-ON	2.7	36.6
	P4-ON-TENF	0.2	77.8

It is interesting to note that surface morphology of the polyHIPE monoliths is complex and different as compared to the beads synthesized by suspension polymerization method using identical monomers under same conditions. In this work, all polyHIPEs were successfully synthesized from UPR/GMA/DVB mixture using monomer ratios of 70:18:12 or 30:50:20.

Figures 5.6 (a) and (b) show SEM images of P1 and P2 which were prepared using the same monomer ratio of 70:18:12 but two different porogens were used. Since toluene is a better solvent for these polymers as compared to THF; the monoliths which were prepared using toluene as the porogen have smaller pores (P1: 8.8 nm) as compared to the monoliths in which THF (P2: 22.3 nm) was used.

At the beginning of the polymerization process the porogenic solvents alter the solvation of polymeric chains. Earlier phase separation occurs if poor solvents such as THF is used, which results in larger pores. These results are in confirmation with pore size analysis of the polyHIPEs using BET instrument (results of which are shown in Table 5.4). Another method to increase the pore size deals with decreasing the monomer to porogen ratio but increased pore sizes results in decreased homogeneity of the macroporous polymers [125,126].

After the π-acceptor was immobilized on these polyHIPEs, the change in porous texture and morphology is shown in Figures 5.6 (c) and (d). The microstructure of P1-ON-TENF consists of quite densely packed overlapping blocks. On the contrary, P2-ON-TENF microstructure consists of extremely fused microgels which results in a rough morphology. Since THF was used as the solvent for these types of polymers, the particles have agglomerated into large and ill-defined clusters. This has resulted in the polymers with low surface areas. However, relatively small change in the range of 0.01-0.04% in pore size of polyHIPEs was observed in case of π-acceptor immobilized polymers.

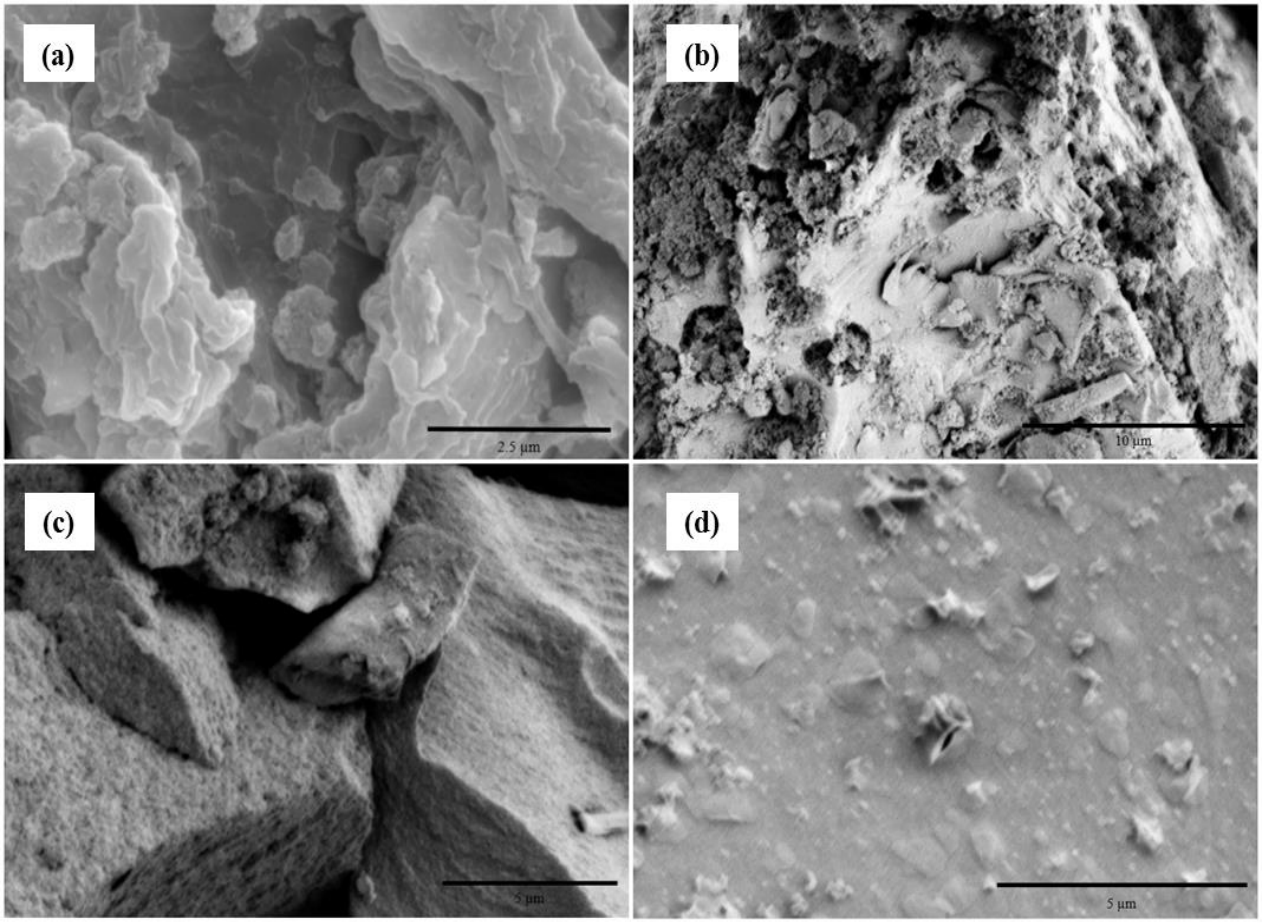

Figure 5.6: SEM micrographs of: (a) P1, (b) P2, (c) P1-ON-TENF, and (d) P2-ON-TENF.

Figures 5.7 (a) and (b) represent the difference in the degradation profiles of polyHIPEs as compared to the polyHIPEs modified with linker and the π-acceptor. The first decomposition peak for P1 ($T_{max}1$ = 368 °C) is larger as compared to the second decomposition peak at 400 °C. It is vice versa for P1-ON and P1-ON-TENF series i.e. their respective smaller peaks appear at $T_{max}1$ (300-340 °C) while, larger peaks appear at about 378-395 °C ($T_{max}2$). Moreover, P1-ON-TENF series has two clearly distinct decomposition peaks, as compared to P1 and P1-ON series. The distinguishable change in the degradation profiles of all three stages of polymer synthesis indicate that the overall functionality has changed by attaching the TENF on polyHIPEs via oxime linker. As shown in Table 5.5, for all four polyHIPE-linker-TENF particles, the average temperature range is ~ 302 °C (for the first degradation step) and ~ 384 °C (for the second degradation step). Furthermore, the amount of TENF grafted on these polyHIPEs was calculated based on the first

degradation step. The particles with higher GMA composition than UPR have higher grafting of TENF. Total graft amount of 0.47 mmol/g and 0.25 mmol/g was found in P1-ON-TENF and P2-ON-TENF, respectively, while, P3-ON-TENF and P4-ON-TENF have total grafting of 0.78 mmol/g and 0.92 mmol/g, respectively. It is evidently due to the high number of reactive epoxy groups present in GMA.

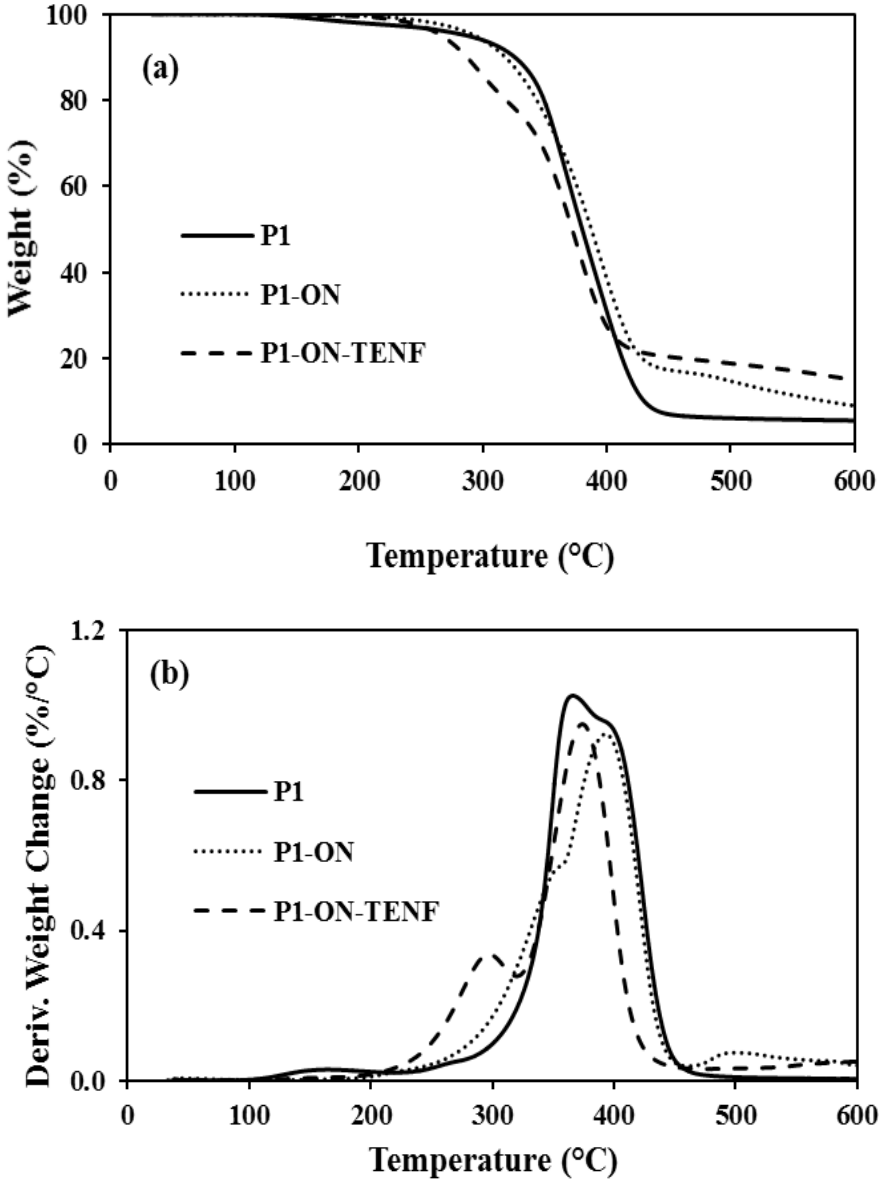

Figure 5.7: Comparison of the thermal decomposition of polyHIPEs, polyHIPE-linker and polyHIPE-linker-TENF series for polyHIPE-1: (a) TGA thermograms, and (b) DTG curves of the particles.

Table 5.5: Characteristic thermal decomposition properties of all the polyHIPE-linker-TENF series particles.

Particles	T_{onset} (°C)	T_{max} (°C)		Residue (wt%) @ 600 °C	Weight loss (wt%) @ 1st step	Total graft amount @ 1st step (mmol/g)
		$T_{max}1$	$T_{max}2$			
P1-ON-TENF	211	300	377	14.9	20.2	0.47
P2-ON-TENF	239	303	376	16.8	11.0	0.25
P3-ON-TENF	212	304	379	21.4	33.1	0.78
P4-ON-TENF	230	302	403	11.7	40.0	0.92

5.4.3 Removal of nitrogen and sulfur containing compounds from light gas oil

Total nitrogen and sulfur removal capacities of TENF immobilized polyHIPEs were investigated using bitumen-derived light gas oil. Its physical and chemical composition is shown in Table 5.6 [22]. In a batch reactor, kept at ambient temperature (23 °C), the adsorbent polymers (P1-ON-TENF, P2-ON-TENF, P3-ON-TENF and P4-ON-TENF) were mixed with light gas oil (LGO) in a ratio of 1:4 (wt./wt.). When the amount of adsorbent was increased, it resulted in a highly viscous mixture; thereby reducing the contact of the mixed stream. Therefore, 1 g of each adsorbent was stirred with 4 g of LGO at 200 rpm for 24 h and then vacuum filtration was used to separate the treated oil from the adsorbent particles. ANTEK Nitrogen/Sulfur analyzer was used to calculate the total nitrogen and sulfur concentrations of untreated and treated light gas oil. To assure the reliability on nitrogen and sulfur concentrations of untreated and treated light gas oil, the adsorption tests were performed three times for all the polymeric adsorbents and the average was taken to report the final results.

Total nitrogen and sulfur removal was calculated as follows [22]:

$$\text{N/S removal (\%)} = \frac{\text{initial N/S content (ppm)- final N/S content (ppm)}}{\text{initial N/S content (ppm)}} \text{ X } 100 \qquad (5.1)$$

Removal percentage of both nitrogen and sulfur compounds present in bitumen derived LGO using polymeric adsorbents was investigated in order to determine the effect of different polymer supports with varying textural properties. As shown in Figure 5.8, P3-ON-TENF has the highest nitrogen removal of 14.6%, followed by P1-ON-TENF and P4-ON-TENF with 3.5% and 1.7% nitrogen removal, respectively; with small influence on the sulfur impurities (0.5-0.7% sulfur removal). However, P2-ON-TENF is ineffective towards nitrogen and sulfur compounds. The results are in agreement with the BET analysis of the adsorbents shown in Table 5.4. TENF immobilized polyHIPEs with higher surface area are capable of adsorbing higher amount of heterocyclic nitrogen impurities with the only exception of P2-ON-TENF. Despite having the surface area of 2.2 m^2/g, P2-ON-TENF does not adsorb nitrogen compounds. On the contrary, P4-ON-TENF has the lowest surface area of 0.2 m^2/g amongst all adsorbents, but it is capable of removing 1.7% of the nitrogen compounds. The large channels (pore size: 77.8 nm) present in the particles facilitate the adsorption of heterocyclic nitrogen compounds.

Table 5.6: Characterization of bitumen-derived light gas oil (LGO).

Parameter	**LGO**
Sulfur content (ppm)	29257
Nitrogen content (ppm)	1676
Density (g/ml)	0.90
Aromatic content (%)	30.2
Simulated distillation	
IBP (ºC)	159
FBP (ºC)	502

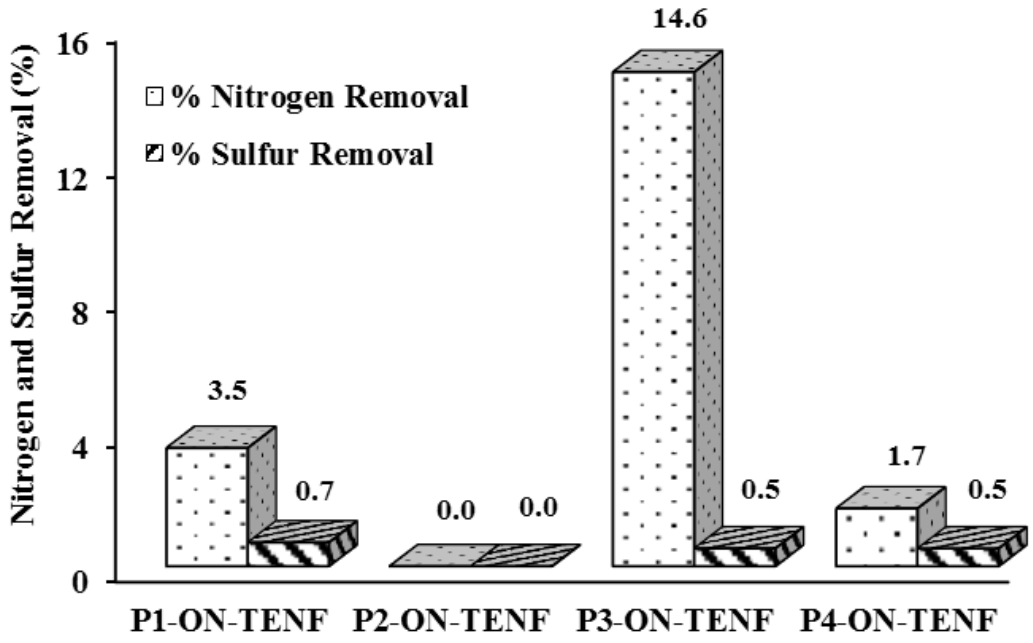

Figure 5.8: Batch adsorption results using fresh polymeric adsorbents and light gas oil in 1:4 particle to oil ratio at 23 ºC mixed for 24 h.

Moreover, the total graft amount of TENF on polyHIPEs calculated from TGA analysis substantiate the obtained results. Based on the studies conducted by several researchers [18–20,22], π-acceptor, TENF was grafted on the polyHIPEs via oxime functionality for the purpose of selectively removing heterocyclic nitrogen compounds from bitumen-derived LGO via charge transfer complex mechanism. As shown in Table 5.5, P3-ON-TENF has higher graft amount of TENF (0.78 mmol/g) as compared to P1-ON-TENF and P2-ON-TENF, having 0.47 mmol/g and 0.25 mmol/g of grafting, respectively. Therefore, P3-ON-TENF attracts higher amount of nitrogen compounds than its corresponding counterparts. However, P4-ON-TENF has the highest TENF grafting of 0.92 mmol/g which should be responsible for its high nitrogen adsorption capacity. Despite that, it removes only 1.7% nitrogen and 0.5% sulfur impurities. Based on the scholarly investigation of the structure of TENF by Sevignon et al. [65], it can be explained as the steric hindrance around TENF molecules. Higher number of TENF molecules present in P4-ON-TENF leads to higher steric hindrance and is clearly reflected in these batch adsorption study results.

5.4.4 Polymer regeneration and reusability tests

Additionally, used polymeric adsorbents were regenerated using soxhlet extraction with toluene as the regenerating solvent at 110 °C for 48 h. The regenerated particles were dried in vacuum at 90 °C for 24 h. BET analysis of the regenerated samples revealed the changes in the textural properties after regeneration. Table 5.7 shows the reduction in the surface area and pore size of all four regenerated polymers which leads to lower percentage of nitrogen and sulfur removal as compared to the fresh particles. As shown in Figure 5.9, the regenerated particles were incapable of removing any sulfur compounds. However, the nitrogen removal declined from 3.5% to 0.6% for Regenerated-P1-ON-TENF, 14.6% to 8.2% for Regenerated-P3-ON-TENF and 1.7% to 0.0% for Regenerated-P4-ON-TENF particles. Notwithstanding the cleaning of the particles using toluene, the textural properties of the regenerated particles did not improve significantly. This is due to the fact that the heterocyclic nitrogen compounds formed strong charge transfer complexes with the π-acceptor (TENF) and were adsorbed onto the polymeric adsorbent particles.

Table 5.7: Textural properties of fresh and regenerated polyHIPE-linker-TENF particles.

Sample Name		**Surface area (m^2/g)**	**Average pore size (nm)**
PolyHIPE-1	P1-ON-TENF	9.0	8.9
	Regenerated-P1-ON-TENF	5.0	7.3
PolyHIPE-2	P2-ON-TENF	2.2	21.4
	Regenerated-P2-ON-TENF	1.9	10.9
PolyHIPE-3	P3-ON-TENF	30.0	9.5
	Regenerated-P3-ON-TENF	29.0	7.9
PolyHIPE-4	P4-ON-TENF	0.2	77.8
	Regenerated-P4-ON-TENF	0.04	18.6

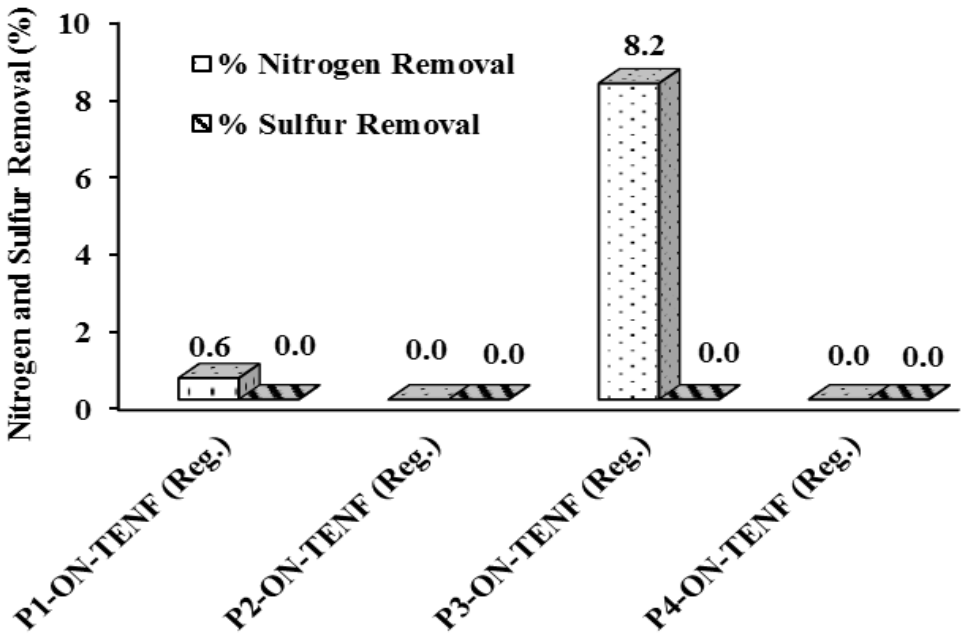

Figure 5.9: Percentage of nitrogen and sulfur compounds removed after contacting the regenerated adsorbents with LGO at conditions: particle to oil ratio = 1:4, 23 ºC, and 24 h.

5.5 Conclusions

In this study, novel polymer based adsorbents were synthesized for their successful application in the removal of nitrogen and sulfur compounds from bitumen-derived light gas oil. The chemical and textural properties of the polymer monoliths were directly related to the type of monomeric mixtures and porogenic solvents used in the synthesis. Among the two porogens (THF and toluene) used in the preparation method, particles with toluene generally had a higher surface area. However, particles with THF were thermally more stable. The polyHIPE with UPR/GMA/DVB (30/50/20 ratio) mixture in the presence of toluene as porogen has the highest surface area, which is a key factor in determining the adsorption capacity of the polyHIPEs. The surface area was in the range of 0.7-6.4 m^2/g. The pore diameter of the polyHIPEs also varied widely from 8.7-22.3 nm. The immobilization of the π-acceptor (TENF) on the polyHIPEs was succeeded via oxime functionality. BET analysis indicated a general increase in the surface area of all the polymeric adsorbents after immobilizing the TENF. For instance, the surface area of polyHIPE-3 increased from 6.4 m^2/g (for P3) to 30 m^2/g (for P3-ON-TENF). Similarly, the surface area of polyHIPE-1 increased from 2 m^2/g (for P1) to 9 m^2/g (for P1-ON-TENF). Both textural and chemical properties

played an important role in the adsorption of heterocyclic compounds. P2-ON-TENF has a surface area of 2.2 m^2/g and pore size of 21.4 nm while its π-acceptor (TENF) loading is 0.25 mmol/g. On the other hand, surface area and pore size of P4-ON-TENF are 0.2 m^2/g and 77.8 nm, respectively with highest TENF loading of 0.92 mmol/g. Suboptimal textural properties along with the least TENF loading were the factors responsible for incompetence of P2-ON-TENF to adsorb nitrogen compounds. Despite having low surface area, the large pores present in P4-ON-TENF along with highest TENF loading facilitated the adsorption of large nitrogen compounds. Based on the batch adsorption studies, the nitrogen removal percent of the adsorbents decrease in order of P3-ON-TENF > P1-ON-TENF > P4-ON-TENF > P2-ON-TENF where P3-ON-TENF is capable of removing 14.6% of nitrogen compounds during the first contact with light gas oil at room temperature. These results clearly showed that TENF immobilized polyHIPEs can be effectively used for the removal of nitrogen and sulfur compounds from light gas oil.

Chapter 6: Denitrogenation and desulfurization of model diesel fuel using functionalized polymer: Charge transfer complex formation and adsorption isotherm study

---

A similar version of this chapter is under review as a research article in Chemical Engineering Journal and a part of this work was presented at the following conference:

- Misra, P., Badoga, S., Chenna, A., Dalai, A. K. & Adjaye, J. "Denitrogenation and desulfurization of model diesel fuel using functionalized polymer: Charge transfer complex formation and adsorption isotherm study". *Chemical Engineering Journal* - In Press, Accepted Manuscript (2017).
- Misra, P., Dalai, A. K. & Adjaye, J. "Selective removal of nitrogen species from bitumen derived gas oil using π-acceptor immobilized polymers: efficient approach towards improving hydrotreatment technology". *AIChE 2014 Annual Meeting*, Atlanta, Georgia, USA, 16-21 November 2014.

Contribution of the Ph.D. candidate

Model feed preparation, polymer synthesis, and characterization of charge transfer complexes was done by Prachee Misra. Adsorption constants and thermodynamic parameters were calculated by Prachee Misra with assistance from Dr. Sandeep Badoga. Akshay Chenna helped Prachee Misra with the batch adsorption experiments for isotherm study and model fitting (in MATLAB®). All the manuscript writing and revision work was done by Prachee Misra based on the suggestions from Drs. Ajay Dalai, John Adjaye, and Sandeep Badoga.

Contribution of this chapter to the overall Ph.D. work

This part of work is focused on the understanding of adsorption mechanism of nitrogen and sulfur compounds over functionalized polymer and charge transfer interactions between electron donors and acceptors.

6.1 Abstract

This study is a perquisite to the fundamental understanding of the adsorption of heterocyclic nitrogen and sulfur compounds present in petroleum feedstock over fluorenone derived π-acceptor functionalized polymers. Quinoline (basic nitrogen compound), 9-ethylcarbazole (non-basic nitrogen compound) and dibenzothiophene (sulfur compound) were scanned to study the adsorptive denitrogenation and desulfurization of model diesel fuel. Batch reactor was used to compare the adsorption capacity and selectivity of these compounds at three sets of temperature (298 K, 313 K and 328 K). Total Nitrogen/Sulfur analyzer measured the change in nitrogen and sulfur content of the model fuels after adsorption over π-acceptor, 2,4,5,7-tetranitro-9-fluorenone (TENF) functionalized polymer. 60% extraction of total nitrogen compounds was obtained in one step, whereas the sulfur reduction was only 23% from a mixed model feed containing 700 ppm each of nitrogen and sulfur compounds. Charge transfer complexes were easily detected by the appearance of new bands in the visible region of UV-vis absorption spectrum. Functionalized polymer contributed towards higher adsorption of quinoline as compared to carbazole derivative and dibenzothiophene. Adsorption of these compounds was found to be reversible and multilayer over the heterogeneous surface of the functionalized polymer. At 298 K, maximum adsorption capacity increases as follows: quinoline > dibenzothiophene > 9-ethylcarbazole. Calculation of the thermodynamic properties revealed that the adsorption is favorable and spontaneous in nature. Molar enthalpies were calculated between -3.9 to -22 kJ/mol; which are characteristic of the electron donor acceptor complexes.

6.2 Introduction

The oil and gas sector can meet the stringent environmental regulations by deploying an improved technology which is capable of supplying cleaner fuels. One of the approaches for increasing the hydrotreating activity of the feed is the removal of catalyst inhibitors prior to hydrotreating. To obtain ultra clean diesel fuel, it is important to reduce sulfur and nitrogen content of the feed before hydrotreating to avoid catalyst inhibition and deactivation. Adsorption is a widely used process for removing toxic contaminants present in varying concentration. Adsorption of nitrogen and sulfur compounds using activated carbon, activated alumina, nickel-based adsorbents, metal organic frameworks, TiO_2 nanoparticles and TiO_2 nanotubes, zeolite based materials and ion-exchange

resins [8,17,50,51,106,127–129] is widely reported in open literature. However, no significant work is reported on the adsorption isotherm study using π-acceptor functionalized polymers. Due to the electron rich nature of the heterocyclic nitrogen and sulfur species, they tend to favor charge transfer complex (CTC) formation with electron deficient compounds [64,130,131]. For different fluorenone based π-acceptors, number of electron withdrawing nitro groups attached to the fluorenone moiety plays an important role in charge transfer complexation. Hence, fluorenone derived, 2,4,5,7-tetranitro-9-fluorenone (TENF) which contains four electron withdrawing nitro groups has been studied as a π-acceptor by researchers and it shows favorable results [132–136]. Meille et al. [137] tested equimolar solution of 4,6-DMDBT and 1-methylnaphthalene in heptane (11 mmol/L) at ambient temperature in the presence of dodecane and found that TENF has the maximum separation factor for 4,6-DMDBT which is reached rapidly. A selectivity factor of 137 was reported for 4,6-DMDBT complexation as compared to 1-methylnaphthalene just after 4.5 h of stirring which increased to >1000 after 29 h. Similarly, Lemaire et al. [5] tested equimolar amounts of 4,6-DMDBT (196 mg), 1-methylnaphthalene (131 mg) and dodecane (157 mg) in heptane for complexation with TENF. They reported that the complex formed between TENF and 4,6-DMDBT is the best in terms of specificity, where high value of selectivity was achieved instantaneously, demonstrating that 1-methylnaphthalene remained in the solution while 4,6-DMDBT formed CTC with TENF. The effect of aromatics in model feed is widely reported in the literature. However, oil contains multifarious compounds which can form CTC with the π-acceptor. Therefore, to make the acceptor selective towards the targeted nitrogen and sulfur impurities, it is immobilized on a polymer support; subsequently improving their separation and filtration after CTC formation.

Based on the nitrogen and sulfur removal results obtained during the screening of different types of functionalized polymers, we have selected fluorenone based π-acceptor, 2,4,5,7-tetranitro-9-fluorenone (TENF) functionalized on the poly glycidyl methacrylate-co-ethylene glycol dimethacrylate (PGMA) polymer support; henceforth referred to as “functionalized polymer” or “PGMA-ON-TENF” to study the adsorption isotherms, owing to its high adsorption efficiency towards sulfur and nitrogen compounds from bitumen-derived gas oil. Carbazole derivatives are found in abundance in the heavy feeds and are responsible for hydroprocessing catalyst inhibition and deactivation [71,138], therefore, 9-ethylcarbazole was selected as one of the model compounds

in this study. Quinoline is a widely used model compound for denitrogenation studies because it is a reasonable representation of the six-membered nitrogen compounds present in crude oil. Hence, quinoline was chosen to represent basic nitrogen in the model feed. Other than heterocyclic nitrogen species, sulfur compounds are also present in crude oil in excessive concentrations. Thiophene, dibenzothiophene and its derivatives are the most refractory sulfur compounds that are present in the heavy complex fuels derived from unconventional resources, and the sulfur removal from these species is difficult during hydroprocessing [139]. Accordingly, dibenzothiophene (DBT) represented the class of thiophenic compounds in this model feed study. With the aim of determining the adsorption mechanism and thermodynamics of the process, the adsorption isotherms were plotted and compared. Selectivity of the functionalized polymer towards nitrogen and sulfur species was found by changing the donor molecules. Charge transfer complex formation between π-acceptor (TENF) and π-donors (quinoline, 9-ethylcarabazole, dibenzothiophene) is the underlying mechanism which leads to the removal of nitrogen and sulfur impurities from oil feed. Therefore, detailed study of the formation of charge transfer complexes was also accomplished in this work. Values of the thermodynamic parameters such as, change in Gibbs free energy, enthalpy, and entropy have been reported for the first time for the complexation of quinoline, 9-ethylcarbazole and dibenzothiophene with TENF functionalized polymer.

6.3 Experimental details and methodology

6.3.1 Materials and analytical methods

Heterocyclic sulfur and nitrogen compounds; dibenzothiophene (≥98%), quinoline (98%), 9-ethylcarbazole (97%) and dodecane (≥99%) were purchased from Sigma Aldrich, Edmonton, Canada. Dimethyl sulfoxide spectrophotometric grade (>99.9%) was purchased from VWR, Edmonton, Canada. All the chemicals were used without additional purification.

Fourier transform infrared (FT-IR) spectra in the range of 400−4000 cm^{-1} were obtained using a Bruker Vertex 70 FTIR spectrometer with a diamond ATR crystal for the spectroscopic analysis of charge transfer complex formed between electron donors and acceptors. Shimadzu UV mini 1240 spectrophotometer was used to record UV-vis spectra. 0.025 M solution of π-acceptor and 0.075 M solutions of π-donors were prepared in dimethyl sulfoxide for UV-vis analysis using

quartz cuvette. TA instrument, Q-5000 model thermo gravimetry analyzer (TGA) was used to calculate the graft amount of π-acceptor on the polymer support. Antek 9000 Nitrogen/Sulfur analyzer was used to calculate the nitrogen and sulfur content of the model fuels.

The adsorbent, PGMA-ON-TENF was synthesized in laboratory using the method described in our previous work, which has the surface area of 57 m^2/g and pore size of 23 nm. The first degradation step of the adsorbent in thermo gravimetry analyzer revealed that 0.89 mmol/g of π-acceptor (TENF) was grafted on PGMA support via oxime linker. The synthesis procedure and detailed characterization of the polymer have been reported previously in literature [140].

6.3.2 Model feed

Four types of model feeds were prepared for this study. First model feed (MF-1) was prepared by adding single nitrogen (quinoline or 9-ethylcarbazole) or sulfur (dibenzothiophene) compound in dodecane in the same molar concentration (75 µmol/g) in order to obtain the adsorption capacity and selectivity of the polymeric adsorbent. The composition of MF-1 is shown in Table 6.1 (a). Second model feed (MF-2) was prepared for the adsorption isotherm study. Single nitrogen (quinoline or 9-ethylcarbazole) or sulfur (dibenzothiophene) compounds were prepared in varying concentration. Molar concentrations for the nitrogen compounds were 5 µmol/g, 12.5 µmol/g, 25 µmol/g, 50 µmol/g, 75 µmol/g and the sulfur compound were 20 µmol/g, 45 µmol/g, 75 µmol/g, 110 µmol/g, 140 µmol/g in dodecane. The composition of MF-2 is shown in Table 6.1 (b).

Third model feed (MF-3) was the mixed compound model feed containing 700 ppm nitrogen and 700 ppm sulfur. It was a mixture of all three: basic nitrogen, non-basic nitrogen and sulfur compounds (350 ppm quinoline, 350 ppm 9-ethylcarbazole and 700 ppm dibenzothiophene were added together). The composition of MF-3 is shown in Table 6.1 (c). Concentration of the fourth model feed, MF-4 is mentioned in Table 6.1 (d), which was prepared to study the effects of increasing sulfur concentration on the adsorption phenomena. All the model feeds were prepared in dodecane, analyzed using N/S analyzer and the calculated concentrations (in ppm) lies between ±5% error.

Table 6.1: Composition of model feeds prepared in dodecane for the adsorption studies.

(a): Composition of MF-1 (individual nitrogen or sulfur compound mixed in dodecane).

Feed name	Compound	Molar concentration (µmol/g)	Concentration (ppmN or ppmS)
Feed-1	Quinoline	75	1050
Feed-2	9-ethylcarbazole	75	1050
Feed-3	Dibenzothiophene	75	2404

(b): Composition of MF-2 (individual nitrogen or sulfur compounds in varying concentrations).

Compounds in MF-2	Molar concentration (µmol/g)				
Quinoline	5	12.5	25	50	75
9-ethylcarbazole	5	12.5	25	50	75
Dibenzothiophene	20	45	75	110	140

(c): Composition of MF-3 (mixed model feed with equal concentration of total nitrogen and total sulfur).

Compounds in MF-3	Molar concentration (µmol/g)	Concentration (ppmN or ppmS)
Quinoline	25	350
9-ethylcarbazole	25	350
Dibenzothiophene	21.9	700

(d): Composition of MF-4 (nitrogen and sulfur mixed model feeds with constant total nitrogen concentration and varying sulfur concentration).

Feed name	Quinoline (µmol/g)	9-ethylcarbazole (µmol/g)	Dibenzothiophene (µmol/g)	Concentration	
				ppmN	ppmS
MMF-1	7.9	7.9	6.9	220	220
MMF-2	7.9	7.9	14.1	220	450
MMF-3	7.9	7.9	21.9	220	700
MMF-4	7.9	7.9	34.4	220	1100
MMF-5	7.9	7.9	46.9	220	1500

6.3.3 Batch adsorption studies

The adsorbent sample was placed in a 20 mL glass vial and heated overnight at 90 °C in a vacuum oven prior to adsorption experiments. The sample was cooled inside the oven and stored in a desiccator later. 3 g of the polymeric adsorbent was stirred with 12 g of the model feed in a glass bottle for 24 h at 200 rpm. To study the effect of temperature on the adsorption capacity, three sets of temperatures (25 ºC, 40 ºC and 55 ºC) were studied. Afterwards, the liquid feed was separated from the adsorbent using vacuum filtration. Model feed samples were carefully withdrawn with glass pipette and were analyzed to obtain the nitrogen and sulfur content. Similar procedure was followed for each adsorption experiment.

6.4 Results and discussion

6.4.1 Spectroscopic characterization of charge transfer complexes

Separation of refractory sulfur and nitrogen compounds from the feed was based on the principle of interaction between electron donor and acceptor molecules [141]. Analysis of molecular orbital interaction of the electron donors and acceptors reveal the stability and strength of the complexes. Overall stability depends on the electronic distribution of higher occupied molecular orbital (HOMO) of electron donor and lowest unoccupied molecular orbital (LUMO) of electron acceptor. During complex formation, the energy gap between HOMO and LUMO is reduced which results in the formation of colored complexes [64]. 0.025 M solution of π-acceptor (TENF) and 0.075 M solutions of π-donors (quinoline, 9-ethylcarbazole and dibenzothiophene) were prepared in dimethyl sulfoxide (DMSO) and mixed in 1:1 ratio; leading to spontaneous color change of the mixture due to the formation of charge transfer complexes. The mixture was stirred at room temperature for 24 h and the resulting colored precipitates (as shown in Figure 6.1) were filtered.

Absorption spectroscopy is the conventional technique used for the characterization of the charge transfer complexes. The electron donor-acceptor (EDA) model mentioned in the work by Hunter and Sanders [142] to describe π-π interactions suggests that charge transfer complexes result in broadened UV-vis absorption spectrum. The appearance of electronic absorption in the UV visible region is due to the intermolecular charge transfer. Hence, UV-vis absorption spectra were obtained

for the charge transfer complex mixtures. For comparison, spectra of individual donor and acceptor molecules were also recorded.

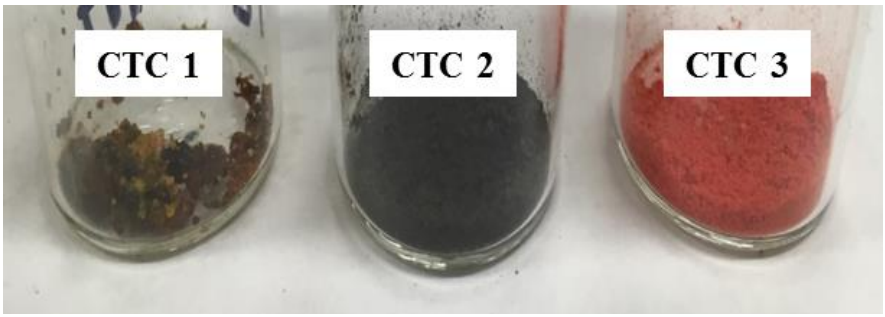

Figure 6.1: Colored crystals of the CTC were obtained by mixing electron donors with the π-acceptor. CTC-1, 2, 3 are charge transfer complexes between TENF and quinoline, 9-ethylcarbazole and dibenzothiophene, respectively.

It was observed that the charge transfer complexes have broadened spectrum in the visible range (λ = 400 to 700 nm) while the donor and acceptor units do not show significant absorption bands in this region, which is in agreement with the intermolecular charge transfer complex studies performed by various researchers [5,81,137,143]. The absorption spectrum of TENF, quinoline, 9-ethylcarbazole, dibenzothiophene and CTC formed between these species are compared in Figure 6.2. Electron acceptor TENF does not show an absorption band after 450 nm, which is consistent with the UV-vis spectra of another nitro substituted derivative of fluorenone (2,4,7-trinitrofluorenone) reported by Hu et al. [83]. Maximum absorption for quinoline was observed at 315 nm which is similar to the quinoline band at 306 nm reported by Correia at al. [144]. Addition of TENF to a solution of quinoline in DMSO resulted in rust colored complex followed by the appearance of a new absorption band in the visible region of the UV-vis spectrum ranging from 450 nm to 700 nm as shown in Figure 6.2 (a).

9-ethylcarbazole has an absorption maximum at 360 nm which is typical for carbazole derivatives [82]. As shown in Figure 6.2 (b), mixture of 9-ethylcarbazole and TENF gave rise to an absorption band in the visible region centered about 600 nm, resulting in black colored complex. The absorption spectra of thiophene derivative used in this study was alike the substituted

dibenzothiophene spectra reported by Meille et al. in their charge transfer complex studies with no absorption band after 350 nm [137]. Dibenzothiophene and TENF formed an orange color CTC which showed a broad absorption band in the visible region in Figure 6.2 (c). These results indicated the strong complex forming ability of TENF with the heterocyclic nitrogen and sulfur compounds.

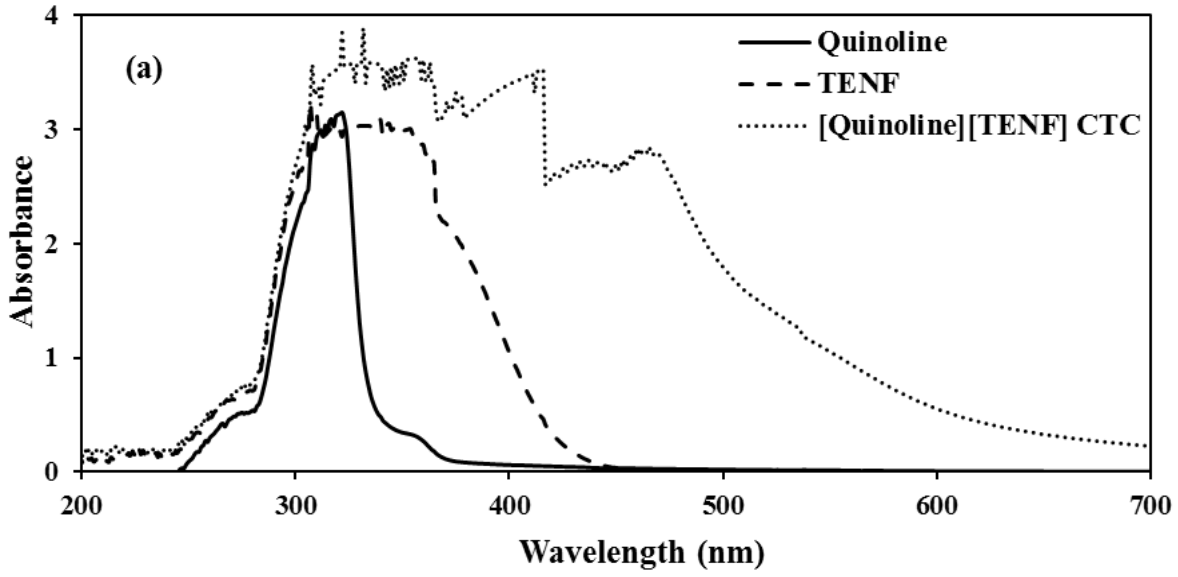

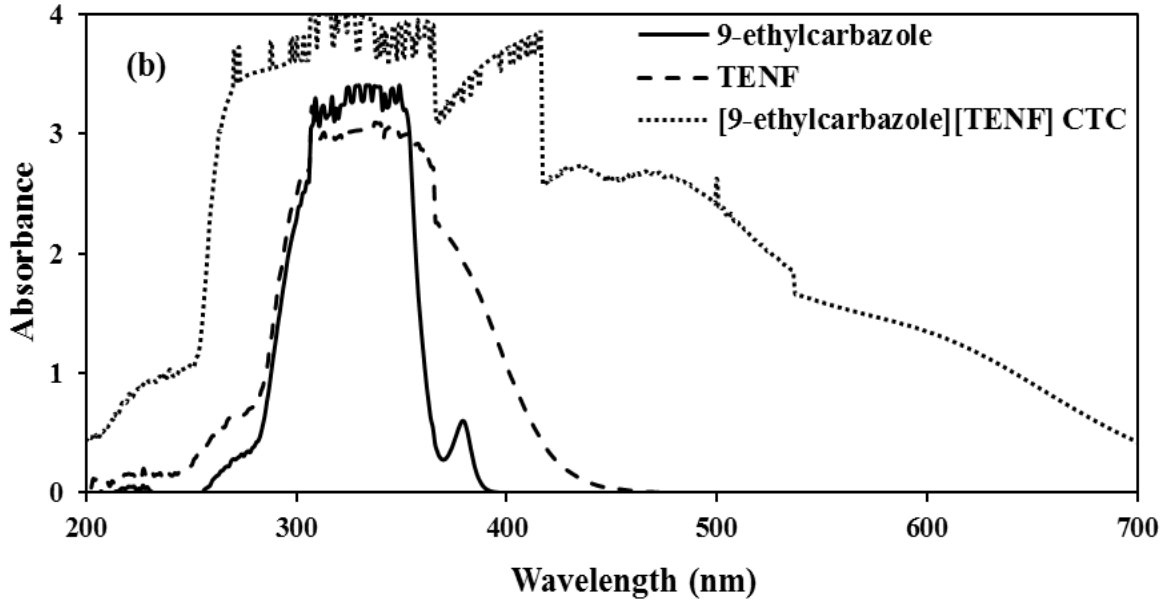

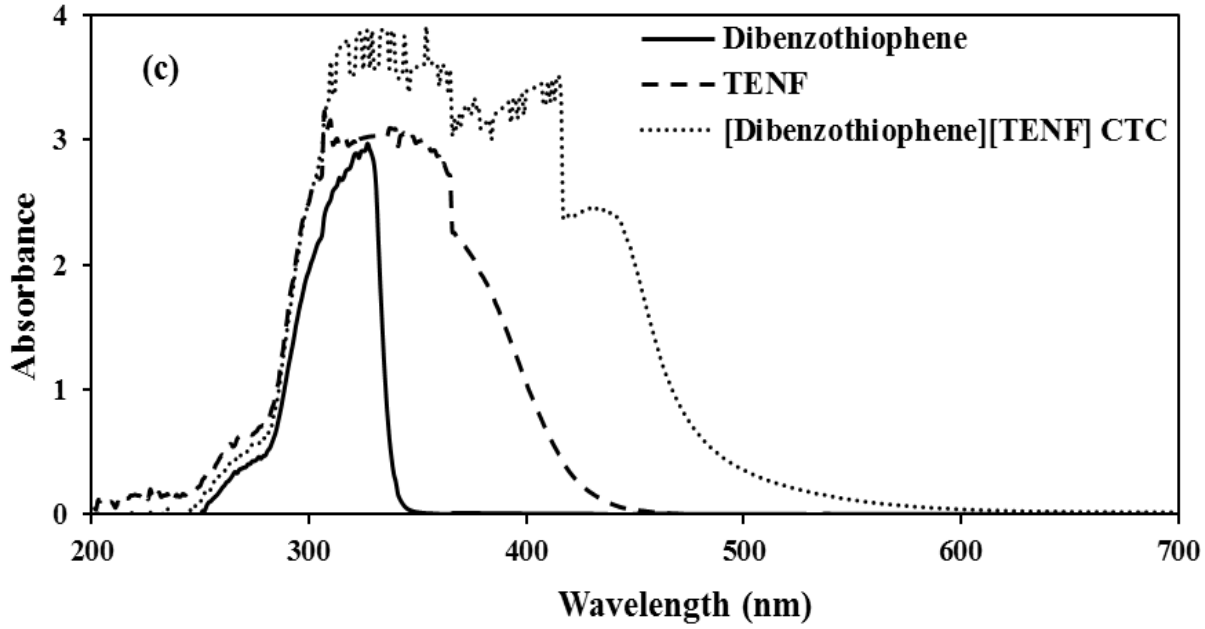

Figure 6.2: UV-vis absorbance spectra of CTC between acceptor TENF and the donors: (a) [Quinoline][TENF] CTC, (b) [9-ethylcarbazole][TENF] CTC and (c) [Dibenzothiophene][TENF] CTC in DMSO for 1:1 molar mixture.

FT-IR spectra also exhibited the formation of strong donor acceptor charge transfer complexes. Comparison of the infrared spectra of the donor (9-ethylcarbazole), acceptor (TENF) and the obtained charge transfer complex, [9-ethylcarbazole][TENF] CTC is shown in Figure 6.3. The C-H stretching vibrations for 9-ethylcarbazole appeared at 3047 cm^{-1} and 2977 cm^{-1}; for TENF at 3085 cm^{-1} and 2979 cm^{-1}; and for [9-ethylcarbazole][TENF] CTC, the vibrations shifted to 2993 cm^{-1} and 2912 cm^{-1}. Peaks at 1594 cm^{-1} and 1598 cm^{-1} are due to C=C bending in 9-ethylcarbazole and TENF, respectively. However, the peak intensity was smaller in the charge transfer complex. The collected bands in the region of 860-680 cm^{-1} were assigned to C-H bending vibrations and were observed at 783 cm^{-1}, 750 cm^{-1} and 721 cm^{-1} for 9-ethylcarbazole; and at 786 cm^{-1}, 769 cm^{-1}, 727 cm^{-1} and 707 cm^{-1} for TENF. These peaks appeared at lower wavenumber values of 756 cm^{-1}, 729 cm^{-1}, 696 cm^{-1} and 667 cm^{-1} for [9-ethylcarbazole][TENF] CTC [145,146].

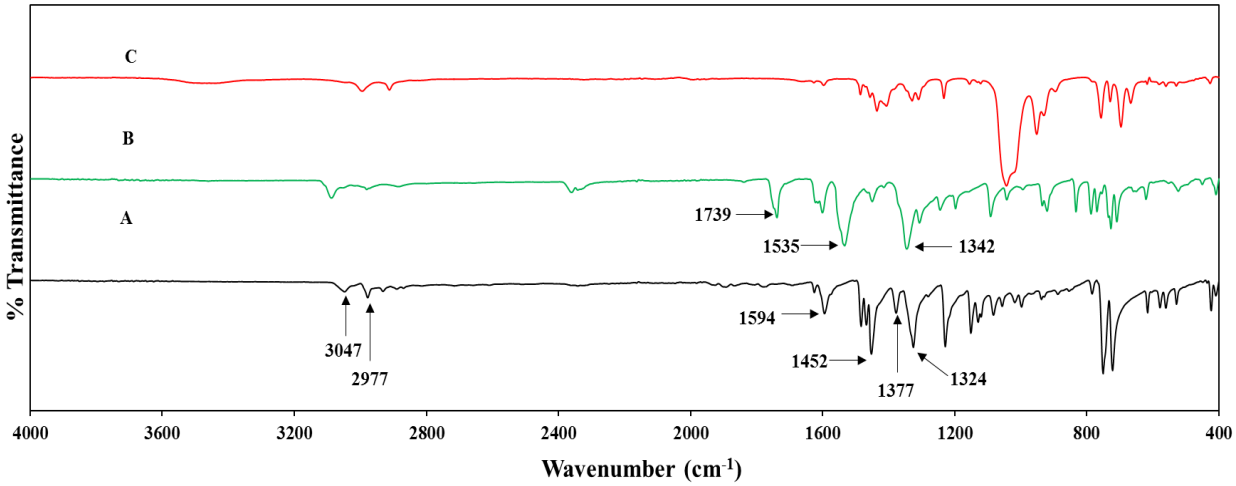

Figure 6.3: FT-IR spectra of (A) 9-ethylcarbazole (B) TENF (C) [9-ethylcarbazole][TENF] CTC.

The most notable change was observed in carbonyl and nitro group vibrations of the electron acceptor. C=O stretching band present in TENF at 1739 cm^{-1} reduced significantly in intensity and appeared at lower frequency at 1625 cm^{-1} in the spectra of charge transfer complex. One reason could be the change in electron density of the region which resulted in the increase in carbonyl bond length and decrease in its frequency [147]. Additionally, two strong bands were observed at 1535 cm^{-1} and 1342 cm^{-1} for asymmetric and symmetric stretching of N=O groups present in TENF while the peaks drastically shifted to lower wavenumber values and lesser intensity at 1485 cm^{-1} and 1330 cm^{-1} which clearly indicates intermolecular interactions between donor and acceptor molecules [148]. It was found that FT-IR spectra of the black colored CTC of 9-ethylcarbazole and TENF contains the principal bands for both the reactants. Nevertheless, shift in the wavenumber frequencies and changes in the band intensities of the CTC as compared with the reactants were observed due to electronic structure modifications during complex formation which concluded the formation of charge transfer complex [149]. Similar spectra were observed for the CTCs formed between the π-acceptor, TENF and other nitrogen and sulfur heterocyclic compounds (quinoline and dibenzothiophene). The π-acceptor, TENF has four strong electron withdrawing nitro groups in conjugation with aromatic rings and allowed for a stronger electron donation from quinoline, 9-ethylcarbazole and dibenzothiophene.

6.4.2 Evaluation of functionalized polymer as adsorbent

In order to evaluate the feasibility of the adsorption process, MF-1 which contains equimolar concentrations of single nitrogen or sulfur compounds, was used to calculate the extraction efficiency, E (%) and distribution coefficient, D according to Equations 6.1 and 6.2, where C_i and C_f are the initial and final concentrations (ppm) of the studied compounds, M_f and M_s are the model feed weight (g) and mass of solid adsorbent (g), respectively [150].

$$E\ (\%) = \frac{(C_i - C_f)}{C_i} \times 100 \qquad (6.2)$$

$$D = \frac{(C_i - C_f)}{C_f} \times \frac{M_f}{M_s} \qquad (6.3)$$

Quantitative assessment of the selectivity of the adsorbent towards nitrogen compounds as compared to sulfur was done by calculating the distribution coefficients and using the following selectivity factor (Equation 6.3), where D_N and D_S are the distribution coefficients of the compounds N and S, respectively.

$$S_{N/S} = \frac{D_N}{D_S} \qquad (6.4)$$

The capacity, q (mmol/g) of the polymer to adsorb nitrogen and sulfur compounds was calculated according to Equation 6.4:

$$q = \frac{M_f\,(C_i - C_e)}{M_s} \qquad (6.5)$$

Where, M_f is the model feed weight (g), C_i and C_e are the initial and equilibrium concentrations of the solute in the model feed (ppm), respectively and M_s is the mass of solid adsorbent (g).

The extraction results from the batch adsorption tests performed at room temperature are reported in Table 6.2. Using pure dodecane as the solvent, distribution coefficient of quinoline was found to be high. The adsorbent showed a higher distribution coefficient of 5.8 for quinoline with high nitrogen/sulfur (quinoline/dibenzothiophene) selectivity ($S_{N/S}$ > 5) which represented higher affinity of the adsorbent towards quinoline. Distribution coefficient of dibenzothiophene was 1.1 which is comparable to the literature value of 1.2, reported by Xie et al. using ionic liquids [150]. The adsorption process was further investigated and higher extraction of quinoline as compared to 9-ethylcarbazole and dibenzothiophene was found. As expected, the adsorption capacity of the

polymer is high (0.18 mmol/g) for quinoline and follows the following order: quinoline > dibenzothiophene > 9-ethylcarbazole.

Additionally, we determined the polymer's adsorption capacity without the acceptor (PGMA only) using MF-1. It was found that the extraction efficiency decreased due to the absence of electron withdrawing π-acceptor on the adsorbent's surface. Moreover, the adsorption capacity of PGMA-ON-TENF was higher as compared to the commercially available ion-exchange resins (IXR) such as, resins bearing pyridinium chloride functionality and Amberjet4200Cl reported in literature [129].

Table 6.2: Functionalized polymer extraction efficiency, distribution coefficient, selectivity factor relative to dibenzothiophene and adsorption capacity at equimolar concentrations of single nitrogen or sulfur compound (adsorbent/model feed = 0.25, 24 h at 298 K).

Feed name	Compound	Molar Conc. (μmol/g)	PGMA E (%)	PGMA-ON-TENF E (%)	D_N or D_S	$S_{N/S}$	q (mmol/g)
Feed-1	Quinoline	75	46	59	5.8	5.2	0.18
Feed-2	9-ethylcarbazole	75	5	17	0.8	0.7	0.05
Feed-3	Dibenzothiophene	75	15	22	1.1	-	0.07

The yield of the adsorption process was found to be promising for MF-3 adsorption on PGMA-ON-TENF. In a mixed feed containing both sulfur and nitrogen in equal concentration, 60% of nitrogen compounds were removed whereas only 23% of sulfur was adsorbed. It signifies that the polymeric adsorbent is more selective towards nitrogen compounds. Also, the adsorbed sulfur was only 27.7% of the total adsorbed nitrogen and sulfur in contrast to 50% of the sulfur present in the initial feed. Therefore, it is worth noting that nitrogen compounds compete with sulfur for the active sites on polymer and the polymer is favorable towards adsorbing nitrogen compounds. With model feed MF-4 as the adsorbate, it was observed that increase in the sulfur concentration had no effect on the nitrogen removal efficiency of the adsorbent (as shown in Figure 6.4). Upon increasing the concentration of sulfur from 220 to 1500 ppm, it was observed that adsorbent's nitrogen extraction efficiency was apparently constant (total nitrogen removal = 55 - 59%).

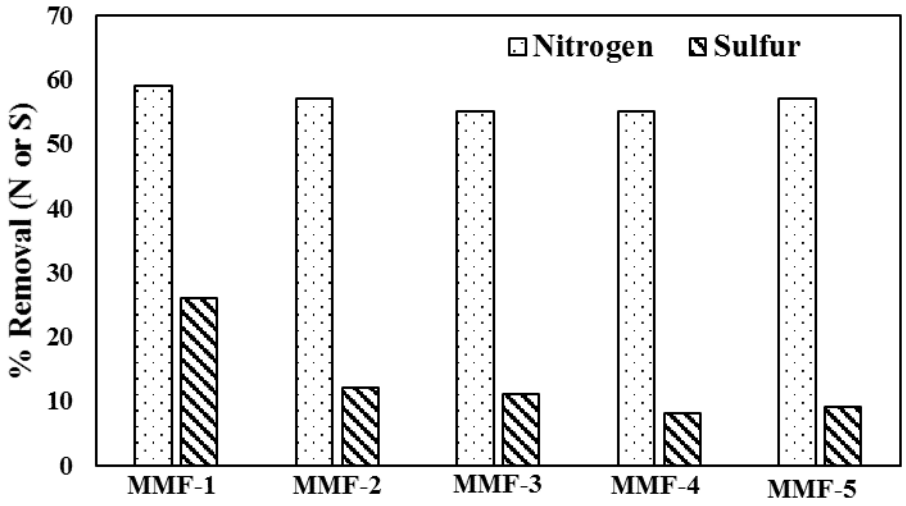

Figure 6.4: Effect of increasing sulfur concentration from 220 to 1500 ppm on the extraction efficiency of the polymer (N conc. = 220 ppm, adsorbent/model feed = 0.25, 24 h at 298 K).

Overall results obtained during evaluation of the functionalized polymer as an adsorbent using different model feeds could be explained by charge transfer between quinoline, 9-ethylcarbazole, dibenzothiophene (electron rich) and the π-acceptor, TENF (electron deficient). Based on the theoretical and experimental studies on the petroleum feedstock; spatial overlap of the frontier molecular orbitals of electron acceptors and donors can be associated with charge transfer complexation capabilities. Considering the electron-rich structure of dibenzothiophene, quinoline and 9-ethylcarbazole, they are capable of forming insoluble CTC with π-acceptors. According to the charge transfer complex studies conducted by Milenkovic et al. [61], determination of highest occupied molecular orbital (HOMO) and oxidation potential of the electron donors can illustrate their CTC formation abilities. Furthermore, the rate of complexation and strength of interaction is best with lowest LUMO energy levels of the π-acceptors (the lower the LUMO level, the stronger will be the interaction with the donor molecules). They observed that the HOMO level 4,6-dimethyldibenzothiophene (4,6-DMDBT) is higher as compared to 1-methylnaphthalene which resulted in stronger complexation of 4,6-DMDBT with the electron acceptor. Therefore, higher the HOMO level of the considered π-donor, the lower will be their oxidation potential and stronger is the alliance with the π-acceptor. HOMO values of the studied electron acceptors are shown in Table 6.3 [61,63,151], which demonstrated their complexing abilities.

Table 6.3: Summary of HOMO energy levels of electron donors.

π-donors	**Name**	**HOMO (eV)**
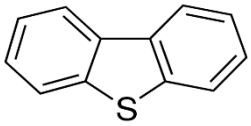	Dibenzothiophene (DBT)	-8.60
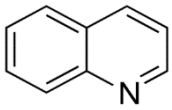	Quinoline	-8.41
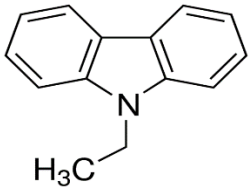	9-ethylcarbazole	-7.36

Removal of quinoline is higher as compared to dibenzothiophene due to the higher HOMO level of quinoline. Regardless of the highest HOMO of 9-ethylcarbazole, the extraction of this compound was found to be the lowest. It can be explained based on the steric hindrance caused by the alkyl substituent in the carbazole derivative. On the contrary, overlap between the molecular orbitals of dibenzothiophene and TENF is more competent because the HOMO of dibenzothiophene is symmetrical with respect to the vertical plane which is the same as LUMO of TENF.

Additionally, the electron acceptor TENF was immobilized on the polar polymer support using a linker to achieve higher complexation of nitrogen compounds. It was mentioned that the nitrogen compounds have similar HOMO as dibenzothiophene. Besides, sulfur compounds are present in higher concentration in real feed and can compete with nitrogen compounds to form charge transfer complexes. Thus, nitrogen/sulfur selectivity of the functionalized polymer can be low. However, the polar nature of heterocyclic nitrogen compounds can be exploited for its interaction with the

complexing agent. The polymer support is required to have at least one polar function which is capable of forming hydrogen bond with polyaromatic nitrogen compounds. The bond can be established between the hydrogen linked to an electronegative heteroatom present in non-basic nitrogen compounds and an electronegative heteroatom present on the polymer or it can be formed between hydrogen linked to an electronegative heteroatom present on the polymer and a negative heteroatom present in basic nitrogen compounds [152]. Therefore, glycidyl methacrylate based polar polymer PGMA favored selective complexation of quinoline. Formation of hydroxylamine linker allowed functionalization of polymer with TENF without replacing electron withdrawing nitro group at the fluorenone moiety and symmetry of the π-acceptor was also preserved. The results demonstrated that the charge transfer complex formation mechanism along with the nature of polymeric support play an important role in the adsorption of nitrogen and sulfur impurities and revealed the extraction properties of the functionalized polymers.

6.4.3 Adsorption isotherms

In this work, adsorption isotherms describe the interaction of quinoline, 9-ethylcarbazole and dibenzothiophene with the TENF functionalized PGMA adsorbent, which is vital for the successful design of the adsorption system and evaluating surface properties, adsorption capacities and affinities. Model feed, MF-2 with varying initial concentrations of quinoline, 9-ethylcarbazole and dibenzothiophene was used for determining the isotherm data. The precise concentration values before and after adsorption were found using NS analyzer. The data were then used to compute the equilibrium adsorption capacity which in turn was employed to determine the isotherm governing the adsorption phenomenon.

Adsorption of heterocyclic nitrogen and sulfur compounds present in the diesel fuels is widely described by Langmuir and Freundlich isotherms [9,17,48,53–56]. Adsorption isotherms of quinoline, 9-ethylcarbazole and dibenzothiophene on the novel polymeric adsorbent were determined and correlated with these empirical models to understand the adsorption equilibrium and mechanisms. The data was regressed using least squares method for linear and non-linear forms of the model using MATLAB 2015a along with Curve-Fitting toolbox (Mathworks Inc.) to estimate the physicochemical parameters.

Langmuir Isotherm [57]: The mathematical expression of the Langmuir isotherm model is as follows:

$$q_e = \frac{q_m K_L C_e}{1+K_L C_e} \qquad (6.5)$$

Where, q_m (mmol/g) is the maximum monolayer coverage capacity on the surface of the polymer, K_L (L/mg) denotes the Langmuir isotherm constant, which is an energy constant, indicating intensity of adsorption and C_e is the equilibrium concentration of the solute in the model feed (ppm).

Freundlich Isotherm [58]: The mathematical expression of the Freundlich isotherm model is as follows:

$$q_e = K_F C_e^{1/n} \qquad (6.6)$$

Where, K_F and 1/n are Freundlich adsorption constants. K_F, (mmol/g) $(L/mg)^{1/n}$ is an indicator of the adsorption capacity, while 1/n is a measure of adsorption intensity or surface heterogeneity. Values of n ranging between 1 and 10 represent favorable adsorption [153].

The model parameters calculated from fitting the adsorption isotherm data obtained at 298 K to these equations are given in Table 6.4. Comparing the Langmuir constant, K_L of the adsorbents, it was found that the adsorption energy of quinoline is the highest. The adsorption of heterocyclic nitrogen and sulfur compounds occurs by the formation of electron donor acceptor complexes. Due to the higher HOMO level of quinoline as compared to dibenzothiophene, it forms more stable complexes with the exception of 9-ethylcarbazole where the ethyl substituent may have caused the steric hindrance. Hence, quinoline has the highest K_L value. The amount adsorbed per gram of adsorbent corresponding to monolayer coverage decreases as follows: quinoline > dibenzothiophene > 9-ethylcarbazole. Comparison of the correlation coefficient R^2 demonstrates that the Freundlich model fits the adsorption of quinoline and 9-ethylcarbazole better than the Langmuir model. However, Langmuir and Freundlich models represent the adsorption of dibenzothiophene equally. Therefore, both models supplemented the understanding of adsorption behavior of the adsorbates.

Freundlich isotherm demonstrated multilayer adsorption where the functionalized polymer presented a heterogeneous surface for the adsorption of quinoline, 9-ethylcarbazole and dibenzothiophene. It is worth considering that the stronger binding sites of "PGMA-ON-TENF" were occupied first, followed by decrease in adsorption energy with increasing degree of site occupancy. K_F represents the adsorption capacity which decreases as follows: quinoline > dibenzothiophene > 9-ethylcarbazole. For all three adsorbates, 1/n values were measured between 0.3 and 0.8 which represents favorable adsorption. Additionally, 1/n value for quinoline is the lowest and follows the same trend as the adsorption energy determined from the Langmuir isotherm. For any adsorbate-adsorbent system, it becomes more heterogeneous as 1/n value gets closer to zero [154]. This indicated that the effect of surface heterogeneity is more pronounced for quinoline, when a stronger adsorbate-adsorbent bond is formed. Quinoline forms more stable complex with the surface functional groups which indicates its higher complexation ability as compared to 9-ethylcarbazole and dibenzothiophene. Concisely, Langmuir parameter, q_m and Freundlich parameter, K_F clearly indicated that the functionalized polymer's capacity to adsorb nitrogen and sulfur heterocyclic compounds follows the following order: quinoline > dibenzothiophene > 9-ethylcarbazole. Langmuir and Freundlich model parameters at 313 K and 328 K are reported in Table 6.5 and Table 6.6, respectively. On comparing the effects of temperature on adsorption, it was found that the adsorption of nitrogen compounds slightly declined with increasing temperature. Conversely, temperature had a noteworthy response on the adsorption of dibenzothiophene which is evident by the increase in the adsorption capacity at higher temperatures. Similar behavior of heterocyclic nitrogen and sulfur compounds during adsorption on activated carbon was reported by Wen at al. [9].

Table 6.4: Summary of Langmuir and Freundlich isotherm parameters[a] of quinoline, 9-ethylcarbazole and dibenzothiophene adsorption on PGMA-ON-TENF at 298 K.

Adsorbate	**Langmuir**				**Freundlich**		
	q_m	**K_L**	**R_L**	**R^2**	**K_F**	**1/n**	**R^2**
Quinoline	0.26	0.55	0.15-0.71	0.857	0.90	0.498	0.928
9-ethylcarbazole	0.08	0.17	0.37-0.88	0.851	0.05	0.686	0.990
Dibenzothiophene	0.12	0.04	0.38-0.80	0.757	0.10	0.517	0.766

[a] The units of parametes are: q_m = mmol/g, K_L = 100 L/mg, K_F = 100 (mmol/g) $(L/mg)^{1/n}$

Table 6.5: Summary of Langmuir and Freundlich isotherm parameters[a] of quinoline, 9-ethylcarbazole and dibenzothiophene adsorption on PGMA-ON-TENF at 313 K.

Adsorbate	Langmuir				Freundlich		
	q_m	K_L	R_L	R^2	K_F	1/n	R^2
Quinoline	0.14	1.26	0.07-0.52	0.986	1.38	0.347	0.909
9-ethylcarbazole	0.03	0.35	0.21-0.78	0.760	0.09	0.467	0.812
Dibenzothiophene	0.15	0.02	0.47-0.86	0.488	0.11	0.516	0.816

[a] The units of parametes are: q_m = mmol/g, K_L = 100 L/mg, K_F = 100 (mmol/g) $(L/mg)^{1/n}$

Table 6.6: Summary of Langmuir and Freundlich isotherm parameters[a] of quinoline, 9-ethylcarbazole and dibenzothiophene adsorption on PGMA-ON-TENF at 328 K.

Adsorbate	Langmuir				Freundlich		
	q_m	K_L	R_L	R^2	K_F	1/n	R^2
Quinoline	0.21	1.02	0.09-0.57	0.897	1.79	0.381	0.785
9-ethylcarbazole	0.03	0.25	0.28-0.84	0.906	0.08	0.482	0.899
Dibenzothiophene	0.35	0.01	0.62-0.92	0.675	0.01	0.842	0.979

[a] The units of parametes are: q_m = mmol/g, K_L = 100 L/mg, K_F = 100 (mmol/g) $(L/mg)^{1/n}$

The adsorption can be further illustrated with a dimensionless constant called the separation factor, R_L [155,156] defined as:

$$R_L = \frac{1}{1 + K_L C_o} \qquad (6.7)$$

Where, K_L (L/mg) refers to the Langmuir isotherm constant and C_o is the adsorbate initial concentration (ppm). Favorable adsorption is associated with the lower R_L values. Separation factor signifies unfavorable ($R_L > 1$), linear ($R_L = 1$), favorable ($0 < R_L < 1$) or irreversible ($R_L = 0$) nature of the adsorption process. Figure 6.5 shows that all the separation factor values were measured between 0 to 1, indicating the favorable adsorption of quinoline, 9-ethylcarbazole and dibenzothiophene on the functionalized polymer at all three sets of temperature.

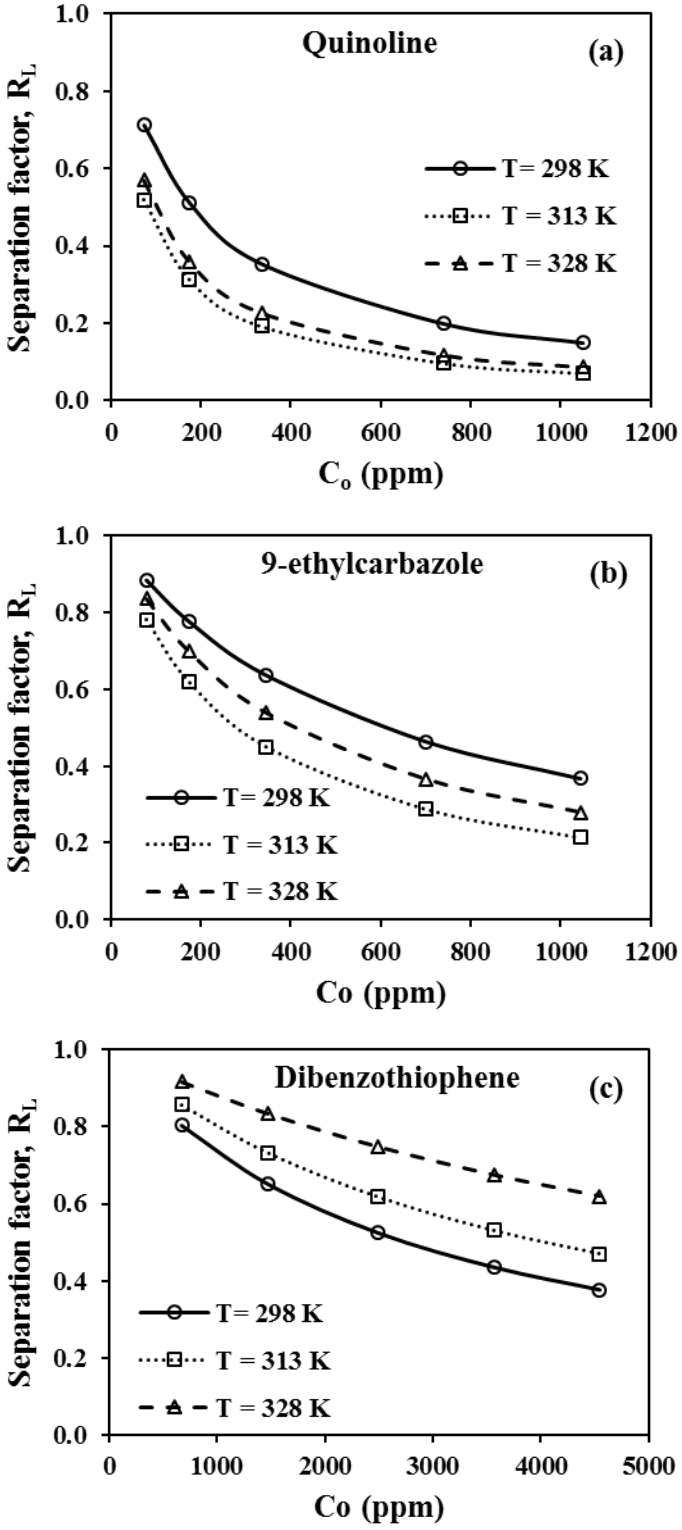

Figure 6.5: Effect of initial concentrations on the separation factor for (a) quinoline, (b) 9-ethylcarbazole and (c) dibenzothiophene adsorption over PGMA-ON-TENF at different temperatures.

Table 6.7: Comparison of quinoline, carbazole and dibenzothiophene adsorption capacity of different adsorbents from the literature.

Adsorbent	**Type of nitrogen or sulfur compounds**	**N adsorption capacity, q_m (mmol/g)**	**S adsorption capacity, q_m (mmol/g)**	**Ref.**
Ni/SiO_2-Al_2O_3	quinoline, dibenzothiophene	0.15	0.07	[128]
Activated alumina	quinoline, dibenzothiophene	0.29	0.04	[128]
Bimetal ion-exchanged zeolite	thiophene		0.42	[157]
Activated carbon	quinoline, dibenzothiophene	0.51	0.42	[8]
Activated alumina	quinoline, dibenzothiophene	0.17	0.02	[8]
Activated carbon	quinoline, carbazole dibenzothiophene	1.18 (quinoline) 1.19 (carbazole)	1.12	[9]
Ion-exchange resin	carbazole, dibenzothiophene	0.09	0.002	[129]
Activated carbon	dibenzothiophene		0.56	[48]
Mesoporous molecular sieve	quinoline	0.21		[53]
Activated carbon	quinoline, dibenzothiophene	0.16	0.09	[158]
Activated carbon	quinoline, dibenzothiophene	1.30	2.74	[56]
Functionalized polymer[a]	quinoline, 9-ethylcarbazole, dibenzothiophene	0.26 (quinoline) 0.08 (9-ethylcabazole)	0.12	Present work

[a] Maximum monolayer adsorption capacity at 298 K.

Table 6.7 compares the capacity of several carbon based adsorbents and non-carbon materials such as, activated alumina, zeolite, ion-exchange resin and molecular sieve towards the adsorption of heterocyclic nitrogen and sulfur compounds present in the diesel feed [8,9,48,53,56,128,129,157,158]. Nonetheless, the comparison of the adsorption capacities is rather inapt because of the reaction conditions and more importantly, the initial concentrations of the adsorbates were different in various studies. The equilibrium adsorption is dependent on the initial adsorbate concentration. The adsorption increases with an increase in the initial adsorbate concentration because of the development of concentration gradient between bulk solution and adsorbent surface which leads to an increase in the mass transfer driving force. However, the adsorption capacity also depends on the surface functional groups of the adsorbents in addition to their chemical and textural properties. Diverse adsorption capacities have been observed for carbon and alumina based adsorbents with different activation methods. Incorporation of functional groups, metallic species and electron withdrawing π-acceptors on the surface of adsorbents can greatly enhance the adsorbent performance and selectivity.

6.4.4 Adsorption thermodynamics

In order to evaluate the effects of temperature on inherent energy changes and thermodynamic feasibility of the adsorption of quinoline, 9-ethylcarbazole and dibenzothiophene on the functionalized polymer; thermodynamic parameters such as change in Gibbs free energy ΔG°, change in enthalpy ΔH° and change in entropy ΔS° were determined by using the following equations:

$$\Delta G^\circ = -RT \ln K \qquad (6.8)$$

$$\ln K = \frac{\Delta S^\circ}{R} - \frac{\Delta H^\circ}{RT} \qquad (6.9)$$

Where, R is the universal gas constant (8.314 J mol^{-1} K^{-1}), K is the thermodynamic equilibrium constant and T is the absolute temperature (K). Thermodynamic equilibrium constant, K is related to enthalpy and entropy of the system which changes with the change in temperature according to Equation 6.9. Values of K for quinoline, 9-ethylcarbazole and dibenzothiophene adsorption on PGMA-ON-TENF at different temperatures were computed by plotting ln (q_e/C_e) vs. q_e and extrapolating to zero qe [159,160]. Good correlation coefficients for the fitted data were obtained

by removing data outliers. It is evident from the Table 6.8 that the values of K decrease with an increase in temperature, indicating exothermic nature of the process. Also, ΔG° has negative values for the temperature range being studied which is an important criteria for the reaction to occur. It is an indicator of the spontaneous nature of the adsorption and the feasibility of the process. All the values of ΔG° indicated that the process of adsorption was favorable and thermodynamically spontaneous for all the nitrogen and sulfur species studied. Decrease in the absolute value of ΔG° with increasing temperature refers that lower temperatures aided adsorption.

Table 6.8: Gibbs free energy and thermodynamic equilibrium constant of quinoline, 9-ethylcarbazole and dibenzothiophene adsorption on functionalized polymer at 298 K, 313 K and 328 K.

Compounds	Thermodynamic equilibrium constant, K			ΔG°(kJ mol^{-1})		
	298 K	313 K	328 K	298 K	313 K	328 K
Quinoline	26.64	17.25	11.82	-7.96	-7.25	-6.59
9-ethylcarbazole	3.23	3.13	2.58	-2.84	-2.90	-2.53
Dibenzothiophene	1.90	1.81	1.64	-1.55	-1.51	-1.33

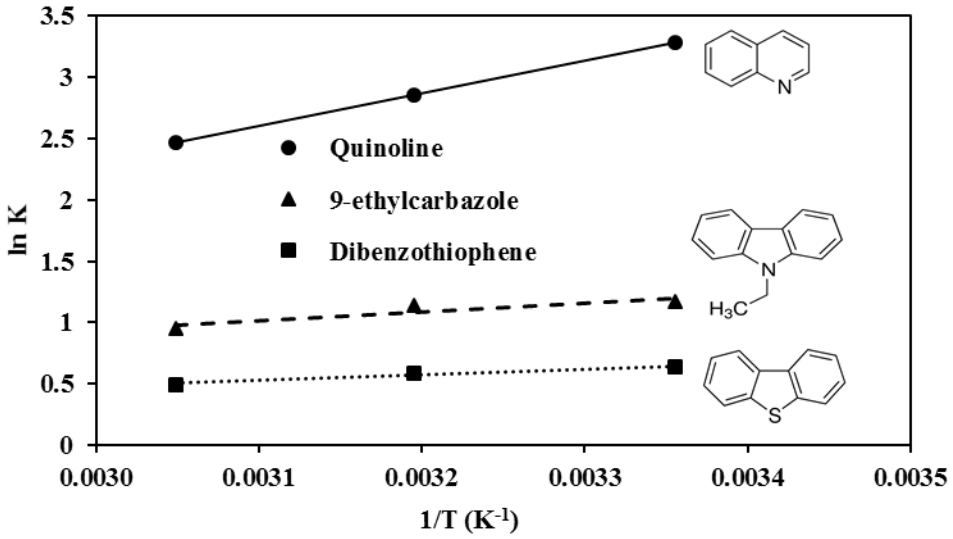

Figure 6.6: Van't Hoff plots of ln K versus 1/T for quinoline, 9-ethylcarbazole and dibenzothiophene adsorption on PGMA-ON-TENF at different temperatures (298 K, 313 K and 328 K).

Figure 6.6 shows the Van't Hoff plots of ln K vs. the inverse of temperature. ΔH° and ΔS° at different temperatures were calculated from the slope and intercept of the plots and the changes in enthalpy and entropy of the species with temperature are reported in Table 6.9. Enthalpy can be utilized to predict the temperature dependence of equilibrium capacity for model-feed-polymer adsorption process. Negative values of ΔH for quinoline, 9-ethylcarbazole and dibenzothiophene indicate that the adsorption interaction is exothermic. It was substantiated by earlier observations made in section 6.4.3 (adsorption isotherms) where the value of adsorption capacity decreased at higher temperatures. Negative values of ΔS showed decreased randomness at the adsorbent-model feed interface during adsorption. Observed negative adsorption entropy for quinoline, 9-ethylcarbazole and dibenzothiophene refers to the ordered arrangement of these compounds on the surface of the polymeric adsorbent. It may be due to the decrease in degree of freedom of the system caused by fixation of nitrogen and sulfur compounds to the adsorption sites. In comparison with the literature, enthalpies of complexation of o-chloranil (electron acceptor) with various aromatic hydrocarbons such as, naphthalene, pyrene and anthracene (electron donors) at 293 K have been measured between -0.75 to -79.07 kJ/mol [161]. Complexation enthalpy of C_{60} (electron acceptor) with aromatic hydrocarbons such as, naphthalene and phenanthrene were reported as -1.7 and -2.8 kJ/mol, respectively [162]. It is important to note that the magnitude of thermodynamic parameters is similar to those of typical electron-donor acceptor complexes reported in the literature.

Table 6.9: Thermodynamic parameters (enthalpy and entropy) for adsorption of nitrogen and sulfur compounds on PGMA-ON-TENF.

Compounds	ΔH°(kJ mol^{-1})	ΔS°(J mol^{-1} K^{-1})	R^2
Quinoline	-22.01	-46.60	0.999
9-ethylcarbazole	-6.00	-10.15	0.835
Dibenzothiophene	-3.86	-7.54	0.955

6.5 Conclusions

Selective adsorption of model nitrogen and sulfur compounds over the polymeric adsorbent was studied to provide a new insight into the desulfurization and denitrogenation of crude oil. Adsorption of quinoline, 9-ethylcarbazole and dibenzothiophene on the functionalized polymer is primarily governed by electron donor-acceptor interaction. Association of electron donors and acceptors leads to the formation of charge transfer complexes. Electronic distribution of higher occupied molecular orbital (HOMO) of the electron donors and lowest unoccupied molecular orbital (LUMO) of the electron acceptor play an important role in determining the strength of complexation. UV-vis spectroscopy established a fundamental comprehension of the role of TENF in removing these impurities by forming charge transfer complexes. FT-IR spectra further confirmed the complexation of heterocyclic sulfur and nitrogen compounds onto TENF functionalized polymer. Assessment of adsorptive capacity and selectivity of the functionalized polymer towards refractory sulfur and nitrogen compounds revealed that the polymer is more selective towards quinoline as compared to 9-ethylcarbazole and dibenzothiophene. Overall, there is competitive adsorption between these compounds and the polymer has higher nitrogen adsorption affinity. Implementation of the two-parameter isotherm equations to fit the batch adsorption data verified that the extent of adsorption was dependent on the HOMO level of the adsorbates where higher HOMO led to higher adsorption with the exception of 9-ethylcarbazole which is due to the hindrance caused by alkyl substituent in the carbazole derivative. The strength and energy of adsorption were dependent on the surface interaction between electron donors and the functionalized polymer, characterized by K_L and 1/n values in the Langmuir and Freundlich isotherms, respectively. Based on the adsorption isotherm studies, it can be concluded that adsorption capacity of the adsorbates decreases in the following order: quinoline > dibenzothiophene > 9-ethylcarbazole. Measurement of the change in Gibbs free energy demonstrated that the process of adsorption was favorable and spontaneous. The adsorption interaction is exothermic in nature and the magnitude of calculated enthalpies are representative of strong charge transfer complexation of heterocyclic nitrogen and sulfur compounds with functionalized polymer. To summarize, TENF functionalized polymer is an efficient adsorbent for the removal of refractory sulfur and nitrogen compounds present in petroleum feed. It can be envisioned as a viable non-catalytic process capable of improving oil refining technology.

Chapter 7: Hydrotreatment of functionalized polymer treated heavy gas oil

A part of this chapter is scheduled for presentation and some parts were presented at the following conferences:

- Misra, P., Badoga, S., Dalai, A. K. & Adjaye, J. "Development of functionalized polymers for the removal of nitrogen and sulfur compounds from bitumen-derived heavy gas oil". *253rd ACS National Meeting & Exposition*, San Francisco, California, 2-6 April 2017.
- Dalai, A. K., Misra, P., & Badoga, S. "Development of functionalized polymers and catalysts for hydrotreating of gas oils". *Asia-Pacific Congress on Catalysis (APCAT-7)*, Mumbai, India, 17-21 January 2017.
- Dalai, A. K., Misra, P., & Badoga, S. "Development of novel catalysts and adsorbents for hydroprocessing of petroleum feedstock". *CHEMCON 2016*, Chennai, India, 27-30 December 2016.

Contribution of the Ph.D. candidate

Polymer synthesis, preparation of polymer treated heavy gas oil feed for hydrotreating, and data analysis was done by Prachee Misra. Hydrotreating reactor experiments were performed by Prachee Misra with assistance from Dr. Sandeep Badoga. All of the written text was prepared by Prachee Misra based on the suggestions from Drs. Ajay Dalai and John Adjaye.

Contribution of this chapter to the overall Ph.D. work

This part of work was focused on comparing the effect of polymer treatment on the hydrotreating activity of bitumen-derived heavy gas oil.

7.1 Abstract

In this part of work, hydrotreatment of polymer treated heavy gas oil was studied. Functionalized polymer, PGMA-ON-TENF was synthesized in bulk and used as an adsorbent for this study because of its high adsorption capacity and reusability. The polymeric adsorbent selectively targeted refractory sulfur and nitrogen compounds present in heavy gas oil through charge transfer complex formation. Functionalized polymer treated feed was referred to as the pre-treated feed, which was further hydrotreated, and hydrodesulfurization, hydrodenitrogenation and hydrodearomatization activities were measured. The catalyst used for hydrotreating was the conventional NiMO/γ-Al_2O_3 synthesized in lab with 13 wt.% molybdenum and 2.5 wt.% nickel. Hydrotreating reactions were carried out using micro scale trickle bed reactor using 5 mL of catalyst. Experiments were performed in the temperature range of 370 – 390 °C, pressure of 8.96 MPa, 1 h^{-1} LHSV and H_2/oil ratio= 600 (v/v). Removal of refractory sulfur and nitrogen species before hydrotreatment has resulted in 94.3 wt.% hydrodesulfurization (HDS) and 63.3 wt.% hydrodenitrogenation (HDN) as compared to 93.1 wt.% HDS and 60.5 wt.% HDN activities. Prior removal of nitrogen and sulfur compounds using functionalized polymer subsequently favored the hydrotreating activity in the trickle bed reactor.

7.2 Introduction

Recent developments in the petroleum refinery processes are focused on the production of ultra-low sulfur fuels due to the stringent environmental regulations [163]. Presently, hydrotreating is the most efficient technique used for the removal of these sulfur and nitrogen impurities found in gas oil. It is a group of technologies which involves HDS (hydrodesulfurization - removal of sulfur compounds), HDN (hydrodenitrogenation - removal of nitrogen compounds), HDM (hydrodemetallization - removal of metals) and HDA (hydrodearomatization - saturation of the aromatics) in the presence of hydrogen at high temperature and pressure. Alumina supported Ni and Mo based catalysts are widely used in industries for hydrotreating of gas oil [164–166]. From decades, rigorous efforts are being made by researchers to enhance the catalyst activity. It is quite challenging to achieve deep HDS with the conventional hydrotreating technology under typical operating conditions. One of the major reasons for the loss of catalyst activity is the presence of heterocyclic nitrogen compounds in the feed [167]. These compounds adsorb onto the catalyst

active sites leading to the inhibition and deactivation of the hydrotreating catalyst [168–170]. This work is focused on enhancing the efficiency of hydrotreating processes by removing nitrogen species from bitumen-derived heavy gas oil (HGO). The feed characteristics of HGO used in this study are reported in Table 7.1. A feed pre-treatment process using functionalized polymers has been developed for the selective removal of heterocyclic nitrogen compounds from HGO by the formation of charge transfer complexes. It was followed by hydrotreatment of both untreated HGO and pre-treated HGO feed to measure the effects of presence or absence of nitrogen species on hydrodesulfurization (HDS) and hydrodenitrogenation (HDN) activities at industrial conditions.

Table 7.1: Feed characteristics of bitumen-derived heavy gas oil.

Parameter	**Heavy gas oil (HGO)**
Sulfur content (ppm)	38000
Nitrogen content (ppm)	4300
Density (g/ml)	0.94
Aromatic content (%)	42.7
Simulated distillation	
IBP (ºC)	208
FBP (ºC)	625

7.3 Experimental details and methodology

7.3.1 Materials

Mo and Ni precursors, ammonium heptamolybdate tetrahydrate (AHM) ($(NH_4)_6Mo_7O_{24}\cdot 4H_2O$) and nickel nitrate hexahydrate ($Ni(NO_3)_2\cdot 6H_2O$); monomers, glycidyl methacrylate and ethylene glycol dimethacrylate; 1-dodecanol (≥98.0%), cyclohexanol (99.0%), N,N-dimethylformamide (anhydrous 99.8%), poly[N-vinyl-2- pyrrolidone] (Mw~55,000 g/mol), acetone oxime (≥98.0%), potassium carbonate (≥99.0%), 9-fluorenone (98%), fuming nitric acid (90%) and p-toluene

sulfonic acid monohydrate (≥98.5%) were purchased from Sigma Aldrich, Edmonton, Canada. The radical initiator Azobisisobutyronitrile was purchased from Molekula Ltd. Ammonium hydroxide (28-30% NH_3 in water), concentrated sulfuric acid (95-98%) and the γ-Al_2O_3 which was used as a support for catalyst were purchased from Fischer Scientific, Saskatoon, Canada. Bitumen-derived heavy gas oil used throughout this study was provided by Syncrude Canada Ltd. All the chemicals were used as received.

7.3.2 Catalyst preparation

The NiMo/γ-Al_2O_3 catalyst was synthesized using wetness sequential impregnation method. 13 wt.% Mo and 2.5 wt.% Ni was loaded on γ-Al_2O_3 using $(NH_4)_6Mo_7O_{24}\cdot 4H_2O$ and $Ni(NO_3)_2\cdot 6H_2O$ as precursors. In a typical synthesis, 2.4 g of AHM was dissolved in 10 mL of water containing few drops of ammonium hydroxide. The resulting solution was impregnated on 8.45 g of γ-Al_2O_3. The material was then dried for 6 h at 110 °C followed by calcination at 550 °C for 5 h at a ramp rate of 1 °C/min. To this material, solution of 1.24 g nickel nitrate in 7 mL water was wet impregnated. The resultant material was dried for 6 h at 110 °C followed by calcination at 550 °C for 5 h at a ramp rate of 1 °C/min to produce 10 g of NiMo/ γ-Al_2O_3 catalyst.

7.3.3 Preparation of functionalized polymer

Functionalized polymer consisting of a polymer support, copolymer of glycidyl methacrylate and ethylene glycol dimethacrylate (PGMA), a fluorenone derived π-acceptor with four nitro groups (2, 4, 5, 7-tetranitroflorenone, TENF), and a hydroxylamine linker was synthesized to create PGMA-ON-TENF polymer. The epoxy group present on PGMA support was opened to attach the linker. Thereafter, the π-acceptor was immobilized on the polymer support via hydroxylamine linker. Detailed synthesis of PGMA and TENF, and the procedure for obtaining functionalized polymer has been reported in chapter 3 of this thesis. Quantities of ingredients for the preparation of functionalized polymers listed in section 3.3.2 were scaled up to synthesize 500 g of PGMA-ON-TENF with the surface area of 57 m^2/g and pore size of 23 nm.

7.3.4 Hydrotreating experimental set-up and catalyst activity studies

The NiMo/γ-Al_2O_3 catalyst was tested for hydrotreating of heavy gas oil in continuous flow fixed bed reactor. The experimental set up consists of a tube type reactor (ID = 14 mm and Length = 240 mm) in which catalyst was loaded. The reactor was heated by furnace and its temperature can be adjusted via controller. The pressure in the system was maintained using back pressure regulator. The heavy gas oil was pumped into the reactor using high pressure Eldex pump, and the hydrogen gas was added in the reactor via mass flow controller. The products (gas and liquid) exiting the reactor were stripped in water scrubber to remove the ammonia produced during hydrodenitrogenation reaction before entering to the gas liquid separator. H_2S produced during hydrodesulfurization was sent out of the system via sodium hydroxide solution to neutralize it. The liquid samples were taken out of the system every 12/24 h and stripped with nitrogen to remove dissolved H_2S before analyzing. Figure 7.1 shows the schematic for hydrotreating experimental setup.

The catalyst was loaded in the reactor using the following protocol [171]. Firstly, based on the temperature calibration for the reactor, nearly 105 mm long catalyst bed zone location was determined. Typically it is located in the middle of the reactor. The reactor was loaded from the top, starting with 4 cm^3 of 3 mm glass beads, followed by 4 cm^3 of 16 mesh silica carbide (SiC). The reactor was tapped from outside to settle the SiC and glass beads. Then, 4 cm^3 of 46 mesh SiC followed by 3 cm^3 of 60 mesh SiC were loaded. Thereafter, 90 mesh SiC was loaded until the start of catalyst bed zone. 5 g catalyst was mixed with 10 mL of 90 mesh SiC to fill the catalyst bed zone. After this, 3 cm^3 of 60 mesh SiC followed by 3 cm^3 of 46 Mesh SiC, 3 cm^3 of 16 mesh SiC and 3 cm^3 of 3mm glass beads were loaded to complete the fixed-bed reactor loading.

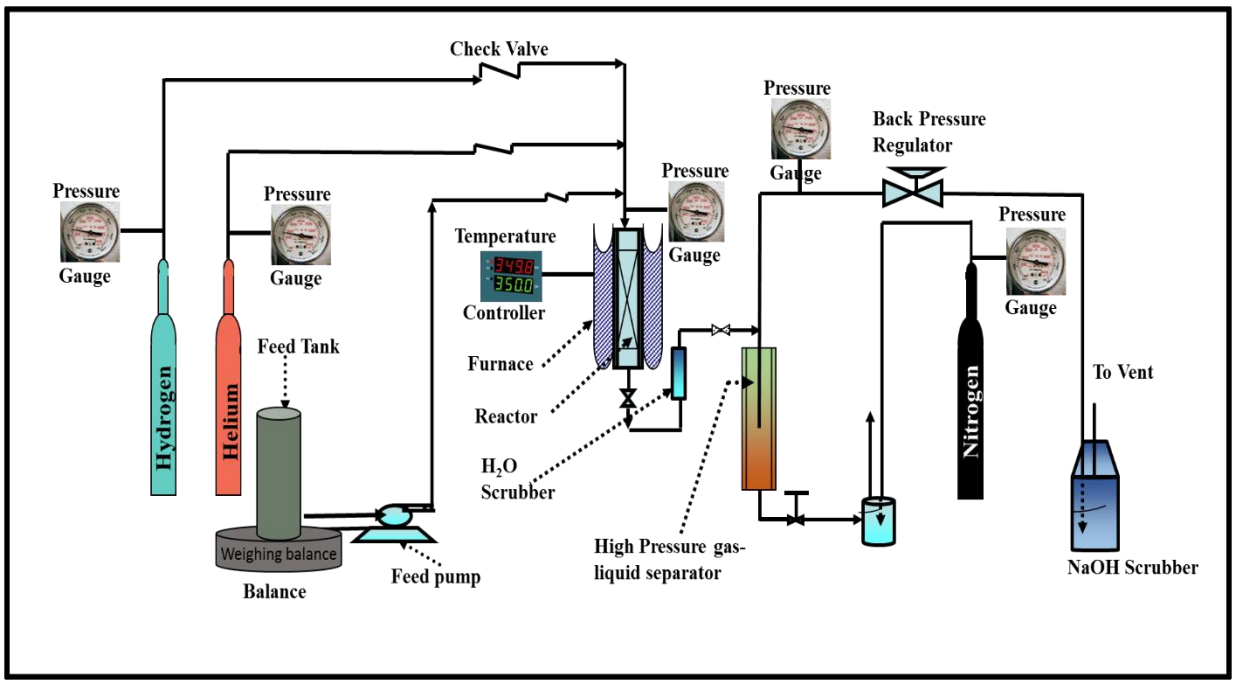

Figure 7.1: Experimental set-up for high pressure and temperature continuous flow fixed-bed reactor.

The catalyst was sulfided in the reactor prior to the hydrotreating reaction with HGO. The sulfiding solution containing 14.5 ml butane-thiol in 500 mL clean oil was pumped in to the reactor at the rate of 5 ml/h. The reactor was pressurized to 8.96 MPa with helium. Hydrogen flowrate was set to 50 ml/min. The reactor temperature was set to 190 °C for 24 h. Then, the temperature was gradually raised to 340 °C and kept at this temperature for the next 24 h. The sulfiding solution was then replaced with HGO and the reactor temperature was increased to 370 °C. The liquid collected in the gas liquid separator was removed and discarded. The HGO was allowed to pump for next 5 days at the same operating conditions and this concluded the catalyst pre-coking phase of the hydrotreating reactions. During these 5 days, the liquid sample was collected every 24 h and tested for nitrogen and sulfur concentration. Initially higher activities were observed and then the catalyst activity stabilized on the 4^{th} day. After activity stabilization, the reaction was continued at same conditions for day 6 and 7 and the hydrotreating activity determined from these sample analysis was reported as the activity at 370 °C. Then, the temperature was raised to 380 °C and the system was allowed to stabilize for 24 h. The sample collected after 24 h was discarded and the reaction was allowed to run for next two days. The samples collected every 24 h were analyzed

and reported for the activity at 380 °C. Similarly, the activity was measured at 390 °C. The sulfur and nitrogen content of the polymer treated and untreated HGO was determined using N/S analyzer.

7.3.5 Instrumentation

Textural properties of the catalyst and polymer samples were determined by Micromeritics 2000 ASAP analyzer (Micromeritics, Nacross, GA, USA) using Brunauer–Emmett–Teller (BET) method. Thermal gravimetric/differential thermal analyzer (TG/DTA) from TA instrument, Q-5000, V20.13 model (TA instruments, New Castle, DE, USA) was used to determine the thermal stability of the polymer. Bruker Advance D8, series II, Powder diffractometer with CuK-α radiation was used to measure diffraction patterns of the sample. H_2-temperature programmed reduction, H_2-TPR of the catalyst was done to analyze the attributes of the reducible metal species using TPD/TPR Micromeritics Autochem 2950 HP (USA) instrument. Aromatic content of the untreated and polymer treated HGO was determined by recording ^{13}C NMR spectra using a 500 MHz Bruker Advance NMR Spectrometer. Inverse gated decoupling with 2000 scans and pulse delay of 4 s were set as the operating parameters. Total sulfur and nitrogen content of the untreated and treated light gas oil was measured by Antek Model 9000 Nitrogen/Sulfur analyzer (ANTEK Instruments Inc., Houston, TX, USA) using pyro-fluorescence and pyro-chemiluminescence techniques.

7.4 Results and discussion

7.4.1 N_2 Adsorption-desorption studies

The textural properties of the γ-Al_2O_3 support and NiMo/γ-Al_2O_3 catalyst were determined using BET and BJH analysis. The N_2 adsorption-desorption isotherm for γ-Al_2O_3 is Type IV with H1 hysteresis loop (as shown in Figure 7.2), which is typical for mesoporous materials. The multi-point BET surface area, pore volume and BJH desorption average pore diameter for γ-Al_2O_3 are shown in Table 7.1. After the addition of Ni and Mo, the surface area decreases from 280 m^2/g to 224 m^2/g due to the filling of pores with nickel and molybdenum oxides. However, there was no change in pore structure in NiMo/γ-Al_2O_3 catalyst as evident by the presence of Type IV isotherm

and unimodal pore size distribution as shown in Figure 7.2. The CO chemisorption analysis was also performed for NiMo/γ-Al_2O_3 catalyst to determine the percentage metal dispersion. Table 7.2 shows a significant amount of metal dispersion on the surface (9.8%). The value of metal dispersion is in accordance with data reported in literature [172,173].

Table 7.2: Textural properties and CO chemisorption data for NiMo/γ-Al_2O_3 catalyst.

Material	BET surface area (m^2/g)	Pore volume (cm^3/g)	Average pore diameter (nm)	Metal dispersion (%)	CO absorbed (μmol/g)
γ-Al_2O_3	280 ± 7	0.78	7.7	-	-
NiMo/γ-Al_2O_3	224 ± 5	0.52	7.2	9.8 ± 0.2	175 ± 10

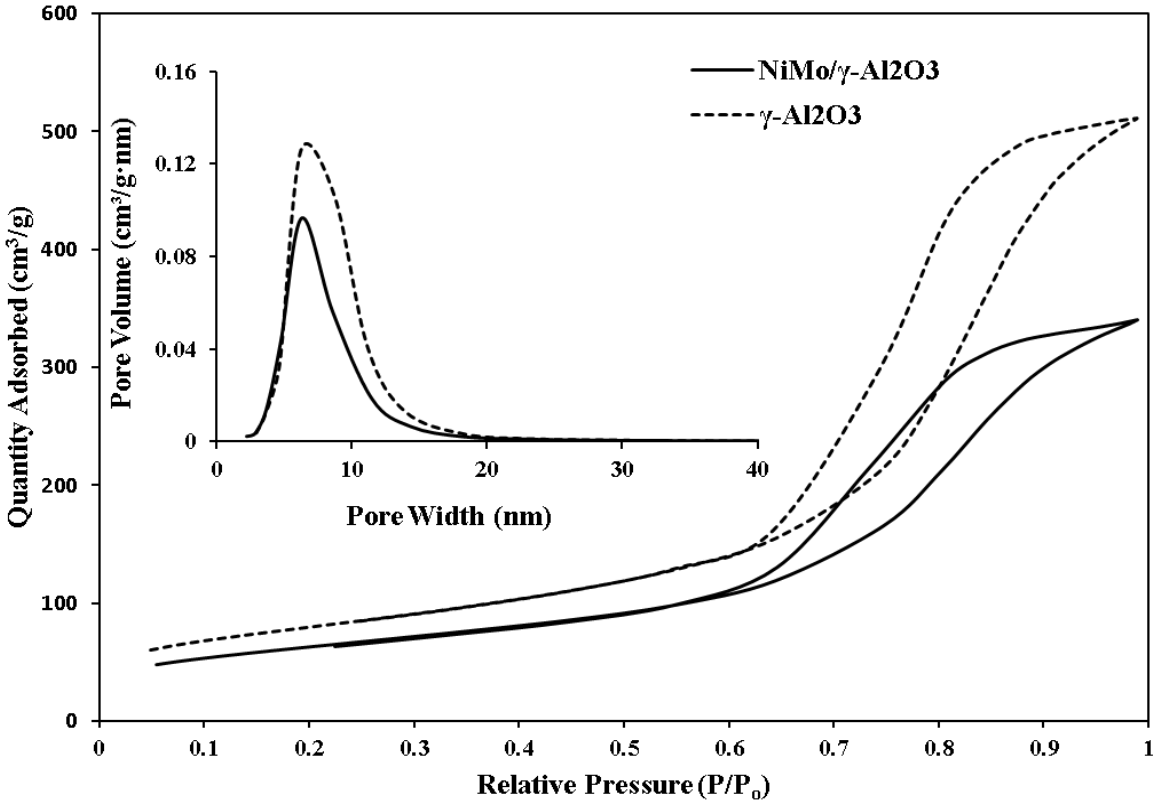

Figure 7.2: N_2 adsorption-desorption isotherms for γ-Al_2O_3 and NiMo/γ-Al_2O_3, and BJH pore size distribution in inset.

7.4.2 X-ray diffraction (XRD)

The powder wide angle diffraction studies were performed to determine the structure of molybdenum oxide in NiMo/γ-Al_2O_3 catalyst. The XRD pattern for NiMo/γ-Al_2O_3 catalyst (as shown in Figure 7.3) showed peak at 2θ=37.2°, 45.9°, and 66.6° which corresponds to 311, 400 and 440 planes of cubic γ-Al_2O_3[174]. The peak at 2θ=26.6° corresponds to presence of β-$NiMoO_4$[175]. No additional peak was detected for the molybdenum oxide, which signifies the fine dispersion of molybdenum. Therefore, XRD analysis confirmed the fine dispersion of molybdenum oxide, and presence of tetrahedrally coordinated molybdenum in β-$NiMoO_4$ which is not hard to sulfide [176].

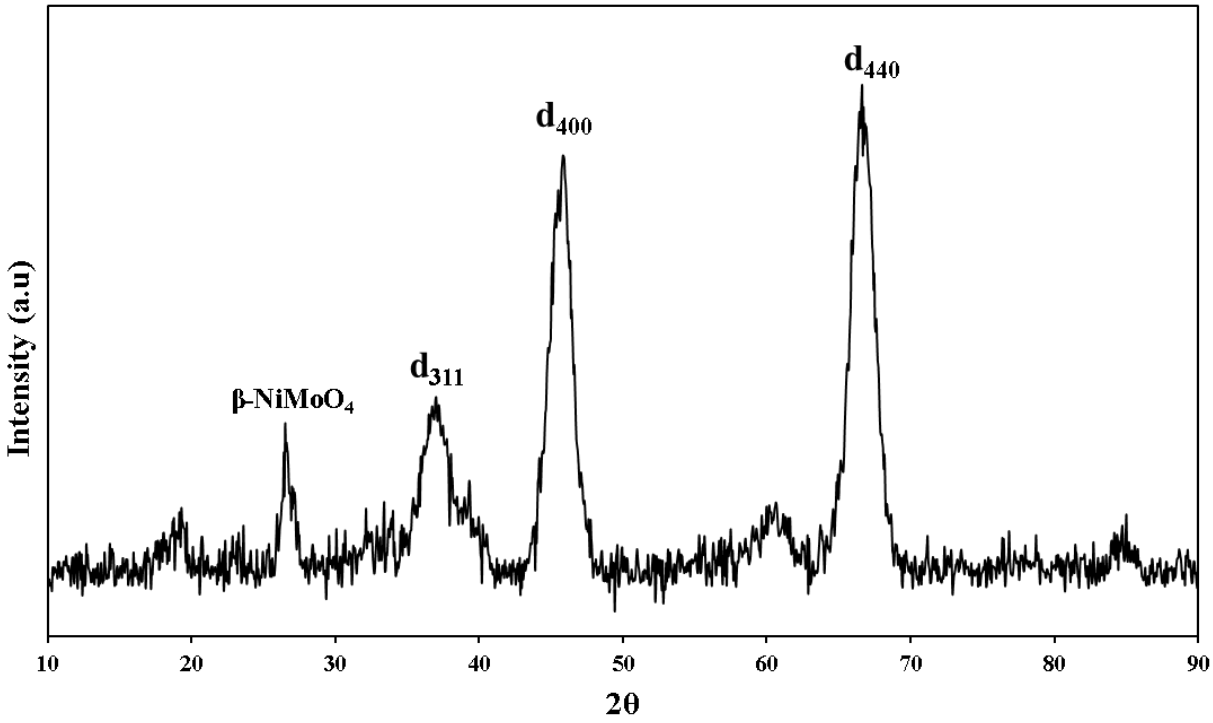

Figure 7.3: X-ray diffraction pattern for NiMo/γ-Al_2O_3 catalyst.

7.4.3 H_2-temperature programmed reduction (H_2-TPR)

The H_2-TPR analysis was performed to determine the ease in molybdenum oxide reduction during catalyst sulfidation/activation. This analysis also provides an estimation for the temperature at

which catalyst reduction should be carried out. The TPR profile for NiMo/γ-Al_2O_3 catalyst is shown in Figure 7.4. The first peak centered at 380 °C corresponds to first stage of molybdenum reduction with hydrogen where Mo^{+6} reduced to Mo^{+4}. The second peak at 715 °C is due to the reduction of Mo^{+4} to Mo^0. During catalyst sulfidation/activation the MoO_3 (Mo^{+6}) converts to MoS_2 (Mo^{+4}), therefore we were interested in the first peak. The appearance of first peak at low temperature signifies the ease in reducibility of molybdenum oxide species to molybdenum sulfide. The temperature of 340 °C was used during catalyst sulfidation instead of 380 °C as predicted by TPR analysis. This is due to the fact that the sulfidation was carried out for 24 h instead of few minutes in TPR analysis, and this will give ample time for catalyst to reduce at 340 °C [177].

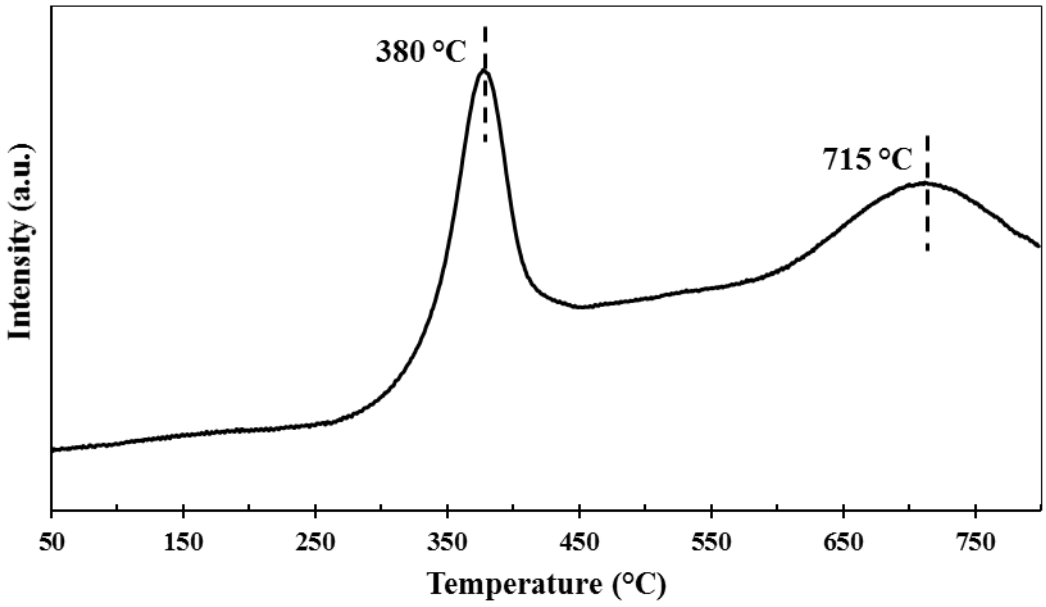

Figure 7.4: H_2-Temperature programmed profile for NiMo/γ-Al_2O_3 catalyst.

7.4.4 Functionalized polymer adsorption studies

For this part of the work, large amount of heavy gas oil was needed to perform the hydrotreating experiments. Hence, 500 g of the polymeric adsorbent sample was heated overnight at 90 °C in a vacuum oven prior to batch adsorption experiments. At ambient temperature (24 °C), 500 g of fresh polymeric adsorbent was stirred with 2500 g of heavy gas oil in 5 batches (one batch = 100

g polymer with 500 g of HGO) for 24 h at 200 rpm. Afterwards, the liquid feed was separated from the adsorbent particles using vacuum filtration. Similar procedure was followed for all adsorption experiments. The treated oil feed was referred to as polymer treated HGO feed. To determine the effectiveness of polymer adsorption process, total nitrogen and sulfur content of untreated and polymer treated HGO samples was measured by N/S analyzer.

As shown in Table 7.3, pre-treatment with functionalized polymer led to a decrease in total nitrogen and sulfur content of heavy gas oil. A total of 8.7 wt.% nitrogen was removed while only 4.4 wt.% sulfur removal was observed in the first contact with the polymer. This is due to the presence of hydrophilic polymer support, PGMA on the functionalized polymer which made the polymer selective towards nitrogen removal. The π-acceptor is itself capable of forming charge transfer complexes with the heterocyclic nitrogen and sulfur compounds present in heavy gas oil. However, it is difficult to recover π-acceptor after adsorption with HGO because of its soluble nature. Moreover, the amount of sulfur present in HGO feed is approximately 10 times higher than the nitrogen concentration and there is a higher possibility of complexing sulfur compounds as compared to nitrogen. Therefore, the π-acceptor was immobilized on the PGMA polymer support for the following reasons: firstly, to prevent the leaching of π-acceptor in HGO feed and secondly, to make the polymer selective towards nitrogen compounds. The polar nature of heterocyclic nitrogen compounds was exploited for its interaction with the complexing agent. PGMA polymer support has the polar function which is capable of forming hydrogen bond with heterocyclic nitrogen compounds. Thereby increasing the nitrogen to sulfur selectivity of the polymeric adsorbent.

Table 7.3: Sulfur and nitrogen content of untreated and polymer treated heavy gas oil (polymer/HGO = 1/5, 24 h at 25 °C).

Parameter	Untreated HGO	Polymer treated HGO
Sulfur content (ppm)	38200	36508
Nitrogen content (ppm)	4380	3998

7.4.5 Adsorbent regeneration and reusability

For industrial application of the process, reusability of the polymeric adsorbent was tested. As described in Section 6.4.1 of this thesis, LUMO (lowest unoccupied molecular orbital) level of the π-acceptor and HOMO (highest occupied molecular orbital) level of the π-donor is the basis of the interaction between electron acceptor (TENF) and electron donors (nitrogen and sulfur compounds) which leads to their complexation and subsequent removal of nitrogen and sulfur impurities from HGO. The LUMO level of TENF represents the deficiency of π orbital which is sufficient to draw electrons from the neighboring electron donor molecules. Therefore, the solvent selected for the regeneration of functionalized polymer should be electron donor type of solvent [66].

It is important to treat the polymeric adsorbent with electron donor solvent which is capable of establishing a donor-acceptor interaction with the π-acceptor, thereby eluting the heterocyclic nitrogen and sulfur compounds from the polymeric adsorbent bed. Regenerating solvents can be selected from a wide range of electron donor solvents, such as benzene, toluene, xylene, and aromatic petroleum fractions having the HOMO level greater than -9.8 eV. Hence, toluene (HOMO = -9.44 eV) was selected as the regenerating solvent for this study. The used polymer from the initial adsorption experiments was regenerated with toluene using a soxhlet apparatus. Regenerated adsorbent was obtained by washing the used polymer with toluene at 110 °C for 6 days, followed by drying at room temperature for 48 h. Regenerated polymer was reused at the same adsorption conditions to produce more polymer treated feed. As shown in Figure 7.5, fresh polymer treated HGO has lower nitrogen and sulfur content as compared to the HGO treated with the regenerated polymer. Based on the literature, it was expected that after regeneration with toluene, adsorption capacity of the polymer can be restored. However, a decrease in polymer adsorption efficiency was observed after regeneration which may be due to the inability of toluene to elute strongly complexed nitrogen and sulfur polyaromatics.

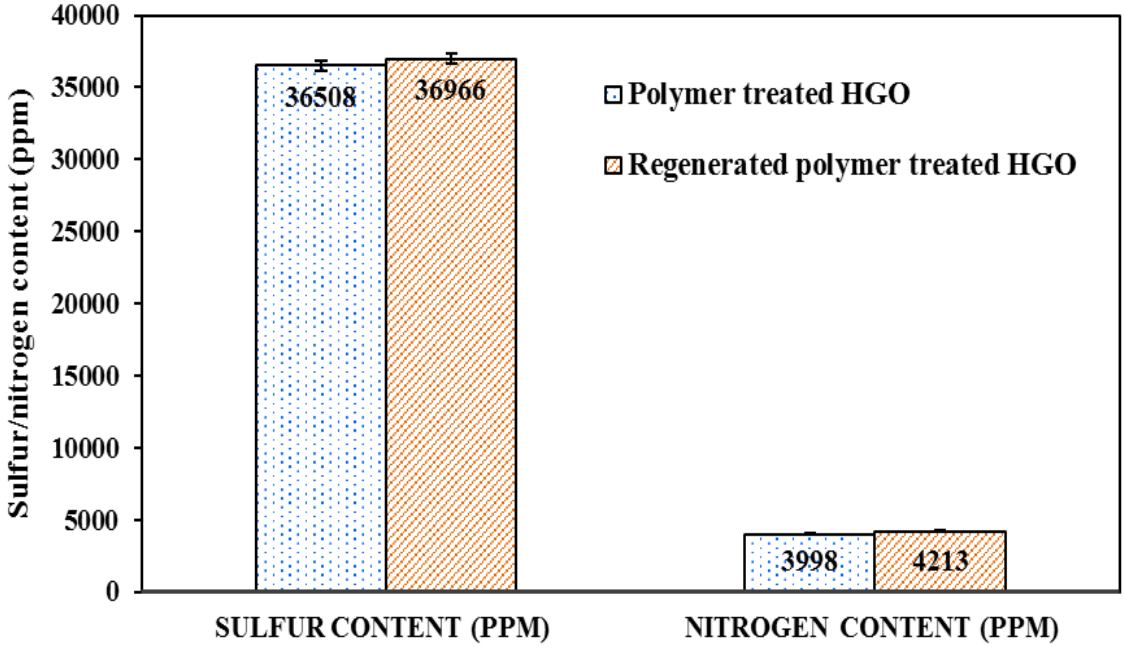

Figure 7.5: Comparison of sulfur and nitrogen content of fresh polymer treated HGO and regenerated polymer treated HGO.

7.4.6 Hydrotreatment Study using untreated and polymer treated heavy gas oil

Bitumen-derived heavy gas oil was used as the feedstock for hydrotreatment studies. The catalytic activity for hydrotreating of gas oil was measured in terms of HDS and HDN activities, reported as percentage removal or the change in nitrogen and sulfur concentration. Three oil samples were analyzed two times each to report the activities as the average of 6 data points. To determine the effect of HGO pre-treatment with polymers, the hydrotreating activity of polymer treated HGO was also performed. The catalyst, NiMo/γ-Al_2O_3 was first sulfided at 190 °C using 2.9% butane-thiol in HGO, followed by catalyst stabilization via pre-coking at 370 °C by reacting with gas oils for 5 days. Afterwards, hydrotreating experiments were performed at three different temperatures: 370 °C, 380 °C and 390 °C, while keeping the reactor pressure, LHSV and H_2/oil ratio constant at 8.96 MPa, 1 h^{-1} and 600 (v/v), respectively. The hydrotreated gas oil samples were collected for two days at each operating condition and analyzed for nitrogen and sulfur conversions in N/S analyzer.

The results from the hydrotreating reactions are shown in Figure 7.6. The hydrotreating results signified that the polymer treated HGO had better HDS and HDN activities as compared to the untreated HGO feed. The higher hydrotreating activity of polymer treated HGO can be assigned to lower concentration of catalyst-inhibiting nitrogen compounds in pre-treated HGO, as shown in Table 7.3.

Based on the literature, it was expected that the selective removal of nitrogen compounds prior to hydrotreating would translate to an increase in HDS activity. Moreover, reduction in total nitrogen content of the feed led to an increase in HDN activity as well. Hydrotreating without prior removal of nitrogen and sulfur impurities is an essential process in petroleum refineries. At 390 °C, hydrotreating alone removed 93.1 wt.% of sulfur compounds and 60.5 wt.% of nitrogen compounds. However, the conversion increased to 94.3 wt.% sulfur and 63.3 wt.% nitrogen removal with the polymer treatment. Although the percentage change is not very high, the ppm of sulfur and nitrogen removed from polymer treated oil is significant. Selective removal of nitrogen and sulfur compounds using polymeric adsorbent led to 17.4% (2636 ppm to 2177 ppm) decrease in total sulfur and 7.1% (1730 ppm to 1607 ppm) decrease in total nitrogen content of the resultant hydrotreated feed.

To further analyze the effect of pre-treatment of heavy gas oil by functionalized polymers, ^{13}C NMR was used to determine the change in aromatic content due to the removal of heterocyclic nitrogen and sulfur impurities before hydrotreating. Hydrodearomatization (HDA) involves the hydrogenation of aromatics present in the feed, and is one of the important hydrotreatment processes used in refineries to improve the quality of the feed. To measure the total aromatics present in the untreated and treated HGO, intensities over saturated hydrocarbon range (0-50 ppm) and aromatic hydrocarbon range (110-150 ppm) in ^{13}C NMR plot were integrated [76] (as shown in Figure 7.7). Percentage aromatic content (% C_{Ar}) in the heavy gas oil samples was calculated according to the following equation:

$$\% \, C_{Ar} = \frac{A}{A + B} * 100 \qquad (7.1)$$

Where, A is the integral of total aromatics, and B is the integral of total saturates.

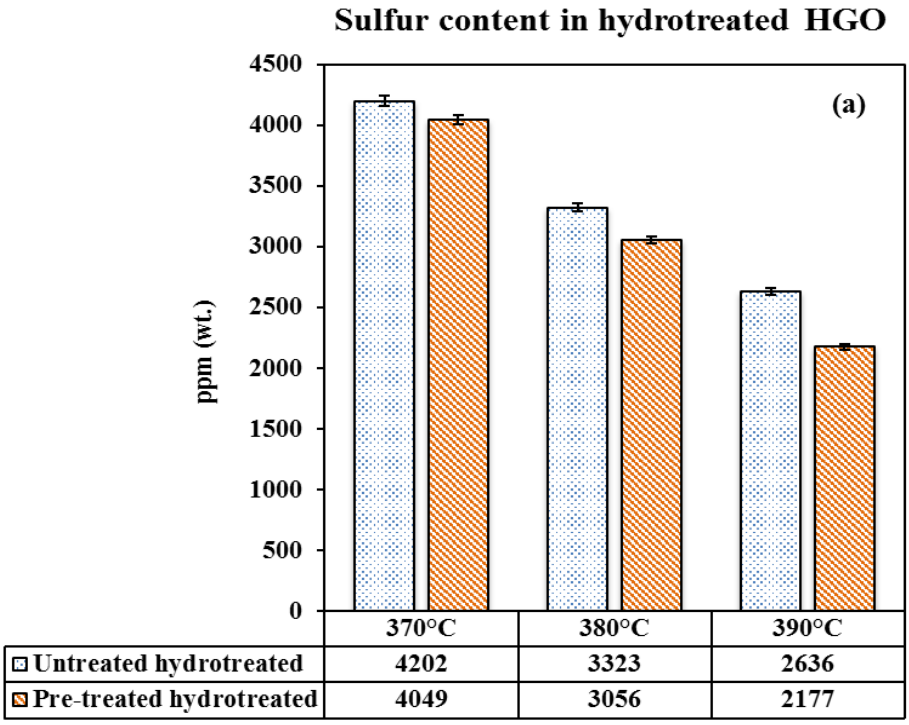

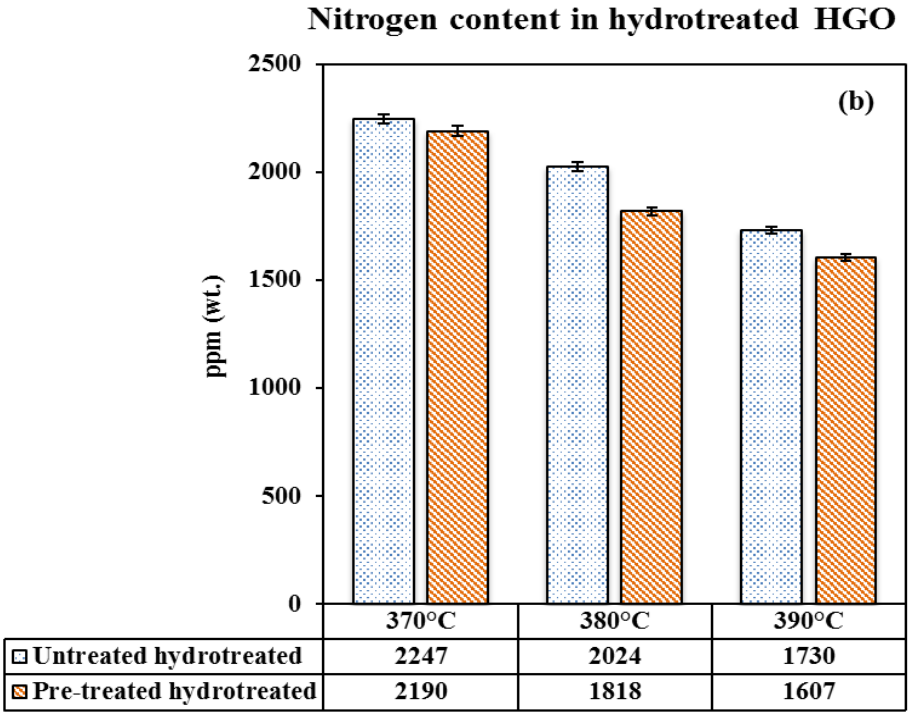

Figure 7.6: (a) HDS and (b) HDN activities of NiMo/γ-Al_2O_3 with untreated and polymer treated HGO at 370 °C, 380 °C and 390 °C (catalyst = 5 cm^3, P = 8.96 MPa, LHSV = 1 h^{-1} and H_2/oil ratio= 600 (v/v)).

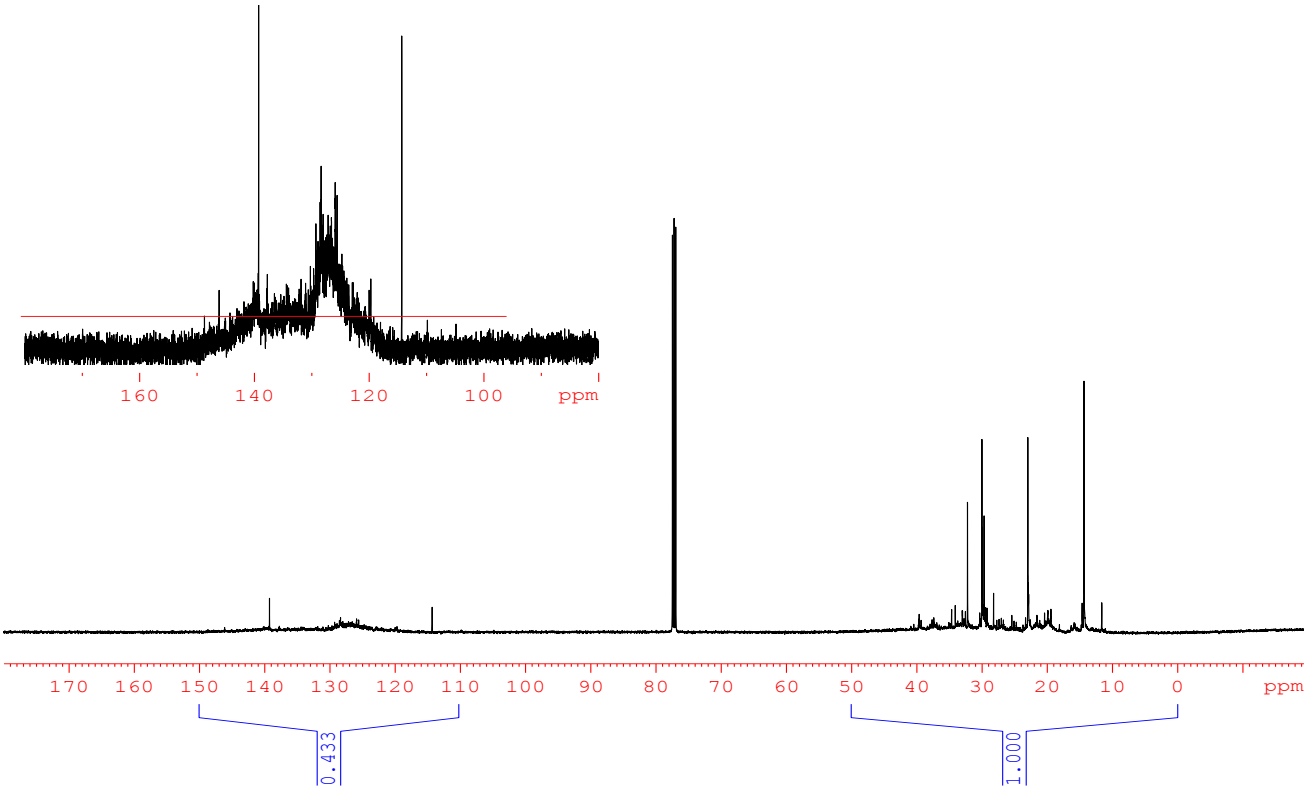

Figure 7.7: ^{13}C NMR sample plot for the calculation of aromatic content of heavy gas oil.

^{13}C NMR analysis revealed that the aromatic content of untreated heavy gas oil feed was 42.8%. Pre-treatment of HGO samples with the functionalized polymer led to a decrease in total aromatics from 42.8% to 39%. The aromatic content of hydrotreated HGO samples at three reaction temperatures (370 °C, 380 °C and 390 °C), pressure = 8.96 MPa, LHSV = 1 h^{-1} and H_2/oil ratio= 600 (v/v) is shown in Figure 7.8. A total of 42.8% aromatic content was found in the analysis of untreated HGO which remarkably decreased in all the polymer treated HGO samples. The highest hydrodearomatization (HDA) was observed for polymer pre-treated HGO feed at 390 °C, where the aromatic content decreased from 23.9% to 21%. Besides, total aromatic content of 22.8% and 21.8% was calculated at 370 °C and 380 °C, respectively for the hydrotreatment of polymer treated HGO. This decrease in the aromatic content is evidently due to the removal of heterocyclic nitrogen and sulfur species present in the gas oil. Charge transfer complex formation favored the adsorption of bulky aromatics via electron donor acceptor interaction, which led to an increase in HDA activity of polymer treated HGO samples.

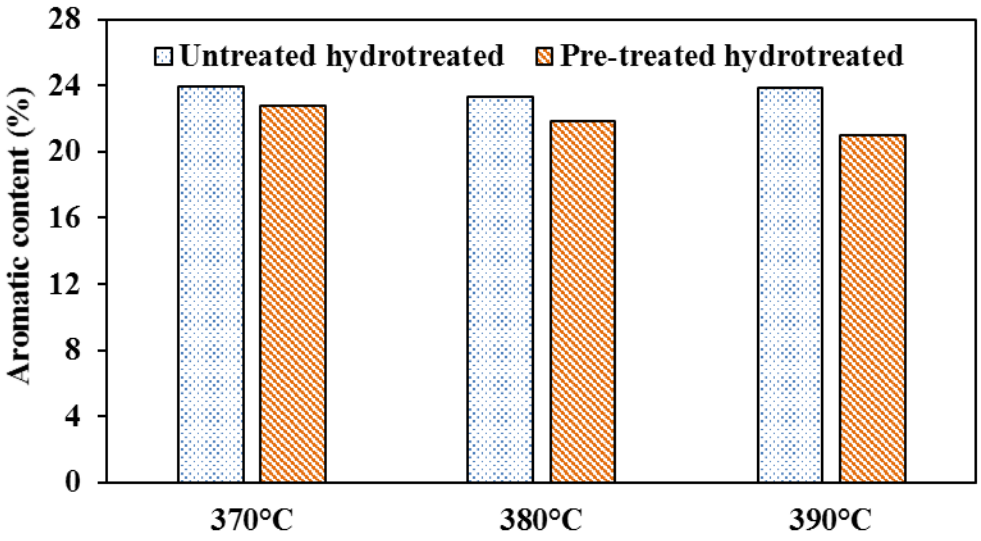

Figure 7.8: HDA activities of NiMo/γ-Al_2O_3 with untreated and pre-treated HGO at 370 °C, 380 °C and 390 °C (catalyst = 5 cm^3, P = 8.96 MPa, LHSV = 1 h^{-1} and H_2/oil ratio= 600 (v/v)).

7.5 Conclusions

This study was conducted to improve the HDS, HDN, and HDA activities of bitumen-derived heavy gas oil by removing the catalyst inhibiting and deactivating compounds such as, refractory sulfur and nitrogen heteroatoms prior to hydrotreating. Because of the high adsorption capacity and regeneration ability, PGMA-ON-TENF was selected as the polymeric adsorbent to remove the impurities at ambient temperature. Functionalized polymer was capable of removing 8.7 wt.% nitrogen and 4.4 wt.% sulfur compounds, respectively in a batch reactor using 1:5 polymer to HGO ratio. Hydrophilic nature of the polymer support, PGMA proved to be beneficial for targeting nitrogen compounds.

Though, nitrogen compounds are present in smaller concentration as compared to sulfur, they irreversibly adsorb on the active sites of the hydrotreating catalyst which leads to catalyst poisoning, resulting in lower HDS, HDN and HDA activities. Conventional NiMo/γ-Al_2O_3 catalyst

was used for hydrotreating in a continuous flow fixed-bed reactor. The N_2 adsorption-desorption isotherm for γ-Al_2O_3 was that of a typical mesoporous materials (Type IV with H1 hysteresis). Significant metal dispersion was observed on the catalyst surface and XRD analysis confirmed the presence of tetrahedrally coordinated molybdenum. Significant effect of removing nitrogen compounds prior to hydrotreating was observed at the temperature of 390 °C; where HDS and HDN activities increased from 93.1 wt.% to 94.3 wt.% and 60.5 wt.% to 63.3 wt.%, respectively. Improvement in HDS and HDN activities of heavy gas oil during hydrotreatment in a trickle bed reactor indicated that the functionalized polymer was reasonably useful in removing nitrogen and sulfur compounds from the gas oil.

Chapter 8: Conclusions and recommendations

8.1 Conclusions

The overall objective of this research was: (i) to improve the efficiency of hydrotreating processes by removing nitrogen and sulfur species from bitumen-derived gas oil using π-acceptor functionalized polymers, (ii) to understand the charge transfer complex formation between electron donors and acceptors, and (iii) to study the effects of changing the components of functionalized polymers on nitrogen and sulfur adsorption.

Various functionalized polymers were synthesized and tested for removing nitrogen and sulfur heterocyclic compounds from bitumen-derived gas oils. It was observed that π-acceptor functionalized polymers can be successfully used for the adsorption of nitrogen and sulfur impurities present in gas oils. Moreover, functionalized polymers were found to be selective towards the removal of nitrogen compounds. Effect of changing the π-acceptors was studied by synthesizing three types of fluorenone based π-acceptors, each containing different number of electron withdrawing nitro groups. All three π-acceptors were immobilized on identical polymer support via hydroxylamine linker. Based on the batch adsorption tests, it can be concluded that, the higher the number of electron withdrawing nitro groups present in π-acceptors, the better is the nitrogen and sulfur removal efficiency. Modification in the linker length of the functionalized polymers also affected the nitrogen and sulfur removal efficiency. Diaminopropane (PGMA-DAP(3)-TENF) substituted polymer gave the highest adsorption, followed by the diaminobutane (PGMA-DAB(4)-TENF)-based polymer. It was observed that the change in linker length did not result in a significant effect on π-acceptor loading as similar amounts of TENF were immobilized on the polymeric particles regardless of the linker length. However, steric hindrance around the TENF molecules, on the surface of the particles, played a major role in the adsorption process rather than the length of the linker. Effect of the polymer support on nitrogen and sulfur removal was studied by synthesizing different polymer supports with high internal phase emulsion (PolyHIPEs). Polymer supports with higher glycidyl methacrylate content as compared to unsaturated polyester resin had higher surface area. TENF immobilized polyHIPE-3 has the highest nitrogen removal efficiency of 14.6 wt.%, while its sulfur removal efficiency is 0.5 wt.%.

Charge transfer complexes were formed between fluorenone derived π-acceptors and heterocyclic nitrogen and sulfur compounds, which was evident by the appearence of new bands in the visible region of absorption spectra. Adsorption of model nitrogen and sulfur compounds (quinoline, 9-ethylcarbazole and dibenzothiophene) was exothermic in nature. The process of adsorption was found to be favorable and thermodynamically spontaneous for quinoline, 9-ethylcarbazole and dibenzothiophene. Nitrogen uptake capacity of functionalized polymers decreases on increasing the temperature. Optimum reaction conditions for batch adsorption were found to be: Temperature = 25 ºC, Mechanical Stirring = 400 RPM and Time = 24 h.

Afterwards, hydrotreating of polymer treated gas oil was studied in a trickle bed reactor. Based on the adsorption efficiency, PGMA-ON-TENF was synthesized in bulk and used for preparing the polymer treated HGO feedstock for hydrotreatment experiments. Functionalized polymer was capable of removing 8.7 wt.% nitrogen and 4.4 wt.% sulfur content in the batch adsorption experiments at ambient temperature, using 1:5 polymer to HGO ratio. With conventional NiMO/γ-Al_2O_3 catalyst, 94.3% HDS and 63.3% HDN activities were observed for polymer treated heavy gas oil, while HDS and HDN activities of untreated HGO were 93.1% and 60.5%, respectively. Reducing the nitrogen and sulfur content prior to hydrotreating led to an increase in HDS, HDN and HDA activities. The combination of adsorption and catalysis has resulted in improved catalyst activities during hydrotreatment in a trickle bed reactor at typical industrial conditions.

8.2 Recommendations for future research work

- Textural properties of the polymer support in particular, surface area and pore volume can be improved to increase the adsorption of refractory sulfur and nitrogen compounds. Activated carbon and alumina supports can be functionalized with π-acceptors to obtain adsorbents with high adsorption capacity, which are also selective towards nitrogen and sulfur impurities.
- Large number of aromatic derivatives are present in petroleum feed which can impede the adsorption of heterocyclic nitrogen and sulfur compounds over functionalized polymers. Impact of the presence of aromatics on adsorption capacity and selectivity of functionalized polymers should be further investigated.

- Toluene was used to regenerate the functionalized polymers, which was not effective in achieving the same adsorption capacity as the fresh polymers. Therefore, different methods for regeneration of adsorbents should be tested to enhance reusability of functionalized polymers for industrial application. Use of other solvents, such as acetone or benzene; chemical methods such as reducing the complex formed; and optimization of regeneration parameters and conditions are worth considering.
- The focus of this research work was to synthesize polymeric adsorbents selective towards nitrogen removal. Polymers targeting sulfur compounds can be studied to further improve the denitrogenation and desulfurization of bitumen-derived gas oils.
- Commercialization of functionalized polymer adsorption process can be investigated by studying adsorption and regeneration in a fixed bed reactor, adsorption kinetics along with techno economic analysis and life cycle assessment.

References

[1] S. Bilgen, Structure and environmental impact of global energy consumption, Renew. Sustain. Energy Rev. 38 (2014) 890–902.

[2] N.A. Owen, O.R. Inderwildi, D.A. King, The status of conventional world oil reserves — Hype or cause for concern?, Energy Policy. 38 (2010) 4743–4749.

[3] I. Elizalde, J. Ancheyta, Application of a three-stage approach for modeling the complete period of catalyst deactivation during hydrotreating of heavy oil, Fuel. 138 (2014) 45–51.

[4] J. Chen, A.G. De Crisci, T. Xing, Review on catalysis related research at CanmetENERGY, Can. J. Chem. Eng. 94 (2016) 7–19.

[5] M. Lemaire, M. Monnet, M. Vrinat, V. Lamure, E. Sanson, A. Milenkovic, Method for separating benzothiophene compounds from hydrocarbon mixture containing them, and hydrocarbon mixture obtained by said method, US 6,441,264 B1, 2002.

[6] J. Fu, G.C. Klein, D.F. Smith, S. Kim, R.P. Rodgers, C.L. Hendrickson, et al., Comprehensive compositional analysis of hydrotreated and untreated nitrogen-concentrated fractions from Syncrude oil by electron ionization, field desorption ionization, and electrospray ionization ultrahigh-resolution FT-ICR mass spectrometry, Energy & Fuels. 20 (2006) 1235–1241.

[7] D. Valencia, T. Klimova, I. García-Cruz, Aromaticity of five- and six-membered heterocycles present in crude oils – An electronic description for hydrotreatment process, Fuel. 100 (2012) 177–185.

[8] M. Almarri, X. Ma, C. Song, Selective adsorption for removal of nitrogen compounds from liquid hydrocarbon streams over carbon- and alumina-based adsorbents, Ind. Eng. Chem. Res. 48 (2009) 951–960.

[9] J. Wen, X. Han, H. Lin, Y. Zheng, W. Chu, A critical study on the adsorption of heterocyclic sulfur and nitrogen compounds by activated carbon: Equilibrium, kinetics and thermodynamics, Chem. Eng. J. 164 (2010) 29–36.

[10] E. Deliyanni, M. Seredych, T.J. Bandosz, Interactions of 4,6-dimethyldibenzothiophene with the surface of activated carbons, Langmuir. 25 (2009) 9302–9312.

[11] D. Liu, J. Gui, Z. Sun, Adsorption structures of heterocyclic nitrogen compounds over Cu(I)Y zeolite: A first principle study on mechanism of the denitrogenation and the effect of nitrogen compounds on adsorptive desulfurization, J. Mol. Catal. A Chem. 291 (2008)

17–21.

[12] S. Velu, X. Ma, C. Song, Selective adsorption for removing sulfur from jet fuel over zeolite-based adsorbents, Ind. Eng. Chem. Res. 42 (2003) 5293–5304.

[13] A.J. Hernandez-Maldonado, R.T. Yang, Desulfurization of Liquid Fuels by Selective Adsorption via π Complexation with Cu (I)-Y and Ag-Y Zeolite, Ind. Eng. Chem. Res. 42 (2003) 123–129.

[14] S. Zhang, Q. Zhang, Z.C. Zhang, Extractive desulfurization and denitrogenation of fuels using ionic liquids, Ind. Eng. Chem. Res. 43 (2004) 614–622.

[15] A.R. Hansmeier, G.W. Meindersma, A.B. de Haan, Desulfurization and denitrogenation of gasoline and diesel fuels by means of ionic liquids, Green Chem. 13 (2011) 1907–1913.

[16] G. Blanco-Brieva, J.M. Campos-Martin, S.M. Al-Zahrani, J.L.G. Fierro, Effectiveness of metal-organic frameworks for removal of refractory organo-sulfur compound present in liquid fuels, Fuel. 90 (2011) 190–197.

[17] I. Ahmed, N.A. Khan, Z. Hasan, S.H. Jhung, Adsorptive denitrogenation of model fuels with porous metal-organic framework (MOF) MIL-101 impregnated with phosphotungstic acid: Effect of acid site inclusion, J. Hazard. Mater. 250–251 (2013) 37–44.

[18] J.M. Chitanda, P. Misra, A. Abedi, A.K. Dalai, J.D. Adjaye, Synthesis and characterization of functionalized poly(glycidyl methacrylate)-based particles for the selective removal of nitrogen compounds from light gas oil: Effect of linker length, Energy & Fuels. 29 (2015) 1881–1891.

[19] A. Abedi, J. Chitanda, A.K. Dalai, J. Adjaye, Synthesis and application of functionalized polymers for the removal of nitrogen and sulfur species from gas oil, Fuel Process. Technol. 131 (2015) 473–482.

[20] M. Macaud, M. Sevignon, A. Favre-Reguillon, M. Lemaire, E. Schulz, M. Vrinat, Novel methodology toward deep desulfurization of diesel feed based on the selective elimination of nitrogen compounds, Ind. Eng. Chem. Res. 43 (2004) 7843–7849.

[21] X. Wei, S.M. Husson, M. Mello, D. Chinn, Removal of branched dibenzothiophenes from hydrocarbon mixtures via charge transfer complexes with a TAPA-functionalized adsorbent, Ind. Eng. Chem. Res. 47 (2008) 4448–4454.

[22] P. Misra, J.M. Chitanda, A.K. Dalai, J. Adjaye, Immobilization of fluorenone derived π-acceptors on poly (GMA-co-EGDMA) for the removal of refractory nitrogen species from

bitumen derived gas oil, Fuel. 145 (2015) 100–108.

[23] U.S. Energy Information Administration, International Energy Outlook 2016, 2016.

[24] Natural Resources Canada, (2017). http://www.nrcan.gc.ca/energy/oil-sands/18085 (accessed March 20, 2017).

[25] M.R. Gray, Upgrading Petroleum Residues and Heavy Oils, CRC Press, Marcel Dekker, Inc, New York, 1994.

[26] S. Lee, J.G. Speight, S.K. Loyalka, Handbook of Alternative Fuel Technologies, CRC Press, Taylor and Francis Group: Boca Raton, FL., 2007.

[27] S. Yui, Producing quality synthetic crude oil from Canadian oil sands bitumen, J. Japan Pet. Inst. 51 (2008) 1–13.

[28] D. Ferdous, A.K. Dalai, J. Adjaye, Comparison of Hydrodenitrogenation of Model Basic and Nonbasic Nitrogen Species in a Trickle Bed Reactor Using Commercial NiMo/Al2O3 Catalyst, Energy & Fuels. 17 (2003) 164–171.

[29] C. Song, X. Ma, New design approaches to ultra-clean diesel fuels by deep desulfurization and deep dearomatization, Appl. Catal. B Environ. 41 (2003) 207–238.

[30] M. Macaud, M. Sevignon, A. Favre-Reguillon, M. Lemaire, Novel Methodology toward Deep Desulfurization of Diesel Feed Based on the Selective Elimination of Nitrogen Compounds, Ind. Eng. Chem. Res. 43 (2004) 7843–7849.

[31] S. Badoga, Synthesis and characterization of NiMo supported mesoporous materials with EDTA and phosphorus for hydrotreating of heavy gas oil, University of Saskatchewan, 2015.

[32] I. Mochida, K.H. Choi, An overview of hydrodesulfurization and hydrodenitrogenation, J. Japan Pet. Inst. 47 (2004) 145–163.

[33] J.G. Speight, The desulfurization of heavy oils and residua, Marcel Dekker, Inc., New York, 1999.

[34] S.L. González-Cortés, S. Rugmini, T. Xiao, M.L.H. Green, S.M. Rodulfo-Baechler, F.E. Imbert, Deep hydrotreating of different feedstocks over a highly active Al 2O3-supported NiMoW sulfide catalyst, Appl. Catal. A Gen. 475 (2014) 270–281.

[35] M. Egorova, R. Prins, Competitive hydrodesulfurization of 4,6-dimethyldibenzothiophene, hydrodenitrogenation of 2-methylpyridine, and hydrogenation of naphthalene over sulfided NiMo/γ-Al2O3, J. Catal. 224 (2004) 278–287.

[36] M. Lu, A. Wang, X. Li, X. Duan, Y. Teng, Y. Wang, et al., Hydrodenitrogenation of quinoline catalyzed by MCM-41-supported nickel phosphides, Energy and Fuels. 21 (2007) 554–560.

[37] T. Koltai, M. Macaud, A. Guevara, E. Schulz, M. Lemaire, R. Bacaud, et al., Comparative inhibiting effect of polycondensed aromatics and nitrogen compounds on the hydrodesulfurization of alkyldibenzothiophenes, Appl. Catal. A Gen. 231 (2002) 253–261.

[38] S. Han, T. Zhou, Y. Chai, H. Zhou, C. Liu, Inhibition effects of quinoline, indole and carbazole on HDS of 4,6-DMDBT over Ni-Mo catalyst, Acta Pet. Sin. 26 (2010) 177–183.

[39] M. Nagai, T. Kabe, Selectivity of molybdenum catalyst in hydrodesulfurization, hydrodenitrogenation, and hydrodeoxygenation: effect of additives on dibenzothiophene hydrodesulfurization, J. Catal. 81 (1983) 440–449.

[40] V. LaVopa, C.N. Satterfield, Poisoning of thiophene hydrodesulfurization by nitrogen compounds, J. Catal. 110 (1988) 375–387.

[41] K.-H. Choi, Y. Korai, I. Mochida, J.-W. Ryu, W. Min, Impact of removal extent of nitrogen species in gas oil on its HDS performance: an efficient approach to its ultra deep desulfurization, Appl. Catal. B Environ. 50 (2004) 9–16.

[42] A.R. Beltramone, S. Crossley, D.E. Resasco, W.E. Alvarez, T. V. Choudhary, Inhibition of the hydrogenation and hydrodesulfurization reactions by nitrogen compounds over NiMo/Al2O3, Catal. Letters. 123 (2008) 181–185.

[43] G.C. Laredo S, J.A. De Los Reyes, J. Luis Cano D, J.J. Castillo M, Inhibition Effects of Nitrogen Compounds on the Hydrodesulfurization of Dibenzothiophene, Appl. Catal. A Gen. 207 (2001) 103–112.

[44] G.C. Laredo, E. Altamirano, J.A. De los Reyes, Inhibition effects of nitrogen compounds on the hydrodesulfurization of dibenzothiophene: Part 2, Appl. Catal. A Gen. 243 (2003) 207–214.

[45] X. Tao, Y. Zhou, Q. Wei, S. Ding, W. Zhou, T. Liu, et al., Inhibiting effects of nitrogen compounds on deep hydrodesulfurization of straight-run gas oil over a NiW/Al2O3 catalyst, Fuel. 188 (2017) 401–407.

[46] G.C. Laredo, P.M. Vega-Merino, F. Trejo-Zárraga, J. Castillo, Denitrogenation of middle distillates using adsorbent materials towards ULSD production: A review, Fuel Process. Technol. 106 (2013) 21–32.

[47] H. Yang, J. Chen, C. Fairbridge, Y. Briker, Y.J. Zhu, Z. Ring, Inhibition of nitrogen compounds on the hydrodesulfurization of substituted dibenzothiophenes in light cycle oil, Fuel Process. Technol. 85 (2004) 1415–1429.

[48] J. Bu, G. Loh, C.G. Gwie, S. Dewiyanti, M. Tasrif, A. Borgna, Desulfurization of diesel fuels by selective adsorption on activated carbons: Competitive adsorption of polycyclic aromatic sulfur heterocycles and polycyclic aromatic hydrocarbons, Chem. Eng. J. 166 (2011) 207–217.

[49] J. Narangerel, Y. Sugimoto, Removal of nitrogen compounds before deep hydrotreatment of synthetic crude oils, J. Japan Pet. Inst. 51 (2008) 165–173.

[50] A.J. Hernandez-Maldonado, R.T. Yang, Desulfurization of commercial liquid fuels by selective adsorption via π-complexation with Cu (I)-Y zeolite, Ind. Eng. Chem. Res. 42 (2003) 3103–3110.

[51] A. Rendon-Rivera, M.A. Cortes-Jacome, E. Lopez-Salinas, M.L. Mosqueira, J.A. Toledo-Antonio, Adsorption of nitrogen and sulphur organic-compounds on titania nanotubes, Int. J. Eng. Res. Sci. 2 (2016) 156–166.

[52] K.Y. Foo, B.H. Hameed, Insights into the modeling of adsorption isotherm systems, Chem. Eng. J. 156 (2010) 2–10.

[53] H. Zhang, G. Li, Y. Jia, H. Liu, Adsorptive removal of nitrogen-containing compounds from fuel, J. Chem. Eng. Data. 55 (2010) 173–177.

[54] N.F. Nejad, E. Shams, M.K. Amini, J.C. Bennett, Ordered mesoporous carbon CMK-5 as a potential sorbent for fuel desulfurization: Application to the removal of dibenzothiophene and comparison with CMK-3, Microporous Mesoporous Mater. 168 (2013) 239–246.

[55] R.N. Fallah, S. Azizian, G. Reggers, R. Carleer, S. Schreurs, J. Ahenach, et al., Effect of aromatics on the adsorption of thiophenic sulfur compounds from model diesel fuel by activated carbon cloth, Fuel Process. Technol. 119 (2014) 278–285.

[56] D. Qu, X. Feng, N. Li, X. Ma, C. Shang, X.D. Chen, Adsorption of heterocyclic sulfur and nitrogen compounds in liquid hydrocarbons on activated carbons modified by oxidation: capacity, selectivity and mechanism, RSC Adv. 6 (2016) 41982–41990.

[57] I. Langmuir, The constitution and fundamental properties of solids and liquids. Part I. Solids, J. Am. Chem. Soc. 38 (1916) 2221–2295.

[58] H.M.F. Freundlich, Over the adsorption in solution, J. Phys. Chem. 57 (1906) 385–471.

[59] A.L. Myers, Thermodynamics of Adsorption, in: Chem. Thermodyn. Ind., ed. T. M., Royal Society of Chemistry, Cambridge, 2004.

[60] C.C. Thompson, Solvent effects on charge-transfer complexes. II. complexes of 1,3,5-trinitrobenzene with benzene, mesitylene, durene, pentamethylbenzene, or hexamethylbenzene, J. Phys. Chem. 69 (1966) 2766–2771.

[61] A. Milenkovic, E. Schulz, V. Meille, D. Loffreda, M. Forissier, M. Vrinat, et al., Selective elimination of alkyldibenzothiophenes from gas oil by formation of insoluble charge-transfer complexes, Energy & Fuels. 13 (1999) 881–887.

[62] M. Kubota, T. Kobayashi, Electronic structures of melatonin and related compounds studied by photoelectron spectroscopy, J. Electron Spectros. Relat. Phenomena. 128 (2003) 165–178.

[63] U. Landman, A. Ledwith, D.G. Marsh, D.J. Williams, Structural variations and multiple charge transfer transitions between chloranil and carbazole derivatives, Macromolecules. 9 (1976) 833–839.

[64] A. Milenkovic, D. Loffreda, E. Schulz, H. Chermette, M. Lemaire, P. Sautet, Charge transfer complexes between tetranitrofluorenone and polyaromatic compounds from gasoil: a combined DFT and experimental study, Phys. Chem. Chem. Phys. 6 (2004) 1169–1180.

[65] M. Sévignon, M. Macaud, A. Favre-Réguillon, J. Schulz, M. Rocault, R. Faure, et al., Ultra-deep desulfurization of transportation fuels via charge-transfer complexes under ambient conditions, Green Chem. 7 (2005) 413–420.

[66] M. Lemaire, E. Schulz, M. Sevignon, M. Macaud, A. Favre-Reguillon, M. Thomas, et al., Polymer-supported π-electron acceptors for charge-transfer-based denitrogenation–desulfurization of petroleum fractions, PCT Int. Appl. 2002024836, 2002.

[67] D. Rizwan, A.K. Dalai, J. Adjaye, Synthesis of novel polymer poly(glycidyl methacrylate) incorporated with tetranitrofluorenone for selective removal of neutral nitrogen species from bitumen-derived heavy gas oil, Fuel Process. Technol. 106 (2013) 483–489.

[68] M. Lemaire, M. Macaud, A. Favre-Reguillon, E. Schulz, M. Sevignon, R. Loutaty, Method for the denitrization of hydrocarbon charges in the presence of a polymeric mass, U.S. Patent No. US 2006/0131213 A1, 2006.

[69] S.K. Bej, A.K. Dalai, J. Adjaye, Effect of Hydrotreating Conditions on the Conversion of Residual Fraction and Microcarbon Residue Present in Oil Sands Derived Heavy Gas Oil,

Energy & Fuels. 15 (2001) 1103–1109.

[70] J.. Woods, J. Kung, G. Pleizier, L.. Kotlyar, B.. Sparks, J. Adjaye, et al., Characterization of a coker gas oil fraction from athabasca oilsands bitumen, Fuel. 83 (2004) 1907–1914.

[71] P.L. Jokuty, M.R. Gray, Resistant nitrogen compounds in hydrotreated gas oil from Athabasca bitumen, Energy & Fuels. 5 (1991) 791–795.

[72] D. Rizwan, Selective Removal of Non-Basic Nitrogen Compounds from Heavy Gas Oil Using Functionalized Polymers, University of Saskatchewan, Saskatoon, 2012.

[73] G.T. Morgan, R.W. Thomason, Nitration of Fluorene. 2 : 5-Dinitrofluorene, J. Chem. Soc. 129 (1926) 2691–2696.

[74] M. Orchin, E.O. Woolfolk, Molecular Complexes with 2,4,7-Trinitrofluorenone, J. Am. Chem. Soc. 68 (1946) 1727–1729.

[75] M.S. Newman, W.B. Lutz, α-(2, 4, 5, 7-Tetranito-9-fluorenylideneaminooxy)-propionic Acid, a New Reagent for Formation, Resolution by Complex Formation, J. Am. Chem. Soc. 78 (1956) 2469–2473.

[76] C. Botchwey, Syntheses, Characterization and Kinetics of Nickel-Tungsten Nitride Catalysts for Hydrotreating of Gas Oil, University of Saskatchewan, Saskatoon, 2010.

[77] X. Jiang, W. Tu, Stable Poly (Glycidyl Methacrylate- co -Ethylene Glycol Dimethacrylate) Microspheres via Precipitation Polymerization, J. Appl. Polym. Sci. 115 (2010) 963–968.

[78] L.K. Minacheva, V.S. Sergienko, S.B. Strashnova, O. V. Avramenko, O.V. Koval'chukova, O.A. Egorova, et al., Crystal Structure and Spectral Characteristics of 2 , 4 , 7-Trinitro-9-Fluorenone, Crystallogr. Reports. 5 (2005) 72–77.

[79] A. ur Rahman, M. Iqbal, F. ur Rahman, D. Fu, M. Yaseen, Y. Lv, et al., Synthesis and Characterization of Reactive Macroporous Poly (glycidyl methacrylate-triallyl isocyanurate-ethylene glycol dimethacrylate) Microspheres by Suspension Polymerization : Effect of Synthesis Variables on Surface Area and Porosity, J. Appl. Polym. Sci. 124 (2012) 915–926.

[80] T. Caykara, S.S. Alaslan, Preparation and Characterization of Novel Poly(glycidyl methacrylate) Beads Carrying Amidoxime Groups, J. Appl. Polym. Sci. 106 (2007) 2126–2131.

[81] T.-S. Gwon, B.-W. Lee, J.-Y. Yoon, M.-K. Doh, Synthesis and electrochromism of intermolecular charge-transfer complex dyes, Bull. Korean Chem. Soc. 19 (1998) 1337–

1341.

[82] J.-F. Morin, M. Leclerc, 2,7-carbazole-based conjugated polymers for blue, green, and red light emission, Macromolecules. 35 (2002) 8413–8417.

[83] J. Hu, J. Wu, Q. Wang, Y. Ju, Charge-transfer interaction mediated organogels from 18β-glycyrrhetinic acid appended pyrene, Beilstein J. Org. Chem. 9 (2013) 2877–2885.

[84] V. Chandra Srivastava, An evaluation of desulfurization technologies for sulfur removal from liquid fuels, RSC Adv. 2 (2012) 759–783.

[85] Q. Gao, T.N.K. Ofosu, S.G. Ma, V.G. Komvokis, C.T. Williams, K. Segawa, Catalyst development for ultra-deep hydrodesulfurization (HDS) of dibenzothiophenes. I: Effects of Ni promotion in molybdenum-based catalysts, Catal. Today. 164 (2011) 538–543.

[86] C. Botchwey, A.K. Dalai, J. Adjaye, Two-Stage Hydrotreating of Athabasca Heavy Gas Oil with Interstage Hydrogen Sulfide Removal: Effect of Process Conditions and Kinetic Analyses, Ind. Eng. Chem. Res. 43 (2004) 5854–5861.

[87] C. Song, An overview of new approaches to deep desulfurization for ultra-clean gasoline, diesel fuel and jet fuel, Catal. Today. 86 (2003) 211–263.

[88] M. Breysse, G. Djega-Mariadassou, S. Pessayre, C. Geantet, M. Vrinat, G. Pérot, et al., Deep desulfurization: Reactions, catalysts and technological challenges, Catal. Today. 84 (2003) 129–138.

[89] N. Rambabu, S. Badoga, K.K. Soni, A.K. Dalai, J. Adjaye, Hydrotreating of light gas oil using a NiMo catalyst supported on activated carbon produced from fluid petroleum coke, Front. Chem. Sci. Eng. 8 (2014) 161–170.

[90] E. Aryee, A.K. Dalai, J. Adjaye, Functionalization and characterization of carbon nanohorns (CNHs) for hydrotreating of gas oils, Top. Catal. 57 (2014) 796–805.

[91] I. V. Babich, J.A. Moulijn, Science and technology of novel processes for deep desulfurization of oil refinery streams: A review, Fuel. 82 (2003) 607–631.

[92] A. Jayaraman, F.H. Yang, R.T. Yang, Effects of nitrogen compounds and polyaromatic hydrocarbons on desulfurization of liquid fuels by adsorption via ??-complexation with Cu(I)Y zeolite, Energy and Fuels. 20 (2006) 909–914.

[93] Z. Liu, Q. Zhang, Y. Zheng, J. Chen, Effects of nitrogen and aromatics on hydrodesulfurization of light cycle oil predicted by a system dynamics model, Energy and Fuels. 22 (2008) 860–866.

[94] J. Wu, X. Li, W. Du, C. Dong, L. Li, Preparation and characterization of bimodal porous alumina-silica and its application to removal of basic nitrogen compounds from light oil, J. Mater. Chem. 17 (2007) 2233–2240.

[95] R. V. Mambrini, A.L.M. Saldanha, J.D. Ardisson, M.H. Araujo, F.C.C. Moura, Adsorption of sulfur and nitrogen compounds on hydrophobic bentonite, Appl. Clay Sci. 83–84 (2013) 286–293.

[96] Y.S. Bae, M.B. Kim, H.J. Lee, C.H. Lee, J.W. Ryu, Adsorptive denitrogenation of light gas oil by silica-zirconia cogel, AIChE J. 52 (2006) 510–521.

[97] J.M. Kwon, J.H. Moon, Y.S. Bae, D.G. Lee, H.C. Sohn, C.H. Lee, Adsorptive desulfurization and denitrogenation of refinery fuels using mesoporous silica adsorbents, ChemSusChem. 1 (2008) 307–309.

[98] P.S. Kulkarni, C.A.M. Afonso, Deep desulfurization of diesel fuel using ionic liquids: current status and future challenges, Green Chem. 12 (2010) 1139–1149.

[99] M. Almarri, X. Ma, C. Song, Adsorption pretreatment of crude oil and its effect on subsequent hydrotreating process, Prepr. - Am. Chem. Soc. Div. Pet. Chem. 50 (2005) 433–435.

[100] M. Almarri, X. Ma, N. Li, C. Song, Adsorptive pretreatment of light cycle oil and its effect on subsequent hydrodesulfurization, ACS Symp. Ser. 1088 (2011) 33–54.

[101] M. Sun, A.E. Nelson, J. Adjaye, First principles study of heavy oil organonitrogen adsorption on NiMoS hydrotreating catalysts, Catal. Today. 109 (2005) 49–53.

[102] Z.K. Li, J. Sen Gao, G. Wang, Q. Shi, C.M. Xu, Influence of nonbasic nitrogen compounds and condensed aromatics on coker gas oil catalytic cracking and their characterization, Ind. Eng. Chem. Res. 50 (2011) 9415–9424.

[103] M. Macaud, E. Schulz, M. Vrinat, M. Lemaire, A new material for selective removal of nitrogen compounds from gasoils towards more efficient HDS processes., Chem. Commun. (Camb). 20 (2002) 2340–2341.

[104] R. Loutaty, S. Kasztelan, F. Diehl, M.L.E.S.M. Vrinat, A.M.M. Macaud, M. Sevignon, et al., Method for denitrogenation of oil fractions by forming charge transfer complexes, WO2002024837 A1, 2002.

[105] D. Horak, J. Straka, J. Stokr, B. Schneider, T.B. Tennikova, F. Svec, Reactive polymers: 61. Reaction of macroporous poly(glycidyl methacrylate-co-ethylene dimethacrylate) with

phenol, Polymer (Guildf). 32 (1991) 1135–1139.

[106] Y. Sano, K.-H. Choi, Y. Korai, I. Mochida, Adsorptive removal of sulfur and nitrogen species from a straight run gas oil over activated carbons for its deep hydrodesulfurization, Appl. Catal. B Environ. 49 (2004) 219–225.

[107] F. Svec, J. Hradil, J. Coupek, J. Kalal, Reactive polymers. I. Macroporous methacrylate copolymers containing epoxy groups, Angew. Makromol. Chemie. 48 (1975) 135–143.

[108] H. Zhou, M. Ye, J. Dong, E. Corradini, A. Cristobal, A.J.R. Heck, et al., Robust phosphoproteome enrichment using monodisperse microsphere-based immobilized titanium (IV) ion affinity chromatography., Nat. Protoc. 8 (2013) 461–480.

[109] A. Nastasovic, S. Jovanovic, D. Dordevic, A. Onjia, D. Jakovljevic, T. Novakovic, Metal sorption on macroporous poly(GMA-co-EGDMA) modified with ethylene diamine, React. Funct. Polym. 58 (2004) 139–147.

[110] L.H. Xiao, T. Wang, T.Y. Zhao, X. Zheng, L.Y. Sun, P. Li, et al., Fabrication of magnetic-antimicrobial-fluorescent multifunctional hybrid microspheres and their properties, Int. J. Mol. Sci. 14 (2013) 7391–7404.

[111] R.E. Burge Jr, G.P. Bradford, V. Epoxy Resins, Anal. Chem. Polym. 12 (1959) 123.

[112] A. Nastasovic, S. Jovanovic, D. Jakovljevic, S. Stankovic, A. Onjia, Noble metal binding on macroporous poly (GMA-co-EGDMA) modified with ethylenediamine, J. Serbian Chem. Soc. 69 (2004) 455–460.

[113] N.S. Pujari, A.R. Vishwakarma, T.S. Pathak, A.M. Kotha, S. Ponrathnam, Functionalized polymer networks: Synthesis of microporous polymers by frontal polymerization, Bull. Mater. Sci. 27 (2004) 529–535.

[114] D. Horak, K. Labsky, J. Pilar, M. Bleha, Z. Pelzbauer, F. Svec, The effect of polymeric porogen on the properties of macroporous poly(glycidyl methacrylate-co-ethylene dimethacrylate), Polymer (Guildf). 34 (1993) 3481–3489.

[115] M.A. Lungan, M. Popa, J. Desbrieres, S. Racovita, S. Vasiliu, Complex microparticulate systems based on glycidyl methacrylate and xanthan, Carbohydr. Polym. 104 (2014) 213–222.

[116] R.M. Silverstein, F.X. Webster, D.J. Kiemle, Spectrometric Identification of Organic Compounds, 7th ed., Wiley, 2004.

[117] A.G. Grigoras, V. Barboiu, Influence of acceptor functionality on charge transfer

interactions in mixtures of poly(9-vinylcarbazole) with nitroaromatic compounds, Cent. Eur. J. Chem. 10 (2012) 313–319.

[118] S.Y. Alqaradawi, A. Mostafa, H.S. Bazzi, Charge-transfer complexes of 4-methylpiperidine with σ- And π-acceptors, Spectrochim. Acta, Part A Mol. Biomol. Spectrosc. 135 (2015) 498–505.

[119] N. Singh, A. Ahmad, Synthesis and spectrophotometric studies of charge transfer complexes of p-nitroaniline with benzoic acid in different polar solvents, J. Mol. Struct. 1074 (2014) 408–415.

[120] S.D. Kimmins, P. Wyman, N.R. Cameron, Amine-functionalization of glycidyl methacrylate-containing emulsion-templated porous polymers and immobilization of proteinase K for biocatalysis, Polymer (Guildf). 55 (2014) 416–425.

[121] M.K. Sharma, P. Rohani, S. Liu, M. Kaus, M.T. Swihart, Polymer and surfactant-templated synthesis of hollow and porous ZnS nano- and microspheres in a spray pyrolysis reactor, Langmuir. 31 (2015) 413–423.

[122] E. Ruckenstein, L. Hong, Binding catalytic sites to the surface of porous polymers and some catalytic applications, Chem. Mater. 4 (1992) 122–127.

[123] E.H. Mert, M.A. Kaya, H. Yıldırım, Preparation and characterization of polyester-glycidyl methacrylate polyHIPE monoliths to use in heavy metal removal, Des. Monomers Polym. 15 (2012) 113–126.

[124] A. Jungbauer, R. Hahn, Polymethacrylate monoliths for preparative and industrial separation of biomolecular assemblies, J. Chromatogr. A. 1184 (2008) 62–79.

[125] J.H.G. Steinke, I.R. Dunkin, D.C. Sherrington, Transparent macroporous polymer monoliths, Macromolecules. 29 (1996) 5826–5834.

[126] E.G. Vlakh, T.B. Tennikova, Preparation of methacrylate monoliths, J. Sep. Sci. 30 (2007) 2801–2813.

[127] A. Zhou, X. Ma, C. Song, Liquid-phase adsorption of multi-ring thiophenic sulfur compounds on carbon materials with different surface properties, J. Phys. Chem. B. 110 (2006) 4699–4707.

[128] J.H. Kim, X. Ma, A. Zhou, C. Song, Ultra-deep desulfurization and denitrogenation of diesel fuel by selective adsorption over three different adsorbents : A study on adsorptive selectivity and mechanism, Catal. Today. 111 (2006) 74–83.

[129] L.-L. Xie, A. Favre-Reguillon, X.-X. Wang, X. Fu, M. Lemaire, Selective adsorption of neutral nitrogen compounds from fuel using ion-exchange resins, J. Chem. Eng. Data. 55 (2010) 4849–4853.

[130] M. Sevignon, M. Macaud, A. Favre-Reguillon, J. Schulz, M. Rocault, R. Faure, et al., Ultra-deep desulfurization of transportation fuels via charge-transfer complexes under ambient conditions, Green Chem. 7 (2005) 413–420.

[131] A.R. Cooper, C.W.P. Crowne, P.G. Farrell, Charge-transfer complexes of some 5-membered heterocyclics and their annellated derivatives with tetracyanoethylene, Trans. Faraday Soc. 62 (1966) 18–28.

[132] V.G. Pavelyev, O.D. Parashchuk, M. Krompiec, T. V. Orekhova, I.F. Perepichka, P.H.M. van Loosdrecht, et al., Charge transfer dynamics in donor−acceptor complexes between a conjugated polymer and fluorene acceptors, J. Phys. Chem. C. 118 (2014) 30291–30301.

[133] M.C. Shah, R.G. Baughman, Structure of charge-transfer complexes. 3. 2,4,5,7-tetranitro-9-fluorenone-2-ethylnaphthalene (1/1), Acta Crystallogr. Sect. C. C50 (1994) 1114–1117.

[134] O. Hutzinger, W.D. Jamieson, Indoles and auxins: IX. Mass spectrometric identification and isolation of indoles as polynitrofluorenone complexes, Anal. Biochem. 35 (1970) 351–358.

[135] E.W. Reinheimer, J.R. Galán-Mascarós, K.R. Dunbar, Synthesis and structure of charge transfer salts of tetrathiafulvalene (TTF) and tetramethyl-TTF with 2,4,7-trinitro and 2,4,5,7-tetranitro-9-fluorenone, Synth. Met. 159 (2009) 45–51.

[136] X. Wei, S.M. Husson, M.V.D. e Mello, D. Chinn, Removal of branched dibenzothiophenes from hydrocarbon mixtures via charge transfer complexes with a TAPA-functionalized adsorbent, US 8,138,369 B2, 2012.

[137] V. Meille, E. Schulz, M. Vrinat, M. Lemaire, A new route towards deep desulfurization : selective charge transfer complex formation, Chem. Commun. (1998) 305–306.

[138] S. Rangarajan, M. Mavrikakis, DFT insights into the competitive adsorption of sulfur- and nitrogen-containing compounds and hydrocarbons on Co-promoted molybdenum sulfide catalysts, ACS Catal. 6 (2016) 2904–2917.

[139] R. Javadli, A. de Klerk, Desulfurization of heavy oil, Appl. Petrochemical Res. 1 (2012) 3–19.

[140] P. Misra, J.M. Chitanda, A.K. Dalai, J. Adjaye, Immobilization of fluorenone derived π-

acceptors on poly (GMA-co-EGDMA) for the removal of refractory nitrogen species from bitumen derived gas oil, Fuel. 145 (2015) 100–108.

[141] J.K. Kochi, Charge-transfer excitation of molecular complexes in organic and organometallic chemistry, Pure Appl. Chem. 63 (1991) 255–264.

[142] C.A. Hunter, J.K.M. Sanders, The nature of π-π interactions, J. Am. Chem. Soc. 112 (1990) 5525–5534.

[143] A.S. Jalilov, J. Lu, J.K. Kochi, Charge-transfer complex formations of tetracyanoquinone (cyanil) and aromatic electron donors, J. Phys. Org. Chem. 29 (2016) 35–41.

[144] F.C. Correia, T.C.F. Santos, J.R. Garcia, L.O. Peres, S.H. Wang, Synthesis and characterization of a new semiconductor oligomer having quinoline and fluorene units, J. Braz. Chem. Soc. 26 (2015) 84–91.

[145] M.S. Refat, O.B. Ibrahim, H. Al-Didamony, K.M.A. El-Nour, L. El-Zayat, Spectroscopic and thermal studies on the charge transfer complexes formed between morpholine as donor with p-chloranil and 7,7',8,8'-tetracyanoquinodimethane, J. Saudi Chem. Soc. 16 (2012) 227–235.

[146] S.K. McNeil, New materials for optical sensing of explosives copolymers containing 2-vinyl-4,6-diamino-1,3,5-triazine and co-crystals of electron rich aromatic molecules and 1,3-dinitrobenzene, The University of Alabama, Tuscaloosa, Alabama, 2013.

[147] G.L. Eakins, J.S. Alford, B.J. Tiegs, B.E. Breyfogle, C.J. Stearman, Tuning HOMO – LUMO levels: trends leading to the design of 9-fluorenone scaffolds with predictable electronic and optoelectronic properties, J. Phys. Org. Chem. 24 (2011) 1119–1128.

[148] C. Browning, J.M. Hudson, E.W. Reinheimer, F.-L. Kuo, R.N. McDougald, H. Rabaâ, et al., Synthesis, spectroscopic properties, and photoconductivity of black absorbers consisting of Pt(Bipyridine)(Dithiolate) charge transfer complexes in the presence and absence of nitrofluorenone acceptors, J. Am. Chem. Soc. 136 (2014) 16185–16200.

[149] A. Mostafa, N. El-Ghossein, G.B. Cieslinski, H.S. Bazzi, UV-Vis, IR spectra and thermal studies of charge transfer complexes formed in the reaction of 4-benzylpiperidine with σ- and π-electron acceptors, J. Mol. Struct. 1054–1055 (2013) 199–208.

[150] L.-L. Xie, A. Favre-Reguillon, X.-X. Wang, X. Fu, S. Pellet-Rostaing, G. Toussaint, et al., Selective extraction of neutral nitrogen compounds found in diesel feed by 1-butyl-3-methyl-imidazolium chloride, Green Chem. 10 (2008) 524–531.

[151] E.E. Ebenso, M.M. Kabanda, T. Arslan, M. Saracoglu, F. Kandemirli, L.C. Murulana, et al., Quantum chemical investigations on quinoline derivatives as effective corrosion inhibitors for mild steel in acidic medium, Int. J. Electrochem. Sci. 7 (2012) 5643–5676.

[152] M. Lemaire, M. Macaud, A. Favre-Réguillon, E. Schulz, M. Sevignon, R. Loutaty, Method for the denitrization of hydrocarbon charges in the presence of a polymeric mass, US 2006/0131213 A1, 2006.

[153] Q.-S. Liu, T. Zheng, P. Wang, J.-P. Jiang, N. Li, Adsorption isotherm , kinetic and mechanism studies of some substituted phenols on activated carbon fibers, Chem. Eng. J. 157 (2010) 348–356.

[154] F. Haghseresht, G.Q. Lu, Adsorption characteristics of phenolic compounds onto coal-reject-derived adsorbents, Energy & Fuels. 12 (1998) 1100–1107.

[155] T.W. Weber, R.K. Chakravorti, Pore and solid diffusion models for fixed-bed adsorbers, AIChE J. 20 (1974) 228–238.

[156] A.D. Dwivedi, S.P. Dubey, M. Sillanpää, Y.-N. Kwon, C. Lee, Distinct adsorption enhancement of bi-component metals (cobalt and nickel) by Fireweed-derived carbon compared to activated carbon: Incorporation of surface group distributions for increased efficiency, Chem. Eng. J. 281 (2015) 713–723.

[157] J.-H. Shan, X.-Q. Liu, L.-B. Sun, R. Cui, Cu-Ce bimetal ion-exchanged Y zeolites for selective adsorption of thiophenic sulfur, Energy & Fuels. 22 (2008) 3955–3959.

[158] J. Xiao, C. Song, X. Ma, Z. Li, Effects of aromatics, diesel additives, nitrogen compounds, and moisture on adsorptive desulfurization of diesel fuel over activated carbon, Ind. Eng. Chem. Res. 51 (2012) 3436–3443.

[159] A.A. Khan, R.P. Singh, Adsorption thermodynamics of carbofuran on Sn (IV) arsenosilicate in H+, Na+ and Ca2+ forms, Colloids and Surfaces. 24 (1987) 33–42.

[160] A. Gunay, E. Arslankaya, I. Tosun, Lead removal from aqueous solution by natural and pretreated clinoptilolite: Adsorption equilibrium and kinetics, J. Hazard. Mater. 146 (2007) 362–371.

[161] B. Chakraborty, A.K. Mukherjee, B.K. Seal, Charge-transfer complex formation between o -chloranil and a series of polynuclear aromatic hydrocarbons, Spectrochim. Acta Part A. 57 (2001) 223–229.

[162] S.P. Sibley, Y.T. Nguyen, R.L. Campbell, H.B. Silber, Spectrophotometric studies of

complexation of C60 with aromatic hydrocarbons, Spectrochim. Acta Part A. 53 (1997) 679–684.

[163] G.C. Laredo, N. V. Likhanova, I. V. Lijanova, B. Rodriguez-Heredia, J.J. Castillo, P. Perez-Romo, Synthesis of ionic liquids and their use for extracting nitrogen compounds from gas oil feeds towards diesel fuel production, Fuel Process. Technol. 130 (2015) 38–45.

[164] M.A. Al-Daous, S.A. Ali, Deep desulfurization of gas oil over NiMo catalysts supported on alumina-zirconia composites, Fuel. 97 (2012) 662–669.

[165] P. Rayo, J. Ramírez, P. Torres-Mancera, G. Marroquín, S.K. Maity, J. Ancheyta, Hydrodesulfurization and hydrocracking of Maya crude with P-modified NiMo/Al2O3 catalysts, Fuel. 100 (2012) 34–42.

[166] K. Nakano, S.A. Ali, H.-J. Kim, T. Kim, K. Alhooshani, J.-I. Park, et al., Deep desulfurization of gas oil over NiMoS catalysts supported on alumina coated USY-zeolite, Fuel Process. Technol. 116 (2013) 44–51.

[167] C. Kwak, J.J. Lee, J.S. Bae, S.H. Moon, Poisoning effect of nitrogen compounds on the performance of CoMoS/Al2O3 catalyst in the hydrodesulfurization of dibenzothiophene, 4-methyldibenzothiophene, and 4,6-dimethyldibenzothiophene, Appl. Catal. B Environ. 35 (2001) 59–68.

[168] Q. Wei, S. Wen, X. Tao, T. Zhang, Y. Zhou, K. Chung, et al., Hydrodenitrogenation of basic and non-basic nitrogen-containing compounds in coker gas oil, Fuel Process. Technol. 129 (2015) 76–84.

[169] J.L. García-Gutiérrez, G.C. Laredo, G.A. Fuentes, P. García-Gutiérrez, F. Jiménez-Cruz, Effect of nitrogen compounds in the hydrodesulfurization of straight-run gas oil using a CoMoP/g-Al2O3 catalyst, Fuel. 138 (2014) 98–103.

[170] E. Furimsky, F.E. Massoth, Deactivation of hydroprocessing catalysts, Catal. Today. 52 (1999) 381–495.

[171] V. Sundaramurthy, A.K. Dalai, J. Adjaye, Effect of EDTA on hydrotreating activity of CoMo/γ-Al2O3 catalyst, Catal. Letters. 102 (2005) 299–306.

[172] S. Badoga, Synthesis and characterization of NiMo supported mesoporous materials with EDTA and phosphorus for hydrotreating of heavy gas oil, University of Sakatchewan, 2015.

[173] S. Badoga, A. Ganesan, A.K. Dalai, S. Chand, Effect of synthesis technique on the activity of CoNiMo tri-metallic catalyst for hydrotreating of heavy gas oil, Catal. Today. Article in

(2017) 1–12.

[174] S. Badoga, R. V. Sharma, A.K. Dalai, J. Adjaye, Synthesis and characterization of mesoporous aluminas with different pore sizes: Application in NiMo supported catalyst for hydrotreating of heavy gas oil, Appl. Catal. A Gen. 489 (2015) 86–97.

[175] S. Badoga, K.C. Mouli, K.K. Soni, a. K. Dalai, J. Adjaye, Beneficial influence of EDTA on the structure and catalytic properties of sulfided NiMo/SBA-15 catalysts for hydrotreating of light gas oil, Appl. Catal. B Environ. 125 (2012) 67–84.

[176] S. Chaturvedi, J.A. Rodriguez, J.L. Brito, Characterization of pure and sulfided NiMoO 4 catalysts using synchrotron-based X-ray absorption spectroscopy (XAS) and temperature-programmed reduction (TPR), Catal. Letters. 51 (1998) 85–93.

[177] S. Badoga, A.K. Dalai, J. Adjaye, Y. Hu, Combined effects of EDTA and heteroatoms (Ti, Zr, and Al) on catalytic activity of SBA-15 supported NiMo catalyst for hydrotreating of heavy gas oil, Ind. Eng. Chem. Res. 53 (2014) 2137–2156.

Appendix A: Additional TGA and DTG curves, and FT-IR spectra of functionalized polymers

Thermal Gravimetric Analysis (TGA) and Fourier Transform-Infrared (FT-IR) spectroscopy were used to investigate the type of functional groups that are possibly lost in the 1st degradation step. One particle sample, PGMA-DAP(3)-TENF, was chosen for this study. TGA was run at the same condition as the other particles, that is, about 15 mg of polymer, a heating rate of 10 °C/min and under nitrogen atmosphere (40 ml/min). In the first instance, the sample was run from ambient temperature to the temperature at the end of the 1st degradation step (350 °C). Its resultant degradation profile compared to the one that was combusted up to 600 °C is shown in Figure A1. It shows a good correlation between the TGA and DTG curves for PGMA-DAP(**3**)-TENF at the two temperatures. After TGA, the remaining sample was crushed in KBr for FT-IR analysis so as to determine the functional groups that are still present in the sample.

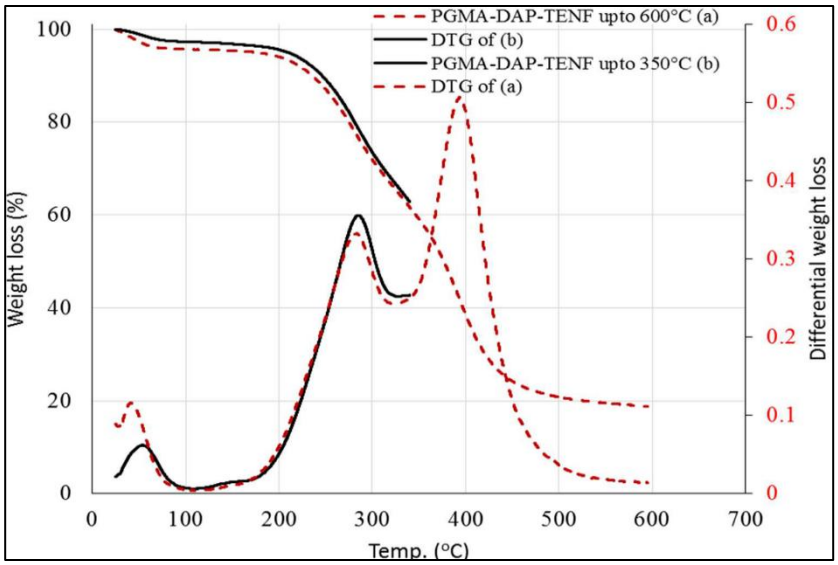

Figure A1: TGA and DTG plot of PGMA-DAP(3)-TENF: (a) heated to 600 °C, and (b) heated to 350 °C.

Figure A2 shows the full spectra (from 400-4000 cm^{-1}) of fresh sample and the one that was heated up to 350 °C (in TGA). Evidently, the spectra showed most of the functional groups, however, O-H, N-H (~3397) and C-H (~ 2950) stretching frequencies have almost disappeared. Upon

expanding the region from 400-2000 cm^{-1} (Figure A3), it is clear that more functional groups have also disappeared. For instance, functional groups related to the ester group (C=O: 1729; C-O: 1160), diamine linker (N-H: 1655, 1389; C-N: 1459) and π-acceptor moiety, TENF (N=O: 1542 and 1343) are missing. The results are consistent with the finding in the literature that the first decomposition step releases the weaker functionality forming olefin type functionality (C=C: 1604) and other unidentified peaks.

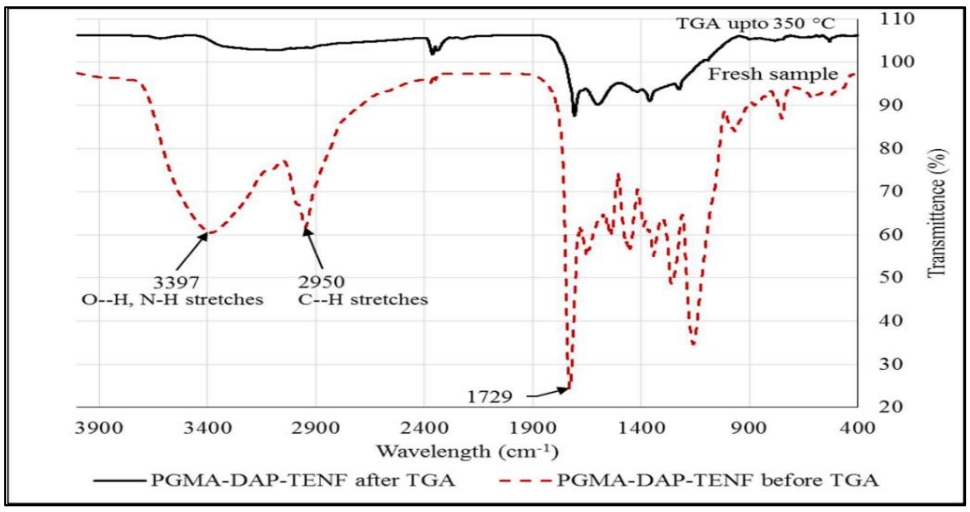

Figure A2: Full FT-IR spectra of PGMA-DAP(3)-TENF before and after TGA analysis.

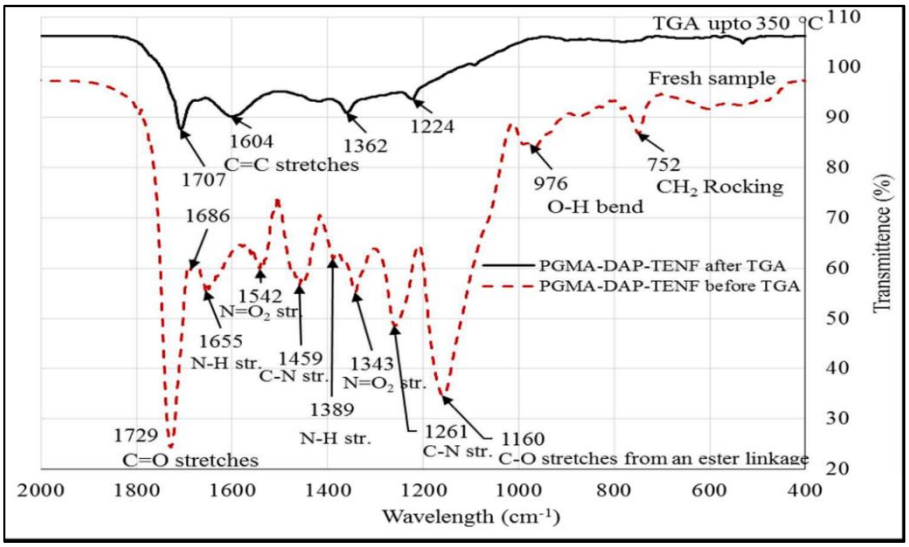

Figure A3: Partial FT-IR spectra of PGMA-DAP(3)-TENF before and after TGA analysis.

Appendix B: Permission to reuse submitted and published papers, and figures

1. Permission to use published paper Immobilization of fluorenone derived π-acceptors on poly (GMA- co-EGDMA) for the removal of refractory nitrogen species from bitumen derived gas oil. *Fuel* 145, 100–108 (2015).

ELSEVIER LICENSE
TERMS AND CONDITIONS

Mar 21, 2017

This Agreement between Prachee Misra ("You") and Elsevier ("Elsevier") consists of your license details and the terms and conditions provided by Elsevier and Copyright Clearance Center.

License Number	4073521422702
License date	Mar 21, 2017
Licensed Content Publisher	Elsevier
Licensed Content Publication	Fuel
Licensed Content Title	Immobilization of fluorenone derived π-acceptors on poly (GMA-co-EGDMA) for the removal of refractory nitrogen species from bitumen derived gas oil
Licensed Content Author	Prachee Misra,Jackson M. Chitanda,Ajay K. Dalai,John Adjaye
Licensed Content Date	1 April 2015
Licensed Content Volume	145
Licensed Content Issue	n/a
Licensed Content Pages	9
Start Page	100
End Page	108
Type of Use	reuse in a thesis/dissertation
Intended publisher of new work	other
Portion	full article
Format	both print and electronic
Are you the author of this Elsevier article?	Yes
Will you be translating?	No
Order reference number	
Title of your thesis/dissertation	Desulfurization and Denitrogenation of Bitumen-Derived Gas Oils using Functionalized Polymers
Expected completion date	Apr 2017
Estimated size (number of pages)	200
Elsevier VAT number	GB 494 6272 12
Requestor Location	Prachee Misra 232 - 103 Cumberland Ave S Saskatoon, SK S7N 1L6 Canada Attn: Prachee Misra
Total	0.00 CAD
Terms and Conditions	

2. Permission to use published paper Synthesis and characterization of functionalized poly(glycidyl methacrylate)-based particles for the selective removal of nitrogen compounds from light gas oil: Effect of linker length. *Energy & Fuels* 29, 1881–1891 (2015).

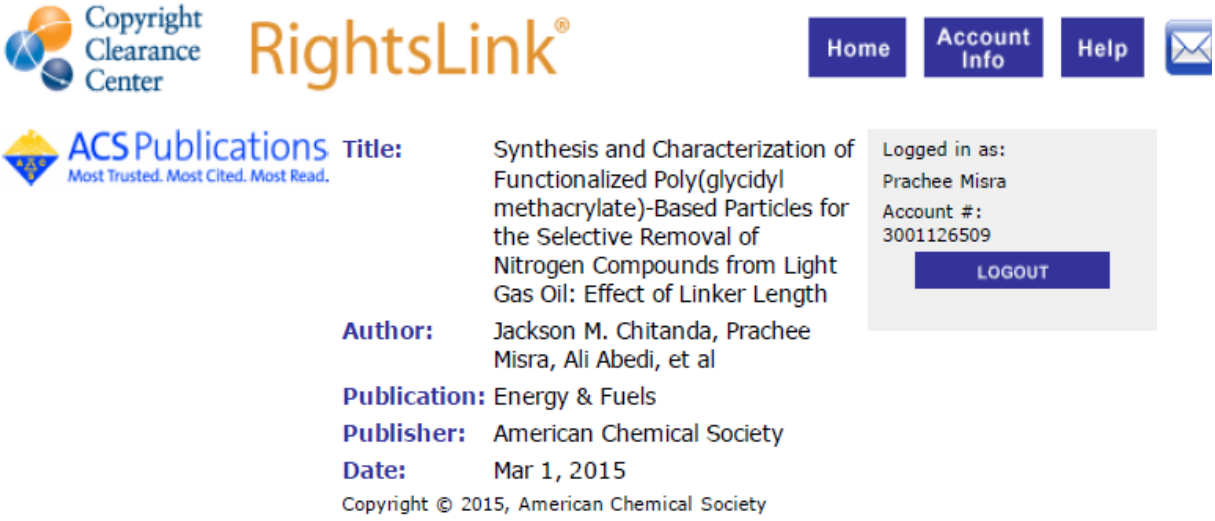

PERMISSION/LICENSE IS GRANTED FOR YOUR ORDER AT NO CHARGE

This type of permission/license, instead of the standard Terms & Conditions, is sent to you because no fee is being charged for your order. Please note the following:

- Permission is granted for your request in both print and electronic formats, and translations.
- If figures and/or tables were requested, they may be adapted or used in part.
- Please print this page for your records and send a copy of it to your publisher/graduate school.
- Appropriate credit for the requested material should be given as follows: "Reprinted (adapted) with permission from (COMPLETE REFERENCE CITATION). Copyright (YEAR) American Chemical Society." Insert appropriate information in place of the capitalized words.
- One-time permission is granted only for the use specified in your request. No additional uses are granted (such as derivative works or other editions). For any other uses, please submit a new request.

3. Permission to use published paper Selective removal of nitrogen compounds from gas oil using functionalized polymeric adsorbents: Efficient approach towards improving denitrogenation of petroleum feedstock. *Chemical Engineering Journal* 295, 109–118 (2016).

ELSEVIER LICENSE
TERMS AND CONDITIONS

Mar 21, 2017

This Agreement between Prachee Misra ("You") and Elsevier ("Elsevier") consists of your license details and the terms and conditions provided by Elsevier and Copyright Clearance Center.

License Number	4073521318251
License date	Mar 21, 2017
Licensed Content Publisher	Elsevier
Licensed Content Publication	Chemical Engineering Journal
Licensed Content Title	Selective removal of nitrogen compounds from gas oil using functionalized polymeric adsorbents: Efficient approach towards improving denitrogenation of petroleum feedstock
Licensed Content Author	Prachee Misra,Jackson M. Chitanda,Ajay K. Dalai,John Adjaye
Licensed Content Date	1 July 2016
Licensed Content Volume	295
Licensed Content Issue	n/a
Licensed Content Pages	10
Start Page	109
End Page	118
Type of Use	reuse in a thesis/dissertation
Intended publisher of new work	other
Portion	full article
Format	both print and electronic
Are you the author of this Elsevier article?	Yes
Will you be translating?	No
Order reference number	
Title of your thesis/dissertation	Desulfurization and Denitrogenation of Bitumen-Derived Gas Oils using Functionalized Polymers
Expected completion date	Apr 2017
Estimated size (number of pages)	200
Elsevier VAT number	GB 494 6272 12
Requestor Location	Prachee Misra 232 - 103 Cumberland Ave S Saskatoon, SK S7N 1L6 Canada Attn: Prachee Misra
Total	0.00 CAD

4. Permission to use Figure 2.5

ELSEVIER LICENSE
TERMS AND CONDITIONS

Mar 21, 201

This Agreement between Prachee Misra ("You") and Elsevier ("Elsevier") consists of your license details and the terms and conditions provided by Elsevier and Copyright Clearance Center.

License Number	4073460581299
License date	Mar 21, 2017
Licensed Content Publisher	Elsevier
Licensed Content Publication	Applied Catalysis A: General
Licensed Content Title	Deep hydrotreating of different feedstocks over a highly active Al2O3-supported NiMoW sulfide catalyst
Licensed Content Author	S.L. González-Cortés,S. Rugmini,T. Xiao,M.L.H. Green,S.M. Rodulfo Baechler,F.E. Imbert
Licensed Content Date	5 April 2014
Licensed Content Volume	475
Licensed Content Issue	n/a
Licensed Content Pages	12
Start Page	270
End Page	281
Type of Use	reuse in a thesis/dissertation
Intended publisher of new work	other
Portion	figures/tables/illustrations
Number of figures/tables/illustrations	1
Format	both print and electronic
Are you the author of this Elsevier article?	No
Will you be translating?	No
Order reference number	
Original figure numbers	Graphical Abstract
Title of your thesis/dissertation	Desulfurization and Denitrogenation of Bitumen-Derived Gas Oils using Functionalized Polymers
Expected completion date	Apr 2017
Estimated size (number of pages)	200
Elsevier VAT number	GB 494 6272 12
Requestor Location	Prachee Misra 232 - 103 Cumberland Ave S Saskatoon, SK S7N 1L6 Canada Attn: Prachee Misra
Total	0.00 CAD
Terms and Conditions	

5. Permission to use Figure 2.6

ELSEVIER LICENSE
TERMS AND CONDITIONS

Mar 21, 2017

This Agreement between Prachee Misra ("You") and Elsevier ("Elsevier") consists of your license details and the terms and conditions provided by Elsevier and Copyright Clearance Center.

License Number	4073470002893
License date	Mar 21, 2017
Licensed Content Publisher	Elsevier
Licensed Content Publication	Journal of Catalysis
Licensed Content Title	Competitive hydrodesulfurization of 4,6-dimethyldibenzothiophene, hydrodenitrogenation of 2-methylpyridine, and hydrogenation of naphthalene over sulfided NiMo/γ-Al2O3
Licensed Content Author	Marina Egorova,Roel Prins
Licensed Content Date	10 June 2004
Licensed Content Volume	224
Licensed Content Issue	2
Licensed Content Pages	10
Start Page	278
End Page	287
Type of Use	reuse in a thesis/dissertation
Intended publisher of new work	other
Portion	figures/tables/illustrations
Number of figures/tables/illustrations	1
Format	both print and electronic

6. Permission to use Figure 2.7

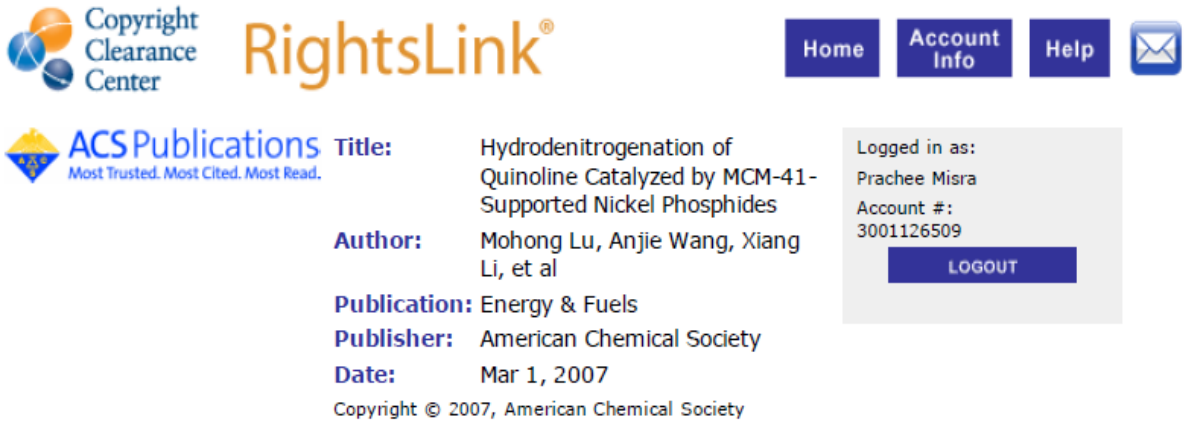

PERMISSION/LICENSE IS GRANTED FOR YOUR ORDER AT NO CHARGE

This type of permission/license, instead of the standard Terms & Conditions, is sent to you because no fee is being charged for your order. Please note the following:

- Permission is granted for your request in both print and electronic formats, and translations.
- If figures and/or tables were requested, they may be adapted or used in part.
- Please print this page for your records and send a copy of it to your publisher/graduate school.
- Appropriate credit for the requested material should be given as follows: "Reprinted (adapted) with permission from (COMPLETE REFERENCE CITATION). Copyright (YEAR) American Chemical Society." Insert appropriate information in place of the capitalized words.
- One-time permission is granted only for the use specified in your request. No additional uses are granted (such as derivative works or other editions). For any other uses, please submit a new request.

If credit is given to another source for the material you requested, permission must be obtained from that source.

7. Permission to use Figure 2.8

ELSEVIER LICENSE
TERMS AND CONDITIONS

Mar 21, 2017

This Agreement between Prachee Misra ("You") and Elsevier ("Elsevier") consists of your license details and the terms and conditions provided by Elsevier and Copyright Clearance Center.

License Number	4073480357842
License date	Mar 21, 2017
Licensed Content Publisher	Elsevier
Licensed Content Publication	Fuel
Licensed Content Title	Inhibiting effects of nitrogen compounds on deep hydrodesulfurization of straight-run gas oil over a NiW/Al2O3 catalyst
Licensed Content Author	Xiujuan Tao,Yasong Zhou,Qiang Wei,Sijia Ding,Wenwu Zhou,Tingting Liu,Xiaohui Li
Licensed Content Date	15 January 2017
Licensed Content Volume	188
Licensed Content Issue	n/a
Licensed Content Pages	7
Start Page	401
End Page	407
Type of Use	reuse in a thesis/dissertation
Intended publisher of new work	other
Portion	figures/tables/illustrations
Number of figures/tables/illustrations	1
Format	both print and electronic

8. Permission to use Figure 2.9

ELSEVIER LICENSE
TERMS AND CONDITIONS

Mar 21, 2017

This Agreement between Prachee Misra ("You") and Elsevier ("Elsevier") consists of your license details and the terms and conditions provided by Elsevier and Copyright Clearance Center.

License Number	4073490457211
License date	Mar 21, 2017
Licensed Content Publisher	Elsevier
Licensed Content Publication	Chemical Engineering Journal
Licensed Content Title	Desulfurization of diesel fuels by selective adsorption on activated carbons: Competitive adsorption of polycyclic aromatic sulfur heterocycles and polycyclic aromatic hydrocarbons
Licensed Content Author	Jie Bu,Gabriel Loh,Chuandayani Gunawan Gwie,Silvia Dewiyanti,Michael Tasrif,Armando Borgna
Licensed Content Date	1 January 2011
Licensed Content Volume	166
Licensed Content Issue	1
Licensed Content Pages	11
Start Page	207
End Page	217
Type of Use	reuse in a thesis/dissertation
Intended publisher of new work	other
Portion	figures/tables/illustrations
Number of figures/tables/illustrations	1
Format	both print and electronic

9. Permission to use Figure 2.10

ROYAL SOCIETY OF CHEMISTRY LICENSE TERMS AND CONDITIONS

Mar 21, 2017

This Agreement between Prachee Misra ("You") and Royal Society of Chemistry ("Royal Society of Chemistry") consists of your license details and the terms and conditions provided by Royal Society of Chemistry and Copyright Clearance Center.

License Number	4073510691679
License date	Mar 21, 2017
Licensed Content Publisher	Royal Society of Chemistry
Licensed Content Publication	Green Chemistry
Licensed Content Title	Ultra-deep desulfurization of transportation fuels via charge-transfer complexes under ambient conditions
Licensed Content Author	Marc Sévignon,Mathieu Macaud,Alain Favre-Réguillon,Jürgen Schulz,Muriel Rocault,René Faure,Michel Vrinat,Marc Lemaire
Licensed Content Date	Apr 26, 2005
Licensed Content Volume	7
Licensed Content Issue	6
Type of Use	Thesis/Dissertation

10. Permission to use Figure 2.11

Copyright Clearance Center RightsLink® Home Account Info Help

ACS Publications Most Trusted. Most Cited. Most Read.

Title:	Novel Methodology toward Deep Desulfurization of Diesel Feed Based on the Selective Elimination of Nitrogen Compounds
Author:	Mathieu Macaud, Marc Sévignon, Alain Favre-Réguillon, et al
Publication:	Industrial & Engineering Chemistry Research
Publisher:	American Chemical Society
Date:	Nov 1, 2004

Logged in as: Prachee Misra Account #: 3001126509 LOGOUT

Copyright © 2004, American Chemical Society

PERMISSION/LICENSE IS GRANTED FOR YOUR ORDER AT NO CHARGE

This type of permission/license, instead of the standard Terms & Conditions, is sent to you because no fee is being charged for your order. Please note the following:

- Permission is granted for your request in both print and electronic formats, and translations.
- If figures and/or tables were requested, they may be adapted or used in part.
- Please print this page for your records and send a copy of it to your publisher/graduate school.
- Appropriate credit for the requested material should be given as follows: "Reprinted (adapted) with permission from (COMPLETE REFERENCE CITATION). Copyright (YEAR) American Chemical Society." Insert appropriate information in place of the capitalized words.
- One-time permission is granted only for the use specified in your request. No additional uses are granted (such as derivative works or other editions). For any other uses, please submit a new request.

If credit is given to another source for the material you requested, permission must be obtained from that source.